The University Of Sheffield.

Department Of Cardiovascular Science.

The Role of the $P2Y_{12}$ Receptor in the Vessel Wall Response to Injury and Inflammation

Laura Elizabeth West

Thesis Submitted for the Degree of Doctor of Philosophy

June 2014

Abstract

Platelets play a fundamental role in thrombosis, but they are increasingly regarded as discrete immune cells due to their pro-inflammatory actions on leukocytes and the endothelium. The $P2Y_{12}$ receptor is responsible for amplifying and sustaining platelet activation. As a result, $P2Y_{12}$ inhibitors, such as ticagrelor and clopidogrel, form an essential component of acute coronary syndrome treatment in preventing thrombotic events. Furthermore, $P2Y_{12}$ receptors have also been identified on vascular smooth muscle cells where they mediate cell contraction and mitogenic responses. This thesis investigates the role of $P2Y_{12}$ in mediating the vessel wall response to injury and to inflammation, specifically in atherogenesis, and considers the use of $P2Y_{12}$ inhibitors in modulating these effects.

I have shown, using a murine ferric chloride injury model, that platelet $P2Y_{12}$ is crucial in mediating thrombus and neointima formation following vessel injury, and that $P2Y_{12}$ inhibition at the time of injury was sufficient to prevent their formation.

To investigate the role of $P2Y_{12}$ in atherogenesis, a novel ApoE/$P2Y_{12}$ double knockout mouse strain was generated and fed a high-fat western diet for 12 weeks, before assessing atherosclerotic burden. Compared to $ApoE^{-/-}$ controls, $P2Y_{12}$-deficency led to a moderate reduction in lesion area, particularly in areas of the vasculature prone to turbulent blood flow, such as the aortic arch. These vessels exhibited characteristics of established disease, with advanced lesions, and so atheroma was also assessed after 4 weeks on a western diet. I demonstrated, using bone marrow transplantations, that platelet $P2Y_{12}$-deficiency profoundly reduced platelet reactivity compared to $ApoE^{-/-}$ controls, but had no effect on atheroma; whereas vessel wall $P2Y_{12}$-deficiency significantly attenuated lesion area and led to a less mature lesion phenotype. Treating mice with ticagrelor or clopidogrel for 4 weeks achieved effective platelet $P2Y_{12}$ inhibition, compared to mice treated with mannitol as a control, but did not block the vessel wall $P2Y_{12}$ effect on atherogenesis.

These data describe a previously unknown role for vessel wall $P2Y_{12}$ in potentiating early atherogenesis. Despite its major contribution to platelet reactivity, platelet $P2Y_{12}$ had no effect at this early stage, and yet is vital in later disease in atherothrombosis and modulating neointima formation following vessel injury. This work emphasises the complexity of cellular roles within atherogenesis, and how the impact of these cell populations may change as disease evolves. Further work is required to clarify the extent to which vessel wall and platelet $P2Y_{12}$ influence atherogenesis throughout disease progression, in order to provide a clearer understanding of potential pharmacological targets in the prevention and management of atherosclerosis.

Publications arising from this thesis

West, L.E., Steiner, T., Judge, H.M., Francis, S.E. & Storey, R.F. (2014) Vessel wall, not platelet, $P2Y_{12}$ potentiates early atherogenesis. *Cardiovascular Research*, **102** (3): 429-435.

Evans, D.J., **Jackman, L.E.**,* Chamberlain, J., Crosdale, D.J., Judge, H.M., Jetha, K., Norman, K.E., Francis, S.E. & Storey, R.F. (2009) Platelet $P2Y_{12}$ receptor influences the vessel wall response to arterial injury and thrombosis. *Circulation*, **119**: 116-122.

*Publication in maiden name.

Copyright notice

Acknowledgements

Throughout the course of my PhD I have received tremendous encouragement, support, and guidance from family, friends, and colleagues, without whom this 8 year journey would not have been possible. For this I am truly grateful. Although it is impossible for me to name every individual who has helped me along the way, there are some important people I wish to thank, and to whom I owe a debt of gratitude for their continual and immeasurable support.

Firstly, I would like to thank my supervisors Professor Robert Storey and Professor Sheila Francis for their helpful thoughts and guidance, and for the time they invested in me throughout the course of this thesis. Thank you also to Dr Heather Judge who is always willing to listen and has been a huge support, both as a friend, and unofficial mentor. As a member of the Department of Cardiovascular Science, I am fortunate to be surrounded by a group of extremely supportive colleagues, who are always happy to offer their help and advice. In particular, I would like to thank Dr Janet Chamberlain for her guidance with histology, and Dr Mark Ariaans for his technical expertise and continual willingness to help. Thank you also to Tanja Steiner for her assistance during the ticagrelor/clopidogrel feeding study. I especially wish to thank Dr David Evans for the time, effort, and patience he invested in training me in the surgical and histological skills, which I have used throughout my PhD. Furthermore, I would like to thank him for kindly providing the $P2Y_{12}^{+/+}$ and $P2Y_{12}^{-/-}$ thrombus and neointima datasets in Chapter 3 (Figures 3.1 and 3.2), which are displayed along with my own clopidogrel data, in addition to the short-term clopidogrel treatment (Figure 3.3) and BMT studies (Figure 3.4), which were performed jointly by Dr David Evans and myself.

I would like to thank my past and present colleagues Kirstie, Abi, Martin, and Nadine, who I am also very privileged to call my friends, for their support and encouragement. In particular, I wish to say a special thank you to Claudia, Amanda, and Louise for their invaluable discussions over lunch and coffee, but most of all for their friendship, countless laughs, and for making work such a happy place.

A support network is vital in life and I am blessed to have an amazing group of friends and family, without whom I would be lost. First and foremost, I would like to say thank you to my parents and step-parents for their endless love, encouragement, and for never limiting my dreams and ambitions. Thanks also to Rosie for her tremendous care and continual support. To my treasured friends Jen, Janine, Alex, and Wendy thank you for always being there. Finally, and most importantly, thank you to my loving husband, Pete, for being my inspiration, my rock, and my guiding light.

Table of contents

List of figures

List of tables

Abbreviations

α-SMA	α-Smooth muscle actin
5HT	5-hydroxytryptamine (Serotonin)
AC	Adenylyl cyclase
ACS	Acute coronary syndrome
ADAMTS	A disintegrin and metalloproteinase with a thrombospondin type 1 motif
ADP	Adenosine diphosphate
ALT	Alanine transaminase
ANOVA	Analysis of variance
ApoE	Apolipoprotein E
aPTT	Activated partial thromboplastin time
AST	Aspartate transaminase
ATP	Adenosine triphosphate
BMS	Bare metal stent
BMT	Bone marrow transplant
CABG	Coronary artery bypass graft
CAD	Coronary artery disease
CAM	Cell adhesion molecule
cAMP	Cyclic adenosine monophosphate
CHD	Coronary heart disease
COX	Cyclooxygenase
CRP	C-reactive protein
CSA	Cross-sectional area
CVD	Cardiovascular disease
DAB	3,3′-diaminobenzidine tetrahydrochloride
DES	Drug-eluting stent
ECG	Electrocardiogram
ECM	Extracellular matrix
EDTA	Ethylenediaminetetraacetic acid
EEL	External elastic lamina
ELISA	Enzyme-linked immunosorbent assay
EVG	Alcian blue/elastic van Gieson
FBS	Fetal bovine serum
FITC	Fluorescein isothiocyanate
GPCR	G protein-coupled receptor
GTT	Glucose tolerance test
Gy	Gray [SI unit of radiation]
HBSS	Hanks buffered salt solution
HDL	High density lipoprotein
H&E	Haematoxylin and eosin
HEPES	N-2-hydroxyethylpiperazine-N′-2-ethanesulfonic acid
HRP	Horseradish peroxidase
HSI	Hue, saturation and intensity
HT buffer	HEPES-Tyrode's buffer
ICAM-1	Intracellular adhesion molecule-1
IEL	Internal elastic lamina
IL	Interleukin
i.p.	Intraperitoneal
ITT	Insulin tolerance test
i.v.	Intravenous
IVC	Individually ventilated cages
LAMP	Lysosomal-associated membrane protein
L/CSA	Lesion:cross-sectional area ratio
LDL	Low density lipoprotein
LDL-R	Low density lipoprotein receptor
MAC	Membrane attack complex

MAPK	Mitogen-activated protein kinase
MCP-1	Monocyte chemotactic protein-1
M-CSF	Macrophage colony stimulating factor
MI	Myocardial infarction
MLCK	Myosin light chain kinase
MMP	Matrix metalloproteinase
MSB	Martius scarlet blue
NF-κB	Nuclear factor kappa-light-chain-enhancer of activated B cells
N/M	Neointima:media ratio
NO	Nitric oxide
NOS	Nitric oxide synthase
NSTEMI	Non-ST-elevation myocardial infarction
ox-LDL	Oxidised low density lipoprotein
P2	Purinergic receptor
PAI-1	Plasminogen activator inhibitor-1
PAR-4	Protease-activated receptor-4
PBS	Phosphate buffered saline
PCI	Percutaneous coronary intervention
PCR	Polymerase chain reaction
PDGF	Platelet-derived growth factor
PE	Phycoerythrin
PECAM-1	Platelet/endothelial cell adhesion molecule-1
PF4	Platelet factor 4
PFA	Paraformaldehyde
PGI_2	Prostaglandin I_2 (Prostacyclin)
PI3K	Phosphoinositide 3-kinase
PIP_2	Phosphatidylinositol 4,5-bisphosphate
PLA2	Phospholipase A2
PLC	Phospholipase C
PKC	Protein kinase C
PS	Phosphatidylserine
PSGL-1	P-selectin glycoprotein ligand-1
PT	Prothrombin time
rad	Radiation absorbed dose [unit of radiation]
RANTES	Regulated upon activation, normal T-cell expressed and secreted
RBC	Red blood cell
RGB	Red, green and blue
SEM	Standard error of the mean
SM-MHC	Smooth muscle myosin heavy chain
SNARE	Soluble N-ethylmaleimide-sensitive factor activating protein receptor
STEMI	ST-elevation myocardial infarction
TBS	Tris buffered saline
TF	Tissue factor
TGF-β	Transforming growth factor-β
T/M	Thrombus:media ratio
TNF-α	Tumour necrosis factor-α
TRAP	Thrombin receptor activating protein
TxA_2	Thromboxane A_2
USP	United States pharmacopoeia [unit]
UV	Ultraviolet
VCAM-1	Vascular cell adhesion molecule-1
VLA-4	Very late antigen-4
VSMC	Vascular smooth muscle cell
vWF	von Willebrand factor
WHO	World Health Organisation

1 Introduction

1.1 The cardiovascular system

The vertebrate cardiovascular system is a remarkably intricate, versatile, and yet robust network. Our understanding of the heart and its vessels has grown from the very first speculations of Aristotle (384 BC), suggesting the heart was the source of all blood vessels, to our modern understanding of a closed circulatory system, first described by William Harvey (1578-1657).

Prior to Harvey, the concept of blood 'circulating' was inconceivable. The established doctrine of Galen (130-199), promoted an open-ended vascular system, whereby blood moved from the right to left ventricle via invisible pores in the septum, and slowly ebbed to tissues when needed. This dogma remained unchallenged for nearly 1500 years until, in 1628, William Harvey published the findings of his extensive experiments, defining the closed vascular system we understand today. He demonstrated that blood *must* form a circuit, with the right ventricle pumping blood to the lungs, via the pulmonary artery, and returning to the left ventricle by the pulmonary vein, although he never favoured the idea of a direct link. Nevertheless, just 4 years after Harvey's death, Malpighi demonstrated the existence of capillaries using light microscopy, proving Harvey's theory conclusively (Aird 2011).

1.1.1 Diseases of the circulatory system

Beating continuously over 2.5 billion times on average in a lifetime (based on a life expectancy of 80 years), the heart is a truly resilient organ. However, it is not surprising, given the intensive nature and crucial role for the circulatory system, coupled with a modern lifestyle that cardiovascular diseases (CVD) remain the leading cause of death in the world, accounting for 30% of the 57 million deaths annually. Estimated at 17.3 million a year, deaths from CVD outstrip cancer over two-fold (7.6 million), and this figure is expected to rise to 23.6 million by 2030 (WHO 2008).

Although a disease primarily associated with the ageing and wealthier West, this is a misconception as over 80% of cardiovascular deaths occur in low and middle income regions of the world and is the leading cause of death, second only to lower respiratory infections in the lowest income countries (WHO 2008). An epidemiologic transition is evident in these areas, with a shift in deaths from infectious diseases to chronic non-communicable diseases such as CVD. Changes in lifestyle and improved nutrition, coupled with inadequate access to appropriate healthcare, have led to increased obesity and diabetes, particularly in countries such as India, China, and East Asia. As a result,

cardiovascular deaths are rising, and at a faster rate than can be explained by demographic changes alone, posing a potential time bomb for developing nations (Yusuf *et al.* 2001).

Advances in medical treatment and emerging pharmaceuticals have begun to impact in high income regions and slow rates of cardiovascular-related death. Despite this, cardiovascular disease still accounts for 50% of deaths in Europe (WHO 2008) and a third of those in the UK. A confounding issue is that of obesity, which is an increasing problem with age and one which continues to rise year on year. In the school year 2008/2009, 23% of reception children were either obese or overweight, and by year 6 this rose to 33%. By the age of 65 to 74 years, 85% of men and 75% of women are either overweight or obese (Scarborough *et al.* 2010).

Perhaps another factor to consider is the economic cost of tackling cardiovascular disease. Estimated at £30 billion a year in the UK, treatment and care for these diseases, with obesity rising, could stretch NHS resources to breaking point. Therefore, development of more effective treatments, with a focus on prevention, is a very desirable prospect.

In the face of such stark statistics, the battle against cardiovascular diseases clearly has a long way to go, and without intervention is set to become a global epidemic.

1.1.2 Coronary heart disease and acute coronary syndromes

Cardiovascular disease is a term which covers a broad spectrum of diseases, including ischaemic heart and cerebrovascular diseases, cardiomyopathies, and rheumatic and hypertensive heart disease. Although the aetiology of these conditions may vary, the majority stem from vascular dysfunction as a direct result of the inflammatory disease atherosclerosis, in which vessels become stenosed from the development of complex, fatty lesions within the vessel wall. Coronary heart disease (CHD), also termed coronary artery disease (CAD), specifically refers to lesions within the coronary vessels, which compromise the lumen and restrict blood flow to the myocardium resulting in diminished cardiac function. Of all the cardiovascular diseases, coronary heart disease has the highest mortality, accounting for 48% of total deaths from CVD in the UK (Scarborough *et al.* 2010).

Ischaemia caused by stenosed vessels in CHD manifests as angina, acute chest pain experienced upon strenuous activity. However, as disease develops, lesions can become unstable, increasing the risk of thrombosis, which is the dominant cause of acute coronary syndromes (ACS) such as myocardial infarction (MI). The formation of non-occlusive thrombus in coronary vessels may present as either unstable angina or non-ST-elevation myocardial infarction (NSTEMI). Both have similar onset, but prolonged ischaemia in MI causes tissue necrosis, which is not seen in unstable angina (Cannon and Braunwald 2008; Cannon and Lee 2008). Occlusive thrombus formation is ultimately more life threatening. It

is estimated that approximately 70% of fatal MIs and sudden coronary deaths are as a result of atherosclerotic plaque rupture and formation of an occlusive thrombus (Naghavi *et al.* 2003). Complete vessel blockage can cause catastrophic damage to the myocardium from transmural necrosis, severely compromising cardiac function. This type of MI often manifests as an ST-elevation myocardial infarction (STEMI), so-called due to an abnormal electrocardiogram (ECG) output in the ST segment of the wave.

1.1.3 Risk factors

A large number of risk factors are associated with coronary heart disease (see Table 1.1). These are proven to have causative effect and are the basis on which predictive models, such as the Framingham risk score, calculate cardiovascular risk. Although seen as the gold standard for many years, the Framingham score is now outdated and demonstrated poor calibration to actual outcomes (Anderson *et al.* 1991). In 2010, the UK National Institute for Health and Care Excellence (NICE) withdrew its recommendation of using the score, leaving the choice of risk model to local organisations (Dent 2010). More recently, the QRISK2 model (Collins and Altman 2012), developed and validated in the UK, includes additional variables such as ethnicity and socio-economic deprivation, and shows superior calibration and discrimination over Framingham.

In addition to conventional risk factors, a variety of molecular biomarkers are closely linked with CHD, including C-reactive protein (CRP), homocysteine, lipoprotein(a), and fibrinogen levels. However, the usefulness of these biomarkers is intensely debated, as a close association between the molecule and CHD may not necessarily translate into improved risk estimation. Furthermore, proving a causal effect of these molecules on CHD can often be confounded by other factors such as inflammation, although this may not detract from their overall value as a biomarker. Nevertheless, questions have been asked as to what advantage they bring to existing prediction models and further investigation is necessary (Dent 2010).

Table 1.1 – Risk factors for coronary heart disease.

Many risk factors are associated with the development of atherosclerosis and, in particular, coronary heart disease. These can be described as either behavioural or medical risk factors, and are used in predictive models to calculate cardiovascular risk (Yusuf *et al.* 2001; Dent 2010; Dent 2010; Scarborough *et al.* 2010).

Medical	Behavioural
Elevated LDL cholesterol *	Diet
Low HDL-cholesterol *	Smoking *
Hypertension *	Physical inactivity
Overweight and obesity	Alcohol consumption
Diabetes mellitus *	
Genetic susceptibility	
Infection (e.g. Chlamydia pneumonia)	

*****Framingham risk factors

1.2 Atherogenesis

Through his extensive investigations and dissections of the heart, Leonardo da Vinci (1452-1519) was the first to describe atherosclerotic vessels. He noted, “the coat thickens so much as to close up and stop the movement of blood” and attributed this as a result of, “absorbing increased nourishment from the blood” (Keele 1951). Da Vinci’s observations were astonishing for the time, and his hypothesis echoes with a surprising similarity to the hypercholesterolaemia (elevated blood cholesterol) theory of recent times.

Supported by abundant data, the link between hypercholesterolaemia and atherosclerosis led it to be described simply as a lipid-storage disease for many years. It was not until the 1970s, when fundamental work by Russell Ross began to uncover the complex nature of atherogenesis, involving cells of the vessel wall and platelets. Further research by others in the 1980s and 90s, established the intrinsic role of the immune system and network of signalling pathways involved. Atherosclerosis is now understood to be a chronic inflammatory disease influenced by many factors, and involving a vast array of inflammatory cells, cytokines, and pathways (Ross 1999; Libby 2002).

1.2.1 Aetiology

The pathogenesis of atherosclerosis is influenced by a multitude of lifestyle choices, along with medical conditions, and the haemodynamics of blood flow itself. It is a chronic disease which develops over a lifetime. Lesions can take many years, even decades to develop, with those affected often remaining symptomless for the majority of their lives, unaware of underlying disease. Evidence shows the process can even begin before birth, with the discovery of fatty streaks and intimal accumulation of low density lipoprotein (LDL) in foetal aortas aged 5-7 months (Napoli *et al.* 1997). This was enhanced with maternal hypercholesterolaemia and is a clear example of how lifestyle can translate into disease. However, despite the many factors and elements to atherogenesis, all begin with an initial insult to the artery wall.

1.2.2 Response to injury hypothesis

The concept of atherogenesis as a response to injury is not a new one. Rudolph Virchow, in 1856, was among the first to suggest, “an inflammation of the inner arterial coat to be the starting point of the so-called atheromatous degeneration” as a result of an initial ‘irritation’ (Virchow 1971). However, 120 years later, Ross and Glomset proposed a modified and more detailed response-to-injury hypothesis, which has since become the cornerstone of atherosclerosis research. This suggested lesions develop as a result of subtle injury to the vasculature caused by a range of factors such as mechanical injury, chemical factors, infection, or the effects of chronic hyperlipidaemia on the vascular endothelial cells (Ross and Glomset 1976).

Their initial hypothesis suggested that injury may alter cells of the vessel wall, possibly leading to their detachment altogether. Platelet adherence and aggregation would ensue, permitting infiltration of platelet-derived factors and lipoproteins at the site of injury, and initiating vascular smooth muscle cell (VSMC) mitogenesis (Ross *et al.* 1977). Investigations in later years favoured endothelial dysfunction over denudation. One such, in a rat model of hypercholesterolaemia, observed leukocytes adhering to the endothelium at sites where atherosclerotic plaques later formed (Joris *et al.* 1983). Crucially, no endothelial denudation was seen, and so concluded it was not necessary in the pathogenesis. Thus, in the early 1990s, the response to injury hypothesis was modified to describe endothelium dysfunction following injury, and include the key role of inflammatory cells such as monocytes, macrophages, and T lymphocytes in lesion formation (Ross 1993). The concept of stem and progenitor cell involvement in atherogenesis has also been considered (Sata *et al.* 2002). This has gained increasing attention, with a recent study suggesting MI can instigate stem cell release from the bone marrow and elicit a secondary inflammatory response by enhancing monocyte recruitment, consequently accelerating atherosclerosis (Dutta *et al.* 2012). Likewise, increasing evidence of platelet interactions with the inflammatory system has generated great interest in their involvement in atherogenesis. As the focus of this thesis, platelet biology, and the specific role of platelets in inflammation and atherogenesis will be discussed later in detail from section 1.4 onwards. However, I will first describe the established cell roles and processes involved in lesion formation and atherothrombosis.

1.2.3 Endothelial activation

The healthy endothelium acts as a protective barrier, separating surrounding tissues from circulating blood, and controlling the passage of cells and molecules across its surface. It has natural anti-thrombogenic properties (Rosenberg and Rosenberg 1984), and crucially resists the attachment of cells to its surface. When dysfunction ensues following injury, the endothelium loses these properties and becomes pro-thrombotic, has increased permeability to circulating cells, and begins to express adhesion molecules on its surface.

The selectins (E, L and P), along with their ligands, are among the first to be expressed, and mediate leukocyte capture and rolling on the endothelial surface (Alon *et al.* 1995). Specifically monocytes, T lymphocytes and neutrophils are captured, as well as platelets. Initial tethering is via either P-selectin (CD62P), found on the endothelium and activated platelets, or L-selectin (CD62L), expressed constitutively on all leukocytes, which binds to CD34 on the endothelium (Baumhueter *et al.* 1994). P-selectin glycoprotein ligand-1 (PSGL-1), present on all leukocytes and activated platelets, and upregulated in activated endothelial cells, enables leukocyte capture and platelet adherence via P-selectin (Norman *et al.* 1995; Frenette *et al.* 2000). PSGL-1 is also a ligand for E-selectin (CD62E), expressed

on the endothelium, and is important in slow rolling, an essential step for firm leukocyte adhesion (Asa *et al.* 1995; Ley *et al.* 1998).

Integrins and cell adhesion molecules (CAM) are expressed on a variety of cell types, and permit cells to bind to each other, as well as to extracellular matrix (ECM). They are responsible for the firm arrest of leukocytes on to the endothelium where integrins, such as very late antigen-4 (VLA-4), bind to their respective CAMs, including vascular cell adhesion molecule-1 (VCAM-1) and intracellular adhesion molecule-1 (ICAM-1), expressed on the activated endothelial surface (Springer 1995). In addition, ICAM-1 has a binding domain for fibrinogen (D'Souza *et al.* 1996), which is converted by thrombin into fibrin as part of the coagulation cascade, thus enhancing the procoagulant properties of the dysfunctional endothelium.

Once adherent to the endothelium, leukocytes migrate to the vessel intima through endothelial cell junctions as the final stage of the leukocyte adhesion cascade (diapedesis). This is facilitated by adhesion molecules such as platelet/endothelial cell adhesion molecule-1 (PECAM-1), expressed on leukocytes, endothelial cells, and platelets (Muller 1995), and ICAM-1 (Shaw *et al.* 2004).

1.2.4 Predisposed sites

The location of VCAM-1 and ICAM-1 expression in the vasculature corresponds to the areas prone to lesion development, as demonstrated in animal models of atherogenesis (Li *et al.* 1993; Nakashima *et al.* 1998). Presence of these adhesion molecules are an early indicator of endothelial dysfunction, preceding fatty streak formation (Nakashima *et al.* 1998), and are rapidly upregulated in response to injury. In a rabbit model of hypercholesterolaemia, focal VCAM-1 expression was evident after only 1 week of feeding on a high-fat diet (Li *et al.* 1993).

Elevated cholesterol is a systemic issue, yet atherosclerosis is a phenomenon that is often only seen at very specific points in the vasculature, typically the branches, bifurcations, and curvatures of vessels. These predisposed sites correspond to areas of disturbed blood flow, characterised by oscillatory flow and recirculation of blood, resulting in low and fluctuating wall shear stress (Ku *et al.* 1985; Asakura and Karino 1990). Where blood flow is steady and unidirectional, laminar shear stress is exerted across the artery wall. Endothelial cells can transduce these haemodynamic forces into cellular responses, and are thought to detect shear stress via receptors such as PECAM-1 (Tzima *et al.* 2005).

In response to laminar shear stress, nitric oxide synthase (NOS) and cyclooxygenase-2 (COX-2) are upregulated (Topper *et al.* 1996). These have a role in regulating vascular tone by producing nitric oxide (NO) and prostaglandin I_2 (PGI_2), which are potent vasodilators.

NO also has an athero-protective role, as it has been shown to significantly inhibit VCAM-1, ICAM-1, and E-selectin expression, as well as suppress leukocyte chemoattractant secretion, such as interleukin-6 (IL-6) and 8 (CXCL8). The effects of shear stress on gene expression are thought to be regulated by flow-responsive transcription factor activity (De Caterina *et al.* 1995; Peng *et al.* 1995; Tsao *et al.* 1996).

Therefore in areas of disturbed blood flow and resulting low shear stress, athero-protective mechanisms of the endothelium are no longer initiated and adhesion molecule expression is upregulated. The endothelium then takes on a pro-inflammatory profile, which promotes leukocyte adhesion to the endothelial surface.

1.2.5 Modified LDL

Uptake and retention of LDL within the vessel wall is a potent stimulus for atherogenesis (Schwenke and Carew 1989). Native LDL is taken into the endothelium, via the LDL receptor (LDL-R) (Brown and Goldstein 1986), and becomes progressively oxidised by free radicals (Morel *et al.* 1984) and lipoxygenases (Harats *et al.* 2000). Oxidised LDL (ox-LDL) is chemotactic for monocytes (Quinn *et al.* 1987), and can induce pro-inflammatory cytokine secretions, such as monocyte chemotactic protein-1 (MCP-1/CCL2) (Cushing *et al.* 1990) and macrophage colony stimulating factor (M-CSF) (Rajavashisth *et al.* 1990). Furthermore, ox-LDL stimulates expression of endothelial adhesion receptors, including VCAM-1 (Khan *et al.* 1995) and P-selectin (Gebuhrer *et al.* 1995), thereby enhancing leukocyte recruitment and adhesion to the endothelium.

1.2.6 Early lesion development

Monocytes and macrophages

Stary *et al*. astutely described the distinct morphological and histological changes observed during atherogenesis, as lesions develop. The very earliest vascular changes seen are subtle, characterised by small clusters of lipid-laden macrophages (foam cells) confined to the intima (Stary *et al.* 1994) (see Figure 1.1). This signifies one of the main consequences of endothelial dysfunction, with expression of adhesion receptors enabling leukocytes, primarily monocytes, to bind to the endothelium. Once adherent, monocytes migrate between endothelial cells in response to chemokines, such as MCP-1 and IL-8, secreted from monocytes and endothelial cells, respectively (Papadopoulou *et al.* 2008). In the intima, macrophage M-CSF augments the differentiation of monocytes into macrophages (Clinton *et al.* 1992), thus enabling the uptake of LDL via scavenger receptors, and leading to foam cell formation.

Leukocyte attachment to the endothelium results in activation of both cells and initiates a cascade of events, such as the expression of adhesion receptors and secretion of a vast array of pro-inflammatory cytokines and enzymes. The intention of this immune response is

to recruit further cytokine-releasing leukocytes to the site of inflammation, and so a positive feedback loop is established. Innate cytokines IL-1 and tumour necrosis factor (TNF)-α, released from monocytes, macrophages, and endothelial cells, are central mediators of these inflammatory mechanisms, and are involved in cell activation, proliferation, production of further cytokines, and upregulation of adhesion receptors (Loppnow *et al.* 2011). Secreted chemokines MCP-1 and IL-8 have been shown to have an additional role in leukocyte recruitment, triggering firm arrest of monocytes to the endothelium (Gerszten *et al.* 1999). Furthermore, mice deficient in TNF-α (Ohta *et al.* 2005), MCP-1 (Boring *et al.* 1998), M-CSF (Smith *et al.* 1995), and IL-1 (Kirii *et al.* 2003; Kamari *et al.* 2007), or its receptor IL-1R1 (Chamberlain *et al.* 2009), all exhibit significantly reduced atherosclerotic lesion formation, demonstrating the important role of these cytokines in the early pathogenesis of atherosclerosis.

T Lymphocytes

MCP-1 has also been shown to be a strong chemoattractant for T lymphocytes (Carr *et al.* 1994; Roth *et al.* 1995), which are present in early lesions (Hansson *et al.* 1989), albeit in smaller numbers than macrophages. Another T cell chemokine RANTES (regulated upon activation, normal T cell expressed and secreted/CCL5) is released from activated T cells to aid further leukocyte recruitment (Schall *et al.* 1990).

Neutrophils

Despite being the most abundant white blood cell, little is known of the involvement of neutrophils in atherosclerosis. Although rarely detected, neutrophils are present in lesions (Rotzius *et al.* 2010), and are recruited via IL-8 and RANTES release. It is postulated that neutrophils may contribute to atherogenesis via their activation and degranulation, causing release of leukocyte chemokines such as cathepsin G (Drechsler *et al.* 2011).

CD40/CD40L

Among this potent cocktail of inflammatory cytokines involved in atherogenesis, is a receptor-ligand pair of particular importance in cell cross-talk. CD40 and its ligand (CD40L/CD154) mediate signalling between virtually all cells within this inflammatory system. Both present on endothelial, smooth muscle, and T cells, macrophages, and platelets, CD40 and CD40L initiate many inflammatory responses, and are expressed in atherosclerotic lesions (Mach *et al.* 1997). Blockade of CD40 signalling inhibits lesion formation (Mach *et al.* 1998; Schonbeck *et al.* 2000), and in existing atherosclerosis, promotes plaque stability (Lutgens *et al.* 2000). Ligation of CD40 evokes VCAM-1 and P-selectin expression in endothelial cells (Kotowicz *et al.* 2000), and IL-1β release (Schonbeck *et al.* 1997).

Figure 1.1 – Summary of the key features of lesion progression, which occur during atherogenesis.

In the healthy vessel, factors such as laminar blood flow and high shear stress promote athero-protective mechanisms in the vessel wall. These include an increase in nitric oxide production, which supresses the expression of adhesion receptors on endothelial cells. Upon an insult to the vessel wall, such as high levels of circulating LDL, the endothelium becomes activated and begins to express a range of selectins, integrins, and cell adhesion molecules. These permit leukocytes, lymphocytes and platelets to adhere to the vessel wall, which in turn causes the release of further cytokines to recruit additional inflammatory cells to the area. Monocytes migrate into the vessel intima where they differentiate into macrophages, and begin to phagocytosis LDL, after which they become foam cells. The continued release of cytokines and growth factors promotes the migration and proliferation of further cells into the intima, including vascular smooth muscle cells from the vessel media. An accumulation of these lipid-laden cells, and the synthesis of collagen and other extracellular matrix components, cause the intima to thicken and protrude into the vessel lumen. Cell apoptosis and necrosis leads to the formation of a lipid-rich necrotic core and the release of matrix metalloproteinases, which degrade the extracellular matrix and de-stabilise the lesion. Plaque erosion, fissure, or rupture ensues, and causes the pro-thrombotic contents of the lesion to be exposed to circulating blood, initiating atherothrombosis. Platelets rapidly activate and aggregate to form a thrombus, which may then block the vessel and lead to an acute coronary syndrome.

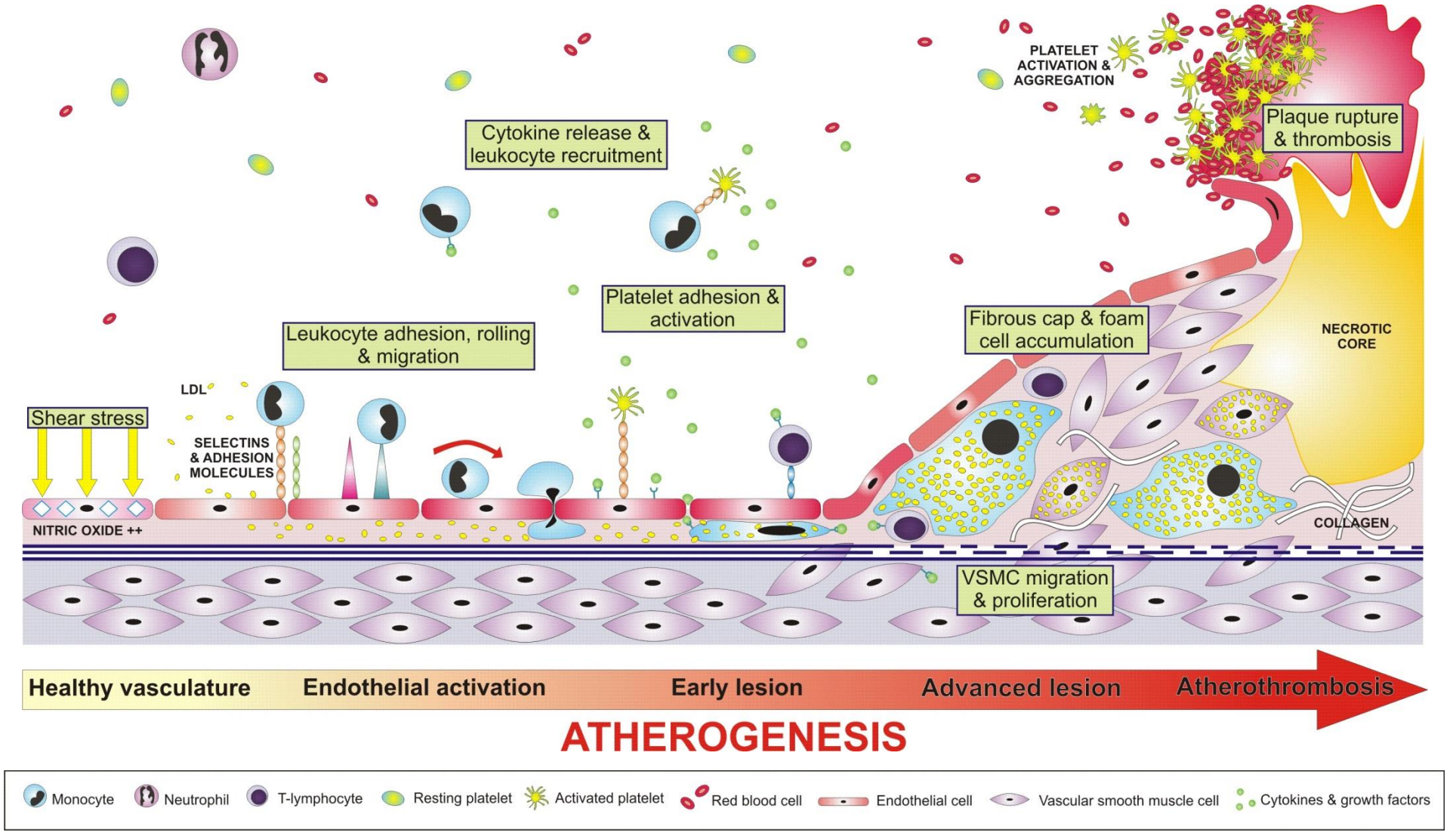
PLATELET ACTIVATION & AGGREGATION
Plaque rupture & thrombosis
Cytokine release & leukocyte recruitment
Platelet adhesion & activation
Leukocyte adhesion, rolling & migration
Fibrous cap & foam cell accumulation
NECROTIC CORE
LDL
Shear stress
SELECTINS & ADHESION MOLECULES
NITRIC OXIDE ++
COLLAGEN
VSMC migration & proliferation
Healthy vasculature
Endothelial activation
Early lesion
Advanced lesion
Atherothrombosis
ATHEROGENESIS
Monocyte
Neutrophil
T-lymphocyte
Resting platelet
Activated platelet
Red blood cell
Endothelial cell
Vascular smooth muscle cell
Cytokines & growth factors

1.2.7 Advanced lesion development

So-called 'early' atherosclerotic lesions do not necessarily occur early in life, like their name may suggest, as these lesions can be found in the vessels of adults and children alike. Atheroma growth itself is by no means a continuous process, with periods of stabilisation followed by bursts of growth. Indeed, lesion progression is not automatic and may halt, requiring further stimulus for growth to proceed. It is thought that progression to so-called 'advanced' lesions requires an added impetus, such as other CVD risk factors (see section 1.1.3), or areas of disturbed blood flow (Stary *et al.* 1994; Libby 2002).

Characteristics of advanced lesions, as defined by Stary *et al.*, include accumulations of cells, lipid, and matrix components, and thickening of the intima causing deformity of the arterial wall (see Figure 1.1). In addition, the build-up of products from apoptosis and necrosis lead to the formation of a necrotic core. These now complex, fibrotic and sometimes calcified lesions, completely obliterate the once normal cell and matrix structure of the original vessel wall (Stary *et al.* 1995). Despite these extensive changes to the vessel, lumen area may not initially be affected due to outward remodelling of the artery, and consequently individuals can remain symptomless (Glagov *et al.* 1987; Clarkson *et al.* 1994). However, these lesions may still be clinically significant since, with or without vessel stenosis, they are prone to fissures and rupture that can lead to thrombosis and acute coronary syndromes.

Vascular smooth muscle cells

VSMCs play a role throughout all stages of atherosclerosis as they too express adhesion receptors (Braun *et al.* 1995) and release an array of cytokines when activated, such as IL-1, TNF-α, M-CSF, and MCP-1, contributing to leukocyte recruitment. Yet their ability to migrate, proliferate, and to synthesise and deposit collagen and extracellular matrix make VSMCs particularly important in transforming atherosclerotic lesions from early to mature plaques (Ross 1999; Raines and Ferri 2005).

Induction of migration and proliferation is driven through release of growth factors, such as platelet-derived growth factor (PDGF) and transforming growth factor (TGF) β, from activated cells in the vessel wall. As the name suggests, PDGF was first identified as a platelet releasate that demonstrated mitogenic effects on cultured VSMCs (Ross *et al.* 1974). However, various isoforms (PDGF A-D) are also released from macrophages (Shimokado *et al.* 1985) and endothelial cells (DiCorleto and Bowen-Pope 1983), as well as smooth muscle cells themselves, acting in an autocrine manner (Nilsson *et al.* 1985). Action of cytokines, such as IL-1 and TNF-α, can also influence VSMC proliferation through induction of PDGF secretion (Hajjar *et al.* 1987; Raines *et al.* 1989). Indeed, the expression of PDGF and its receptors have been found to be increased in atherosclerotic lesions

(Barrett and Benditt 1987; Rubin *et al.* 1988), and *in vivo* models blocking the action of PDGF have clearly shown a reduction in atheroma (Lamb *et al.* 2001; Sano *et al.* 2001).

TGF-β is another growth regulatory molecule, which tightly controls cell proliferation and differentiation in many cell types, including VSMCs (Bobik 2006). Cellular expression levels of TGF-β determine either its inhibitory, or stimulatory effect on VSMC proliferation via PDGF. Low concentrations of TGF-β induce endogenous secretion of PDGF from smooth muscle cells, creating an autocrine loop. In contrast, high levels limit proliferation via down regulation of the PDGF receptor (Battegay *et al.* 1990).

Extracellular matrix deposition

In addition to their effects on proliferation, TGF-β and PDGF are also potent inducers of collagen and proteoglycan production in VSMCs (Amento *et al.* 1991; Schonherr *et al.* 1993). Indeed, TGF-β-mediated matrix deposition is crucial in plaque progression, fibrosis, and stabilisation. Inhibition of TGF-β signalling, via a soluble recombinant TGF-β receptor, dramatically altered plaque composition to a pro-inflammatory phenotype prone to haemorrhage, characterised by large lipid cores and decreased fibrosis (Lutgens *et al.* 2002). Moreover, analysis of TGF-β expression in human carotid lesions noted a 3-fold increase in asymptomatic lesions compared with those of patients presenting with stroke, further supporting the role of TGF-β in plaque stabilisation (Cipollone *et al.* 2004).

VSMC phenotype

Vascular smooth muscle cells demonstrate great plasticity, and have the ability to modulate their phenotype in response to environmental cues. VSMCs are largely described as switching between either quiescent, 'contractile' or proliferative, 'synthetic' states; however, these fall at opposite ends of the spectrum with many intermediate phenotypes in between. Subtle or profound changes in migratory and mitogenic responses, matrix production, expression of cell markers and adhesion receptors, and secretion of cytokines result in a widely heterogeneous population (Owens *et al.* 2004).

Contractile cells of the media migrate to the intima in response to inflammatory stimuli. In doing so, VSMCs switch to a synthetic phenotype and down regulate their characteristic contractile markers, including α-smooth muscle actin (α-SMA), desmin, and smooth muscle myosin heavy chain (SM-MHC). So-called 'synthetic' VSMCs are able to migrate and proliferate, and have increased capacity for ECM deposition and cytokine secretion (Owens *et al.* 2004). Key mediators of phenotypic modulation include PDGF (Chen *et al.* 2006), TGF-β (Hautmann *et al.* 1997), ECM (Thyberg and Hultgardh-Nilsson 1994), shear stress (Reusch *et al.* 1996), and lipids (Pidkovka *et al.* 2007).

As VSMCs proliferate in the lesion, structural reorganisation occurs from ordered concentric layers, to a large jumbled mass of cells abundant in rough endoplasmic reticulum and golgi bodies, a clear indicator of ECM synthesis (Ross and Klebanoff 1971; Thyberg *et al.* 1983). Accumulation of ECM, and fibrous cap formation, alter the mechanical properties of the lesion and arterial wall. VSMCs that are incorporated in the cap, revert back to a contractile phenotype and contribute to the stabilisation of the plaque (Babaev *et al.* 1990; van der Loop *et al.* 1997).

The concept that lesional VSMCs originate from the vessel media is an issue which is hotly debated. Whilst several studies have identified the recruitment of bone marrow-derived progenitor cells as an additional, alternative source (Sata *et al.* 2002; Tanaka *et al.* 2003; Yu *et al.* 2011), others dispute the involvement (Hu *et al.* 2002; Bentzon *et al.* 2006) and lineage of these cells (Iwata *et al.* 2010), and so the matter continues to be contested.

1.3 Atherothrombosis

Classically, acute coronary events were thought to be caused by the rupture of thin capped atheromas with a large lipid-rich core. Although this is true, clinicians now understand many different types of lesions can led to coronary events and be vulnerable not only to rupture, but erosion and fissure also. A wide spectrum of lesions, including those with evidence of previous thrombus or intra-plaque haemorrhage, and those with fibrotic, calcified, and critically stenotic plaques, are all at risk of atherothrombosis (Naghavi *et al.* 2003; Schaar *et al.* 2004).

1.3.1 The vulnerable lesion

Plaque disruption is facilitated by a loss of structural integrity within the plaque due to degradation of extracellular matrix proteins by matrix metalloproteinases (MMP), a process that is then further fuelled by apoptosis and necrosis.

The accumulation of macrophages and their eventual death occurs throughout lesion progression. In early disease, macrophage apoptosis is thought to be beneficial and limits lesion growth (Liu *et al.* 2005); however, in advanced disease, the phagocytosis of these apoptotic cells becomes impaired (Schrijvers *et al.* 2005), leading to necrosis and the formation of a necrotic core (Ball *et al.* 1995; Tabas 2005). This impaired clearance of apoptotic macrophages further promotes inflammation via the release of cytokines, including TNF-α (Grainger *et al.* 2004), which has itself been shown to stimulate macrophage-induced VSMC apoptosis (Boyle *et al.* 2003) and induce MMP expression (Galis *et al.* 1994).

Matrix metalloproteinases are a group of proteases consisting of collagenases, gelatinases, and stromelysins, amongst other subclasses, which catalyse the breakdown of ECM. MMPs are elaborated from macrophages, endothelial, and vascular smooth muscle cells in

response to cytokines, such as IL-1 and TNF-α (Galis *et al.* 1994; Saren *et al.* 1996), and T lymphocyte-mediated CD40 ligation (Mach *et al.* 1997; Mach *et al.* 1999; Schonbeck *et al.* 1999; Horton *et al.* 2001). Collagenases (MMP-1, 8 and 13) are responsible for collagen fibre degradation, and have been found to be expressed at rupture-prone sites in atherosclerotic plaques (Galis *et al.* 1994; Sukhova *et al.* 1999; Herman *et al.* 2001), along with stromelysins (MMP-3 and 11), and gelatinases (MMP-2 and 9) (Henney *et al.* 1991; Galis *et al.* 1994; Schonbeck *et al.* 1999), which degrade other ECM proteins. The action of these MMPs, coupled with a reduction in matrix-producing VSMC due to apoptosis, lead to a dramatic loss of ECM within the lesion. Fuelled by macrophage apoptosis and necrosis, it is therefore not surprising that these processes are all associated with unstable lesions and sites of plaque rupture (Galis *et al.* 1994; van der Wal *et al.* 1994; Bauriedel *et al.* 1999).

1.3.2 The pro-thrombotic lesion

Just as in early atherogenesis where they were among the driving forces of inflammation, macrophages and VSMCs are equally influential in advanced disease by increasing the thrombogenicity of the lesion. Wilcox *et al.* were the first to identify the presence of tissue factor (TF), a potent catalyst of the coagulation cascade, within the media of healthy vessels, but noticed that atherosclerotic lesions had much higher levels, which was localised to macrophages, the necrotic core, and ECM (Wilcox *et al.* 1989). Others later discovered that macrophage apoptosis and TF content both correlated with the thrombogenicity of the lesion (Kaikita *et al.* 1997; Toschi *et al.* 1997; Hutter *et al.* 2004).

As mentioned previously, CD40 and its ligand are expressed on many cells within the lesion (Mach *et al.* 1997). In addition to potentiating atheroma, CD40 ligation has also been shown to induce TF expression on the surface of macrophages (Mach *et al.* 1997) and VSMCs (Schonbeck *et al.* 2000), rendering the lesion pro-thrombotic. Furthermore, microparticles shed from apoptotic cells within the lesion have been found to not only contain TF, but also bear the phospholipid phosphatidylserine (PS) on their surface, which also promotes thrombosis (Mallat *et al.* 1999).

1.3.3 Thrombosis

Plaque disruption is understood to be brought about by either the physical forces of blood flow acting on weaker areas of the lesion, or as a result of internal destabilisation of the lesion, although perhaps the more likely scenario is a combination of both (Fuster *et al.* 2005). Upon rupture, the TF-rich contents of the plaque are released into the blood, initiating the extrinsic pathway of the coagulation cascade and contributing to thrombosis. Platelets (Schwertz *et al.* 2006; Panes *et al.* 2007), leukocytes (Giesen *et al.* 1999), and their microparticles (Rauch *et al.* 2000) are known to be additional sources of TF.

Exposure of collagen in the damaged vessel wall, as well as activated platelets, initiate the intrinsic coagulation pathway, which later converges with the extrinsic pathway in the final common steps which lead to thrombin and fibrin generation. Platelets rapidly activate in response to thrombin, a potent platelet agonist, or upon adhering to vessel collagen, and quickly form platelet aggregates. These become incorporated within the developing fibrin matrix, along with trapped leukocytes and red blood cells (RBC), to form a large platelet and fibrin-rich thrombus capable of occluding vessels. In addition, activated platelets further promote thrombosis by enabling thrombin generation on their outer membrane, following the exposure of PS on their surface (Dahlback 2000).

In the following section, platelet biology, activation and aggregation, and the role of the $P2Y_{12}$ receptor in these processes will be discussed in greater detail.

1.4 Platelets

In 1865, German anatomist Max Schultze (1825-74) was the first to describe the presence of colourless 'sphericules', approximately 2 µm in diameter, in the blood (Schultze 1865). However, ground-breaking work by Giulio Bizzozero (1846-1901) discovered platelets were important in thrombosis and coagulation, and able to rapidly adhere to the vessel, forming a thrombus. Bizzozero considered platelets as the third constituent of the blood, morphologically distinct from red, and white blood cells, as granulated anucleate cells or 'corpuscles' (Bizzozero 1882; Brewer 2006).

As Bizzozero correctly postulated, the primary physiological role of platelets is detecting vascular damage, via exposure of vessel substratum, and rapidly aggregating. Platelet activation leads to thrombin generation, which activates the coagulation cascade and ultimately results in the development of a fibrin-rich haemostatic plug, halting any blood loss. Nevertheless, in addition to haemostasis, there is a growing appreciation of the important role of platelets in the innate and adaptive immune response (Semple *et al.* 2011).

1.4.1 Production

Platelets are derived from megakaryocytes in the bone marrow, and enter the bloodstream following a complex process of mass assembly and release. A single megakaryocyte is capable of producing thousands of platelets, and does so by amplifying its DNA many times over. The cells enlarge, and the cytoplasm fills with ribosomes, organelles, granules, and a vast membranous and tubular network (Patel *et al.* 2005).

Now packed with platelet components, the megakaryocytes develop pseudopodia, which elongate into long pro-platelet strings. Platelet granules, organelles, and membrane network are packaged into the pro-platelet ends, where platelets are assembled (Italiano *et al.* 1999). Pro-platelet formation is amplified by continual elongation and branching, driven by sliding of

the microtubules (Patel *et al.* 2005), until the entire megakaryocyte cytoplasm is converted into pro-platelets. These are released, leaving an extruded nucleus behind. Individual platelets are then liberated from the pro-platelet ends, and have a lifespan of 8 to 10 days (Patel *et al.* 2005). With a normal platelet count between 150 and 400 x 10^9 platelets per litre of blood, an average adult has approximately one trillion platelets circulating at any one time.

1.4.2 Structure

In their resting state, platelets circulate as small, oval, lentiform discs. This shape is maintained by a specialised cytoskeleton which, upon platelet activation, can reorganise, altering the platelet structure into spiny spheres. Inside the platelet, α granules, dense granules, and lysosomes act as storage compartments for a plethora of molecules, including inflammatory mediators, adhesive proteins, coagulation factors, and platelet agonists. An immense intracellular membrane network, called the open canalicular system, permeates the cytoplasm and connects to the surface of the platelet, functioning as an exit route for granule contents. In addition, the self-contained dense tubular system acts as an intracellular store for calcium, the release of which is important in many phases of platelet activation. Surface receptors mediate platelet activation in response to a range of stimuli, including adhesion to matrix proteins, or exposure to soluble agonists, such as thrombin, adenosine diphosphate (ADP), and thromboxane A_2 (TxA_2) (see Figure 1.2) (White 2006).

1.4.3 Adhesion

Following plaque rupture, or other instances of vessel damage, ECM components, including collagen, von Willebrand factor (vWF), and fibronectin are exposed to blood flow. Integrins and receptors mediate initial platelet tethering to these components, followed by platelet activation via receptor-mediated signalling. Downstream events from these pathways include calcium release from intracellular stores, platelet shape change, granule secretion, and ultimately activation of platelet integrins, GPIaIIa ($\alpha_2\beta_1$) and GPIIbIIIa ($\alpha_{IIb}\beta_3$), enabling firm adhesion and aggregation (Nieswandt *et al.* 2011).

Due to their small size, platelets naturally accumulate and flow adjacent to the vessel walls by a process called margination. This positioning is beneficial to their role in haemostasis; however, flowing at high shear, platelets need to be slowed prior to firm adhesion and activation. Initial platelet attachment to the sub-endothelium occurs via collagen-bound vWF, and platelet receptor GPIb, part of the receptor complex GPIb-IX-V (also referred to as GPIb-IX). High shear flow rates stretch the platelet membrane around GPIb, bound to vWF, to form elongated tethers, which may break, but ultimately slow the platelet to allow activation and firm adherence (Dopheide *et al.* 2002).

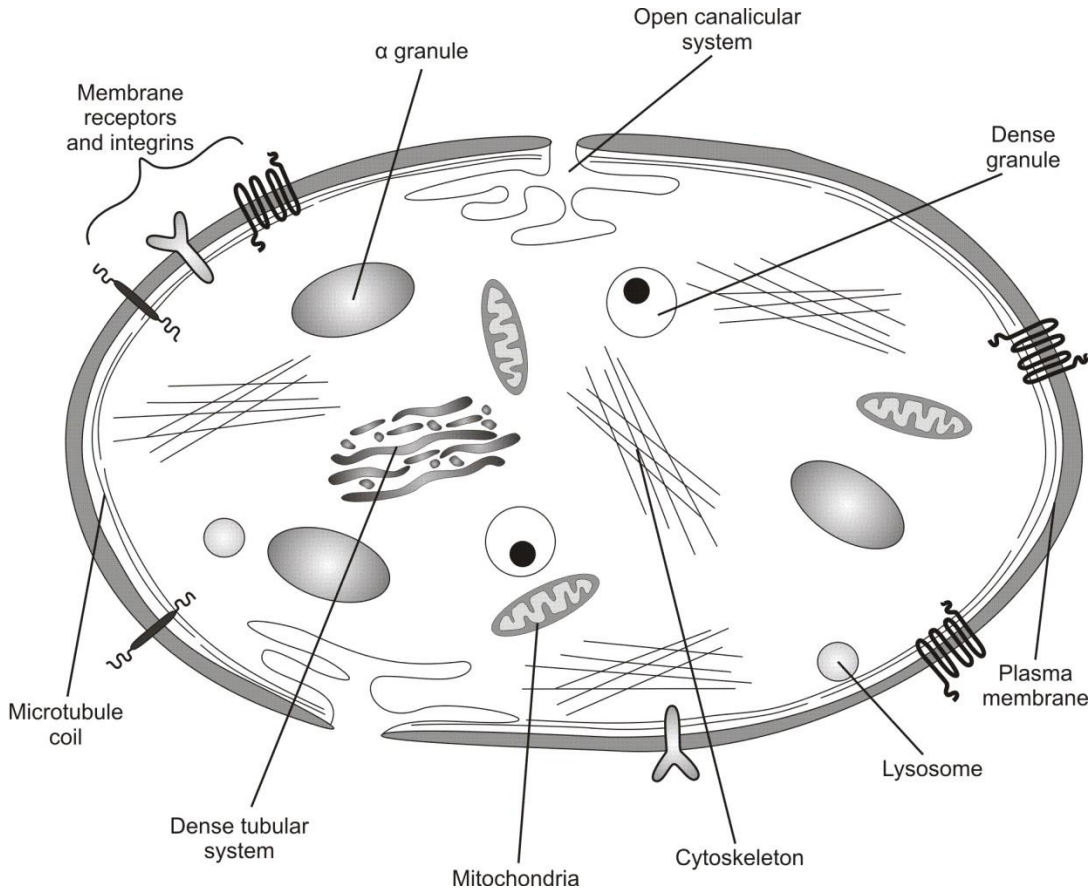

Figure 1.2 – Ultrastructure of a resting platelet.

The lentiform shape of a resting platelet is maintained by the specialised cytoskeleton and microtubule coil. Lysosomes, dense, and α granules act as storage compartments, releasing their contents upon platelet activation. The open canalicular system permeates the cytoplasm, and is connected to the plasma membrane, which provides an exit route for granule contents during release. Intracellular calcium is stored in the dense tubular network, and is rapidly mobilised upon platelet activation. Membrane receptors initiate these activation responses, following platelet adhesion or exposure to soluble agonists.

Tethered platelets are then able to interact with collagen, the most reactive ECM component, via the Ig receptor GPVI. Ligation of this receptor elicits an intracellular signalling response, leading to firm arrest of the platelet through activation of integrins GPIaIIa, which binds to collagen, and GPIIbIIIa, enabling both vWF and fibrinogen binding (Nieswandt and Watson 2003). In the absence of GPVI signalling, mouse platelets were unable to adhere to collagen in either static or flow conditions, despite normal expression of GPIb-IX and the platelet integrins; therefore, demonstrating the essential role of GPVI in platelet activation and adhesion (Nieswandt *et al.* 2001).

1.4.4 Activation and receptor signalling

Platelets are able to respond to a range of agonists due to the wide variety of receptors present on their membranes (see Figure 1.3). Activation can occur via adhesion to ECM, as described above, or by exposure to soluble agonists, signalling via G protein-coupled receptors (GPCR). The activation response can be viewed as a 2-step process, with initial receptor signalling followed by secondary amplification from the release of endogenous agonists stored within the dense granules (Li *et al.* 2010).

A network of signalling pathways lie between the initial activating stimulus of receptor ligation, and their end-point responses of shape change, granule secretion, and platelet aggregation. These pathways are complex, involve multiple feedback loops, and are interlinking, with phospholipase C (PLC), calcium (Ca^{2+}) mobilisation, and Src family kinase forming common intermediary steps for signal transduction through many receptors. In addition, several GPCRs are coupled to the same G protein, for example thrombin, TxA_2, serotonin (5HT), and ADP all signal via Gq (see Figure 1.4).

1.4.5 Shape change

The earliest physiological response to activation is platelet shape change, brought about by rearrangement of the actin cytoskeleton. Regulatory proteins control the dynamics of the cytoskeleton, and mediate the disassembly of actin filaments upon platelet activation. Platelets take on a spherical form, and the reassembly of new actin filaments result in finger-like protrusions extending from the plasma membrane. If adhered to a surface, the platelets then flatten and spread (Hartwig 2006).

Initiation of this cascade of events is mediated by Ca^{2+} mobilisation (Rosenberg *et al.* 1981), and phosphorylation of myosin II, a cytoskeleton regulatory protein, by myosin light chain kinase (MLCK) (Daniel *et al.* 1994). Virtually all platelet receptors result in Ca^{2+} mobilisation from the dense tubules due to the activation of PLCβ or γ in their signalling pathways. However, investigations by Paul *et al.* demonstrated that shape change can also occur in the absence of calcium, via activation of RhoA and its kinase, which can stimulate MLCK and myosin II phosphorylation independently of calcium (Paul *et al.* 1999).

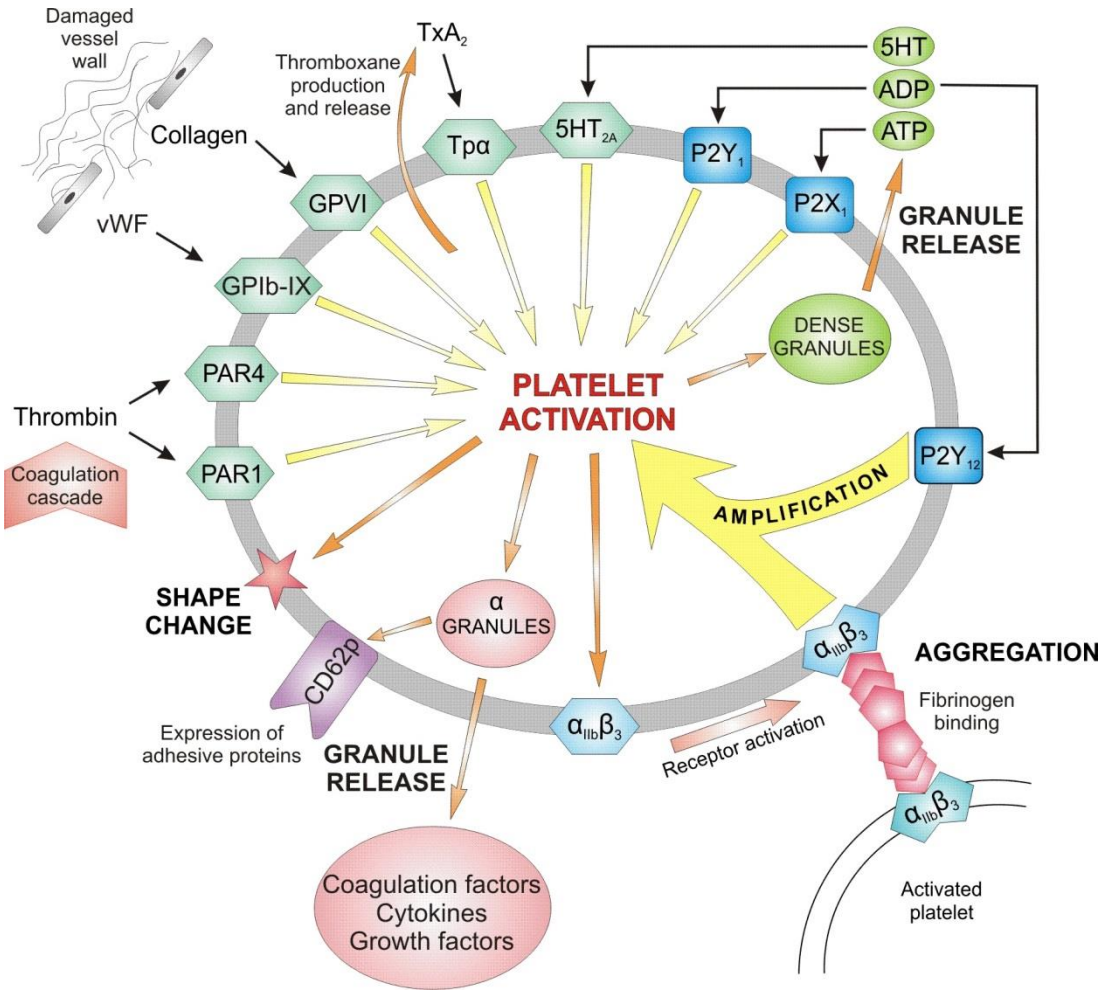

Figure 1.3 – Overview of platelet receptors and activation responses.

Platelets possess many surface receptors for a variety of ligands capable of inducing platelet activation. GPIb-IX and VI initiate activation responses via adhesion to the vessel wall to either collagen, or von Willebrand factor (vWF). Soluble mediators, such as thrombin, serotonin (5HT), and thromboxane (TxA_2), act via their respective receptors shown. Platelet activation results in shape change, granule release, and aggregation. Dense and α granules release their contents, including platelet agonists and inflammatory mediators. Adenosine diphosphate (ADP) released from the dense granules acts on the purinergic receptors $P2Y_1$ and $_{12}$, shown in bright blue. $P2Y_{12}$ is of particular importance, as this plays a key role in amplifying the activation response. This includes the transformation of integrin GPIIbIIIa ($\alpha_{IIb}\beta_3$) from a low to high affinity state, enabling it to bind fibrinogen, and form platelet aggregates. Adapted from Storey (2006).

Figure 1.4 – Summary of platelet receptor signalling pathways.

Platelets become activated upon adhesion to extracellular membrane proteins, via receptors GPIb-IX and GPVI, or by exposure to soluble agonists, signalling via G protein-coupled receptors. A network of signalling pathways lie between the initial activating stimulus of receptor ligation, and their end-point responses of shape change, granule secretion, and platelet aggregation. These complex pathways involve multiple feedback loops, and have a degree of cross-over, with phospholipase C (PLC), calcium (Ca^{2+}) mobilisation, and Src kinases forming common intermediary steps for signal transduction through many receptors. In addition, several G protein-coupled receptors are coupled to the same protein, for example thromboxane (TxA_2), thrombin, serotonin (5HT), and adenosine diphosphate (ADP) all signal via Gq. The important role of $P2Y_{12}$ signalling in platelet activation is highlighted by the blue arrows. $P2Y_{12}$ is coupled to Gi and inhibits adenylyl cyclase (AC) activity. $P2Y_{12}$ works in a synergistic manner with $P2Y_1$ to bring about ADP-induced platelet aggregation, through phosphoinositide 3-kinase (PI3K) activity and integrin $\alpha_{IIb}\beta_3$ (GPIIbIIIa) activation, leading to irreversible platelet aggregation. Importantly, $P2Y_{12}$ also amplifies and sustains platelet activation in response to other platelet agonists, including thrombin, TxA_2 and collagen, demonstrating its crucial role in platelet reactivity.

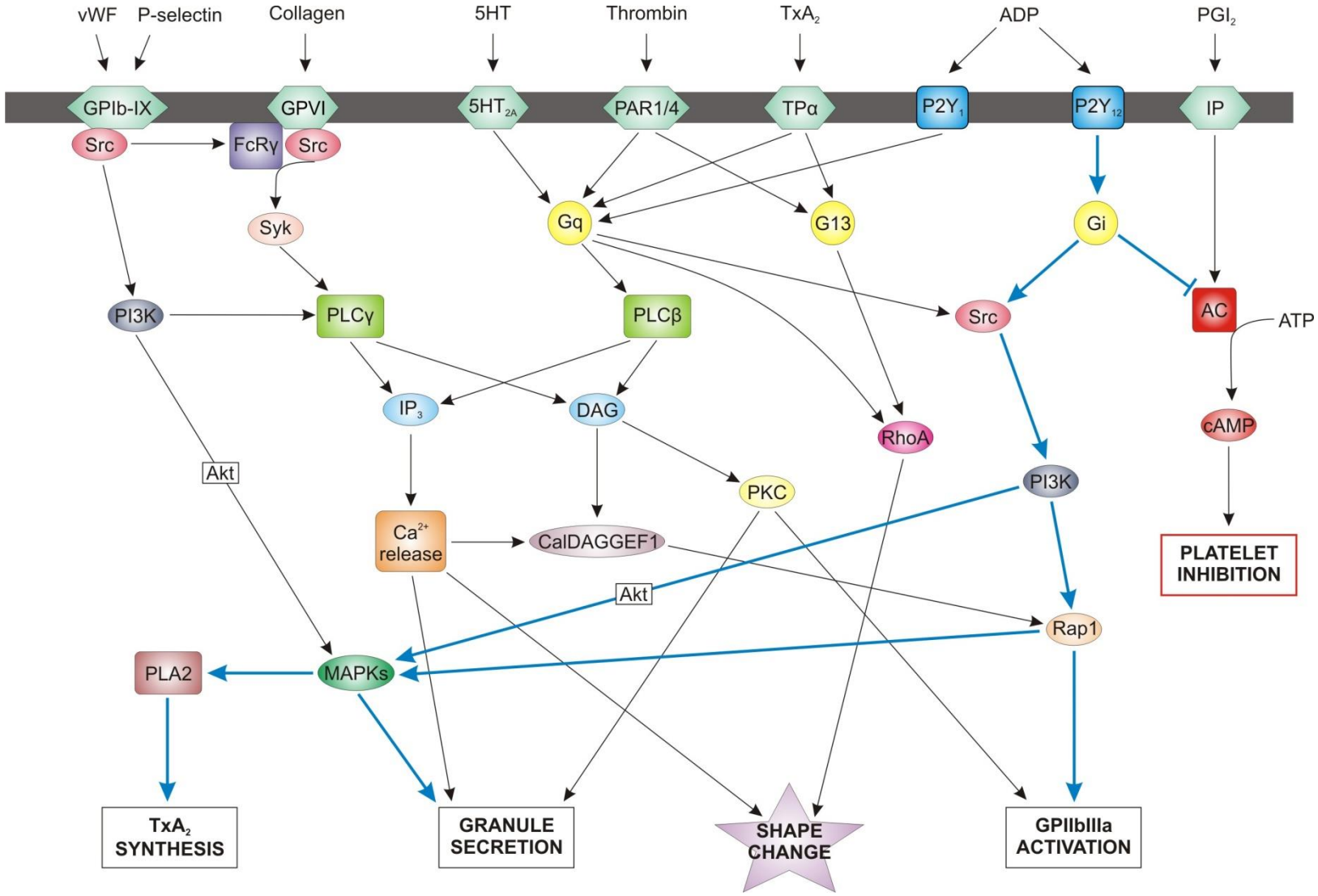
vWF
P-selectin
Collagen
5HT
Thrombin
TxA2
ADP
PGI2
GPIb-IX
GPVI
5HT2A
PAR1/4
TPα
P2Y1
P2Y12
IP
Src
FcRγ
Src
Syk
Gq
G13
Gi
PI3K
PLCγ
PLCβ
Src
AC
ATP
IP3
DAG
RhoA
cAMP
Akt
PKC
PI3K
Ca2+ release
CalDAGGEF1
PLATELET INHIBITION
Akt
Rap1
PLA2
MAPKs
TxA2 SYNTHESIS
GRANULE SECRETION
SHAPE CHANGE
GPIIbIIIa ACTIVATION

1.4.6 Secretion

An activation response common to all signalling pathways is platelet secretion, including the release of granule contents, incorporation of granule membranes with the plasma membrane, and the generation and secretion of TxA_2. Platelets contain a variety of storage vesicles, which are pre-packaged with a vast array of proteins, receptors, and molecules capable of inducing pro-thrombotic, atherogenic, and bactericidal effects upon exocytosis (see Table 1.2). The dense and α granules are the most abundant of these vesicles, and play an important role in the amplification of platelet activation, coagulation, and the inflammatory response. In particular, the release of platelet agonists ADP and 5HT from the dense granules, leads to activation of their respective receptors, amplifying the activation response (Rendu and Brohard-Bohn 2001). Lysosomes also secrete their contents upon platelet activation (Ciferri *et al.* 2000), but will not be discussed further in this thesis.

Granule release is initiated by many signalling events (see Figure 1.4), including calcium release, the mitogen-activated protein kinase (MAPK) pathway, phosphoinositide 3-kinase (PI3K), and protein kinase C (PKC). These events regulate the activity of soluble N-ethylmaleimide-sensitive factor activating protein receptor (SNARE) and GTPase proteins, which augment the docking and fusion of granules with the open canalicular system and plasma membranes. Granule contents such as ADP, cytokines, and coagulation factors are released into the extracellular compartment, whilst granule membrane components, including P-selectin (CD62p) and CD40L, are then expressed on the platelet surface (Rendu and Brohard-Bohn 2001; Blair and Flaumenhaft 2009; Li *et al.* 2010).

Other activation events include the generation and secretion of TxA_2 via the activity of phospholipase A2 (PLA2), which liberates arachadonic acid from the plasma membrane, and is converted to TxA_2 by cyclooxygenase-1 (COX-1) and thromboxane synthase. Released TxA_2 is able to activate platelets via the thromboxane receptor (TPα), and provides another route for amplification of the activation response. Blockade of TxA_2 production is the mechanism by which the COX-1 inhibitor, aspirin, irreversibly inhibits platelet activation (Paul *et al.* 1999).

1.4.7 Aggregation

Receptor-mediated integrin activation is important, not only for firm adhesion to the vessel wall, but also for platelet aggregation, and subsequent thrombus formation. Of all platelet integrins, GPIIbIIIa ($\alpha_{IIb}\beta_3$) is the most abundant, and is able to bind fibrinogen, vWF, and several other matrix proteins, allowing interactions with the vessel wall and, crucially, between platelets. GPIIbIIIa is found in a low affinity state on the surface of resting platelets, unable to bind to any of its ligands. Following platelet activation, intracellular 'inside-out' signalling induces a conformational change in the integrin, transforming it from a low to high affinity, 'activated' state. This is mediated by the binding of talin and kindlin cytoskeletal

Table 1.2 - Platelet granule contents and membrane components.

A summary of the main α, dense, and lysosomal granule contents and membrane components, with a particular focus on those elements highlighted in this thesis and relating to atherogenesis (McNicol and Israels 1999; Rendu and Brohard-Bohn 2001; Nurden).

	Contents	Membrane components
α granules	*Adhesive proteins:* vWF, fibrinogen, fibronectin, laminin, vitronectin	*Glycoproteins:* Ib-IX, VI, IIbIIIa
		CD40L
	Coagulation factors: V, XI	CD63
	Cytokines and growth factors: IL-1, IL-8, MCP-1, RANTES, TGF-β, PDGF, PF4	P-selectin (CD62p), PSGL-1
		PECAM-1
	Fibrinolytic factors: Plasminogen, PAI-1	
	Proteases: MMP-1, 2, 4, 9, ADAMTS13	
	Anti-microbial proteins	
	Immunoglobulins	
Dense granules	ADP, ATP, 5HT, calcium	*Glycoproteins:* Ib, IIbIIIa
		P-selectin
Lysosomes	Acid proteases, glycohydrolases	CD63, LAMP1,2

*All abbreviations are in the full text except: a disintegrin and metalloproteinase with a thrombospondin type 1 motif (ADAMTS)13; adenosine triphosphate (ATP); lysosomal-associated membrane protein (LAMP); plasminogen activator inhibitor-1 (PAI-1) and platelet factor 4 (PF4).

proteins to the cytoplasmic domain of the β_3 subunit. Integrin ligation, via fibrinogen or vWF, augments platelet-platelet interactions through GPIIbIIIa, forming platelet aggregates and initiating further signalling events. This so-called 'outside-in' signalling results in granule secretion, platelet spreading, and clot retraction (Shattil and Newman 2004; Li *et al.* 2010).

1.5 Platelet purinergic receptors

The $P2Y_{12}$ receptor belongs to a larger family of membrane-bound molecules, the purinergic (P2) receptors, which are important in mediating extracellular signalling. P2 receptors are expressed on a variety of cells throughout the body, and are activated by nucleotides, such as ADP and adenosine triphosphate (ATP). They are divided into two groups, ATP-gated ion channels (P2X) and G-protein-coupled receptors (P2Y), of which there are several subtypes. Platelets possess three P2 receptors; $P2X_1$, $P2Y_1$, and $P2Y_{12}$ (Erlinge and Burnstock 2007).

1.5.1 $P2X_1$

ATP released from damaged cells or platelet dense granules, causes a rapid influx of extracellular Ca^{2+} via $P2X_1$ (MacKenzie *et al.* 1996), and this is considered to prime activation of the P2Y receptors by working in a synergistic manner to enhance intracellular Ca^{2+} signalling, and its effects (Vial *et al.* 2002). $P2X_1$ has also been shown to amplify collagen-induced granule secretion, aggregation (Oury *et al.* 2002), and contribute to thrombus formation (Hechler *et al.* 2003).

1.5.2 $P2Y_1$

As part of a duo of ADP receptors found on platelets, $P2Y_1$ mediates a rapid ADP-induced platelet activation response, which is then amplified and sustained by its counterpart, $P2Y_{12}$ (Storey *et al.* 2000). $P2Y_1$ is coupled to Gq and, when activated, causes a rapid rise in intracellular Ca^{2+} through PLCβ, resulting in platelet shape change (see Figure 1.4) (Offermanns *et al.* 1997; Jin *et al.* 1998). Furthermore, $P2Y_1$ is essential for initiating ADP-induced platelet aggregation, and it also potentiates aggregation to other agonists such as collagen (Fabre *et al.* 1999; Leon *et al.* 1999); however, $P2Y_1$ stimulation alone results in only a small, reversible aggregation response that requires $P2Y_{12}$ activation for completion (Hechler *et al.* 1998; Jin and Kunapuli 1998).

1.5.3 $P2Y_{12}$

The identity of the second platelet ADP receptor was elusive for some time, but much was discovered about its activity prior to its eventual cloning (Foster *et al.* 2001; Hollopeter *et al.* 2001). It was known to be coupled to Gi (Ohlmann *et al.* 1995), and Daniel *et al.* demonstrated that this mystery receptor, referred to previously as P_{2T}, $P2T_{AC}$, $P2Y_{ADP}$, or $P2Y_{cyc}$, inhibited adenylyl cyclase (AC) activity, but did not induce shape change as did $P2Y_1$ and therefore must be a distinct receptor (Daniel *et al.* 1998). $P2Y_{12}$, as it's now known, is

required, along with $P2Y_1$, to achieve complete ADP-induced aggregation (Jin and Kunapuli 1998). However, the importance of $P2Y_{12}$ lies in its ability to amplify and sustain platelet activation responses to not only ADP, but also other platelet agonists, including TxA_2, thrombin, and collagen, since activation of platelets by these agonists inevitably lead to release of ADP from dense granules (Storey *et al.* 2000). This capacity to enhance platelet reactivity, regardless of the initiating stimulus, is why $P2Y_{12}$ inhibition has been established as, and continues to be, a vital treatment for preventing thrombotic events following ACS or percutaneous coronary intervention (PCI).

1.5.4 $P2Y_{12}$ in platelet activation

Although a relatively weak agonist compared to thrombin and collagen, which are markedly more potent, ADP acts a vital co-factor in the platelet activation response. ADP is released from the dense granules, following platelet activation in response to various agonists, including thrombin, and stimulates the P2Y receptors on the source, and neighbouring platelet(s). As a result, this nucleotide, when bound to the $P2Y_{12}$ receptor, initiates the Gi signalling pathway, and brings about irreversible GPIIbIIIa activation and complete aggregation in response to any platelet agonist (Dorsam and Kunapuli 2004; Storey 2006). Accordingly, synergistic activation of the Gq (Quinton *et al.* 2002), G13 (Nieswandt *et al.* 2002), GPVI (Ohlmann *et al.* 2000), or GPIb-IX (Turner *et al.* 2001) pathways, in addition to Gi stimulation, is required for these effects. Thus, in the absence of $P2Y_{12}$ activation, platelet aggregation is readily reversible, with GPIIbIIIa reverting to its inactive form (Jin and Kunapuli 1998; Quinton *et al.* 2002).

$P2Y_{12}$ potentiates these activation responses by sustaining elevated Ca^{2+} levels within the platelet, which would otherwise diminish (Storey *et al.* 2000). This is thought to be mediated by inhibition of AC activity and stimulation of PI3K (Hardy *et al.* 2004). Induced via endothelial PGI_2, adenylyl cyclase regulates platelet activity *in vivo* by the production of cyclic adenosine monophosphate (cAMP), which inhibits intracellular Ca^{2+} release (Smolenski 2012). Consequently, $P2Y_{12}$ inhibition of AC removes the inhibitory effects of cAMP on Ca^{2+} mobilisation; however, Hardy *et al*. demonstrated this was only partially responsible for the calcium levels. $P2Y_{12}$-mediated activation of PI3K was also shown to contribute the sustained Ca^{2+} levels (Hardy *et al.* 2004) via activation of PLC (van der Meijden *et al.* 2008).

PI3K activity is also responsible for $P2Y_{12}$-induced TxA_2 and granule secretion (Dangelmaier *et al.* 2001; Garcia *et al.* 2010), as well as irreversible aggregation (Trumel *et al.* 1999; Kauffenstein *et al.* 2001). Other agonists, such as thrombin, are known to induce PI3K activity. Yet, thrombin stimulation alone results in reversible aggregation, not stable aggregates as seen following $P2Y_{12}$ activation. These $P2Y_{12}$ specific effects, it appears, are mediated by the generation of a particular PI3K product, phosphatidylinositol 4,5-

bisphosphate (PIP_2), which is linked to irreversible aggregation (Trumel *et al.* 1999). Furthermore, $P2Y_{12}$-induced PI3K is also involved in platelet spreading on immobilised fibrinogen (O'Brien *et al.* 2012). In addition, $P2Y_{12}$ activation is associated with GTPase Rap1 activity, a key mediator of GPIIbIIIa integrin activation (see Figure 1.4), although it can be activated independently of $P2Y_{12}$ also (Larson *et al.* 2003).

In summary, the $P2Y_{12}$ receptor is extremely influential in platelet activation, by potentiating platelet secretion and aggregation (Storey 2006). Furthermore, $P2Y_{12}$ activation also promotes procoagulant responses by enhancing surface membrane PS expression (Leon *et al.* 2003), and contributing to platelet microparticle formation (Storey *et al.* 2000; Kahner *et al.* 2008), which are another source of PS and TF (Owens and Mackman 2011). As a result, $P2Y_{12}$ activity plays an important role in thrombosis.

1.5.5 $P2Y_{12}$ in thrombosis

The effects of $P2Y_{12}$ antagonists, such as clopidogrel, on reducing thrombotic events in ACS patients had been known for some time (CAPRIE 1996). Similarly animal models had shown $P2Y_{12}$ antagonist treatment prolonged bleeding time and reduced thrombus formation (Samama *et al.* 1992; Herbert *et al.* 1998; Huang *et al.* 2000), but how these drugs provided a therapeutic benefit was less apparent. However, cloning of the $P2Y_{12}$ receptor (Hollopeter *et al.* 2001) enabled the development of $P2Y_{12}^{-/-}$ mice (Foster *et al.* 2001), and permitted the study of its role in thrombosis *in vivo*.

Foster *et al*. were the first to generate $P2Y_{12}^{-/-}$ mice and demonstrated that their platelets displayed $P2Y_{12}$-deficient characteristics as expected, such as reduced aggregation in response to ADP, collagen, and thrombin. In addition, they showed this translated into substantially prolonged bleeding times following tail tip transection (Foster *et al.* 2001). Further studies on $P2Y_{12}^{-/-}$ mice revealed, using arterial injury models, that $P2Y_{12}$ controls both thrombus growth and stability (Andre *et al.* 2003).

1.5.6 Other cells expressing $P2Y_{12}$

The $P2Y_{12}$ receptor was first identified on platelets; however, its expression has since been discovered in other cell types, although often little is known of its role in these tissues, and its function remains to be fully elucidated in some cases (see Table 1.3). The most notable and well-documented roles for $P2Y_{12}$, outside of the platelet, are in VSMCs and microglia.

Wihlborg *et al*. revealed that $P2Y_{12}$ receptors on VSMCs mediated cell contraction in response to ADP. In addition, he discovered that the $P2Y_{12}$ antagonist cangrelor, but not clopidogrel, was able to block ADP-induced contraction in denuded vessels (Wihlborg *et al.* 2004). A more recent study showed ticagrelor is also capable of inhibiting this response,

Table 1.3 - $P2Y_{12}$ receptor expression.

An overview of the tissues and cell types in which the $P2Y_{12}$ receptor has been identified, including its function in these cells, if known.

Tissue	Cell	Function	
Blood	**Platelets**	Amplification of platelet activation	(Storey *et al.* 2000)
	Dendritic cells	Enhance T-cell activation	(Ben Addi *et al.* 2010)
Vessel wall	**Vascular smooth muscle cells**	Cell contraction and promote pro-inflammatory and mitogenic responses	(Wihlborg *et al.* 2004; Rauch *et al.* 2010)
	Endothelial cells	Unknown	(Shanker *et al.* 2006)
Brain	**Microglia**	Chemotaxis in response to injury	(Sasaki *et al.* 2003; Haynes *et al.* 2006)
Liver	**Cholangiocytes**	Postulated to act as chemosensors detecting biliary nucleotides	(Masyuk *et al.* 2008)
Pancreas	**Islet cells**	Postulated to stimulate insulin secretion	(Lugo-Garcia *et al.* 2008)
Spleen	**Splenic sinus endothelial cells**	Unknown	(Uehara and Uehara 2011)

but prasugrel, another thienopyridine-class drug similar to clopidogrel, had no effect (Grzesk *et al.* 2012). Furthermore, *in vitro* studies in cultured VSMCs revealed that $P2Y_{12}$ receptors are linked to mitogenic and pro-inflammatory responses in VSMCs, through a thrombin-induced pathway (Rauch *et al.* 2010).

Microglia are the macrophages of the brain, and their role is to detect injury, infection, remove apoptotic cells, and in addition, they are also important in brain development (Schlegelmilch *et al.* 2011). $P2Y_{12}$ receptors are involved in microglia activation, and mediate chemotaxis in response to injury (Haynes *et al.* 2006); however, their involvement in other microglia functions is unknown.

1.6 Antiplatelet drugs in CVD

For those presenting with an ACS following atherothrombosis, antiplatelet drugs form a dominant part of the treatment strategy, in addition to revascularisation via PCI, usually involving the insertion of a metal stent, or coronary artery bypass graft (CABG) surgery. These are followed by long-term antiplatelet drug treatment as an outpatient, to reduce the risk of further thrombotic events (Capodanno *et al.* 2013).

1.6.1 Percutaneous coronary intervention

Balloon angioplasty, as a method of coronary revascularisation, was developed by Andreas Gruentzig, who performed the first human coronary angioplasty in 1977 (Gruntzig 1978). This paved the way for the development of the balloon expandable Palmaz-Schatz stent (Schatz *et al.* 1991), which became the forebear of modern stents due its improved outcomes (Fischman *et al.* 1994). Over 80,000 stenting procedures are now carried out annually in the UK (Scarborough *et al.* 2010).

For patients with multiple diseased vessels and complicating conditions, such as diabetes, CABG is traditionally the favoured procedure, demonstrating a lower mortality in comparison with PCI (Hlatky *et al.* 2009).

1.6.2 Dual antiplatelet therapy

Since platelet activation is central to thrombus formation, the drugs which inhibit this activation are crucial in the treatment and prevention of ACS. Aspirin is a COX-1 inhibitor that irreversibly blocks the production of platelet agonist TxA_2 from arachadonic acid, and was the first such antiplatelet drug to be used (Patrono 1994). Several clinical studies demonstrated that both acute and long-term aspirin treatment reduced the risk of MI or death in unstable patients (Theroux *et al.* 1988; Wallentin 1991; Antiplatelet_Trialists'_Collaboration 1994). However, the prolonged use of aspirin is also associated with an increased incidence of gastrointestinal bleeding (Roderick *et al.* 1993).

The $P2Y_{12}$ antagonist clopidogrel offered an alternative to aspirin, and demonstrated not only superior platelet inhibition, but also an enhanced reduction in thrombotic events (CAPRIE 1996). Combination of the two drugs, however, offered the greatest risk reduction (Yusuf *et al.* 2001), and as a result this dual antiplatelet therapy of aspirin plus $P2Y_{12}$ antagonist continues to be the cornerstone of ACS treatment and prevention (Hamm *et al.* 2011).

1.6.3 Clopidogrel

Clopidogrel and its predecessor, ticlopidine, belong to a group of drugs called thienopyridines. These are pro-drugs that first require metabolism by various isoforms of the hepatic cytochrome P450, in a 2-step process to produce the active metabolite, which then binds irreversibly to the $P2Y_{12}$ receptor (Cattaneo 2012). Platelet inhibition, denoted as 50% inhibition of aggregation, is achieved within 2-4 hours of administration and, due to its irreversible binding, these inhibitory effects are apparent for 3-10 days, dependent on platelet turnover (Hamm *et al.* 2011). Drug metabolism is therefore directly linked to its activity, and genetic polymorphisms of the cytochrome P450 isoforms have now been linked to poor clopidogrel response in some individuals (Shuldiner *et al.* 2009). Furthermore, they are also associated with an increased risk of thrombotic events (Mega *et al.* 2010).

Although an effective platelet inhibitor, ticlopidine use was limited due to its severe side effects, which were less evident in its more potent replacement, clopidogrel (Bertrand *et al.* 2000). Since its introduction, the efficacy of clopidogrel, in combination with aspirin, has been tested by various clinical studies. The CURE study set out to test combination therapy versus aspirin alone for 3-12 months in ACS patients, and found that the addition of clopidogrel reduced the incidence of adverse events, including MI or death. This did, however, also come with a moderately increased risk of major, but not fatal, bleeding (Yusuf *et al.* 2001). In an extension of this study, PCI-CURE revealed that dual clopidogrel and aspirin treatment prior to PCI and for prolonged treatment afterwards, for an average of 8 months, reduced MI and death by 31% versus aspirin treatment alone (Mehta *et al.* 2001). Later, the CREDO study found that dual treatment for up to 1 year, versus 30 days, after PCI reduced adverse events by 27%, and that a loading predose of clopidogrel at least 6 hours prior to PCI may be advantageous and reduce further events (Steinhubl *et al.* 2002).

1.6.4 Ticagrelor

Development of the orally active $P2Y_{12}$ antagonist ticagrelor offers an alternative for poor clopidogrel responders. It belongs to a new drug class of cyclopentyltriazolopyrimidines, and binds directly and reversibly to the $P2Y_{12}$ receptor (Capodanno *et al.* 2013). As ticagrelor is orally active, its onset of action is more rapid compared to clopidogrel, and 50% platelet inhibition is typically achieved after 30 minutes of administration. Drug activity is

linked to ticagrelor plasma levels and, with a half-life of approximately 12 hours, the duration of effect lasts 3-4 days (Hamm *et al.* 2011).

A comparison of the efficacy of ticagrelor versus clopidogrel treatment in ACS patients was investigated in the PLATO study. This revealed that ticagrelor treatment led to a significant reduction in MI, stroke, or death compared to clopidogrel, and had no effect on procedure-related major bleeding rates. An increase in non-procedure-related bleeding was, however, noted (Wallentin *et al.* 2009). In addition, the PLATO substudy clearly demonstrated that ticagrelor achieved a superior level of platelet inhibition to clopidogrel, including immediately following a single loading dose (Storey *et al.* 2010). The pharmacodynamic profile of these drugs was further investigated in the ONSET/OFFSET study, which showed ticagrelor had a more rapid onset of inhibitory action and wore off more quickly compared to clopidogrel, making it advantageous for use when antiplatelet drugs need to be halted prior to surgical procedures (Gurbel *et al.* 2009).

In light of its superior inhibitory effects and improved clinical outcomes, ticagrelor is now recommended for all patients. Only in cases where ticagrelor and other $P2Y_{12}$ antagonists, such as prasugrel (see section 1.6.5), are unsuitable, should clopidogrel be considered as an alternative. In all cases, the use of a $P2Y_{12}$ antagonist, in addition to aspirin, is recommended to be given for a period of 12 months (Hamm *et al.* 2011).

Non-$P2Y_{12}$-mediated effects of ticagrelor have been noted, but currently are not fully understood. Recently van Giezen *et al*. demonstrated that ticagrelor inhibits adenosine reuptake by erythrocytes (van Giezen *et al.* 2012). Adenosine is a purine that is known to have anti-inflammatory effects on the vessel wall (Smits *et al.* 1995; Dubey *et al.* 1998). In addition, the PLATO study revealed that ticagrelor led to an unexpected reduction in total mortality, to a greater extent than could be explained by cardiovascular deaths alone, raising questions about the mechanisms behind this mortality reduction (Wallentin *et al.* 2009). Further analyses of the PLATO findings showed that ticagrelor-treated patients were also less likely to have pulmonary adverse events, such as infection and sepsis (Storey *et al.* 2012).

1.6.5 Other $P2Y_{12}$ antagonists

Prasugrel, another thienopyridine class drug, has emerged as a potent alternative to clopidogrel. It is similar to clopidogrel in that it too is a pro-drug and requires metabolism to form the active metabolite, which binds irreversibly to $P2Y_{12}$; however, this process is much more efficient leading to its enhanced antiplatelet effects and rapid onset (Sugidachi *et al.* 2007; Capodanno *et al.* 2013). The TRITON-TIMI 38 study compared prasugrel versus clopidogrel treatment in ACS patients undergoing PCI and revealed that prasugrel reduced

the incidence of adverse events, such as MI and death, but was associated with an increase in major and fatal bleeding, although overall mortality was unchanged (Wiviott *et al.* 2007).

Cangrelor is an ATP-analogue drug given via intravenous (i.v.) infusion, which achieves effective platelet inhibition within seconds and, due to a short half-life of 3-6 minutes, enables recovery of platelet function within 60 minutes after cessation of treatment (Capodanno *et al.* 2013). Pharmacodynamic studies have revealed that cangrelor demonstrates superior platelet inhibition compared to clopidogrel (Storey *et al.* 2002), but this did not translate to significantly improved outcomes in patients undergoing PCI in the CHAMPION-PCI and –PLATFORM studies (Bhatt *et al.* 2009; Harrington *et al.* 2009). However, despite the later CHAMPION-PHEONIX and BRIDGE studies showing cangrelor was superior to clopidogrel in reducing ischaemic events (Bhatt *et al.* 2013), and sustaining platelet inhibition during procedures (Angiolillo *et al.* 2012), cangrelor is not yet approved for clinical use and its future is still unsure.

1.7 Platelets in restenosis

1.7.1 Neointimal hyperplasia

Ironically, PCI as a treatment for CHD can itself lead to a recurrence of symptoms due to restenosis, i.e. the re-occlusion of the vessel, caused by growth of neointima. Restenosis is viewed as a wound healing response gone awry, with excessive neointima formation (hyperplasia) in response to injury (Steele *et al.* 1985; Forrester *et al.* 1991; Schwartz *et al.* 1992), similar to that described by Russell Ross in the initiation of atherosclerosis (Ross 1993). Neointima formation is brought on by vascular injury incurred at the site of stent deployment, with the severity of restenosis directly correlated to the degree of vessel injury sustained (Schwartz *et al.* 1992; Farb *et al.* 2002). Endothelial denudation followed swiftly by platelet adhesion and thrombus formation, are all precursors of early neointima (Steele *et al.* 1985; Harker 1987; Chandrasekar and Tanguay 2000). Leukocyte recruitment (Farb *et al.* 2002), VSMC proliferation (Komatsu *et al.* 1998; Christen *et al.* 2001), and ECM synthesis (Glover *et al.* 2002) fuel neointimal growth, which is characterised by the re-organisation of mural thrombus (Steele *et al.* 1985; Richter *et al.* 2000; Glover *et al.* 2002). More recent studies have shown that stem cells also contribute to neointimal growth, suggesting that not all endothelial and smooth muscle cells in neointima originate from the vessel wall (Tsai *et al.* 2012).

1.7.2 Treatment and prevention

Initial restenosis rates following balloon angioplasty or bare metal stent (BMS) implantation have been documented at between 30 and 40% (Holmes *et al.* 1984; Fischman *et al.* 1994). Developments, particularly in the field of stent design and the use of anti-proliferative and immunosuppressive drug-eluting stents (DES), have significantly reduced restenosis rates. Promising results from clinical studies of sirolimus- and paclitaxel-eluting stents showed

dramatic reductions in the incidence of restenosis when compared to BMS, reporting rates of 3.2% vs. 35.4% for sirolimus DES versus BMS at 6 months post-PCI (Moses *et al.* 2003), and 7.9% vs. 26.6% for paclitaxel-eluting stents after 9 months (Stone *et al.* 2004). Many other DES have since been developed, including zotarolimus- (Fajadet *et al.* 2006) and everolimus-eluting stents (Palmerini *et al.* 2012). Despite limiting neointima, DES also delay the formation of an intact endothelium. Safety concerns have since arisen following the BASKET-LATE study results, showing an increased risk of late stent thrombosis with DES (4.9%) compared to BMS (1.3%) following discontinuation of antiplatelet therapy (Pfisterer *et al.* 2006), and this continues to be a major complication.

1.7.3 Platelets and antiplatelet drugs in restenosis

Many animal studies have highlighted the close relationship between platelet activation, aggregation, and restenosis. Platelet, rather than endothelial, P-selectin has been shown to be important in promoting neointima formation (Manka *et al.* 2004) through deposition of platelet RANTES onto leukocytes and the endothelium, thereby enhancing leukocyte recruitment (Schober *et al.* 2002). Further studies have demonstrated platelets also facilitate neointimal hyperplasia via platelet MCP-1-dependent monocyte recruitment (Schober *et al.* 2004), and through PDGF release (Ferns *et al.* 1991). In addition, blockade of platelet activation via thrombin (Unterberg *et al.* 1995), collagen (Konishi *et al.* 2002), TxA_2, serotonin and ADP (Willerson *et al.* 1991; Anderson *et al.* 2001), or increased cAMP levels (Faxon *et al.* 1984) also lead to reduced neointimal hyperplasia. However, translation of these studies into humans has not always offered such positive results. Combined inhibition of platelet integrins GPIIbIIIa and $\alpha_v\beta_3$ led to attenuated neointima formation in a hamster model of vessel injury (Matsuno *et al.* 1994), but this was not reflected in human studies, such as ERASER, which showed that integrin blockade had no effect on restenosis post-PCI (ERASER 1999).

Investigations into the direct impact of $P2Y_{12}$ antagonists on restenosis are limited, and offer differing results. The ISAR clinical study demonstrated that ticlopidine treatment did not reduce restenosis (Kastrati *et al.* 1997). In addition, low clopidogrel responsiveness has been shown to have no effect on restenosis, compared to those patients who achieved high levels of $P2Y_{12}$ inhibition (Schulz *et al.* 2010). Yet other studies of ticlopidine in humans (Nagaoka *et al.* 2001), and clopidogrel with nitroaspirin in mice (Momi *et al.* 2005), indicate beneficial effects of these inhibitors on neointimal thickening. Furthermore, reductions in the rate of target vessel revascularisation following large-scale clinical studies of $P2Y_{12}$ antagonists clopidogrel (Steinhubl *et al.* 2002), ticagrelor (Wallentin *et al.* 2009), and prasugrel (Wiviott *et al.* 2007) suggest a positive impact of these drugs on reducing restenosis rates, although these trials were not powered to prove such an effect.

1.7.4 Murine model of vascular injury and restenosis

Murine models have been used extensively to investigate the vascular response to injury, primarily studying thrombosis using various injury methods, such as wire injury, ligation, laser injury, and ferric chloride (Westrick *et al.* 2007). In the study of restenosis, few murine models of stent implantation exist due to the technical difficulties posed by small vessel size (Chamberlain *et al.* 2010). Wire injury is an alternative method, which results in neointimal hyperplasia following mechanical endothelial damage caused by the repeated insertion of a metal wire into a vessel (Westrick *et al.* 2007). Other chemical methods, such as the topical application of ferric chloride, achieve endothelial injury and neointima formation with the vessel remaining physically intact.

The ferric chloride injury method was originally developed as an *in vivo* model of arterial thrombosis (Kurz *et al.* 1990); however, due to the 2-stage nature of the vessel wall response, it has also been used to study neointima formation (Schafer *et al.* 2002). Topical application of a ferric chloride solution to the outer surface of an intact vessel causes localised endothelial denudation, VSMC, and endothelial damage, and collagen exposure due to oxidative damage (Woollard *et al.* 2009; Eckly *et al.* 2011). Ferric ions are transported through the vessel wall via an endocytosis/exocytosis pathway, resulting in the generation of reactive oxygen species that disrupt the vessel wall (Tseng *et al.* 2005). The resulting damage leads to exposure of vessel wall TF, which further promotes thrombosis by triggering the coagulation cascade (Wang *et al.* 2009).

Kurz *et al*. discovered that applying a piece of ferric chloride-soaked filter paper (5-65% w/v) to the carotid artery of a rat resulted in the rapid formation of an occlusive platelet and fibrin-rich thrombus. In addition, the total vessel occlusion time was related to the ferric chloride concentration in a dose-dependent manner (Kurz *et al.* 1990). Further investigation in mice revealed lower concentrations (2-10% w/v) would be more sensitive to unmask anti-thrombotic effects, with concentrations greater than 5% w/v achieving consistent vessel occlusion (Wang and Xu 2005). Several studies have adopted the same method of 10% w/v ferric chloride solution applied to the carotid artery for 3 minutes to investigate both thrombus (Farrehi *et al.* 1998; Konstantinides *et al.* 2001), and neointima formation (Zhu *et al.* 2001; Schafer *et al.* 2002).

1.8 Platelets in atherogenesis

Even in the early days of atherosclerosis research, platelets were linked to atherogenesis and observed as having mitogenic effects. In 1974, Ross noted that platelets activated with thrombin released a ‘serum factor’, later identified as PDGF, which stimulated the proliferation of arterial smooth muscle cells *in vitro* (Ross *et al.* 1974). We now understand that the role of platelets extends far beyond haemostasis; however, the full extent and impact of their role in atherogenesis is becoming clearer with the help of animal models.

1.8.1 Interactions with leukocytes and the endothelium

Upon activation, platelets release a cocktail of pro-inflammatory cytokines from their granules, and express a variety of adhesion receptors and proteins (Rendu and Brohard-Bohn 2001), which facilitate interactions with both leukocytes and the endothelium. Among these are P-selectin (CD62p) and its ligand PSGL-1, which enable platelets to adhere to reciprocal proteins on endothelial cells (Frenette *et al.* 1998; Frenette *et al.* 2000), and form platelet-leukocyte conjugates (Larsen *et al.* 1989; Diacovo *et al.* 1996; Storey *et al.* 2002). Platelet P-selectin and endothelial PSGL-1 ligation causes P-selectin release from Weibel-Palade bodies, and thereby enhances leukocyte rolling on the endothelium (Dole *et al.* 2005; Dole *et al.* 2007). In addition, activated platelets have been shown to further promote leukocyte recruitment via the deposition of the chemokines RANTES and platelet factor 4 (PF4/CXCL4) on the surface of endothelial cells and leukocytes, in a process which is platelet P-selectin dependent (von Hundelshausen *et al.* 2001; Schober *et al.* 2002; Huo *et al.* 2003). Microparticles shed from activated platelets similarly contribute to RANTES delivery (Mause *et al.* 2005). Activated platelets also modulate pro-inflammatory responses via IL-1 release (Lindemann *et al.* 2001), which causes MCP-1 release and ICAM-1 expression in endothelial cells (Gawaz *et al.* 2000). In addition, MCP-1 also binds to adherent platelets and triggers leukocyte arrest onto these cells (Schober *et al.* 2004).

Animal experiments conducted to assess the contribution of platelets in atherosclerotic lesion development demonstrated, using transgenic mice, that platelet P-selectin enhanced lesion growth, and promoted an advanced lesion phenotype (Burger and Wagner 2003). Similarly, Huo *et al*. found that circulating activated platelets readily formed platelet-leukocyte conjugates and exacerbated atherosclerotic lesion development. Furthermore, these effects were attributed to platelet P-selectin-mediated chemokine deposition (Huo *et al.* 2003). This is supported by findings showing that mice treated with a RANTES receptor antagonist demonstrated reduced neointimal lesions after injury (Schober *et al.* 2002). Likewise, $PF4^{-/-}$ mice also showed significantly attenuated atheroma (Sachais *et al.* 2007).

Platelet adherence can also occur independently of P-selectin through the GPIb-IX receptor complex and endothelial P-selectin (Romo *et al.* 1999), membrane attack complex (MAC)-1 on leukocytes (Wang *et al.* 2005), or vWF (Andre *et al.* 2000). Indeed blockade of GPIb in mice, by use of an antibody, led to a significant reduction in atheroma, demonstrating a clear role for platelet adhesion in atherosclerosis (Massberg *et al.* 2002). Likewise, GPVI antibody treatment had a similar limiting effect on lesion progression (Bultmann *et al.* 2010).

CD40-CD40L signalling between platelets, leukocytes, and endothelial cells plays an important role in atherogenesis by mediating cytokine release and adhesion molecule expression (Lievens *et al.* 2009). Platelets possess both proteins, they constitutively express CD40 (Inwald *et al.* 2003), but also CD40L upon activation (Henn *et al.* 1998).

CD40 ligation provides another mechanism for platelet activation, and also results in RANTES release (Danese *et al.* 2004). However, platelet CD40L triggers inflammatory responses in other cells. Henn *et al*. demonstrated that CD40L upregulated VCAM-1, ICAM-1, and E-selectin expression in endothelial cells, and also led to IL-8 and MCP-1 release (Henn *et al.* 1998). Furthermore, CD40L mediates platelet-leukocyte conjugate formation, and has a direct impact on leukocyte recruitment and adherence to the endothelium (Lievens *et al.* 2010). In this *in vivo* model, atherosclerotic mice were injected with CD40L-deficient platelets and, in addition to diminished platelet-leukocyte interactions, also displayed reduced atherosclerosis. Earlier studies have shown similar findings, demonstrating that CD40L is important in promoting lesion development, as well as an unstable lesion phenotype (Mach *et al.* 1998; Lutgens *et al.* 1999; Lutgens *et al.* 2000; Schonbeck *et al.* 2000).

1.8.2 Mitogenic effects on the vessel wall

PDGF and TGF-β are known to regulate VSMC mitogenesis and synthesis of ECM proteins, both of which are important processes in advanced lesion development (Raines and Ross 1993). When activated, platelets release these growth factors, inducing VSMC migration and proliferation (Schini-Kerth *et al.* 1997; Massberg *et al.* 2003), and collagen synthesis (Amento *et al.* 1991). Consequently *in vivo* rabbit and mouse models, where the action of PDGF was blocked by use of an antibody, demonstrated reduced atheroma (Lamb *et al.* 2001; Sano *et al.* 2001), and delayed the fibrous cap formation (Kozaki *et al.* 2002).

1.8.3 Murine model of atherosclerosis

Given the timescale in which atherosclerosis develops in humans, early research using animal models proved difficult as many species appeared resistant to the disease and did not develop spontaneous lesions. Administration of a high-cholesterol diet enabled the study of fatty lesions in rabbits; however, such models had limited usefulness as these lesions were dissimilar to those observed in humans (Jawien *et al.* 2004). Despite many mouse strains being highly resistant, it was noted that C57/BL6 mice fed a high-fat 'Paigen' diet developed small lesions (Paigen *et al.* 1985).

The later development of the apolipoprotein E (ApoE)$^{-/-}$ (Piedrahita *et al.* 1992) and LDL-R$^{-/-}$ mouse strains (Ishibashi *et al.* 1993) revolutionised research into this disease. Given the rapidity of onset of atherogenesis in both strains, athero-progression from simple to complex lesions could be achieved in a matter of weeks, particularly with the addition of a paigen, or the less toxic 'western' diet (Jawien *et al.* 2004; Getz and Reardon 2006). This has given rise to a second generation of double and triple knockout mouse lines, to investigate the role of various cells and proteins in atherosclerosis.

ApoE is a component of all the lipoproteins, with the exception of LDL, and is responsible for the trafficking of lipids between organs and cells. It also acts as a ligand, and facilitates the excretion of lipids and cholesterol from the blood plasma via receptor-mediated pathways in the liver (Mahley 1988). ApoE-deficient mice have demonstrated both spontaneous and diet-induced atherosclerotic lesions, and so they provide a well-characterised model for atherosclerosis (Zhang *et al.* 1992; Reddick *et al.* 1994). In addition, the $ApoE^{-/-}$ mouse strain is renowned for the development of complex fibrous lesions found throughout the arterial tree, similar to those observed in human disease (Nakashima *et al.* 1994). LDL-R-deficient mice, however, do not develop spontaneous lesions but, once fed a high-fat diet, can develop large lesions similar to those seen in ApoE-deficient mice (Jawien *et al.* 2004; Maeda 2011).

1.9 Hypothesis and aims

The classical role of platelets is thought to be in maintaining vascular integrity and haemostasis, in such processes as atherothrombosis, where they play a fundamental role. However, platelets are increasingly regarded as discrete inflammatory cells, and are known to interact with both the endothelium and leukocytes. Given that platelets can, upon activation, elicit an inflammatory response in these cells, I hypothesised that the $P2Y_{12}$ receptor, which is crucial in amplifying platelet activation, would also be involved in modulating the vessel wall response to injury and inflammation.

The aims of this thesis were to study the role of the $P2Y_{12}$ receptor, using murine *in vivo* models of injury and atherogenesis, and specifically to:

- Investigate the role of $P2Y_{12}$ in thrombus and neointima formation following vessel injury, using the well-established ferric chloride injury model.
- Generate an ApoE/$P2Y_{12}$ double knockout colony to study the role of $P2Y_{12}$ in atherogenesis, and to characterise the phenotype of this novel strain.
- Assess the effect of $P2Y_{12}$ deficiency on atherogenesis and lesion composition.
- Investigate the role of platelet versus vessel wall $P2Y_{12}$ in early atherogenesis using bone marrow transplantations (BMT).
- Consider the use of $P2Y_{12}$ antagonists, ticagrelor and clopidogrel, in modulating atherogenesis.

2 Materials and methods

2.1 Preface

This materials and methods chapter has been organised into main themes of work, to provide a clear and distinct description of the methods, and to avoid repetition. As certain techniques have been used throughout the work, each has been described in detail once and referred to in all other sections. The order of this chapter has also been designed to form a logical progression through the project.

2.2 Animals

2.2.1 Licensing

All experimental procedures were approved by The University of Sheffield Ethics Committee, and were performed in accordance with UK and European legislation under the Animals (Scientific Procedures) Act 1986 and European Directive 2010/63/EU. Work was carried out under project licence PPL 40/3307 (previously 40/2732), and personal licence PIL 40/8420.

2.2.2 Husbandry

Animals were housed in a controlled environment with a 12 hour light/dark cycle at 22°C and a constant air pressure. Where possible, littermates were housed together with a maximum of 6 animals per cage. All cages were provided with environmental enrichment, and animals were fed standard laboratory chow (Harlan 18% protein rodent diet) *ad libitum*, unless otherwise stated. See Appendix I (section 10.1) for diet ingredients and specification.

2.2.3 Breeding

2.2.3.1 Established colonies

Transgenic mice were obtained from in-house colonies derived from breeding pairs sourced externally. $P2Y_{12}^{-/-}$ and genetically matched wild-type $P2Y_{12}^{+/+}$ mice were derived from breeding pairs provided by Schering Plough Research Institute, NJ (courtesy of Dr M Chintala). $ApoE^{-/-}$ breeding pairs (JAX 2052) were supplied by Jackson Laboratories (Bar Harbor, ME). Both the ApoE and $P2Y_{12}$ strains were developed on a C57BL/6 background and backcrossed 10 generations (Piedrahita *et al.* 1992) (Foster *et al.* 2001).

2.2.3.2 Generation of ApoE/$P2Y_{12}$ double knockout colony

An ApoE/$P2Y_{12}$ double knockout (DK) colony was developed by cross breeding of the in-house ApoE and $P2Y_{12}$ colonies. $ApoE^{-/-}$ mice were crossed with $P2Y_{12}^{-/-}$ mice to produce an F_1 generation of heterozygotes. Offspring were crossed to produce a subsequent F_2 generation, of which 1 in 16 were expected to be the desired genotype (see Table 2.1). Mice from all generations were ear clipped and genotyped by polymerase chain reaction

(PCR) to identify double knockouts for further breeding. Prior to processing, ear clips were stored in the freezer at -25°C until needed.

2.3 Genotyping

2.3.1 Materials

DNEasy® blood and tissue kit was purchased from Qiagen (Crawley, UK). Ethidium bromide and PCR primers were from Sigma-Aldrich (Poole, UK). BioMix™ Red and agarose was from Bioline (London, UK). GoTaq® DNA polymerase, and all other PCR buffers and markers, were produced by Promega (Southampton, UK).

2.3.2 DNA extraction from murine tissue

The DNEasy® blood and tissue kit was used for all samples to extract purified DNA from the mouse ears clips. DNA was extracted as per the kit protocol handbook (Purification of total DNA from animal tissues – Spin-column Protocol, page 28). In summary, this involved incubating the ear clips in lysis buffer and proteinase K overnight at 56°C to digest the tissue. The following day, samples underwent a series of wash and centrifugation steps in spin columns, ending with an elution of purified DNA into AE buffer (supplied with kit).

2.3.3 Polymerase chain reaction for genotyping

Extracted DNA was subsequently amplified by PCR to determine the genotype of each animal. ApoE and $P2Y_{12}$ PCRs were analysed separately, to determine whether each animal was a homozygote or heterozygote for the ApoE and $P2Y_{12}$ gene. Primers specific to the ApoE or $P2Y_{12}$ gene were used to amplify the particular gene of interest in each case. The sequences of the primers used are shown in Table 2.2. All primers were reconstituted in sterile water to 100 µmol/L stock solutions, from which 20 µmol/L working solutions were made. These were added in differing volumes to each of the PCRs to provide optimum DNA amplification for each gene. All PCRs were carried out in a G-Storm GS1 thermocycler (GRI Ltd, Braintree, UK).

2.3.3.1 ApoE PCR reaction conditions

PCR reaction tubes were prepared for each individual DNA sample, as detailed in Appendix II (section 10.2.1). ApoE primers were used to a final concentration of 0.4 µmol/L in the reaction mix. BioMix™ Red contained 2 mmol/L $MgCl_2$, nucleotides, DNA polymerase, and a red dye, eliminating the need to use a loading dye when running the gel following PCR. BioMix™ was used to increase efficiency and reduce variability. Sterile water was then added to the reaction mix to make a final volume 25 µL for each sample. The reaction tubes were placed in a G-Storm thermocycler, and the PCR was carried out using the cycle program also detailed in Appendix II.

Table 2.1 – Genotype outcomes of the ApoE/P2Y$_{12}$ colony F$_2$ generation.

A summary of all possible genotype outcomes of the ApoE/P2Y$_{12}$ colony F$_2$ generation, achieved from crossing the F$_1$ generation of heterozygotes (ApoE$^{+/-}$P2Y$_{12}^{+/-}$).

	AP	***Ap***	***aP***	***ap***
AP	AAPP	AAPp	AaPP	AaPp
Ap	AAPp	AApp	AaPp	Aapp
aP	AaPP	AaPp	aaPP	aaPp
ap	AaPp	Aapp	aaPp	**aapp**

A - ApoE wild-type allele
a - ApoE knockout allele
P - P2Y$_{12}$ wild-type allele
p - P2Y$_{12}$ knockout allele

Table 2.2 – List of ApoE and P2Y$_{12}$ primers used for polymerase chain reaction.

Primer Name		***Sequence (5'-3')***
ApoE	180	GCCTAGCCGAGGGAGAGCCG
	181	TGTGACTTGGGAGCTCTGCAGC
	182	GCCGCCCCGACTGCATCT
P2Y$_{12}$	NEO	ACGCGTCACCTTAATATGCG
	DP308	GGCTGCCTTGAGAAATATCAAGT
	DP310	GGCACTCTAGTGATGCTTTGCCTA

2.3.3.2 $P2Y_{12}$ PCR reaction conditions

PCR was performed according to methods provided by Schering Plough Research Institute, NJ. Reaction tubes were prepared as detailed in Appendix II (section 10.2.2), using individual nucleotides, 1.5 mmol/L $MgCl_2$, GoTaq® DNA polymerase, and GoTaq® green buffer. Green GoTaq® buffer eliminated the need to use loading dye when running the gel. Sterile water was added to the reaction mix, to make a final volume of 25 µL. PCR was carried out using the cycle program also detailed in Appendix II.

2.3.4 Agarose gel electrophoresis and analysis

ApoE PCR products were electrophoresed in 1.5% w/v agarose gels, and $P2Y_{12}$ PCR products in 2% w/v gels; in addition, each contained 10 µL of ethidium bromide. Gels were submerged in TAE buffer (40 mmol/L Tris, 1 mmol/L EDTA, 0.1% v/v glacial acetic acid; section 10.2.4) prior to sample loading. For all PCR products, 10-15 µL of sample was loaded into each well. As described previously, loading dyes were not required as the PCR mix already contained either a red or green dye. To determine the length of DNA fragments in each sample, a Phix174/HAEIII DNA marker (see section 10.2.5) was added to the first well of each row. Agarose gels were run at 90 volts for 1-2 hours.

When completed, gels were viewed under ultraviolet (UV) light in a ChemiGenius^2 transilluminator (Syngene, Cambridge, UK) to assess the migration of DNA. An image of the gel was captured using Syngene GeneSnap Bio imaging software. DNA migration patterns were compared in relation to the DNA markers, to determine the sizes of the bands. For ApoE PCR products, a lower (smaller) band of 155 bp indicated a wild-type genotype ($ApoE^{+/+}$). An upper (larger) band of 245 bp specified a knockout ($ApoE^{-/-}$). The presence of both bands denoted a heterozygote, $ApoE^{+/-}$. For $P2Y_{12}$ PCR products, a lower band of 510 bp similarly indicated a wild-type ($P2Y_{12}^{+/+}$). An upper band of 650 bp showed a knockout ($P2Y_{12}^{-/-}$), and both bands denoted a heterozygote ($P2Y_{12}^{+/-}$).

2.4 Ferric chloride injury model for rodents

2.4.1 Materials

Clopidogrel (Plavix®) was purchased from Bristol Myers Squibb Pharmaceuticals Ltd (Uxbridge, UK). Ferric chloride was from Sigma-Aldrich (Poole, UK) and used at 10% w/v dissolved in sterile water. Saline (0.9% w/v $NaCl_2$) was from Baxter Healthcare Ltd (Thetford, UK). Whatman® grade 1 filter paper was purchased from Whatman International (Maidstone, UK). Hypnorm® was purchased from VetaPharma Ltd (Leeds, UK); Midazolam (Hypnovel®) was from Roche (Welwyn Garden City, UK).

2.4.2 Animals

Male $P2Y_{12}^{-/-}$ mice and genetically matched wild-types, $P2Y_{12}^{+/+}$, underwent ferric chloride injury. All mice were aged between 8 and 12 weeks, and weighed 22-28 g at the time of surgery.

2.4.3 Pharmacological inhibition of $P2Y_{12}$

To examine the effects of $P2Y_{12}$ inhibition on thrombus and neointima formation following arterial injury, some $P2Y_{12}^{+/+}$ mice were also treated with the $P2Y_{12}$ antagonist clopidogrel, or sterile water as a control. Clopidogrel was prepared as a suspension in 200 µL of sterile water, at a dose of 20 mg/kg, and administered orally by gavage, a method of delivering a substance directly to the stomach via a tube or needle.

Mice were scruffed in an upright position and a blunt, curved 18-gauge needle, approximately 2 inches in length, passed slowly down the oesophagus to the neck of the stomach. The drug suspension or vehicle control was deployed from the syringe into the stomach, and the needle carefully removed. This particular method of drug delivery was employed to ensure swift, timely, and accurate dosing of the drug to each mouse.

Both long- and short-term clopidogrel treatment regimens were investigated. For long-term treatments, mice were gavaged 24 hours before ferric chloride injury, with either clopidogrel or water, followed by a second dose, 1-2 hours before surgery. Some mice were sacrificed at 30 minutes post injury to investigate thrombus formation. The remaining mice were allowed to recover from the procedure, and then continued to be gavaged once daily. At 21 days post injury the mice were sacrificed to examine neointima formation.

For short-term clopidogrel treatment, mice were gavaged 4 hours before injury, followed by a second dose 24 hours after surgery. These mice were not gavaged again for the duration of the procedure, and were sacrificed at 21 days post injury.

2.4.4 Bone marrow transplants in $P2Y_{12}$ mice

Bone marrow transplantation (BMT) is a procedure in which bone marrow is taken from a donor mouse, and transplanted into a lethally irradiated recipient mouse. The purpose is to isolate the role of bone marrow-derived circulating cells, such as platelets, from the constituent genotype of the body. Further detailed description of the entire BMT procedure, including irradiation dosing and chimera generation, can be found later in section 2.6.

Briefly, male $P2Y_{12}^{+/+}$ and $P2Y_{12}^{-/-}$ mice, aged 4-6 weeks old, underwent bone marrow transplantation prior to ferric chloride injury. Mice received a lethal dose of whole body irradiation, followed by an i.v. tail vein injection of bone marrow cells from donor females.

Mice were kept in ventilated caging and treated with antibiotic water for 5 weeks after transplantation, prior to ferric chloride injury. Animals were sacrificed at 21 days post injury.

2.4.5 Surgical procedure for ferric chloride injury

Animals were anaesthetised by intraperitoneal (i.p.) injection of an anaesthetic solution (0.008 mL/g), consisting of Hypnorm® (fluanisone 2.5 mg/mL; fentanyl citrate 0.07875 mg/mL) and midazolam (1.25 mg/mL).

An incision, approximately 1 cm in length, was made to the right of the midline of the neck, and the salivary glands were separated by blunt dissection. The right common carotid artery was then exposed and carefully isolated from the surrounding tissues using forceps. Subsequently a piece of Whatman® grade 1 filter paper (1 mm x 2 mm) was soaked in 10% w/v ferric chloride solution and placed on the artery, just below the bifurcation into the internal and external carotid arteries, where it was left for 3 minutes (see Figure 2.1). The artery was then washed with saline and the dermis sutured with 5/0 silk. At 30 minutes post-injury, some mice were sacrificed to study thrombus formation, whilst the others were allowed to recover in order to study neointima (Evans *et al.* 2009). These animals were placed in a hospital cage within an incubator set to 30°C. Upon recovery from anaesthesia, mice were monitored for any signs of stroke before being returned to standard housing. Any sick animals were culled. The combined incidence of death, during procedure, and stroke, leading to the animal being culled, was 8%.

2.4.6 End of procedure

Mice were killed at either 30 minutes or 21 days post-injury, and the right common carotid arteries harvested, as detailed later in section 2.8, followed by histological analysis (see section 2.9).

2.5 Atherogenesis studies

2.5.1 Materials

Western diet was purchased from Special Diet Services (SDS; Witham, UK). This is a high-fat, no cholate diet used specifically to study diet related diseases, and contains supplementary cholesterol to aid induction of atherosclerosis. Chow diet was a Teklad Global diet from Harlan (Indianapolis, IN). See Appendix I (section 10.1) for diet ingredients and specification. D(+) glucose was obtained from Sigma-Aldrich (Poole, UK) and Actrapid® human insulin purchased from Novo Nordisk (Crawley, UK).

2.5.2 Animals

$ApoE^{-/-}$ and $ApoE/P2Y_{12}$ DK mice were fed *ad libitum* either standard laboratory chow or western diet for 12 weeks. All mice used were male, and aged between 8 and 10 weeks upon commencement of feeding.

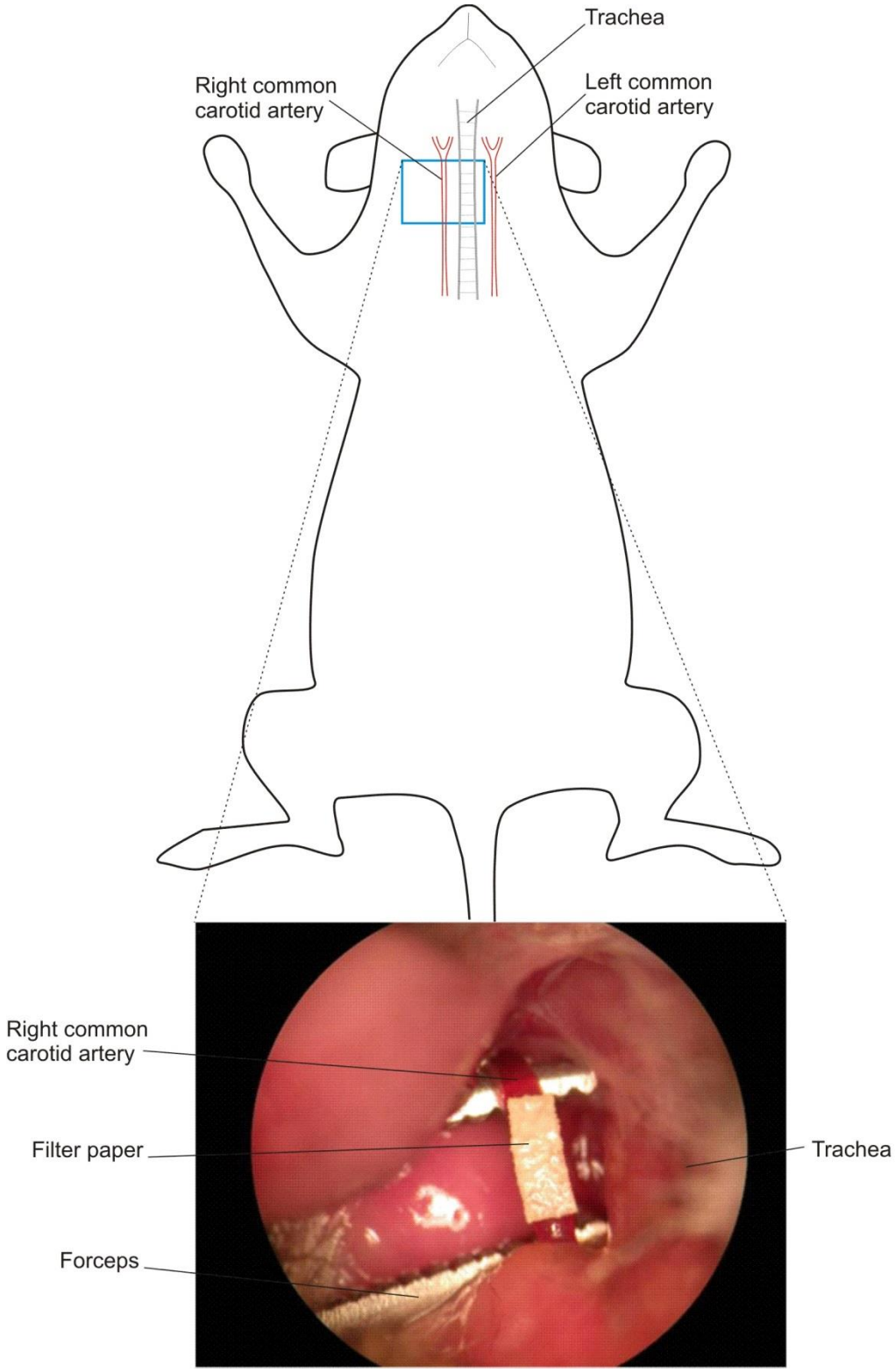

Figure 2.1 – Ferric chloride injury surgical procedure.

The right common carotid artery was isolated by blunt dissection using forceps. A piece of filter paper, 2 mm x 1 mm in size, was soaked in 10% w/v ferric chloride solution and placed on the artery, carefully avoiding contact with the surrounding tissue. The filter paper was left in place for 3 minutes, causing injury to the vessel. After 3 minutes the paper was removed, the vessel washed with saline, and the dermis sutured.

2.5.3 Weight measurements

Mice were ear clipped to identify individual mice within a cage. Weekly weight measurements were taken for both chow and western fed ApoE$^{-/-}$ and ApoE/P2Y$_{12}$ DK mice. Readings were taken at the start of each week over 12 weeks, beginning with a baseline weight before feeding commenced and a final weight after 12 weeks of feeding. Measurements were taken to the nearest 0.1 g. Individual weights each week were combined to give a mean weight for each genotype and diet.

2.5.4 Food consumption

Over a period of 12 weeks, the food consumption of a cage of 4 ApoE$^{-/-}$ and 4 ApoE/P2Y$_{12}$ DK mice on western diet was measured. Bags of food were weighed out (140 g each) and added to a cage, one at a time, when the food hopper was empty. All food added to a cage was recorded, and no food was removed or thrown away. At the end of 12 weeks, any remaining food in the hopper was weighed and subtracted from the total weight of food added to each cage over the course of 12 weeks.

2.5.5 Blood pressure measurements

Daily blood pressure readings were taken of ApoE$^{-/-}$ and ApoE/P2Y$_{12}$ DK mice on western diet via a tail cuff device on the Bp-2000 blood pressure analysis system (Visitech Systems Inc, Apex, NC). Individual mice were identified by ear clips and were trained for one week on the equipment prior to commencement of the study. To help reinforce this daily routine, readings were always taken by the same operator, at the same time each day. Efforts were also made to ensure similar lighting levels, room temperature, and low noise levels. Following training, baseline readings were taken whilst mice were on standard chow, the week prior to feeding. Mice were then switched to western diet at the start of week 1, and readings were taken thereafter until the end of week 12. The system was calibrated daily using a manometer and the cuff elastic changed on a weekly basis to ensure consistent experimental conditions.

Specimens were placed on a heated platform at 34°C ± 0.5°C and secured in a magnetic holder. The tail was threaded through the cuff and secured with tape, and finally the sensor positioned on top of the tail. A total of 30 readings were taken for each mouse, every day, with the first 10 readings discarded. The final 20 readings were taken to calculate the mean blood pressure and pulse rate for each animal. These values were also used to generate a weekly mean blood pressure for each genotype.

2.5.6 Metabolic studies

Glucose tolerance tests (GTT) and insulin tolerance tests (ITT) were carried out after 10 and 11 weeks, respectively, of feeding on a western diet. These studies were carried out on ApoE$^{-/-}$ and ApoE/P2Y$_{12}$ DK mice undergoing daily blood pressure readings.

Mice were restrained on the heated blood pressure platform, and a small sample of blood was obtained by puncturing the tail vein using a 21-gauge needle. Blood glucose levels were measured using an Optium Xceed portable glucose meter and disposable test strips (Abbott Laboratories Limited, Maidenhead, UK). Measurements were given in mmol/L.

2.5.6.1 Glucose tolerance test

Fed baseline glucose levels were taken 1-2 days prior to starting the metabolic studies and each mouse weighed. All mice were fasted from 5pm the evening before the GTT, and a fasted blood glucose level was taken the following morning.

Mice received an i.p. injection of 20% w/v D(+) glucose in sterile water, at a dose of 10 µL/g (2 mg/g). Blood glucose readings were taken at 30, 60, 90, and 120 minutes post injection (Crossey *et al.* 2000; Wheatcroft *et al.* 2004; Zhang 2011). When blood glucose levels had returned to baseline levels, mice were returned to their cages.

2.5.6.2 Insulin tolerance test

The week following glucose tolerance testing, the same mice were weighed again, and a fed baseline glucose level was taken. Each mouse received Actrapid® human insulin at a dose of 0.75 U/kg by i.p. injection. Blood glucose readings were taken at 20, 40, and 60 minutes post injection (Wheatcroft *et al.* 2004). Mice were monitored throughout for signs of hypoglycaemia, upon which a glucose injection would have been administered. When blood glucose levels had risen to baseline levels, mice were returned to their cages.

2.5.7 End of procedure

Mice were sacrificed after 12 weeks of feeding on western or chow diet. Blood was taken by cardiac puncture, either for plasma or flow cytometry. Various tissues were harvested for histological analysis, including the brachiocephalic and right common carotid arteries, the aortic sinus, the aorta, and major organs (see section 2.8 and 2.9).

2.6 Detailed method for bone marrow transplantations

2.6.1 Materials

RPMI-1640 (modified, with sodium bicarbonate, without L-glutamine and without phenol red) was purchased from Sigma-Aldrich (Poole, UK). FBS was from Lonza (Slough, UK). HBSS was purchased from Thermo Scientific (Epsom, UK). Acetic acid was from VWR International Inc. (Lutterworth, UK). Neomycin trisulphate salt hydrate and polymyxin B sulphate salt were obtained from Sigma-Aldrich (Poole, UK).

2.6.2 Animals and chimeras generated

Transplanting bone marrow between strains of transgenic mice generates chimeras (see section 2.4.4), a mouse which is composed of 2 genetically distinct cell populations or

tissues. The chimeras generated in the following studies are detailed in Tables 2.3 and 2.4. The method described is based on a protocol which has successfully been used previously by my group (Chamberlain *et al.* 2006; Evans *et al.* 2009; West *et al.* 2014).

2.6.2.1 Ferric chloride studies

BMT was carried out on male $P2Y_{12}^{+/+}$ and $P2Y_{12}^{-/-}$ mice, aged 4-6 weeks old, to create 2 chimeras and 2 control groups (see Table 2.3). Female mice were used as donors in a ratio of 1 donor to 2 recipient mice. After BMT, mice underwent ferric chloride injury, as described earlier in section 2.4.

2.6.2.2 Atherogenesis studies

$ApoE^{-/-}$ and ApoE/$P2Y_{12}$ DK mice were used to create the chimeras detailed in Table 2.4. Females were used as donors, where possible, and recipient males were aged 8-10 weeks at the time of transplantation.

All mice were housed in individually ventilated caging (IVC), fed standard chow and given neomycin (1 mmol/L, final concentration) and polymyxin B (1000 USP units/mL) in drinking water, provided in covered bottles (see Appendix I, section 10.1). In addition, atherogenesis mice were switched to western diet 5 weeks after transplantation, and maintained on this diet for 4 weeks until the end of the procedure.

2.6.3 Total body irradiation

Recipient mice were given a lethal dose of whole body irradiation totalling 11 Gy (1100 rad). This was split into 2 doses of 5.5 Gy (550 rad), 4 hours apart. Following the final irradiation, mice were placed in an incubator at 35°C for 1 hour prior to receiving donor bone marrow via a tail vein injection.

2.6.4 Bone marrow cell preparation and transplantation

Donor mice were killed by cervical dislocation, and the femurs and tibias removed under aseptic conditions. Bone marrow was flushed from the bones with RPMI-1640 media + 10% v/v fetal bovine serum (FBS) using a syringe and 26-gauge needle. The cell-media solution was passed through a 40 µm cell strainer, and then centrifuged at 500 x g for 5 minutes. The supernatant was removed and the small cell pellet resuspended in Hank's buffered salt solution (HBSS) + 10% v/v FBS. Cells were counted on a haemocytometer, using 1% v/v acetic acid to lyse the RBCs, and then placed on ice until the tail vein injections. Each preparation produced an average yield of 20 x 10^6 cells/mL.

Mice were injected with 200 µL of whole bone marrow via the tail vein. Each mouse received between 2 and 4 x 10^6 cells in total and were monitored daily, on day 0-6 after transplant and twice daily on day 7-14, for signs of non-engraftment. Mortality due to this

Table 2.3 – $P2Y_{12}$ chimeras generated from bone marrow transplantations for ferric chloride studies.

Chimera	*Donor*	*Recipient*
1	$P2Y_{12}^{+/+}$	$P2Y_{12}^{+/+}$
2	$P2Y_{12}^{-/-}$	$P2Y_{12}^{+/+}$
3	$P2Y_{12}^{-/-}$	$P2Y_{12}^{-/-}$
4	$P2Y_{12}^{+/+}$	$P2Y_{12}^{-/-}$

Table 2.4 – ApoE/$P2Y_{12}$ chimeras generated from bone marrow transplantations for atherogenesis studies.

Chimera	*Donor*	*Recipient*
1	$ApoE^{-/-}$	$ApoE^{-/-}$
2	ApoE/$P2Y_{12}$ DK	$ApoE^{-/-}$
3	ApoE/$P2Y_{12}$ DK	ApoE/$P2Y_{12}$ DK
4	$ApoE^{-/-}$	ApoE/$P2Y_{12}$ DK

cause was 0% for these experiments, although an incidence of up to 30% can be expected for bone marrow transplantations.

2.6.5 End of procedure

For atherogenesis studies, mice were killed at 9 weeks post-transplant, after 4 weeks of feeding on western diet. Blood was taken by cardiac puncture, either for plasma or flow cytometry. The brachiocephalic and right common carotid arteries, aortic sinus, aorta, and major organs were harvested for histological analysis (see section 2.8 and 2.9).

2.7 Pharmacological inhibition of $P2Y_{12}$ in a model of early atherogenesis

2.7.1 Materials

Ticagrelor (Brilique™) was supplied by AstraZeneca UK Ltd (Luton, UK) and clopidogrel (Plavix®) was from Bristol Myers Squibb Pharmaceuticals Ltd (Uxbridge, UK). Mannitol was obtained from Sigma-Aldrich (Poole, UK). Hartley's blackcurrant flavoured concentrated jelly was used in these experiments.

2.7.2 Animals

$ApoE^{-/-}$ and $ApoE/P2Y_{12}$ DK male mice were fed western diet for 4 weeks, in addition to either twice-daily doses of ticagrelor (100 mg/kg), daily clopidogrel (20 mg/kg), or mannitol (control) in jelly. This method of voluntary drug delivery was adapted from a published method by Zhang (Zhang 2011). The doses of ticagrelor and clopidogrel were based on previous studies that established these as optimal for providing a high, sustained level of platelet $P2Y_{12}$ inhibition (Evans *et al.* 2009). Mannitol is a main constituent of ticagrelor and clopidogrel tablets, and was therefore selected as a control.

2.7.3 Preparation of drug doses

Ticagrelor and clopidogrel tablets had the film coating removed and were crushed into powder. Ticagrelor, clopidogrel, or mannitol powder was weighed into separate shallow moulds according to the appropriate doses for each drug, weighing 12 doses per mould. Flavoured jelly was dissolved in hot water, according to the manufacturer's instructions, and allowed to cool, then poured into each mould and mixed with the drug to achieve an even suspension. Moulds were placed immediately in a freezer and later cut into 12 equal cubes, measuring approximately 1 cm^3, containing a single dose of drug.

2.7.4 Dosing strategy

Mice were housed individually and fed a chow diet during one week of training, where mice received twice-daily meals of jelly only. Mice were then switched to a western diet upon commencing drug treatment. Due to the short half-life of ticagrelor, mice were dosed twice-

daily with ticagrelor and mannitol. Clopidogrel-fed mice were given one dose of clopidogrel and one dose of mannitol. Mice received daily doses approximately 9 hours apart and were observed daily to monitor jelly consumption.

2.7.5 End of procedure

Mice were killed after 4 weeks of drug treatment and western diet. Blood was taken by cardiac puncture for flow cytometry. In addition, various tissues were harvested for histological analysis, including the brachiocephalic artery, aortic sinus, and whole aorta (see section 2.8 and 2.9).

2.8 Harvesting of tissues

2.8.1 Materials

Sodium pentobarbital was provided by J M Loveridge Ltd (Southampton, UK). Hirudin (900 anti-IIa units/mL, 5 µg/mL) was purchased from Canyon Pharmaceuticals™ (Basel, Switzerland). Sodium citrate was supplied from Sigma-Aldrich (Poole, UK). PBS was purchased from Oxoid (Basingstoke, UK). All fixative reagents were from VWR International Ltd (BDH brand, Lutterworth, UK), except sodium phosphate, which was supplied from Sigma.

2.8.2 Sacrifice of animals and blood withdrawal

At the end of the procedure, mice were killed by injection of 0.2 mL sodium pentobarbital (200 mg/mL) given i.p. If blood was required, cardiac puncture was performed following pentobarbital injection, and prior to cessation of breathing.

Blood was taken directly from the heart through the chest wall into a 1 mL syringe, following loss of the pedal reflex. For plasma, blood was taken into a heparinised syringe and centrifuged at 2000 x g for 5 minutes at room temperature in a Beckman microfuge® R (Beckman Coulter, High Wycombe, UK). For platelet flow cytometry, blood was taken into 10% v/v hirudin at a final concentration in the blood of 1%. Blood was kept at room temperature and processed for flow cytometry immediately (see section 2.10.4). For coagulation studies (see section 2.10.5), blood was taken into 3.8% w/v sodium citrate at a ratio of 1 part anticoagulant to 9 parts blood, as used in previous murine studies (Palm *et al.* 1997; Bolliger *et al.* 2010).

2.8.3 Perfusion fixation

Once breathing had ceased, the abdominal cavity was exposed and the lower aorta cut to provide a route for blood loss. The chest cavity was then opened, and the circulation perfused via intraventricular injection of 1 mL phosphate buffered saline (PBS), followed by 1 mL of 10% v/v buffered formalin (33.3 mmol/L NaH_2PO_4, 50 mmol/L Na_2HPO_4, 10% v/v formaldehyde; see Appendix III, section 10.3.1).

2.8.4 Tissue excision

2.8.4.1 Carotid artery

An incision was made into the neck and the right carotid artery carefully dissected from the surrounding tissue. A segment of the vessel, approximately 1 cm in length, was excised originating from the bifurcation. For ferric chloride injuries, this included the entire injured area and some surrounding healthy tissue. The arteries were fixed in 10% v/v buffered formalin before processing for histological analysis (see section 2.9).

2.8.4.2 Organs

The spleen, liver, and lungs were taken from $ApoE^{-/-}$ and $ApoE/P2Y_{12}$ DK mice to assess differences in organ weights between the genotypes. Organs were removed by blunt dissection and placed in 10% v/v buffered formalin.

2.8.4.3 Dissection of the aortic tree

To expose the aortic tree, the rib cage, lungs, thymus, and oesophagus were removed. Beginning at the descending aorta, above the diaphragm, and working towards the aortic arch, fat was carefully dissected from the aorta, breaking any small branching vessels along its length. The vena cava was then broken to expose the upper aorta. The arch and its 3 main vessels, the brachiocephalic, left common carotid, and left subclavian arteries, were dissected free of the surrounding tissue. The brachiocephalic artery was then excised from its origin at the aortic arch, to the bifurcation into the right common carotid and right subclavian arteries, and placed in 10% v/v buffered formalin.

The left common carotid and left subclavian arteries were cut at the arch, and the aorta excised from its origin at the heart, ending at the diaphragm. The aorta was placed in a petri dish with PBS, and blunt forceps were used to remove any remaining adventitial fat from the vessel. Sprung vanus scissors were used to open the vessel and expose the inside surface. Vessels were cut along the outside curve of the arch, ending at the top of the descending aorta and along the inside curve for its entire length (see Figure 2.2). Aortae were then placed in 4% w/v paraformaldehyde in PBS (PFA; see Appendix III, section 10.3.1).

The heart was removed by blunt dissection from any surrounding tissue, and transected along the midline below the atria at a slight angle (see Figure 2.2). Both pieces of heart were placed in 10% v/v buffered formalin.

All tissues were stored at 4°C and kept in either 10% v/v buffered formalin or 4% w/v PFA for 24 hours, and then transferred to PBS for longer term storage. Tissues were processed for histological analysis, as described below.

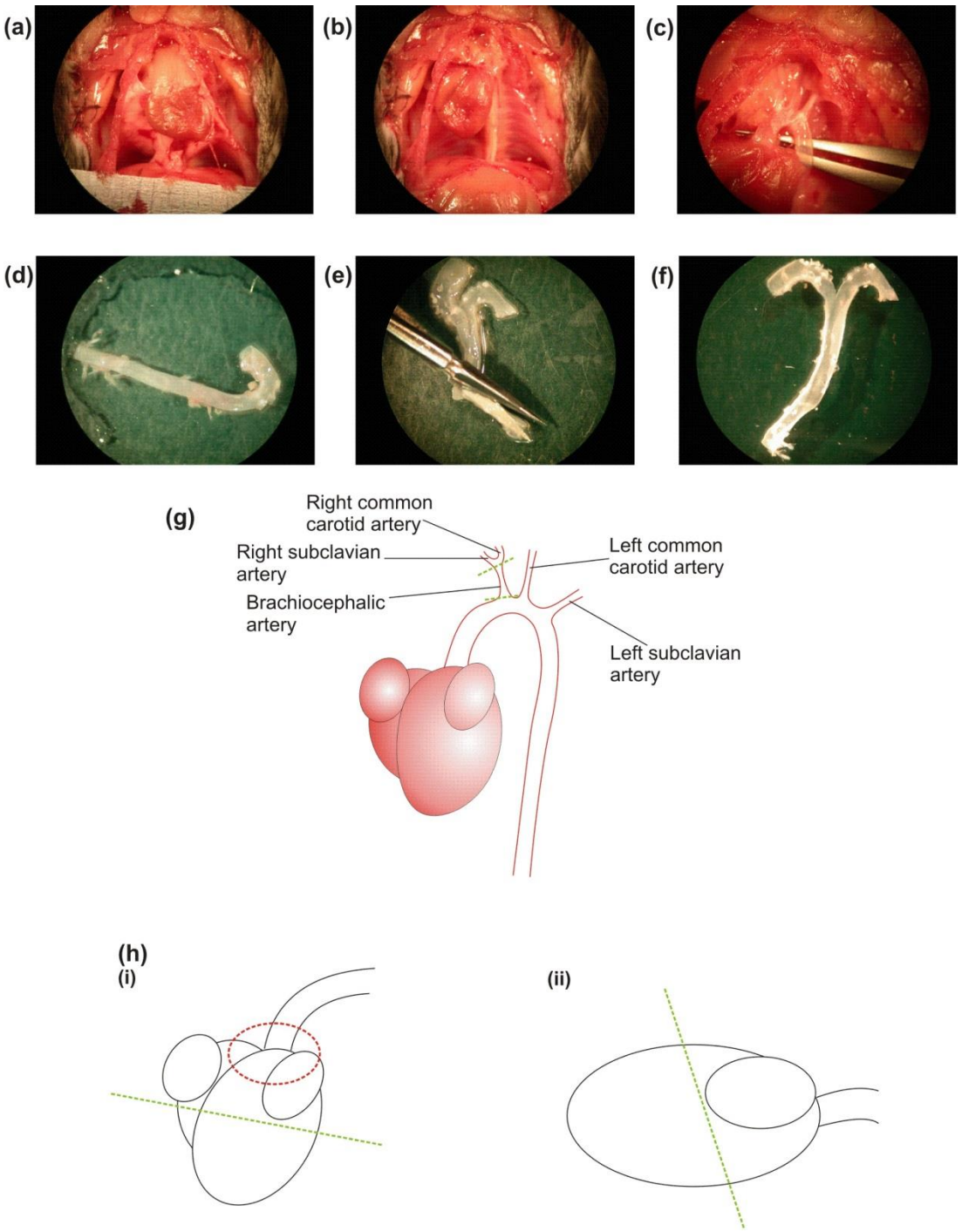

Figure 2.2 – Aortic dissection.

These images show the chest cavity **(a)** before and **(b)** after removal of the lungs, thymus, and oesophagus. The aorta and arch **(c)** were then dissected free of the surrounding tissue, before the entire aorta was removed **(d)**. The aorta was then stripped of any remaining adventitial fat and cut open using vanus scissors **(e)** to expose the inside surface of the aorta **(f)**. Diagram **(g)** shows the aortic arch and the branching vessels. The green dashed lines indicate the point at which the brachiocephalic artery was excised. Diagram **(h)** shows the heart from a front **(i)** and lateral **(ii)** view. The red dashed ellipse indicates the position of the aortic sinus, and the green dashed lines show the position and angle at which the heart was transected.

2.9 Histology, immunohistochemistry and morphometry

2.9.1 Materials

All histological cassettes, moulds and paraffin wax were purchased from Raymond A Lamb Ltd (now Thermo Fisher Scientific, Epsom, UK). Alcohols and xylene were also from Thermo Fisher Scientific. All stains, Polysine™ glass slides, coverslips and DPX resin were purchased from VWR International Ltd (Lutterworth, UK). Whatman® grade 1 filter paper was obtained from Whatman International (Maidstone, UK). Fine insect pins (#26002-20) were from Fine Science Tools (Heidelberg, Germany). Primary antibodies: mouse monoclonal anti-human α-smooth muscle actin (M0851; clone 1A4) and mouse monoclonal anti-human MAC387 (M074701) were supplied by Dako (Ely, UK), rat anti-mouse F4/80 (ab6640) was purchased from Abcam (Cambridge, UK), and rabbit polyclonal anti-$P2Y_{12}$ (APR-012) was from Alomone Labs (Jerusalem, Israel). Secondary antibodies: biotinylated goat anti-mouse IgG and goat anti-rat IgG were purchased from Vector Labs (Peterborough, UK), Alexa Fluor® 488 goat anti-mouse IgG H+L (A-11034) and Alexa Fluor® 594 goat anti-rabbit IgG H+L (A-11037), both highly cross adsorbed, were supplied by Invitrogen™ Life Technologies (Paisley, UK). Vectastain® ABC-HRP kit and Vectorshield® mounting media with DAPI (H-1200) was also from Vector Labs. Hydrogen peroxide (30% v/v), Triton X-100, Sigma*FAST*™ 3,3′-Diaminobenzidine tablets, and Tris buffered saline (TBS) powder (0.05 mol/L Tris, 0.138 mol/L NaCl, 2.7 mmol/L KCl) were from Sigma-Aldrich (Poole, UK). Trypsin 250 was obtained from BD Biosciences (Oxford, UK). Citric acid monohydrate was purchased from Alfa Aesar (Ward Hill, MA). Commercially available Marvel skimmed milk powder was used for immunohistochemistry.

2.9.2 Tissue preparation

2.9.2.1 Carotid and brachiocephalic arteries

Arteries (except aortae, see section 2.9.5.1) were removed from formalin or PBS, and each laid on a sheet of Whatman® grade 1 filter paper, straightened and a second sheet of filter paper placed on top, leaving the artery sandwiched in between. Each sample was labelled and placed in a plastic histological cassette for processing. Arteries were dehydrated through graded alcohols and xylene, prior to embedding in paraffin wax for cutting. Details of the dehydration protocol can be found in Appendix III (see section 10.3.2).

2.9.2.2 Aortic sinus and other tissues

Tissues were weighed prior to processing for histological analysis. Each organ was removed from formalin or PBS and gently shaken to remove excess liquid. Gross wet weights were measured on fine scales in micrograms (mg). Some tissues were also processed for histology.

As described in section 2.8.4.3, hearts were excised and transected along the midline below the atria. Both pieces of tissue were kept and weighed on fine scales to find the total heart

weight. The bottom half was then discarded and only the top half, containing the aortic sinus, retained and placed in a plastic cassette with filter paper. Organ tissues were first cut into 0.5 cm slices, using a scalpel blade, and 2 or 3 pieces placed in a cassette with filter paper. These were then dehydrated as outlined in Appendix III (see section 10.3.2).

2.9.3 Embedding in wax

2.9.3.1 Carotid and brachiocephalic arteries

The next day, following dehydration, in which samples were left overnight in molten wax, cassettes were taken from the oven. The arteries were removed and each placed horizontally at the base of a shallow plastic mould. Molten paraffin wax was then poured around the vessel and allowed to cool for 2-3 hours. Once set, the wax block was removed and trimmed down to a small cuboid shape containing the artery. This was then rotated and placed vertically in the centre of a deeper mould, placing the artery perpendicular to the base (see Figure 2.3). Fresh molten wax was then poured into the mould, around the cube, and a microtome block placed on top. The wax was left overnight to set. This process corrects the orientation of the artery in preparation for sectioning.

2.9.3.2 Aortic sinus and other tissues

For all other tissues, cassettes were removed from the oven, and each piece of tissue placed in the bottom of a shallow plastic mould with the flat surface facing down. In the case of the aortic sinus, this positioned the heart correctly to allow entire cross-sections of the sinus, including all 3 valve leaflets. Molten wax was then poured around the tissue and a microtome block placed on top. The blocks were allowed to set and harden overnight.

2.9.4 Tissue sectioning

Wax blocks were pressed from the moulds, and placed on ice for at least 1 hour prior to cutting on a Leica RM2135 microtome (Leica Microsystems, Wetzlar, Germany). Overnight storage of the wax blocks in a fridge can also aid the cutting process, particularly when sectioning in a warm room.

All vessel sections were cut to a 5 micron (μm) thickness and floated out on a water bath, heated to approximately 35°C, to flatten the sections. Aortic sinus and organ sections were cut slightly thicker, at 7 μm, to help ensure the tissue remained intact during transfer to the water bath. Sections were then mounted on Polysine™ glass slides by using the slide to ‘pick up’ the sections from the surface of the water bath. The slides were first allowed to air dry in racks, before placing them in an oven at 40°C overnight to dry completely and adhere to the coated slide surface. The following day, slides were removed from the drying oven and stored at room temperature until staining.

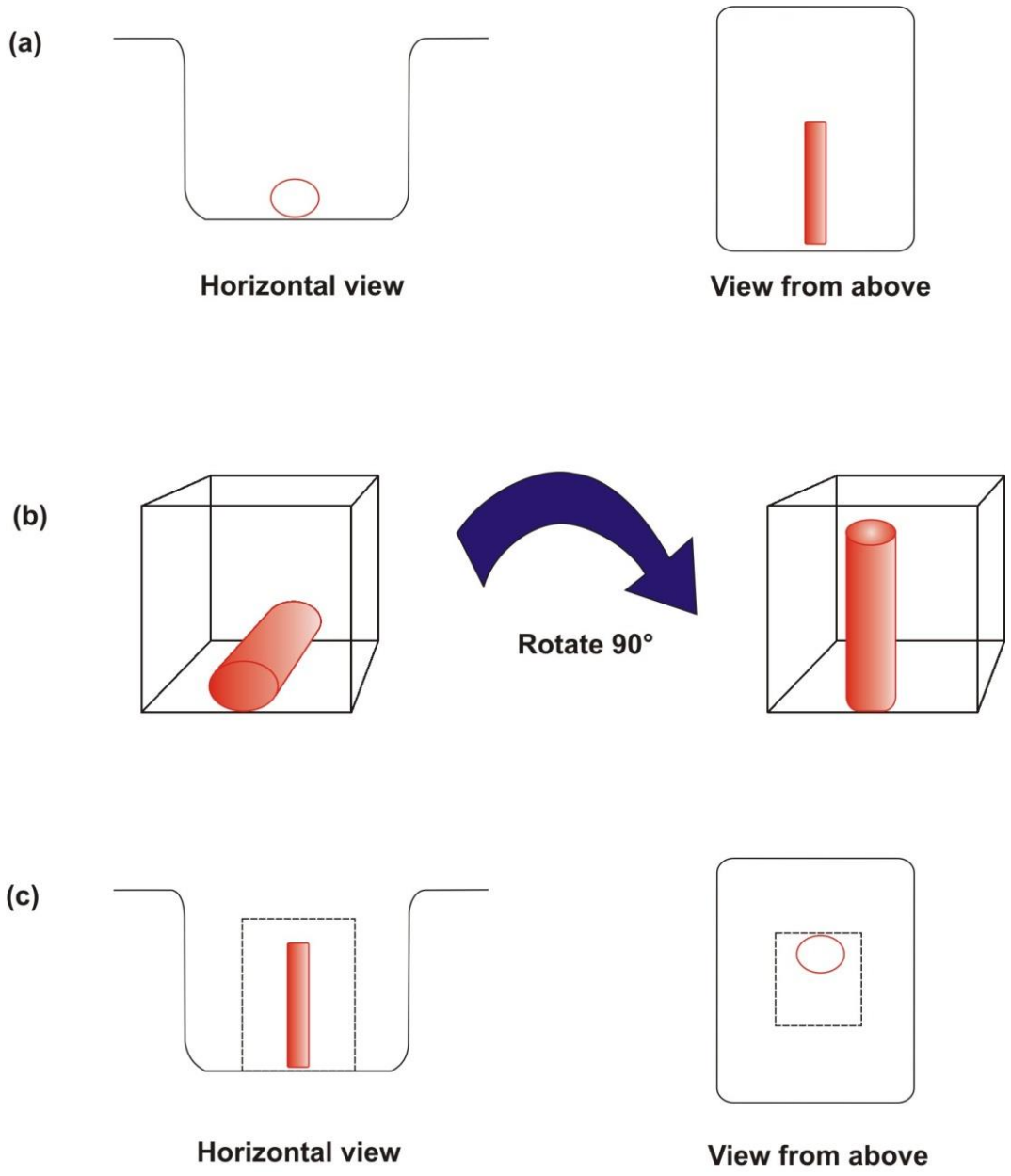

Figure 2.3 – Embedding of vessels.

To facilitate sectioning of vessels, a 2-step embedding process is needed to correctly orientate the vessels. First vessels were laid along the bottom of a plastic mould **(a)** and molten wax poured around the tissue. Once set, the block was removed from the mould and the excess wax trimmed away, leaving only a small cube containing the vessel. Next, this was rotated 90° **(b)** and placed in the bottom of another mould, with the vessel perpendicular to the base **(c)**. Molten wax was poured around the block and finally a microtome blocked placed on top. Once set, the block was pressed from the mould and was ready for sectioning.

2.9.4.1 Carotid and brachiocephalic arteries

Cross-sections were taken at intervals along the full length of the artery. Typically 10 x 5 µm sections were mounted onto 4 slides, encompassing a 50 µm length of vessel. An interval of 100 µm was then left between each set of 10 sections. This method of sectioning allowed assessment of the entire artery, and encompassed either the site of injury (ferric chloride injuries), or areas of atherosclerotic lesion (atherogenesis studies).

2.9.4.2 Aortic sinus

Blocks were cut until the appearance of the valve leaflets of the aortic sinus. Sections were then collected continually from this point onwards until the end of the sinus and the beginning of the aorta, leaving no intervals.

2.9.5 Histology

2.9.5.1 *En face* oil red O staining of whole aortae

Whole aortas were removed from PFA or PBS and stained *en face* with oil red O, an inert oil-soluble bis-azo dye for lipids. This is a sensitive technique, and is commonly used to identify and measure areas of atherosclerotic lesion, as previously described (Nunnari *et al.* 1989). For details of the staining protocol, see Appendix III (section 10.3.3).

Molten paraffin wax was poured into petri dishes and allowed to cool. Once the wax had set, aortae were positioned to expose the inside of the vessels and pinned onto the surface using fine insect pins, approximately 0.2 mm in diameter (Fine Science Tools, Heidelberg, Germany), with the aid of a magnifying lamp. When pinned, the vessels were covered with PBS before capturing images of each aorta.

2.9.5.2 Histological staining of tissue sections

Brachiocephalic artery, aortic sinus, carotid artery, and liver cross-sections were stained using histological dyes to identify tissue constituents and structure. Briefly, slides were dewaxed and rehydrated through graded alcohols to water. Sections were then stained using various protocols, including alcian blue/elastic van Gieson (EVG), haematoxylin and eosin (H&E), or martius scarlet blue (MSB). For details of these staining protocols, see Appendix III (section 10.3.3). Following staining, the tissue was dehydrated, and mounted with coverslips using DPX resin.

2.9.6 Immunohistochemistry

Aortic sinus sections were stained for α-smooth muscle actin (α-SMA), F4/80, and MAC387 using standard immunohistochemical techniques. Detailed protocols can be found in Appendix III (see section 10.3.4). Briefly, sections were dewaxed, rehydrated and blocked for both endogenous peroxidases with hydrogen peroxide, and non-specific antibody binding with milk buffer. Antigen retrieval was performed if necessary. Sections were incubated

with primary antibody for 1 hour at room temperature, or overnight at 4°C, followed by incubation with biotinylated secondary antibody (1:200 dilution in PBS) for 30 minutes at room temperature. Negative control sections were incubated in PBS only, followed by secondary antibody. Positive staining was amplified using avidin-biotinylated enzyme complexes with horseradish peroxidase (HRP), and detected using Sigma*FAST*™ 3,3′-diaminobenzidine tetrahydrochloride (DAB) as the substrate. Tissue was then counterstained with Carazzi's haematoxylin, dehydrated, and mounted with DPX.

2.9.7 Immunofluorescence

Aortic sinus sections were dual stained for α-SMA and $P2Y_{12}$ using immunofluorescence. A detailed protocol, including buffer constituents, can be found in Appendix III (section 10.3.5). Briefly, sections were dewaxed, rehydrated, and blocked for non-specific antibody binding with blocking buffer containing 5% v/v goat serum. Sections were then incubated with α-SMA (1:150) and $P2Y_{12}$ (1:100) primary antibodies in dilution buffer at 4°C overnight. Sections were then incubated with Alexa Fluor® 488 anti-mouse IgG and Alexa Fluor 594® anti-rabbit IgG secondary antibodies (1:200) for 2 hours at room temperature in the dark. Tissue was mounted using Vectashield® mounting medium with DAPI, and sealed with nail varnish.

2.9.8 Morphometry

Images of stained sections were captured using a camera mounted to a light microscope, or dissecting microscope for whole aortae, and analysed on NIS-elements software (Nikon Instruments, Kingston upon Thames, UK). Fluorescent images were captured using a Leica DM6000b fluorescence microscope with LMD BGR filter cube.

2.9.8.1 Quantification of lesions in whole aortae

Individual aortae were captured at x15 magnification, and the software was calibrated using an image of a ruler taken at the same magnification. This ensured all subsequent measurements were accurate and in the appropriate units. Total surface area of each aorta was measured by manually tracing the perimeter of the vessel. Areas of positive oil red O staining were then selected using a threshold function with hue, saturation, and intensity (HSI) filters to identify red regions in the image. Lesion area was quantified and expressed as a percentage of the total aortic surface area (see Figure 2.4). This method was then used to assess lesion area in the aortic arch and descending aorta regions.

2.9.8.2 Quantification of thrombus, neointima and lesions in vessels

Carotid and brachiocephalic artery sections were captured at either x100 or x200 magnification. Typically one section per 150 µm interval (approximately) was assessed along the length of the artery, generating a mean area for each of the vessel parameters measured. The internal and external elastic lamina area (IEL and EEL respectively) and

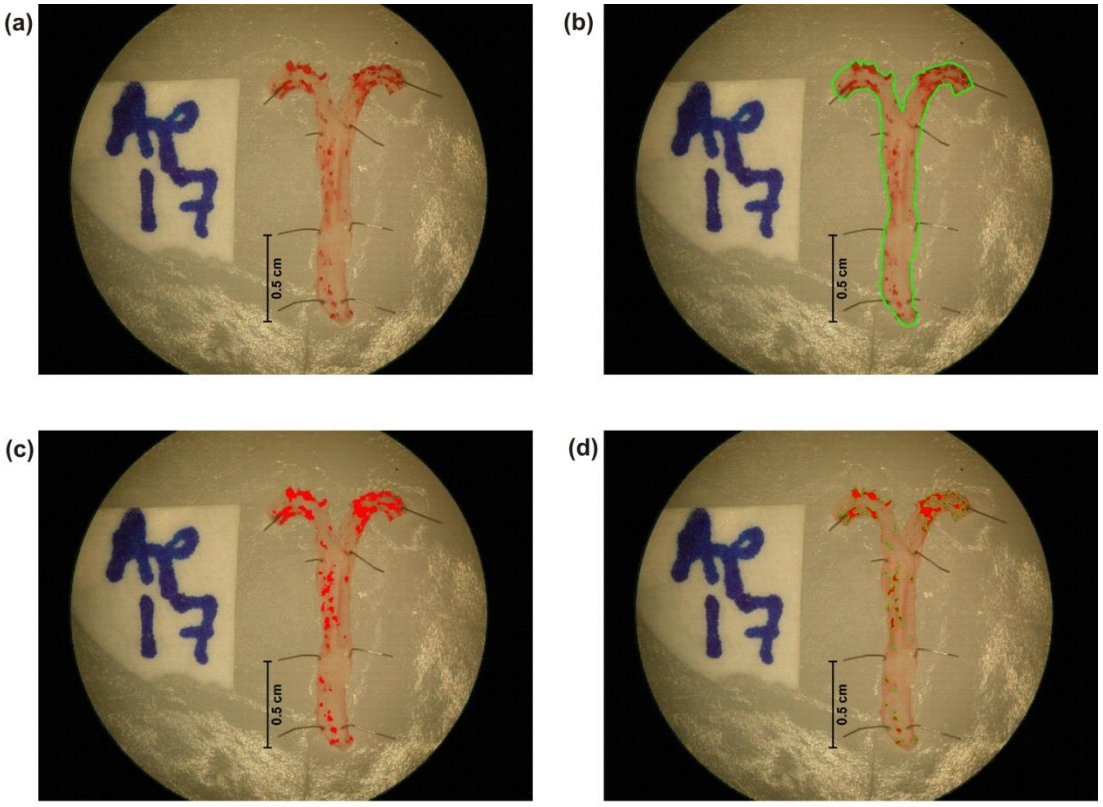

(e) ***Example:***

Total surface area (TSA) = 0.36cm^2

Number of objects = 60
Mean object area = 0.0007cm^2
Total lesion area (TLA) = 60 x 0.0007
= 0.042cm^2

% lesion area = (TLA/TSA) x 100
= (0.042/0.36) x 100
= 11.67%

Figure 2.4 – Quantification of *en face* oil red O staining of whole aortae.

(a) Image of a whole aorta stained with oil red O, showing positively stained areas in red. Original image captured at x15 magnification. **(b)** NIS-elements analysis software was used to calculate the total vessel area by manually tracing the perimeter of the vessel (outlined in green). **(c)** The software was then used to select areas of positive staining by using hue, saturation and intensity filters. Selected areas are highlighted in bright red. **(d)** The software then identified separate objects (outlined in green) and calculated the mean object area. **(e)** Shows a worked example of how the percentage lesion area was calculated. NIS-elements software was calibrated using an image of a ruler taken at the same magnification as the vessels. Scale bars = 0.5 cm.

circumference were measured by manually tracing the outer perimeter of the structures (see Figure 2.5). Due to the often fragmented nature of its structure, the thrombus, neointima, or lesion area were indirectly measured by quantifying lumen area, and subtracting this from the IEL. Luminal area was determined using a threshold function with red, green, and blue filters (RGB) to select the white area of the lumen.

Aortic sinus sections were captured at x40, x200, or x400 magnification. Typically 5 sections, each with 3 valves present, were assessed from each animal generating a mean area for each of the vessel parameters measured. Due to the presence of the valve leaflets, it was not possible to calculate lesion area by indirect measurement of the lumen, as with arterial sections. Instead, total lesion area was quantified by tracing around each individual lesion (see Figure 2.5).

Using the assumption that the vessels were originally circular, the circumference measurements were then used to re-calculate the IEL and EEL areas, to correct for any distortion of the vessel during processing (see below for calculation). Total cross-sectional area (CSA) of the vessel was attributed as c-EEL (corrected) area. Medial area was determined by subtracting c-IEL from c-EEL. Furthermore, to enable direct comparison between vessels of differing size, the thrombus:media (T/M), neointima:media (N/M) (Evans *et al.* 2009; Patil *et al.* 2010), and lesion:CSA (L/CSA) ratios (West *et al.* 2014) were also calculated.

Calculation for corrected area (using formulas for circle area):

$$\text{Circumference } (C) = 2\pi r \rightarrow \text{rearrange} \rightarrow r = C/2\pi$$

$$\text{Area of a circle} = \pi r^2$$

$$\text{Corrected area} = \pi(C/2\pi)^2$$

2.9.8.3 Quantification of collagen and α-smooth muscle actin

Collagen content of was determined using martius scarlet blue (MSB), and quantifying areas of blue positive staining within the lesions. Smooth muscle actin content was determined by immunohistochemistry using DAB, in which positive cells were stained with a brown precipitate. Similarly, as with oil red O, collagen and α-SMA content was measured using the threshold function with HSI filters to select areas of positive staining, which was then quantified and expressed as a percentage of the total lesion area.

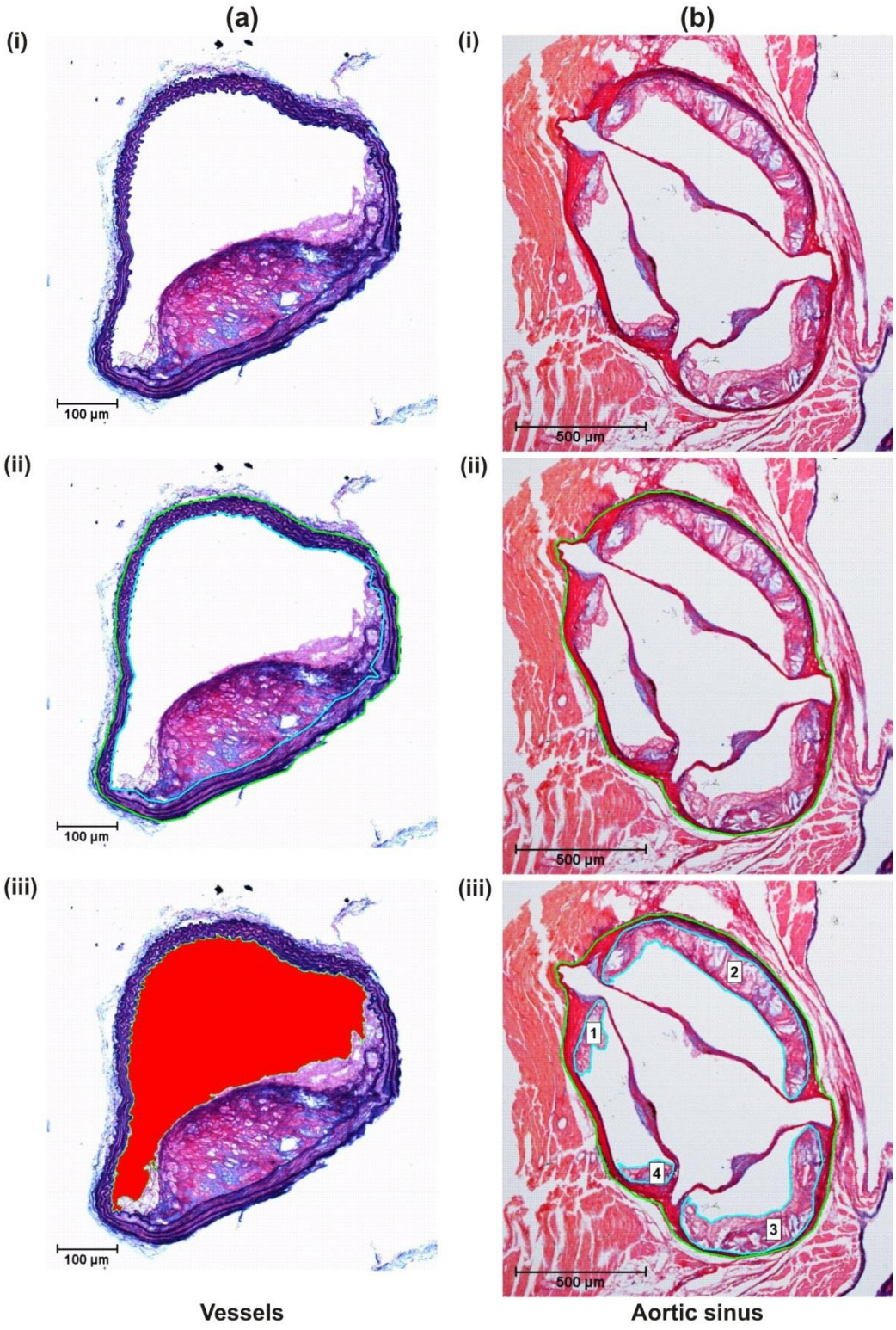

Figure 2.5 – Measurement of vessel and aortic sinus parameters using image analysis.

(a)(i) Original vessel image x100, scale bar = 100 µm. **(ii)** Using a polygon tool, the IEL (outlined in blue) and EEL (outlined in green) were manually traced. **(iii)** Lumen area was then selected using red, green, and blue (RGB) filters on the threshold function. Selected areas are highlighted in bright red. The software then measures the selected area (perimeter of area outlined in green). **(b)(i)** Original sinus image x40, scale bar = 500 µm. **(ii)** Using a polygon tool, the total CSA of the sinus was manually traced (outlined in green). **(iii)** Lesions were then traced (outlined in blue) and the individual areas (1-4) combined to give a total lesion area.

2.10 *In vitro* assays

2.10.1 Materials

An ultra-sensitive mouse insulin ELISA kit was purchased from Crystal Chem Inc. (Downers Grove, IL). PAR-4 TRAP peptide (AYPGKF) was synthesized by Almac Sciences (East Lothian, UK). All HT buffer reagents, EDTA, and formaldehyde (37% w/v) containing methanol for FACS fix, were from Sigma-Aldrich (Poole, UK). FITC anti-mouse CD62p and FITC isotype rat $IgG_1\lambda$ polyclonal antibodies were purchased from BD Pharmingen™ (BD Biosciences, Oxford, UK). PE anti-mouse JON/A (CD41/61) was purchased from Emfret Analytics (Eibelstadt, Germany). FACSFlow™ was obtained from BD Biosciences (Oxford, UK). Dade® Actin® FS; Innovin® thromboplastin; thrombin reagent; Owren's veronal buffer and standard human reference plasma (all Dade Behring, Liederbach, Germany) were supplied from Sysmex (Milton Keynes, UK).

2.10.2 Blood biochemistry

Plasma from $ApoE^{-/-}$ and $ApoE/P2Y_{12}$ DK mice fed on western and chow diet were sent to Sheffield Teaching Hospitals Biochemistry Department for analysis. A full lipid profile including high and low density lipoproteins (HDL and LDL), triglycerides, and cholesterol levels were obtained, plus liver enzymes, aspartate transaminase (AST), and alanine transaminase (ALT).

2.10.3 Insulin ELISA

Plasma from $ApoE^{-/-}$ and $ApoE/P2Y_{12}$ DK mice fed on western diet for 12 weeks was analysed by enzyme-linked immunosorbent assay (ELISA) to determine plasma insulin levels. Samples were prepared and processed according to the kit protocol for the low range assay (0.1 - 6.4 ng/mL), as previous data from our group showed insulin levels should fall within this range.

In brief, 5 µL of plasma or mouse insulin standard was added to 95 µL of sample diluent in antibody-coated microplate wells and allowed to incubate for 2 hours at 4°C. The plate was washed repeatedly before adding anti-insulin enzyme conjugate, and was allowed to incubate for a further 30 minutes at room temperature. The plate was again washed, and the enzyme substrate solution added before the final 40 minute incubation at room temperature. The reaction was stopped with 0.5 mol/L sulphuric acid and the absorbance measured at A_{450}, with the reference at A_{630}, on an Opsys MR™ plate reader (Dynex Technologies Ltd, East Grinstead, UK). A standard curve was generated using the absorbance of the insulin standards and the plasma samples read from the curve.

2.10.4 Platelet function studies

A flow cytometry based platelet function assay was carried out on blood taken from $ApoE^{-/-}$ and $ApoE/P2Y_{12}$ DK mice, to demonstrate either $P2Y_{12}$ deficiency or inhibition. Blood was

exposed to thrombin receptor activating protein (TRAP, AYPGKF), a potent platelet agonist of the protease-activated receptor (PAR)-4, to induce cell surface expression of P-selectin (CD62p) and activation of the receptor GPIIbIIIa (CD41/61), which are both markers of platelet activation. The presence of these activation markers were detected and quantified by flow cytometry, a method of using fluorescently labelled antibodies which bind specifically to their target receptor or marker, in this case either P-selectin or activated GPIIbIIIa.

Briefly, blood was collected via cardiac puncture into hirudin, as described in section 2.8.2. For each mouse 100 µL of blood was diluted into 1.9 mL HEPES-Tyrode's (HT) buffer (129.6 mmol/L NaCl, 8.8 mmol/L $NaHCO_3$, 2.8 mmol/L KCl, 800.9 µmol/L KH_2PO_4, 5.7 mmol/L dextrose, 10 mmol/L HEPES; see Appendix IV, section 10.4.1) and 20 µL (100 mmol/L) $CaCl_2$. Tubes were prepared with 10 µL fluorescein isothiocyanate (FITC) anti-CD62p (1:200 dilution in HT buffer), 5 µL phycoerythrin (PE) JON/A (anti-CD41/61, used neat), 2 µL PAR-4 TRAP (0, 0.1, 0.3, 1 or 3 mmol/L), and 33 µL diluted blood. Non-specific binding was determined by use of a FITC rat $IgG_1\lambda$ polyclonal isotype antibody in place of anti-CD62p, with no agonist. For JON/A (anti-CD41/61), ethylenediaminetetraacetic acid (EDTA, 100mmol/L, pH 8.0) was used in place of TRAP as an unstimulated control. Tubes were incubated in the dark for 20 minutes at room temperature, before adding 500 µL of either FACSFlow™ or FACS fix (1% v/v formaldehyde in PBS) to each tube. Samples were analysed on a BD™ LSRII flow cytometer using FACSDiva™ software (BD Biosciences, Oxford, UK). The platelet population was gated on forward versus side scatter plots and 10,000 events were collected. Expression was denoted as increase in median fluorescence of the entire platelet population over baseline values (Evans *et al.* 2009; West *et al.* 2014).

2.10.5 Coagulation studies

To determine any differences in thrombin and fibrin generation, activated partial thromboplastin time (aPTT) and prothrombin time (PT) were measured to assess the intrinsic (aPTT) and extrinsic (PT) coagulation pathways. Fibrinogen levels were a measure of the final common coagulation pathway.

Blood was taken, as described in section 2.8.2, from $ApoE^{-/-}$ and $ApoE/P2Y_{12}$ DK mice which had undergone BMT procedures. Samples were sent to Sheffield Teaching Hospitals Coagulation Department within 2 hours of blood withdrawal, for centrifugation to obtain plasma, and subsequent analysis.

Briefly, for aPTT, Dade® Actin® FS (containing phospholipids) was added to citrated plasma to activate the 'intrinsic' contact coagulation pathway, and the clotting time measured. PT was measured by adding Dade® Innovin® thromboplastin (containing tissue factor) to citrated plasma to activate the extrinsic coagulation pathway, and the clotting time measured. Finally, fibrinogen levels were determined by diluting citrated plasma in Dade®

Owren's veronal buffer, before adding thrombin reagent. Clotting time was measured and converted to a fibrinogen concentration by reference to a calibration curve of standard reference plasma. All steps were carried out by a Sysmex coagulation auto-analyser CA1500 or CS2100i, which were cross-calibrated by the manufacturer to give equivalent results (Sysmex, Milton Keynes, UK).

2.11 Statistics

Data are expressed as mean values and presented with standard error of the mean (SEM), or as individual data. Analyses were performed using Prism (Version 6; GraphPad, San Diego, CA) or SPSS software (Version 19; IBM, New York, NY).

Levene's test was performed on all data to assess for equality of variance. Where the *P* value yielded >0.05, equal variances were assumed, and the data was analysed using parametric tests, including the independent samples t test, one-, or two-way analysis of variance (ANOVA). The choice of post hoc test for one- and two-way ANOVA was dependent on the number of groups to be compared. Bonferroni's multiple comparison was used for datasets involving a small number of comparisons, whereas Tukey's multiple comparison was applied to those which required a large number of comparisons to be made. Significance was attributed to *P* values <0.05.

Where the Levene's test yielded a *P* value <0.05, equal variances were not assumed and the data was analysed using the Mann-Whitney test. In datasets involving multiple group comparisons, separate Mann-Whitney tests were performed for each group pair and the level of significance was adjusted to reflect the number of comparisons, such that significance was attributed to *P* values <0.01.

Genotype frequencies of the ApoE/P2Y$_{12}$ F$_2$ generation, in Chapter 4, were analysed using the Pearson's chi-squared test to assess whether this population followed the Hardy-Weinberg principle and test the null hypothesis that genotype frequencies remain constant within a population. Where the *P* value yielded <0.05, the null hypothesis was rejected.

Power analyses determined that, in the vascular injury model, a sample size of 6 was required to have a 90% power of detecting a difference in neointima:media ratio of 0.8 (standard deviation 0.4) with a 5% significance level. In atherogenesis studies, a sample size of 8 was required to have a 90% power of detecting a difference in lesion:CSA ratio of 0.05 (standard deviation 0.02) with a 5% significance level.

3 Investigating the role of $P2Y_{12}$ in the vessel wall response to vascular injury

Studying the vessel wall response to injury, using *in vivo* models, offers a useful insight into the processes which may be important in vessel repair following PCI, restenosis, plaque rupture, and atherothrombosis, as well as the inflammatory response atherogenesis, commonly termed as a 'response to injury'. A better understanding of these processes is vital to delivering effective treatment and management, and may improve clinical outcomes.

The development of neointima at the site of vascular injury is a wound healing response, preceded by the formation of an initial platelet-rich thrombus, which is remodelled primarily by invasion of smooth muscle and inflammatory cells (Steele *et al.* 1985; Harker 1987; Komatsu *et al.* 1998; Christen *et al.* 2001; Glover *et al.* 2002). Moreover, platelets are thought to further enhance this process via the release of pro-inflammatory cytokines and growth factors. Given that platelet activation is amplified and sustained by the $P2Y_{12}$ receptor (Storey *et al.* 2000), I hypothesised that $P2Y_{12}$ would play a key role in thrombus and neointima formation. In addition, I considered the use of the $P2Y_{12}$ antagonist clopidogrel in modulating these processes. Furthermore, $P2Y_{12}$ is also expressed on vascular smooth muscle cells (Wihlborg *et al.* 2004), and so bone marrow transplantations were employed to investigate the role of platelet versus vessel wall $P2Y_{12}$.

In this chapter, I investigated the role of $P2Y_{12}$ in thrombus and neointima formation using a murine ferric chloride injury model. Ferric chloride solution was topically applied to the outer surface of the right common carotid artery, resulting in localised endothelial denudation. I chose to use an established model, applying a 10% w/v ferric chloride solution for 3 minutes, which has been shown to produce occlusive thrombi within 10 minutes of application (Kurz *et al.* 1990; Farrehi *et al.* 1998; Konstantinides *et al.* 2001; Wang and Xu 2005), and neointima formation at 21 days post injury (Schafer *et al.* 2002).

3.1 $P2Y_{12}$ mediates thrombus and neointima formation following vessel wall injury

$P2Y_{12}^{+/+}$ and $P2Y_{12}^{-/-}$ mice underwent ferric chloride injury, and carotid arteries were harvested at either 30 minutes post injury, to assess thrombus, or 21 days following injury, to quantify neointima formation. For detailed methods refer to section 2.4.

3.1.1 Thrombus

At 30 minutes post injury, $P2Y_{12}^{-/-}$ mice demonstrated a significant reduction in thrombus compared to $P2Y_{12}^{+/+}$ controls (see Figure 3.1a and c): thrombus area was 0.039 ± 0.006 vs. 0.003 ± 0.001 mm^2 (+/+ vs. -/-; $P<0.001$). Similarly, thrombus was significantly attenuated in

$P2Y_{12}^{+/+}$ mice treated with clopidogrel (0.011 ± 0.003 mm^2 vs. +/+; *P*<0.05). As expected, luminal area was increased in those mice with reduced thrombus. No difference was noted between the mean media area of each group; however, vessel CSA was significantly larger in clopidogrel-treated mice compared to both untreated groups.

To minimise the effect of variations in vessel size, I also calculated thrombus:media ratio (T/M). Mirroring the attenuated thrombus formation, as seen in Figure 3.1a and c, T/M ratio was significantly attenuated in $P2Y_{12}^{-/-}$ mice compared to $P2Y_{12}^{+/+}$ controls (see Figure 3.1b): T/M ratio was 3.148 ± 0.379 vs. 0.257 ± 0.062 (+/+ vs. -/-; *P*<0.001). Likewise, in $P2Y_{12}^{+/+}$ mice treated with clopidogrel, T/M ratio was also significantly reduced (1.029 ± 0.300 vs. +/+; *P*<0.01).

3.1.2 Neointima

At 21 days post ferric chloride injury, neointima formation was quantified. $P2Y_{12}^{-/-}$ mice showed a substantial attenuation in neointimal area compared to $P2Y_{12}^{+/+}$ control mice (see Figure 3.2a and c): neointima area was 0.061 ± 0.006 vs. 0.011 ± 0.001 mm^2 (+/+ vs. -/-; *P*<0.001). Pharmacological inhibition of $P2Y_{12}$ in control mice with clopidogrel produced a similar reduction in neointima (0.003 ± 0.001 mm^2 vs. +/+; *P*<0.001). As a result, both $P2Y_{12}^{-/-}$ and $P2Y_{12}^{+/+}$ mice treated with clopidogrel exhibited a greater lumen area compared with untreated controls (*P*<0.001). No difference was noted between the mean media area of each group; however, CSA was slightly increased in $P2Y_{12}^{-/-}$ mice compared to clopidogrel treated mice.

The neointima:media ratio (N/M) was significantly attenuated in $P2Y_{12}^{-/-}$ mice compared to $P2Y_{12}^{+/+}$ controls (see Figure 3.2b): N/M ratio was 2.667 ± 0.273 vs. 0.4026 ± 0.029 (+/+ vs. -/-; *P*<0.001). Similarly, N/M ratio was greatly reduced in clopidogrel-treated mice compared to untreated controls (0.111 ± 0.049 vs. +/+; *P*<0.001).

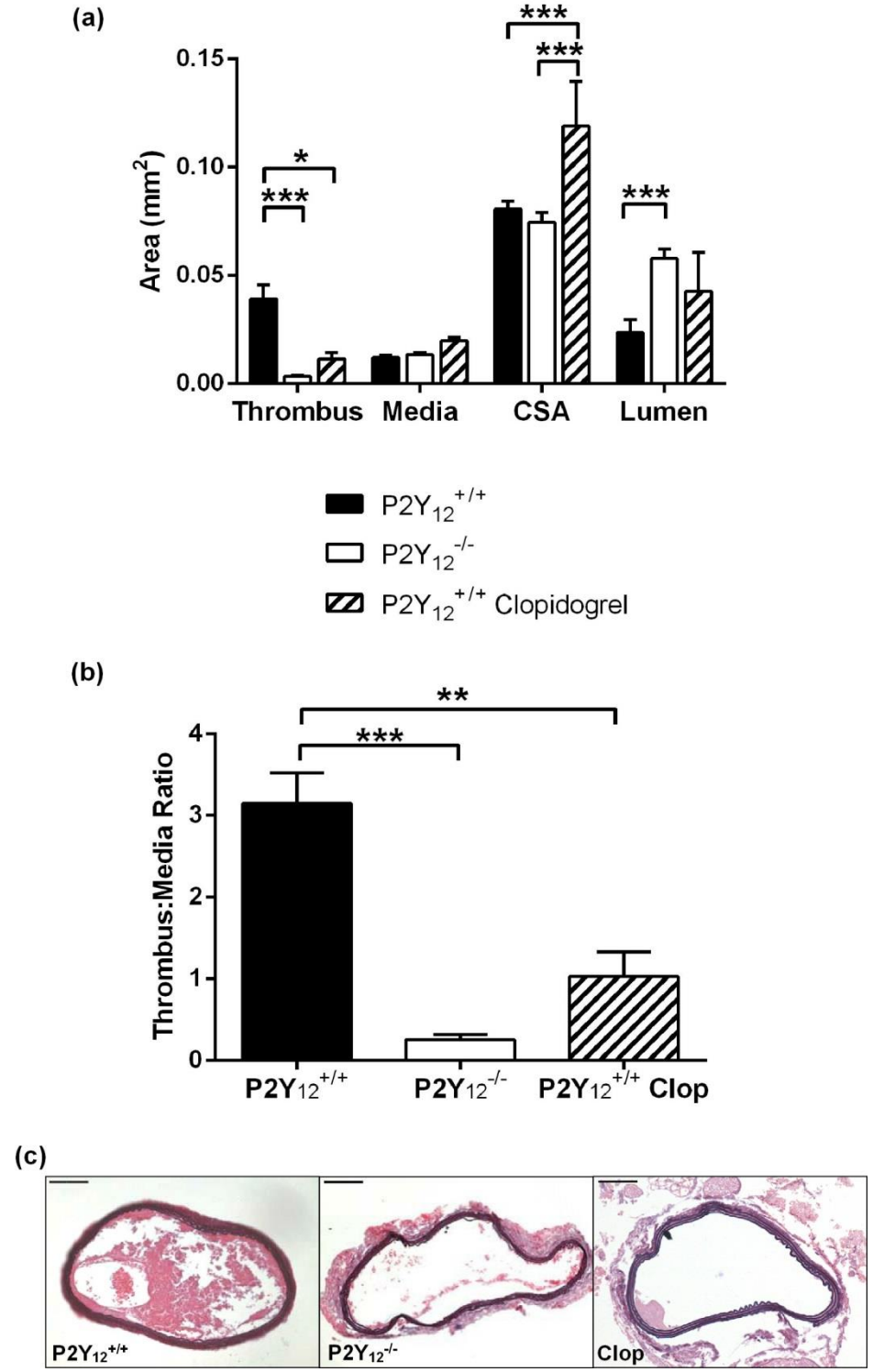

Figure 3.1 – Thrombus formation was attenuated in $P2Y_{12}^{-/-}$ mice, and clopidogrel-treated wild-types, at 30 minutes post ferric chloride injury.

Carotid arteries were excised from $P2Y_{12}^{+/+}$ (n=5), $P2Y_{12}^{-/-}$ (n=5), and $P2Y_{12}^{+/+}$ mice treated with clopidogrel (n=3) at 30 minutes post ferric chloride injury. Mice treated with clopidogrel were administered 20 mg/kg by gavage at 24 hours and 1-2 hours before surgery. **(a)** Thrombus, media, lumen, and cross-sectional area (CSA), and **(b)** thrombus:media ratio were calculated for each vessel. **(c)** Representative vessel cross-sections are shown. Images taken at x100 magnification, scale bar = 250 µm. Data are mean ± SEM; **P*<0.05, ***P*<0.01, ****P*<0.001; **(a)** two-way and **(b)** one-way ANOVA with Tukey's multiple comparison.

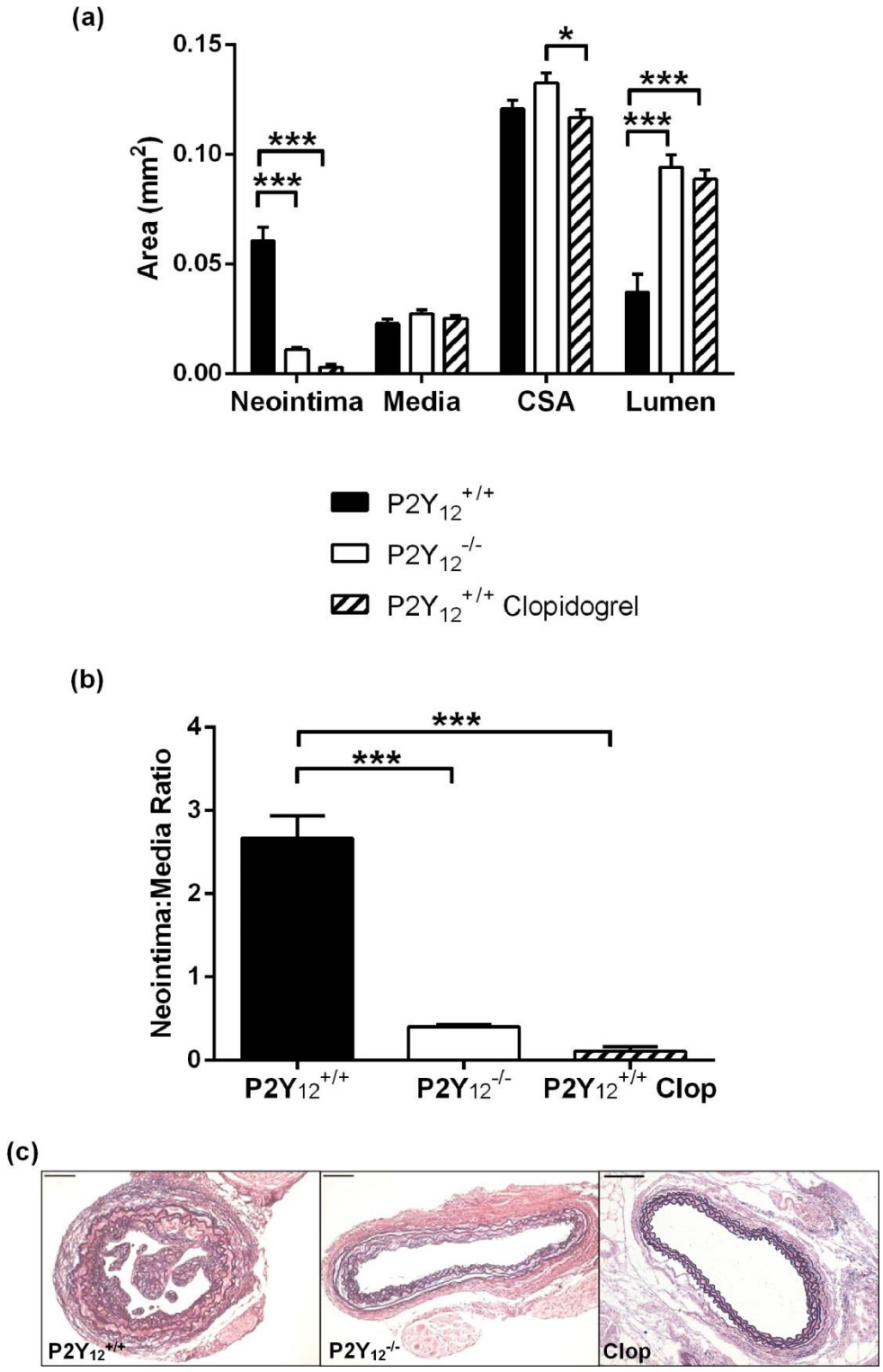

Figure 3.2 – Neointima formation was attenuated in $P2Y_{12}^{-/-}$ mice, and clopidogrel-treated wild-types, at 21 days post ferric chloride injury.

Carotid arteries were excised from $P2Y_{12}^{+/+}$, $P2Y_{12}^{-/-}$, and $P2Y_{12}^{+/+}$ mice treated with clopidogrel (all n=4) at 21 days post ferric chloride injury. Mice treated with clopidogrel were administered 20 mg/kg by gavage at 24 hours and 1-2 hours before surgery, followed by single daily doses. **(a)** Neointima, media, lumen, and cross-sectional area (CSA), and **(b)** neointima:media ratio were calculated for each vessel. **(c)** Representative vessel cross-sections are shown. Images taken at x100 magnification, scale bar = 250 µm. Data are mean ± SEM; **P*<0.05, ****P*<0.001; **(a)** two-way and **(b)** one-way ANOVA with Tukey's multiple comparison.

3.2 Short-term blockade of $P2Y_{12}$ attenuates neointima formation at 21 days post vessel injury

Following either long- or short-term treatment with clopidogrel or water, neointima formation at 21 days post ferric chloride injury was quantified. All mice treated with clopidogrel showed a non-significant trend towards reduced neointimal area compared to control mice given water (by gavage) (see Figure 3.3a): neointima area was 0.036 ± 0.011 in control mice, 0.006 ± 0.003 in short-term treated mice (*P*=0.056 vs. control), and 0.003 ± 0.001 mm^2 in long-term treated mice (*P*=0.032 vs. control). Furthermore, mice given only short-term treatment with clopidogrel, at the time of injury, demonstrated a similar reduction in neointimal area compared to those mice treated daily throughout the duration of the study. As expected, luminal area was increased in those mice with reduced neointima; however, there was no difference between the media or CSA of each group.

N/M was greatly reduced in clopidogrel-treated mice, compared to controls (see Figure 3.3b): N/M ratio was 1.453 ± 0.5039 in control mice, 0.191 ± 0.073 in short-term treated mice (*P*=0.056 vs. control), and 0.111 ± 0.049 in long-term treated mice (*P*=0.063 vs. control). As demonstrated in the neointimal areas, short-term treatment with clopidogrel was as effective as prolonged treatment in reducing neointima formation.

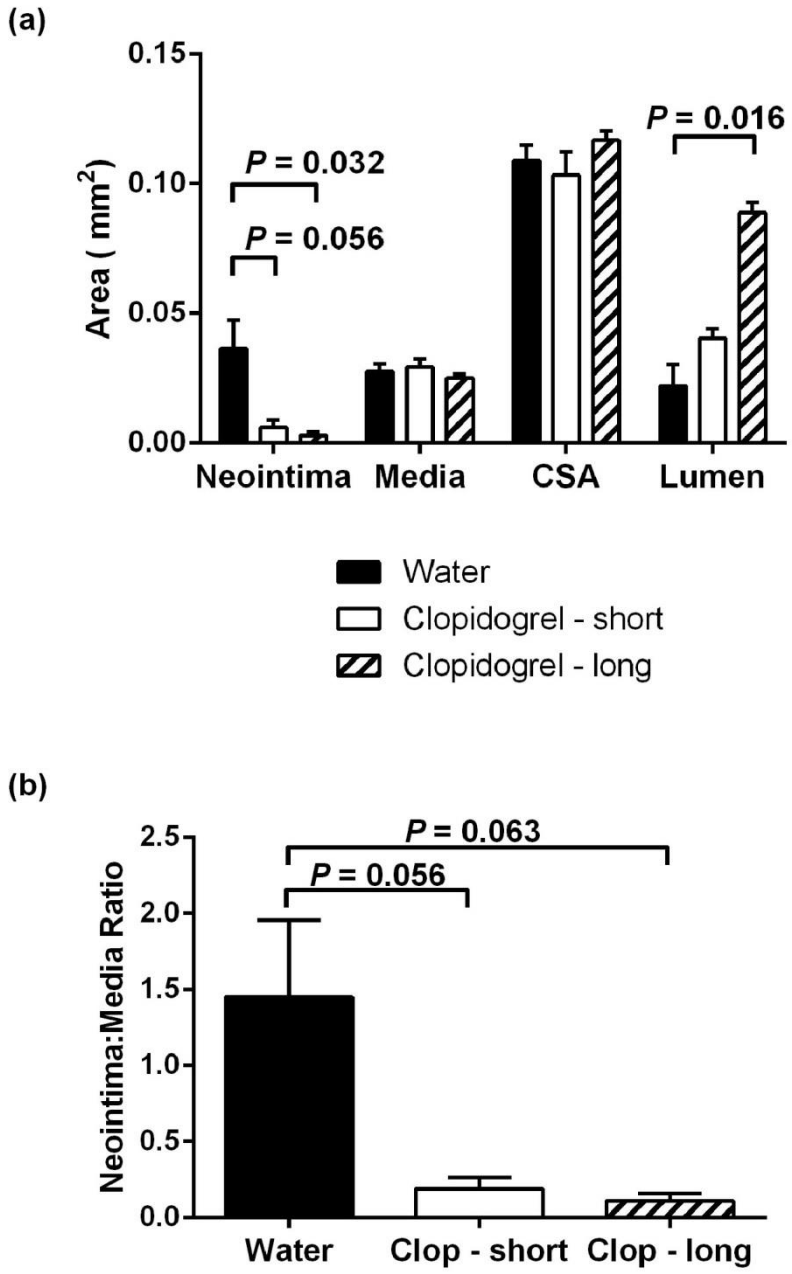

Figure 3.3 – Short-term clopidogrel treatment was as effective as prolonged treatment in attenuating neointima formation, at 21 days post ferric chloride injury.

Carotid arteries were excised from $P2Y_{12}^{+/+}$ mice treated with water (n=5), short-term (n=5), or long-term clopidogrel treatment (n=4) at 21 days post ferric chloride injury. For long-term treatments, mice were gavaged with either water or 20 mg/kg clopidogrel at 24 hours and 1-2 hours before surgery, followed by a single daily dose thereafter. Mice receiving short-term treatment were gavaged with clopidogrel 4 hours prior to injury followed by a final dose 24 hours after surgery. **(a)** Neointima, media, lumen, and cross-sectional area (CSA), and **(b)** neointima:media ratio were calculated for each vessel. Data are mean ± SEM; *P*=ns; Mann-Whitney test (adjusted level of significance *P*<0.01 for multiple group comparisons).

3.3 Neointima formation is predominantly platelet, rather than vascular smooth muscle cell, $P2Y_{12}$-mediated

$P2Y_{12}^{+/+}$ and $P2Y_{12}^{-/-}$ mice underwent BMT to generate 2 control and 2 chimeric groups, deficient in either platelet or vessel wall $P2Y_{12}$. Ferric chloride injury was performed 5 weeks after transplantation, and neointima formation at 21 days post injury was assessed.

Chimeric mice deficient in platelet, but not vessel wall, $P2Y_{12}$ demonstrated a significant reduction in neointimal area compared to $P2Y_{12}^{+/+}$ controls (see Figure 3.4a): neointima area was 0.0233 ± 0.0067 in control mice and 0.001 ± 0.0004 mm^2 in platelet $P2Y_{12}$-deficient mice (P<0.05 vs. control). As expected, neointima was also reduced in mice completely deficient in $P2Y_{12}$ (0.0021 ± 0.001 vs. control; P<0.05). Interestingly mice which did express platelet $P2Y_{12}$, but were vessel wall $P2Y_{12}$-deficient, did not demonstrate any significant effects on neointima formation compared to control mice (0.0171 ± 0.0062 vs. control; P=ns).

This pattern of results was also mirrored when assessing N/M ratio, with mice deficient in platelet $P2Y_{12}$ having a significantly attenuated N/M ratio compared to control mice (see Figure 3.4b): N/M ratio was 0.9247 ± 0.2984 in control mice and 0.0343 ± 0.011 in platelet $P2Y_{12}$-deficient mice (P<0.01 vs. control). The N/M ratio was also reduced in mice completely deficient in $P2Y_{12}$ (0.0796 ± 0.0352 vs. control; P=0.011). Similarly, vessel wall $P2Y_{12}$-deficiency alone did not have any significant effects on the N/M ratio (0.4996 ± 0.1653 vs. control; P=ns).

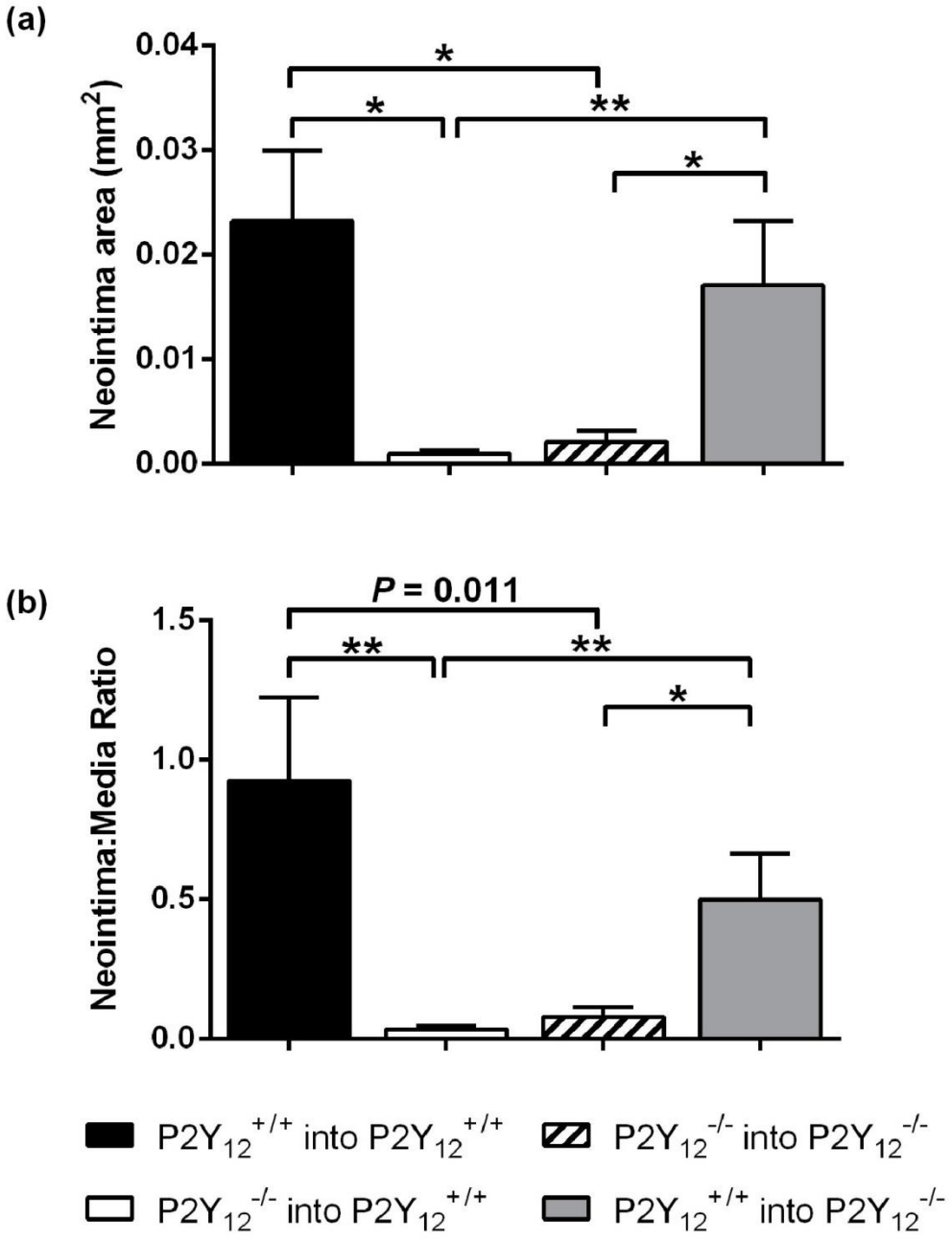

Figure 3.4 – Bone marrow transplantation indicated neointima formation, following ferric chloride injury, was predominantly platelet, rather than vascular smooth muscle cell, $P2Y_{12}$-mediated.

$P2Y_{12}$ mice underwent bone marrow transplantation to generate chimeric groups: $P2Y_{12}^{+/+}$ into $P2Y_{12}^{+/+}$ (n=9), $P2Y_{12}^{-/-}$ into $P2Y_{12}^{+/+}$ (n=8), $P2Y_{12}^{-/-}$ into $P2Y_{12}^{-/-}$ (n=8), and $P2Y_{12}^{+/+}$ into $P2Y_{12}^{-/-}$ (n=11). Ferric chloride injury was performed 5 weeks following transplantation, and carotid arteries were excised 21 days post injury. **(a)** Neointima and **(b)** neointima:media ratio were calculated for each vessel. Data are mean ± SEM; **P*<0.01, ***P*<0.001; Mann-Whitney test (adjusted level of significance *P*<0.01 for multiple group comparisons).

3.4 Summary

This chapter has described the contribution of platelet $P2Y_{12}$ receptor in the vessel wall response to injury, by examining thrombus and neointima formation following ferric chloride induced vascular injury. In summary:

- $P2Y_{12}$-deficient mice had significantly less thrombus at 30 minutes after injury, compared to wild-type ($P2Y_{12}^{+/+}$) control mice.
- Pharmacological inhibition of $P2Y_{12}$ in wild-type mice, using clopidogrel, resulted in a similar reduction in thrombus compared to untreated animals.
- Likewise, $P2Y_{12}$ deficiency or inhibition also lead to significantly attenuated neointima formation compared to control, at 21 days following injury.
- Further studies demonstrated that only short-term clopidogrel treatment, of 2 doses before and one immediately after injury, was required to cause a reduction in neointima at 21 days, as seen with prolonged (daily) clopidogrel treatment.
- Bone marrow transplantations revealed platelet $P2Y_{12}$-deficient mice had significantly attenuated neointima at 21 days, compared to $P2Y_{12}^{+/+}$ control mice, and demonstrated a similar reduction to mice completely deficient in $P2Y_{12}$.
- Vessel wall $P2Y_{12}$-deficiency alone had little effect on neointima formation.

3.5 Discussion

The fundamental role of platelets, and specifically the $P2Y_{12}$ receptor, in thrombosis is irrefutable, with $P2Y_{12}$ inhibitors forming a key component of acute coronary syndrome treatments (Yusuf *et al.* 2001; Wiviott *et al.* 2007; Wallentin *et al.* 2009). However, their involvement in restenosis and the vascular response to injury was less clear. In this chapter, I demonstrated that $P2Y_{12}$ indeed mediates the vessel wall response to injury, and show a clear relationship between the initial thrombus and subsequent neointima formation. These data reaffirm the importance of $P2Y_{12}$ inhibitor treatment following PCI in the prevention of restenosis and provide a rationale for further investigation into the role of $P2Y_{12}$ in atherogenesis.

In vivo models of thrombosis and neointima formation induce vessel injury via a range of methods, including by chemical or mechanical means. In this study I used the application of a 10% w/v ferric chloride solution, which results in vessel denudation following ferric ion oxidation of endothelial cells (Tseng *et al.* 2005), and causes the rapid formation of occlusive thrombi (Kurz *et al.* 1990; Farrehi *et al.* 1998). Although traditionally employed in thrombosis research, ferric chloride injury has also been used to study neointima formation (Zhu *et al.* 2001; Schafer *et al.* 2002), for which the less thrombogenic mechanical methods of wire injury and ligation are usually applied.

At 30 minutes and 21 days post ferric chloride injury, thrombus and neointima area were assessed, respectively. Differences observed in vessel CSA represented the variation in animal size between groups, and so the thrombus or neointima to media ratios were calculated to account for these differences. $P2Y_{12}$-deficiency led to a substantial reduction in thrombus and neointimal area, the effects of which were reproduced by treatment with the $P2Y_{12}$ antagonist, clopidogrel. Furthermore, as $P2Y_{12}$ is expressed on VSMCs as well as platelets (Wihlborg *et al.* 2004), bone marrow transplants revealed that platelet, but not vessel wall, $P2Y_{12}$ was responsible for potentiating neointima formation.

The effects of $P2Y_{12}$-deficiency or inhibition on thrombosis have been reported previously (Andre *et al.* 2003; Wang and Xu 2005); however, a role for $P2Y_{12}$ in neointima formation had, until now, only been inferred from clinical trial data, demonstrating a reduction in repeat vessel revascularisation post-PCI following clopidogrel (Mehta *et al.* 2001; Steinhubl *et al.* 2002), ticagrelor (Wallentin *et al.* 2009), or prasugrel treatment (Wiviott *et al.* 2007). Neointima development is characterised by the accumulation and proliferation of VSMCs and macrophages within the vessel intima, and a role for platelets in this process has been implicated in several studies. Transgenic mouse lines have revealed P-selectin is required for neointima formation, and cite its role in mediating leukocyte rolling and adhesion as the mechanism by which it promotes neointima (Manka *et al.* 2001). Further investigation demonstrated platelet, rather than endothelial, P-selectin was responsible for these effects (Manka *et al.* 2004). By enabling the formation of platelet-leukocyte conjugates, P-selectin allows leukocyte arrest onto thrombus, at the site of injury, and subsequent infiltration. Furthermore, P-selectin is required for the deposition of platelet RANTES onto the surface of leukocytes and the endothelium, which further promotes leukocyte recruitment (Schober *et al.* 2002). Investigation into the expression of another chemokine revealed MCP-1 binds to the surface of platelets and results in monocyte arrest onto these cells (Schober *et al.* 2004). Platelets also induce VSMC migration and proliferation through release of PDGF (Schini-Kerth *et al.* 1997; Massberg *et al.* 2003), and blockade of PDGF via antibody treatment has been attributed to a reduction in neointima (Ferns *et al.* 1991).

From this evidence it is clear that platelets have a substantial role to play in promoting neointima formation through the recruitment of leukocytes, by deposition of chemokines RANTES and MCP-1, and enabling their adhesion onto thrombus at the site of injury via P-selectin. In addition, platelets induce mitogenic effects on VSMCs by release of growth factors. It is apparent that these platelet effects commence from the initial thrombus formation at the site of vascular injury, allowing the infiltration of leukocytes and VSMCs, and thus causing the eventual remodelling of thrombus into neointima. By inhibiting $P2Y_{12}$ using clopidogrel, thrombosis is virtually abolished and, with little thrombus present, all ensuing platelet-mediated effects on neointima development are eliminated. Short-term clopidogrel treatment demonstrated that $P2Y_{12}$ inhibition is only required at the time of injury to instigate

these effects, highlighting the innate relationship between thrombosis and neointima formation. This is supported by similar data showing a single treatment with either a P-selectin or PSGL-1 antibody at the time of vessel injury was sufficient to cause a reduction in later neointima formation, due to the blockade of platelet interactions with the vessel wall and leukocytes (Phillips *et al.* 2003).

However, it must also be noted that clopidogrel binds irreversibly to the $P2Y_{12}$ receptor, and so its inhibitory effects would have been sustained for several days after the final dose, despite only short-term treatment, until clopidogrel-bound platelets were removed naturally from the body. Clopidogrel activity is therefore dependent on platelet turnover. This is highlighted by Gurbel *et al.* who compared the offset of platelet inhibition by clopidogrel and ticagrelor, i.e. how these drugs wore off over time, in the ONSET/OFFSET clinical study (Gurbel *et al.* 2009). Following a final dose of drug, platelet inhibition was sustained for a longer period in patients that had received clopidogrel, compared to those that were given the reversible drug ticagrelor, in which the antiplatelet effects diminished at a much quicker rate. Further work into the relationship between the timing of $P2Y_{12}$ inhibition and neointima formation, using ticagrelor, has been pursued by our group and confirms that $P2Y_{12}$ inhibition is indeed required at the time of injury, both before and immediately after, in order to prevent neointimal hyperplasia (Patil *et al.* 2010). In addition, the clear role of platelet $P2Y_{12}$ in neointima formation is also evident following a more moderate injury method compared to ferric chloride, using the less thrombogenic wire injury model, as demonstrated by our group (Evans *et al.* 2009).

These data demonstrate the crucial role for $P2Y_{12}$ in the vessel wall response to injury, and validate the importance of $P2Y_{12}$ inhibition in the prevention of thrombosis and restenosis following PCI. Despite evidence to show the clear interaction of platelets with the inflammatory response, little is known of their direct impact on atherogenesis. Given the importance of $P2Y_{12}$ in the development of neointima, I was interested to investigate its role in lesion formation using a model of atherogenesis. In the following chapter, I discuss the development of a novel ApoE/$P2Y_{12}$ double knockout mouse colony in which to test this hypothesis.

4 Physiological and metabolic phenotype of the ApoE/$P2Y_{12}$ double knockout mouse during atherogenesis

Given that platelets, and in particular the $P2Y_{12}$ receptor, are highly influential in the development of thrombus and neointima following arterial injury, and that blockade of $P2Y_{12}$ leads to a dramatic reduction in both (see Chapter 3), I was interested to further investigate the role of $P2Y_{12}$ in an inflammatory setting, during atherogenesis.

The $ApoE^{-/-}$ mouse is a well-established model for studying atherosclerosis, and is favoured due to the similarities seen in lesion composition and development, as compared to human disease (Nakashima *et al.* 1994). In order to investigate the role of $P2Y_{12}$ in atherogenesis, an ApoE/$P2Y_{12}$ double knockout (DK) mouse strain was generated from crossing existing in-house $ApoE^{-/-}$ and $P2Y_{12}^{-/-}$ colonies. As a novel transgenic line, the phenotype of this strain was unknown, and was therefore compared to the $ApoE^{-/-}$ parent line. This chapter outlines the generation of the ApoE/$P2Y_{12}$ DK colony, and describes the characterisation of the physiological and metabolic phenotype of an ApoE/$P2Y_{12}$ DK mouse.

4.1 Generation of an ApoE/$P2Y_{12}$ double knockout mouse strain

Established in-house $ApoE^{-/-}$ and $P2Y_{12}^{-/-}$ colonies were crossed to generate F_1 and F_2 ApoE/$P2Y_{12}$ generations. Offspring were genotyped to select ApoE/$P2Y_{12}$ DK animals as breeding pairs from which to establish the colony.

4.1.1 Genotyping

PCR was performed using DNA extracted from ear clips and primers specific to both the ApoE and $P2Y_{12}$ genes. The original $ApoE^{-/-}$ strain, generated by Nobuyo Maeda (Piedrahita *et al.* 1992), and $P2Y_{12}^{-/-}$ strain, by Madhu Chintala (Foster *et al.* 2001), were developed using a neomycin resistance cassette to disrupt the desired gene. Therefore a set of 3 primers were used to determine homozygotes and heterozygotes. The first primer was common to both wild-type and mutant (knockout) genes; the second was specific to the neo-insert of the mutant gene, and the third corresponded to only the wild-type gene (see Figure 4.1a). In each case, either single (homozygote) or double (heterozygote) bands were produced. The genotype was determined by the length of PCR product.

The primary cross produced an F_1 generation that was heterozygous for both the $P2Y_{12}$ and ApoE genes, demonstrated by the presence of a double band, as shown in Figure 4.1b(i) ($P2Y_{12}$ gel not shown). Heterozygotes were paired to produce an F_2 generation and all mice

were assessed for ApoE genotype in order to select candidate $ApoE^{-/-}$ mice. These were identified by a single PCR product, 245bp in length, as shown in Figure 4.1b(ii) (lanes 4, 5, 9, 10, 16, 17 and 19). Only $ApoE^{-/-}$ mice were then genotyped for the $P2Y_{12}$ gene to select $P2Y_{12}^{-/-}$ animals, denoted by a single band 650bp in length (see Figure 4.1b(iii); lanes 4, 7, 10, 11 and 14). The ApoE/$P2Y_{12}$ DK mice identified were used for establishing the colony.

4.1.2 Genotype frequencies

The F_2 generation, derived from heterozygotes, had 16 possible outcomes, of which only 1 in 16 would be the desired ApoE/$P2Y_{12}$ DK genotype (see Figure 4.2a). The entire F_2 generation (n=119) was genotyped, and the observed and expected frequencies of each genotype are shown in Figure 4.2c. Pearson's chi-squared test (see Figure 4.2b) was applied to test the null hypothesis that genotype frequencies will remain constant within a population, as stated in the Hardy-Weinberg principle. As $P<0.05$ the null hypothesis was rejected ($P=0.0366$).

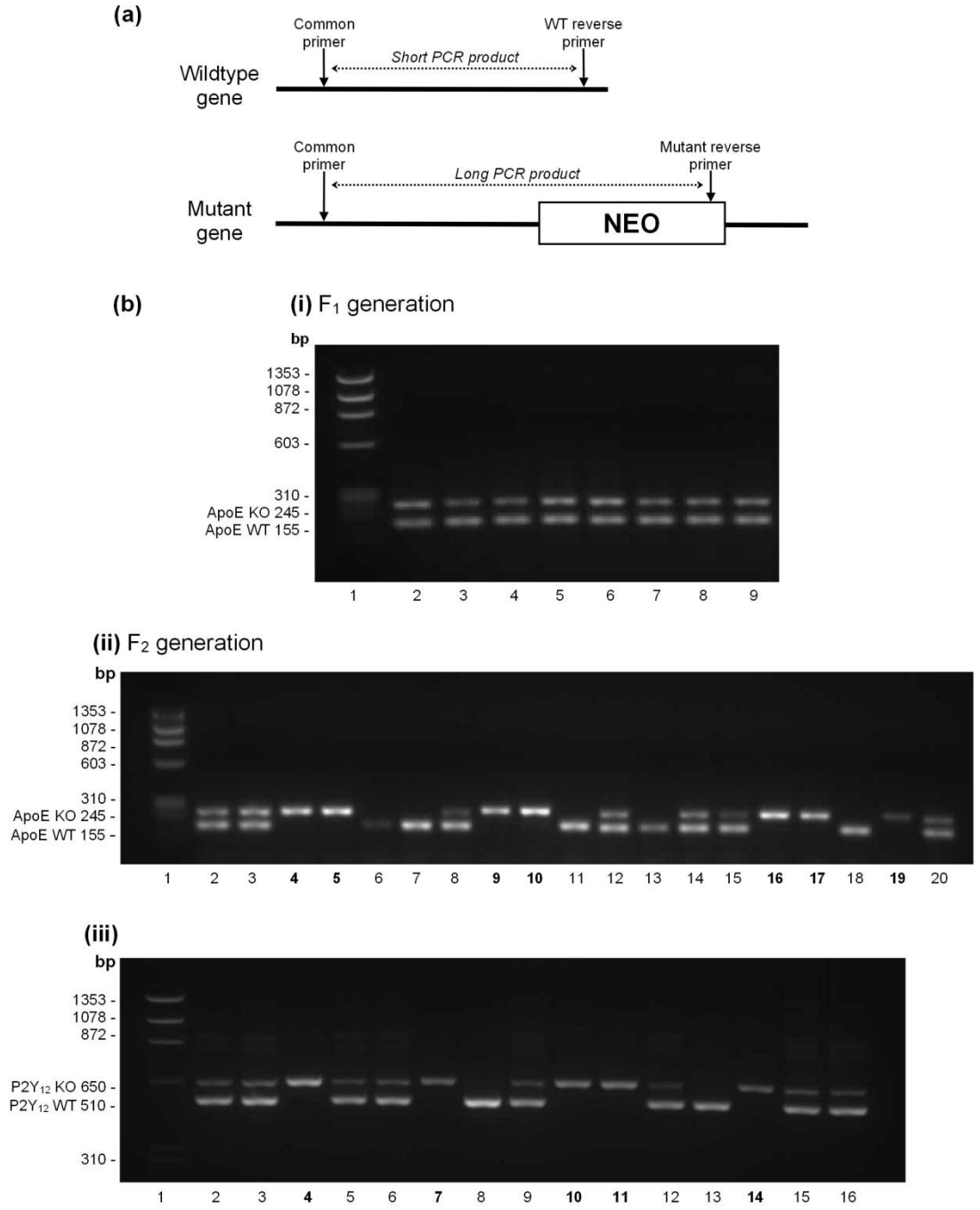

Figure 4.1 – Generation of an ApoE/P2Y$_{12}$ double knockout colony.

Mice were genotyped by PCR using primers specific to either the ApoE or P2Y$_{12}$ gene. **(a)** The first primer was common to both wild-type (WT) and mutant (KO) genes; the second was specific to the neo-insert of the mutant gene, and the third corresponded to only the wild-type gene. In each case, either single (homozygote) or double (heterozygote) bands were produced. The genotype was determined by the length of PCR product**,** referenced against Phix174/HAEIII DNA marker shown in lane 1 of each gel. **(b)(i)** ApoE$^{-/-}$ and P2Y$_{12}^{-/-}$ in-house parent colonies were crossed to produce an F_1 generation, heterozygous for both the P2Y$_{12}$ and ApoE genes (ApoE gel shown). Heterozygotes were paired to produce the F_2 generation. **(ii)** All mice were first genotyped for ApoE to select ApoE$^{-/-}$ mice (lanes 4, 5, 9, 10, 16, 17 and 19). **(iii)** ApoE$^{-/-}$ mice were then genotyped for P2Y$_{12}$ to select ApoE/P2Y$_{12}$ DK mice for future breeding (lanes 4, 7, 10, 11 and 14).

(a)

	AP	***Ap***	***aP***	***ap***
AP	AAPP	AAPp	AaPP	AaPp
Ap	AAPp	AApp	AaPp	Aapp
aP	AaPP	AaPp	aaPP	aaPp
ap	AaPp	Aapp	aaPp	**aapp**

Key: **A** – ApoE wild-type allele **P** - $P2Y_{12}$ wild-type allele

a - ApoE knockout allele **p** - $P2Y_{12}$ knockout allele

(b)

$$\chi^2 = \sum \frac{(O_i - E_i)^2}{E_i}$$

O_i = observed frequency

E_i = expected frequency

(c)

	AAPP	***AApp***	***AAPp***	***AaPP***	***AaPp***	***Aapp***	***aaPp***	***aaPP***	***aapp***
O_i	15	10	8	18	27	9	19	6	**7**
E_i	7.4375	7.4375	14.875	14.875	29.77	14.875	14.875	7.4375	**7.4375**

$\chi^2 = 16.4285$

Degrees of freedom = n - 1 = 8

P = 0.0366

Figure 4.2 – Genotype frequencies and Pearson's chi-squared test of the ApoE/$P2Y_{12}$ F_2 generation.

(a) An F_2 generation was created from crossing the F_1 generation of heterozygotes, which produced 16 possible outcomes, of which only 1 in 16 was expected to be the desired ApoE/$P2Y_{12}$ DK genotype (highlighted in bold). Pearson's chi-squared test **(b)** was applied to test the null hypothesis that genotype frequencies will remain constant within a population (Hardy-Weinberg principle). **(c)** The observed and expected frequencies of each genotype were calculated for the ApoE/$P2Y_{12}$ F_2 population (n=119), and the chi-squared value calculated.

4.2 ApoE/P2Y$_{12}$ double knockout mice demonstrate reduced platelet reactivity

The P2Y$_{12}$ phenotype of platelets from ApoE$^{-/-}$ and ApoE/P2Y$_{12}$ DK mice was further confirmed by a functional assay measuring P-selectin (CD62p) and activated GPIIbIIIa receptor (CD41/61) expression in response to TRAP, which acts via the PAR-4 receptor. Stimulation via the thrombin receptor induces a strong platelet activation response that leads to release of ADP from the platelet dense granules and consequent amplification by P2Y$_{12}$, so that TRAP-induced platelet activation provides a useful measure of P2Y$_{12}$ inhibition or deficiency.

Platelets from ApoE$^{-/-}$ mice displayed high fluorescence of the CD62p and CD41/61 JON-A antibodies, demonstrating these platelets expressed high levels of both P-selectin and activated GPIIbIIIa receptors (see Figure 4.3a and b). In contrast, platelets from ApoE/P2Y$_{12}$ DK mice showed attenuated platelet activation, and exhibited much lower fluorescence levels, shown as a shift to the left in the fluorescence peaks for each antibody. Baseline fluorescence was determined using an isotype (CD62p) or EDTA unstimulated control (CD41/61 JON-A).

CD62p and CD41/61 JON-A fluorescence was measured in response to a range of PAR-4 TRAP concentrations, in addition to a saline control, which showed the cells were not pre-activated. Expression was measured as an increase in median fluorescence over baseline. At each concentration, ApoE$^{-/-}$ mice demonstrated consistently higher P-selectin (Figure 4.3c) and activated GPIIbIIIa receptor expression (Figure 4.3d) compared to ApoE/P2Y$_{12}$ DK mice. This was particularly evident at 3 mmol/L TRAP for which P-selectin median fluorescence was 3088 ± 561 vs. 256 ± 38 (ApoE$^{-/-}$ vs. ApoE/P2Y$_{12}$ DK; P<0.001) and GPIIbIIIa median fluorescence was 24502 ± 2284 vs. 4181 ± 481 (P<0.001). A similar response was also seen for 1 mmol/L TRAP. Attenuated expression of these activation markers confirmed a functional platelet deficiency, and demonstrated reduced platelet reactivity in ApoE/P2Y$_{12}$ DK mice. These results were consistent with our previous findings on P2Y$_{12}^{-/-}$ mice (Evans *et al.* 2009).

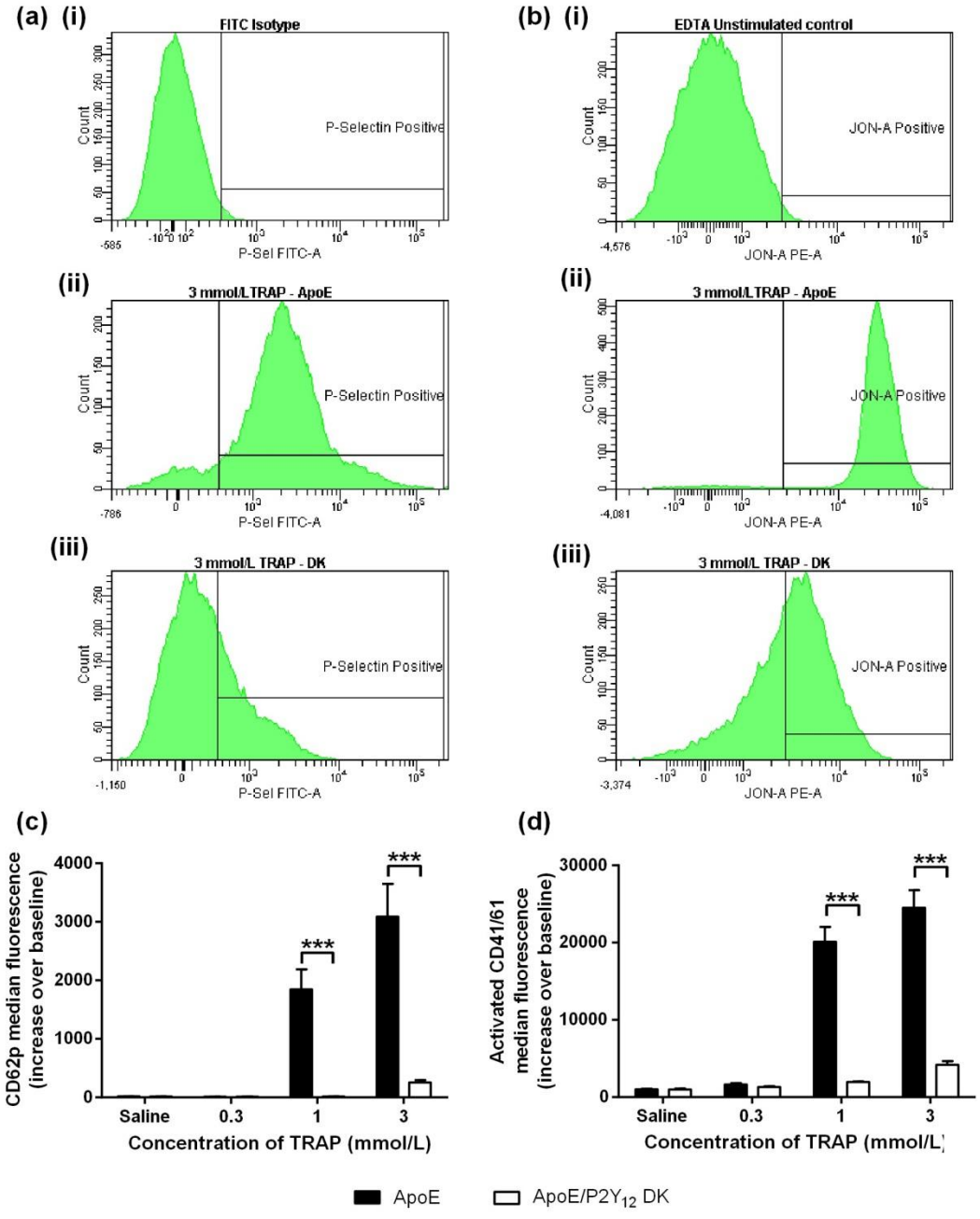

Figure 4.3 – ApoE/P2Y$_{12}$ double knockout mice showed reduced expression of platelet activation markers.

Blood was taken from ApoE$^{-/-}$ and ApoE/P2Y$_{12}$ DK mice (n=3), and analysed by flow cytometry to assess platelet function, via measurement of **(a)** P-selectin (CD62p) expression and **(b)** activation of the GPIIbIIIa receptor (CD41/61) in response to PAR-4 TRAP, a potent platelet agonist. Baseline fluorescence was determined using **(a)(i)** isotype, or **(b)(i)** EDTA unstimulated control for the CD62p and CD41/61 antibodies respectively. Representative fluorescence histograms are shown for **(ii)** ApoE$^{-/-}$ and **(iii)** ApoE/P2Y$_{12}$ DK mice. Median fluorescence was measured, and is shown as increase over baseline for **(c)** CD62p and **(d)** activated CD41/61. Data are mean ± SEM; ****P*<0.001; two-way ANOVA with Tukey's multiple comparison.

4.3 ApoE/P2Y$_{12}$ double knockout mice gain weight more rapidly than ApoE$^{-/-}$ mice when fed a high-fat diet

Atherogenesis was augmented in ApoE$^{-/-}$ and ApoE/P2Y$_{12}$ DK mice by feeding a high-fat (21% w/w) western diet for 12 weeks. Additional mice were fed a standard chow (6% w/w fat) diet, and all mice were weighed weekly (see Methods, section 2.5).

ApoE/P2Y$_{12}$ DK mice fed a western diet gained significantly more weight compared to ApoE$^{-/-}$ mice over 12 weeks (see Figure 4.4a). Baseline weights were similar for both genotypes before feeding commenced: 25.1 ± 0.7 vs. 22.6 ± 0.6 g (ApoE$^{-/-}$ vs. ApoE/P2Y$_{12}$ DK; *P*=ns). Mice gained weight rapidly thereafter, becoming significantly heavier after 4 weeks on a high-fat diet: 33.1 ± 1.0 vs. 28.1 ± 0.6 g; (*P*<0.01). Weight gain persisted throughout 12 weeks of feeding, and continued to diverge from ApoE$^{-/-}$ mice. After 12 weeks on a western diet, ApoE/P2Y$_{12}$ DK mice weighed 42.5 ± 1.4 g compared to 33.8 ± 0.8 g in ApoE$^{-/-}$ mice (*P*<0.001).

Chow-fed animals gained weight steadily throughout 12 weeks of monitoring, from 25.8 ± 2.4 vs. 24.5 ± 0.5 g (ApoE$^{-/-}$ vs. ApoE/P2Y$_{12}$ DK) at baseline, to 31.7 ± 1.4 vs. 31.2 ± 0.9 g at week 12. No significant difference in weight was observed between ApoE$^{-/-}$ and ApoE/P2Y$_{12}$ DK mice at any time point (see Figure 4.4b). Overlaying the weight profiles of mice fed each diet, demonstrated that ApoE$^{-/-}$ mice fed a western or chow diet gained weight to a similar degree and rate, highlighting the magnitude of weight gain observed in western fed ApoE/P2Y$_{12}$ DK mice (Figure 4.4c). This significant weight difference was reflected in a noticeable size difference compared to ApoE$^{-/-}$ mice (see Figure 4.4e).

With such a significant difference in weight, I was interested to monitor the food consumption of a cage of 4 ApoE$^{-/-}$ and 4 ApoE/P2Y$_{12}$ DK mice fed a western diet for 12 weeks. No difference was seen in the mean total food consumption per mouse (see Figure 4.4d). ApoE$^{-/-}$ mice consumed 250 g of western diet each over 12 weeks vs. 266.3 g eaten by ApoE/P2Y$_{12}$ DK mice. This corresponded to 2.98 g per day for an ApoE$^{-/-}$ mouse and 3.17 g per day for an ApoE/P2Y$_{12}$ DK mouse, compared to a mean daily food intake of 3.26 g for a male mouse aged 24 weeks (Evsikova and Svenson 2014), represented by the dashed line in Figure 4.4d.

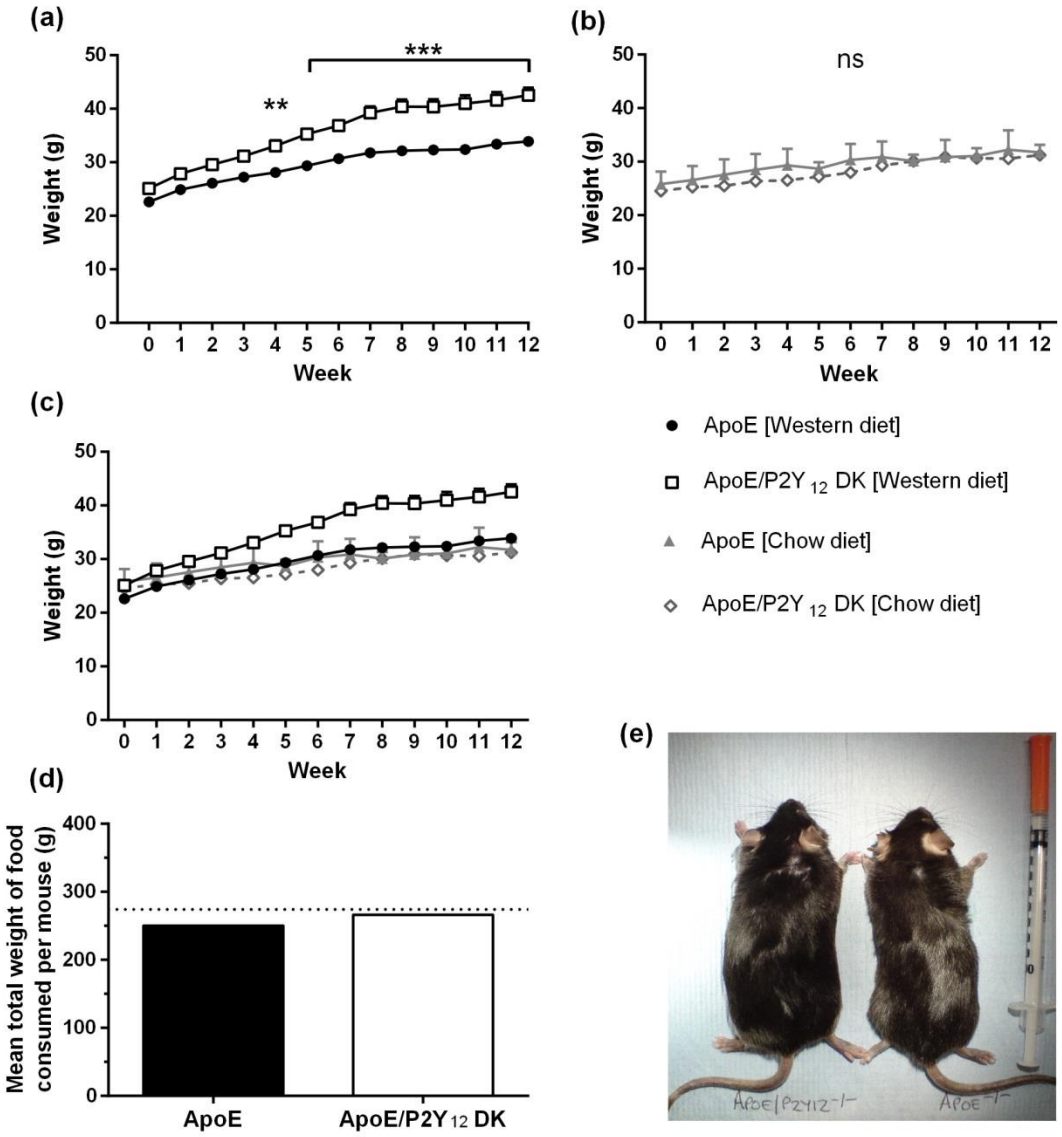

Figure 4.4 – ApoE/P2Y$_{12}$ double knockout mice gained significantly more weight than ApoE$^{-/-}$ mice when fed a western diet.
ApoE$^{-/-}$ and ApoE/P2Y$_{12}$ DK mice were fed either **(a)** western (n=16 & 15 respectively) or **(b)** chow diet (n=7) for 12 weeks and weighed weekly. An overlay of data from both diets can be seen in **(c)**. The food consumption of a cage of 4 mice, of each genotype, fed western diet was measured over 12 weeks, and the mean total weight of food consumed per mouse calculated **(d)**. The dashed line represents the mean intake of an average male mouse, based on a daily intake of 3.26g/day. A visible difference in body size **(e)** was noted between ApoE/P2Y$_{12}$ DK (left) and ApoE$^{-/-}$ mice (right) after 12 weeks of feeding a western diet. Data are mean ± SEM; ***P*<0.01, ****P*<0.001; two-way ANOVA with Bonferroni's multiple comparison.

Source: Mouse Phenome Database.

4.4 ApoE/P2Y$_{12}$ double knockout mice fed a western diet had enlarged livers

Upon dissection, a clear difference in liver size was noted between the 2 genotypes, with ApoE/P2Y$_{12}$ DK mice having noticeably larger livers than their ApoE$^{-/-}$ counterparts (see Figure 4.5a). Weighing each of the main organs revealed no significant difference between the heart, lungs, and spleen weight of ApoE$^{-/-}$ and ApoE/P2Y$_{12}$ DK mice (Figure 4.5b). However, ApoE/P2Y$_{12}$ DK mice had significantly heavier livers than ApoE$^{-/-}$ mice fed a western diet: liver weights were 2.169 ± 0.13 vs. 2.588 ± 0.401 g (ApoE$^{-/-}$ vs. ApoE/P2Y$_{12}$ DK; P<0.05). As expected western fed mice had enlarged livers compared to their chow fed counterparts: chow ApoE$^{-/-}$ livers were 1.514 ± 0.078 g (vs. western; P<0.001) and chow ApoE/P2Y$_{12}$ DK livers were 1.7 ± 0.089 g (vs. western; P<0.001). This pattern was also reflected when liver weight was calculated as a percentage of the mean body weight (see Figure 4.5c).

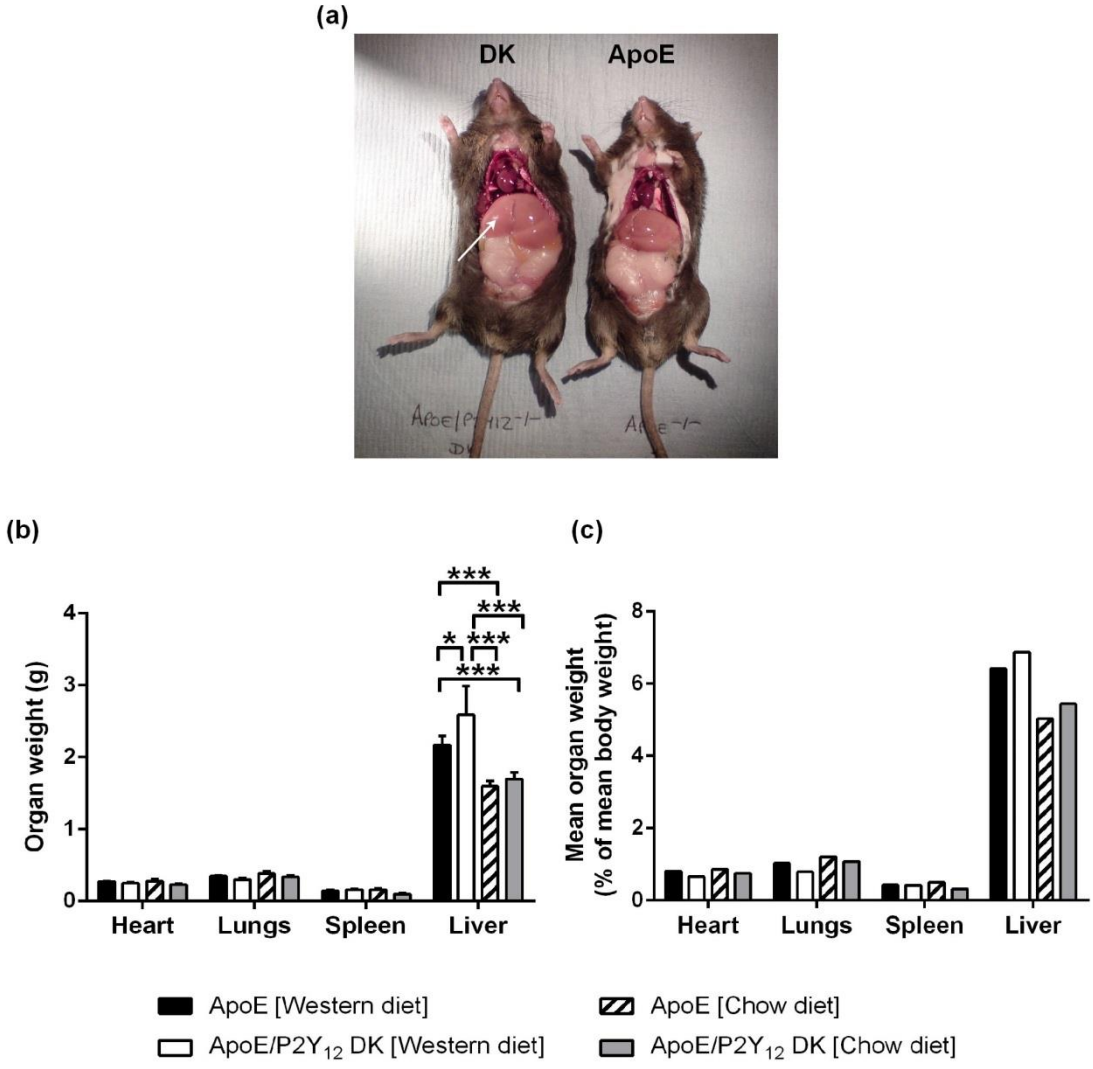

Figure 4.5 – ApoE/P2Y$_{12}$ double knockout mice fed a western diet had enlarged livers.

The heart, lungs, spleen, and liver were excised from ApoE$^{-/-}$ and ApoE/P2Y$_{12}$ DK mice following 12 weeks of feeding. **(a)** Upon dissection, ApoE/P2Y$_{12}$ DK mice fed a western diet appeared to have larger livers (arrow) than those of ApoE$^{-/-}$ mice. All organs were **(b)** weighed, and **(c)** calculated as a percentage of mean body weight. Data are mean ± SEM; **P*<0.01, ****P*<0.001; two-way ANOVA with Bonferroni's multiple comparison.

4.5 The physiological and metabolic phenotype of ApoE/P2Y$_{12}$ double knockout and ApoE$^{-/-}$ mice is similar

ApoE$^{-/-}$ and ApoE/P2Y$_{12}$ DK mice underwent a range of tests to assess both physiological and metabolic parameters throughout, and upon the conclusion of, 12 weeks on a western diet (see Methods, sections 2.5 and 2.10).

4.5.1 Blood pressure

Daily systolic and diastolic blood pressure, and pulse readings were taken for ApoE$^{-/-}$ and ApoE/P2Y$_{12}$ DK mice throughout 12 weeks of feeding on a western diet. Systolic and diastolic pressures were averaged to give a mean blood pressure for each genotype, every week. As these parameters are highly sensitive to stress, mice were trained for one week, to incorporate these readings into their daily routine. In addition, care was taken to ensure consistent environmental conditions, such as lighting, noise levels, operator, and time of day.

Weekly readings for individual mice showed a wide range of mean blood pressures within each genotype group (see Figure 4.6a and b). Individual blood pressures fluctuated from week to week, and the wide range of pressures within each group was maintained throughout the entire 12 weeks of feeding on a western diet. The total mean blood pressure for each genotype showed the overall trend, and there was no significant difference between ApoE$^{-/-}$ and ApoE/P2Y$_{12}$ DK mice on any week (see Figure 4.6c). In both genotype groups, mean blood pressure rose initially from baseline, at 97.8 ± 2.6 vs. 94.3 ± 1.6 mmHg (ApoE$^{-/-}$ vs. ApoE/P2Y$_{12}$ DK), peaking at 106.1 ± 3.3 vs. 99.1 ± 3.8 in week 2, before falling to the lowest recorded pressures of 85.3 ± 2.4 vs. 84.5 ± 3.5 mmHg at week 4. From this time point onwards, mean weekly blood pressure increased incrementally. The final mean blood pressure, following 12 weeks on a western diet, was 97.9 ± 3.1 mmHg in ApoE$^{-/-}$ mice and 99.6 ± 2.3 mmHg in ApoE/P2Y$_{12}$ DK mice.

In addition to blood pressure, the mean pulse rate was also measured, and throughout 12 weeks of assessment there was no significant difference between ApoE$^{-/-}$ and ApoE/P2Y$_{12}$ DK mice (see Figure 4.6d). The mean pulse rate remained relatively constant throughout, ranging between 688-727 beats per minute (bpm) in ApoE$^{-/-}$ mice and 678-730 bpm in ApoE/P2Y$_{12}$ DK mice.

4.5.2 Metabolic studies

ApoE$^{-/-}$ and ApoE/P2Y$_{12}$ DK mice underwent glucose (GTT) and insulin tolerance tests (ITT) after 10 and 11 weeks, respectively, on a western diet. For the GTT, mice were fasted overnight, and baseline blood glucose levels were 7.91 ± 0.83 vs. 8.91 ± 0.57 mmol/L (ApoE$^{-/-}$ vs. ApoE/P2Y$_{12}$ DK) before receiving a glucose bolus. Blood glucose levels were

recorded thereafter, and showed an increase to 26.4 ± 0.8 vs. 23.34 ± 2.14 mmol/L after 30 minutes of administration (see Figure 4.7a). Glucose levels gradually declined back to near baseline levels, 9.43 ± 0.49 vs. 10.73 ± 1.37 mmol/L, after 120 minutes.

The following week, mice underwent insulin tolerance testing. Baseline blood glucose levels were 13.91 ± 0.44 vs. 12.3 ± 0.82 mmol/L ($ApoE^{-/-}$ vs. $ApoE/P2Y_{12}$ DK) before receiving an insulin bolus. Blood glucose levels were recorded thereafter, and showed a steady decrease to 6.1 ± 0.66 vs. 7.23 ± 0.52 mmol/L after 40 minutes of administration (see Figure 4.7b). Glucose levels gradually increased back to near baseline levels, 9.35 ± 1.44 vs. 11.23 ± 0.79 mmol/L, after 60 minutes. Both GTT and ITT revealed no difference in response between $ApoE^{-/-}$ and $ApoE/P2Y_{12}$ DK mice.

After 12 weeks on a western diet, plasma was analysed by ELISA to determine insulin levels, and showed that $ApoE/P2Y_{12}$ DK mice had elevated plasma insulin levels compared to $ApoE^{-/-}$ mice (see Figure 4.7c): insulin levels were 1.22 ± 0.2 vs. 3.27 ± 0.61 ng/ml ($ApoE^{-/-}$ vs. $ApoE/P2Y_{12}$ DK; $P<0.01$). Plasma was sent for biochemical analysis and showed no difference between the final plasma glucose levels of $ApoE^{-/-}$ and $ApoE/P2Y_{12}$ DK mice (see Figure 4.7d).

4.5.3 Blood biochemistry

Plasma from $ApoE^{-/-}$ and $ApoE/P2Y_{12}$ DK mice was sent for biochemical analysis following 12 weeks on either a western or chow diet. The lipid profile, glucose, and liver enzyme levels were assessed, and mean values ± SEM are shown in Table 4.1. As expected, all lipid levels were elevated in western fed mice compared to their chow fed counterparts; however, no differences were noted when comparing $ApoE^{-/-}$ and $ApoE/P2Y_{12}$ DK mice on the same diet. Similarly, liver enzymes, aspartate transaminase (AST) and alanine transaminase (ALT), were elevated as expected in western fed mice compared to chow fed animals. However, when comparing $ApoE^{-/-}$ and $ApoE/P2Y_{12}$ DK mice, AST and ALT levels were higher in western fed $ApoE/P2Y_{12}$ DK mice (see Figure 4.8a and b): AST levels were 116.9 ± 24.9 vs. 177.8 ± 27.5 U/L ($ApoE^{-/-}$ vs. $ApoE/P2Y_{12}$ DK; P=ns), and ALT levels were 58.8 ± 16.2 vs. 137.4 ± 27.7 U/L ($P<0.05$).

4.6 $ApoE/P2Y_{12}$ double knockout mice possess fatty livers

$ApoE/P2Y_{12}$ DK mice fed a western diet had enlarged livers (Figure 4.5b), and elevated AST and ALT liver enzyme levels (Figure 4.8a and b) compared to $ApoE^{-/-}$ mice fed the same diet. I therefore stained liver cross-sections with haematoxylin and eosin (H&E) to assess tissue architecture (see Figure 4.8c). H&E staining showed $ApoE/P2Y_{12}$ DK mice had enlarged, irregular hepatocytes with numerous areas once occupied by fat, which had been removed during histological processing. In comparison, $ApoE^{-/-}$ mice had a well-preserved tissue architecture with intact, regular hepatocytes and few fatty areas.

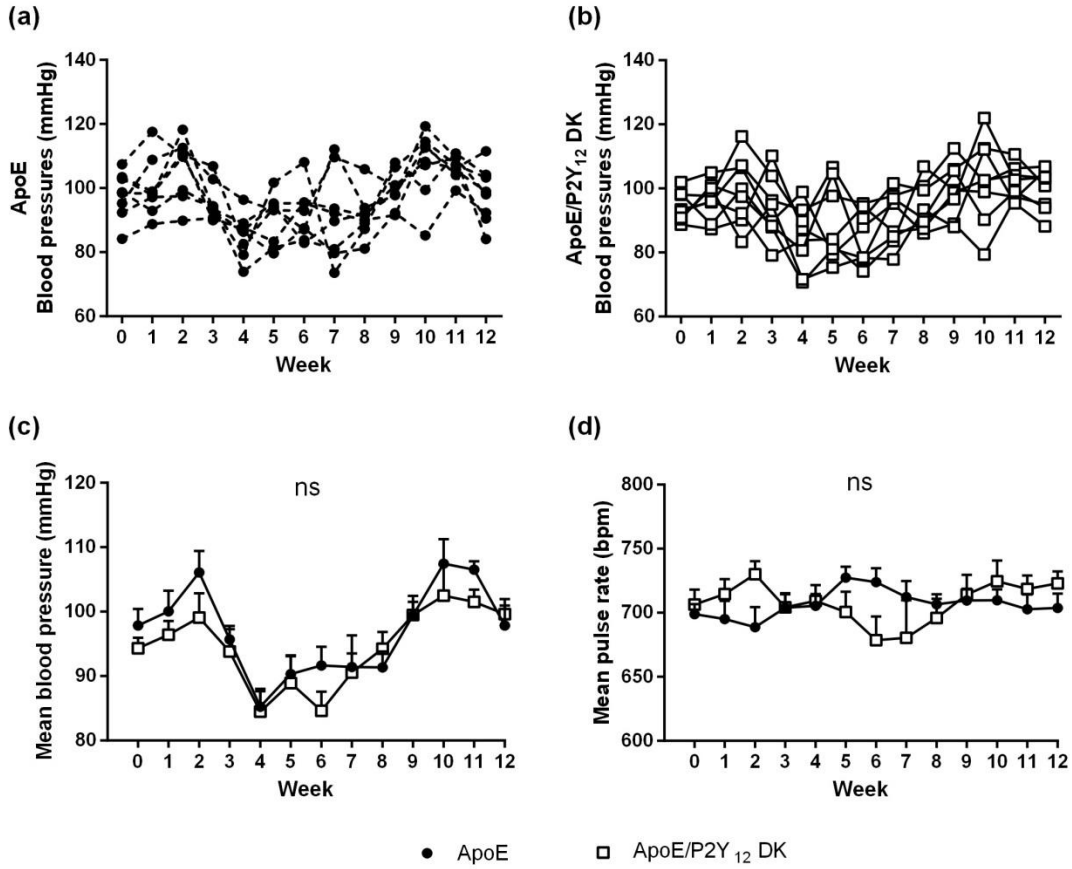

Figure 4.6 – Mean blood pressure and pulse rate were similar for ApoE/P2Y$_{12}$ double knockout and ApoE$^{-/-}$ mice fed a western diet for 12 weeks.

Daily blood pressure and pulse rate readings were taken for **(a)** ApoE$^{-/-}$ and **(b)** ApoE/P2Y$_{12}$ DK mice (n=8) throughout 12 weeks of feeding on a western diet. **(c)** Mean blood pressure and **(d)** pulse rate of each genotype was calculated for each week. Data are mean ± SEM; *P*=ns; two-way ANOVA with Bonferroni's multiple comparison.

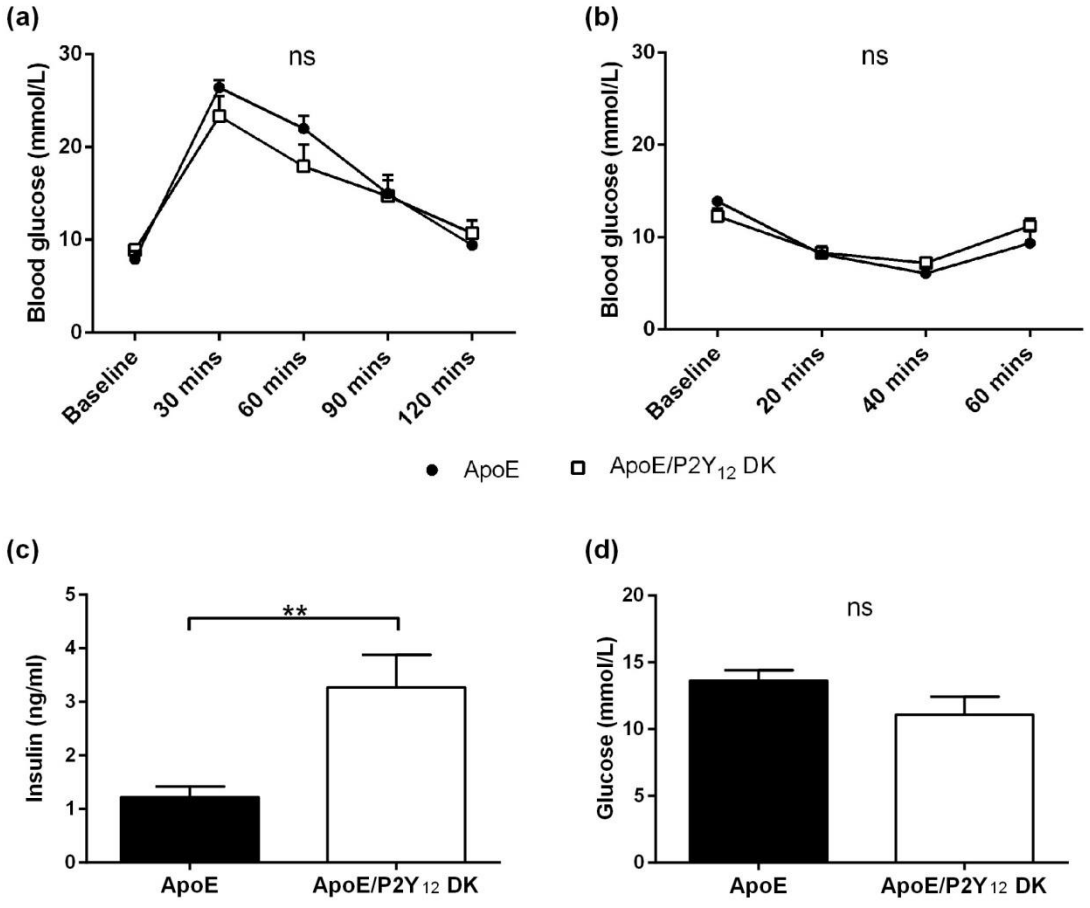

Figure 4.7 – Metabolic studies carried out on ApoE/P2Y$_{12}$ double knockout and ApoE$^{-/-}$ mice fed a western diet showed no difference in response to insulin or glucose.

(a) Glucose and **(b)** insulin tolerance tests were carried out on ApoE$^{-/-}$ and ApoE/P2Y$_{12}$ DK mice after 10 and 11 weeks (respectively) of feeding on a western diet (n=8). Blood glucose readings were taken at intervals following either a glucose or insulin challenge. Following 12 weeks of feeding, plasma was analysed **(c)** by ELISA to determine plasma insulin levels (n=8 & 7 respectively), and **(d)** sent for analysis to determine plasma glucose levels (n=10). Data are mean ± SEM; ***P*<0.01; **(a)** and **(b)** two-way ANOVA with Bonferroni's multiple comparison; **(c)** Mann-Whitney test; **(d)** independent samples t test.

Table 4.1 - Biochemical analysis of plasma from ApoE/P2Y$_{12}$ double knockout and ApoE$^{-/-}$ mice fed either chow or western diet for 12 weeks.

Data are mean (± SEM); *P<0.05; two-way ANOVA with Tukey's multiple comparison.

	ApoE$^{-/-}$ Western n=9	**ApoE/P2Y$_{12}$ DK Western n=10**	**ApoE$^{-/-}$ Chow n=3**	**ApoE/P2Y$_{12}$ DK Chow n=7**
Cholesterol (mmol/L)	24.356 (1.859)	22.820 (1.587)	11.067 (2.298)	10.614 (1.014)
HDL cholesterol (mmol/L)	4.840 (0.356)	4.738 (0.392)	3.267 (0.622)	3.187 (0.371)
LDL cholesterol (mmol/L)	14.850 (0.760)	15.083 (1.505)	6.600 (1.389)	5.720 (0.614)
Triglycerides (mmol/L)	5.222 (0.898)	3.910 (0.767)	2.600 (0.814)	3.633 (0.655)
Total cholesterol/HDL	5.044 (0.252)	4.722 (0.203)	3.400 (0.058)	3.417 (0.060)
Glucose (mmol/L)	13.620 (0.786)	11.070 (1.350)	8.800 (0.945)	9.586 (0.569)
AST (U/L)	116.889 (24.877)	177.800 (27.513)	97.333 (19.548)	81.500 (17.489)
ALT (U/L)	*58.778* ***** *(16.160)*	*137.400* ***** *(27.665)*	28.667 (11.319)	42.429 (10.781)

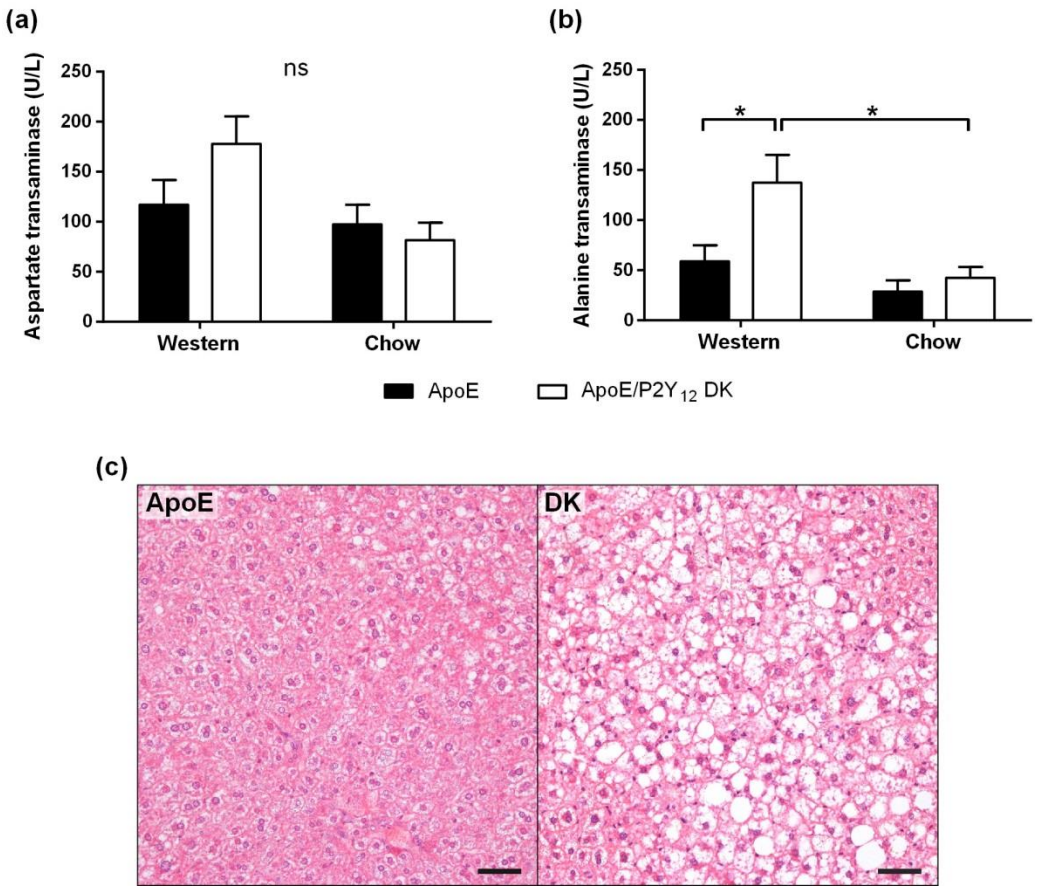

Figure 4.8 – ApoE/P2Y$_{12}$ double knockout mice fed a western diet had significantly elevated levels of alanine transaminase (ALT) and fatty livers compared to ApoE$^{-/-}$ mice.

Plasma from ApoE$^{-/-}$ and ApoE/P2Y$_{12}$ DK mice fed either a western (n=9 & 10 respectively) or chow diet (n=3 & 7 respectively) for 12 weeks was sent for biochemical analysis for liver enzymes **(a)** aspartate transaminase (AST) and **(b)** alanine transaminase (ALT). **(c)** Haematoxylin and eosin (H&E) staining of liver cross-sections from ApoE$^{-/-}$ and ApoE/P2Y$_{12}$ DK mice fed a western diet. Images taken at x200 magnification, scale bars = 50 µm. Data are mean ± SEM; **P*<0.05; two-way ANOVA with Tukey's multiple comparison.

4.7 Summary

This chapter has outlined the generation of a novel ApoE/$P2Y_{12}$ double knockout mouse strain, and described a range of physiological and metabolic phenotype parameters for these mice in comparison to the well-known and well-established $ApoE^{-/-}$ strain. In summary:

- ApoE/$P2Y_{12}$ DK breeding pairs were genotyped and successfully selected using PCR.
- Pearson's chi-squared test of the F_2 generation genotype frequencies yielded a *P* value marginally less than 0.05, and so the null hypothesis, that genotype frequencies remain constant within a population, was rejected.
- Platelets from ApoE/$P2Y_{12}$ DK mice demonstrated reduced P-selectin and activated GPIIbIIIa receptor expression in response to a platelet agonist, and thus confirmed impaired platelet function in these mice.
- ApoE/$P2Y_{12}$ DK mice fed a western diet gained significantly more weight than $ApoE^{-/-}$ mice fed the same diet over 12 weeks. No weight difference was seen in chow fed animals.
- Dissection revealed western fed ApoE/$P2Y_{12}$ DK mice also had enlarged livers compared to their $ApoE^{-/-}$ counterparts.
- No differences were noted in blood pressure or metabolic parameters, such as glucose and insulin tolerance tests.
- Plasma insulin levels were elevated in ApoE/$P2Y_{12}$ DK mice after 12 weeks of western diet.
- Biochemical analysis of plasma showed no difference in the lipid profile of ApoE/$P2Y_{12}$ DK mice compared to $ApoE^{-/-}$ controls. However, liver enzymes, AST and ALT, were elevated in ApoE/$P2Y_{12}$ DK mice fed a western diet.
- Histological staining of liver cross-sections revealed western fed ApoE/$P2Y_{12}$ DK mice also had fattier livers than $ApoE^{-/-}$ mice.

4.8 Discussion

In this chapter, I describe the successful generation of a novel ApoE/$P2Y_{12}$ DK mouse strain to enable studies into the role of $P2Y_{12}$ in atherogenesis. In addition, I identify phenotypic differences in body and liver weight between $ApoE^{-/-}$ and ApoE/$P2Y_{12}$ DK mice following consumption of a high-fat diet, which raises questions regarding the potential involvement of $P2Y_{12}$ in liver function, lipid levels and appetite, and suggests that $P2Y_{12}$ deficiency may affect areas of animal physiology other than haemostasis.

With the emergence of transgenic mouse strains, the development of the $P2Y_{12}^{-/-}$ mouse was a relatively new addition to this ever expanding group (Foster *et al.* 2001). Primarily

they have been used to study platelet aggregation and thrombosis; yet, despite many other platelet atherosclerosis studies having been conducted, $P2Y_{12}^{-/-}$ mice had never been employed in this capacity. I therefore generated a novel ApoE/$P2Y_{12}$ DK mouse strain in order to study the role of $P2Y_{12}$ in atherogenesis. At the time of commencing my research no other group had generated such a cross; however, a recent paper has been published which too developed an ApoE/$P2Y_{12}$ DK mouse strain, as discussed in later chapters (Li *et al.* 2012).

ApoE/$P2Y_{12}$ DK mice were generated from parent $ApoE^{-/-}$ and $P2Y_{12}^{-/-}$ lines, which were derived from the original founding colonies that had been backcrossed for 10 generations onto a C57/BL6 background (Piedrahita *et al.* 1992; Foster *et al.* 2001). To test whether the ApoE/$P2Y_{12}$ DK F_2 generation followed Mendelian genetics, in that the genotype frequencies would remain constant within the population, as stated by the Hardy-Weinberg principle, I performed Pearson's chi-squared test. This assessed to what extent the genotype frequencies I observed deviated from what would be expected for a population of this size, and if this was likely to have occurred by chance, or if another factor was influencing genotype frequency in this population. A significant chi-squared value of 0.0366 was calculated, which in turn meant that there was a 3.6% chance that, following the Hardy-Weinberg principle, this pattern of genotype frequencies occurred at random. As such the null hypothesis, that genotype frequencies remain constant within this population, was rejected and so suggests another factor may have affected genotype frequencies.

The Hardy-Weinberg principle is based on the assumption that allele/genotype frequencies do not change over time, and from generation to generation within a population. This also assumes there are no other influences on the population, such as natural or sexual selection, gene flow, genetic drift, or mutation, which may affect genotype frequencies. In the case of an inbred transgenic mouse strain, where both the ApoE and $P2Y_{12}$ lines were backcrossed onto the same background, it can be assumed that these factors are not at play. Nevertheless, although minimal, the effect of mutations, and the potential for genetic drift should be considered. Another assumption on which the principle is based is that the population size is infinite. When testing the Hardy-Weinberg principle, Pearson's chi-squared test is known to be sensitive to both low sample size and low expected frequencies (Russell 2002). In this limited cohort it is very likely, therefore, that small population size, in combination with single figure expected frequencies in some groups, contributed to a significant chi-squared value.

P-selectin is a platelet activation marker and its expression, determined by flow cytometry, is often used as a measure of platelet function (Leytin *et al.* 2000). As $P2Y_{12}$ activation results in the amplification of α granule release (Storey *et al.* 2000), stimulation of platelets via the PAR-4 receptor provides a sensitive method to determine $P2Y_{12}$ function, by the degree of

P-selectin expression. Attenuation of P-selectin expression, in response to PAR-4 TRAP, in platelets from ApoE/$P2Y_{12}$ DK mice demonstrates $P2Y_{12}$-deficiency, and thus confirms the expected platelet phenotype. These results are consistent with our previous findings (Evans *et al.* 2009).

Although predominantly found on platelets, $P2Y_{12}$ receptors have now also been identified at lower expression levels on VSMCs (Wihlborg *et al.* 2004), microglial cells (Sasaki *et al.* 2003), dendritic cells (Ben Addi *et al.* 2010), liver cholangiocytes (Masyuk *et al.* 2008), pancreatic islet cells (Lugo-Garcia *et al.* 2008), and splenic sinus (Uehara and Uehara 2011) and vascular endothelial cells (Shanker *et al.* 2006). A functional role for $P2Y_{12}$ in some of these cells types is yet to be established; however, it is clear from its wider expression pattern that $P2Y_{12}$-deficiency is no longer limited to affecting platelets alone.

Comparing the physiological and metabolic phenotype of ApoE/$P2Y_{12}$ DK mice with their $ApoE^{-/-}$ counterparts revealed many similarities between the 2 strains; nevertheless, some interesting differences emerged when mice were fed a high-fat diet. In ApoE/$P2Y_{12}$ DK mice, it appeared that $P2Y_{12}$-deficiency led to an increase in body and liver weight, in conjunction with elevated liver enzymes and evidence of fat deposition within the liver tissue, with less effect seen in $ApoE^{-/-}$ mice, and no effect in either genotype when fed a chow diet. It must also be noted that no such effects have been documented in our own or other published studies using $P2Y_{12}^{-/-}$ mice. Following the original development of the $P2Y_{12}^{-/-}$ mouse strain, Foster *et al*. assessed histological cross-sections of the major organs and found no abnormalities (Foster *et al.* 2001). These data pose the interesting notion that $P2Y_{12}$-deficiency, in cells other than platelets, may influence further physiological systems around the body in a diet-dependent manner.

Vascular smooth muscle cell $P2Y_{12}$ has been shown to mediate cell contraction, and promote pro-inflammatory and mitogenic responses in VSMCs (Wihlborg *et al.* 2004; Rauch *et al.* 2010). These receptors may contribute to inflammatory responses, such as atherogenesis, and this role will be discussed in later chapters; however, vessel wall $P2Y_{12}$-deficiency is unlikely to result in such specific, diet-dependent physiological effects in ApoE/$P2Y_{12}$ DK mice.

Microglia are macrophage-like cells, which police the brain and spinal cord for injury and infection. They are also responsible for the removal of apoptotic and necrotic cells, as well as modulation of synapses. In addition, they are also important in the early development of the brain in eliminating synapses during brain maturation (Schlegelmilch *et al.* 2011). As a result of CNS injury, nucleotides are released, and act as signalling molecules for microglia (Davalos *et al.* 2005). Research into the role of $P2Y_{12}$ on microglia discovered these nucleotides directly activate microglia through the $P2Y_{12}$ receptor, and mediate chemotaxis

in response to injury (Haynes *et al.* 2006). Although $P2Y_{12}$-deficient microglia retained basic motility, their ability to migrate in response to nucleotides was eliminated. The long-term physiological and behavioural impacts of diminished microglia response to injury, as a result of $P2Y_{12}$-deficiency, are unknown. Yet links have been made between microglial function and behaviour, demonstrating that deficient microglia-neuron signalling results in impaired brain function and altered behaviour (Zhan *et al.* 2014). It is not known whether $P2Y_{12}$-deficiency directly affects brain development and behaviour; however, given these findings, further investigation is warranted. Nevertheless, microglia $P2Y_{12}$-deficiency is unlikely to be totally responsible for the phenotype I observed, although alterations in appetite and activity could influence body weight. A crude analysis showed no difference in food consumption between genotypes, though a more sensitive and accurate investigation, using metabolic cages, is necessary to conclude this decisively.

Cholangiocytes are epithelial cells that line the bile ducts, and their function is to modify bile composition by regulating water, electrolyte, and organic solute secretion and absorption. Cilia on these cells act as mechano- and osmosensory organelles, and regulate bile composition via calcium and cAMP signalling (Alpini *et al.* 1996). $P2Y_{12}$ receptors on cholangiocyte cilia are thought to act as chemosensors detecting biliary nucleotides, and are known to transduce these into a cAMP response (Masyuk *et al.* 2008). It is therefore plausible that $P2Y_{12}$-deficiency in the liver may result in impaired sensory function, and $P2Y_{12}$-mediated signalling from cholangiocyte cilia, directly altering bile composition. Modifications of this sort could therefore affect both cholesterol excretion in the bile, and lipid digestion and absorption in the intestine. Biochemical analysis of plasma from ApoE/$P2Y_{12}$ DK mice showed no overall difference in lipid profile or total cholesterol systemically compared to $ApoE^{-/-}$. However, it must be considered that subtle changes may still have a local impact on liver physiology and function, and so offers a potential mechanism by which $P2Y_{12}$-deficiency may lead to lipid accumulation in the liver causing a rise in liver enzymes.

In pancreatic islet cells, $P2Y_{12}$ is proposed to have a role in stimulation of insulin secretion, but its true function has yet to be formally identified (Lugo-Garcia *et al.* 2008). Elevated baseline insulin levels measured in ApoE/$P2Y_{12}$ DK mice would lend support to this theory; however, no overall effect was seen in the metabolic response of these animals compared to $ApoE^{-/-}$ mice, when glucose or insulin tolerance tests were performed. $P2Y_{12}$ receptors have also been identified in dendritic cells, where they are thought to enhance T-cell activation (Ben Addi *et al.* 2010), and in cultured vascular endothelial cells, where their role is currently unknown (Shanker *et al.* 2006). Another study also found $P2Y_{12}$ to be expressed on splenic sinus endothelial cells. These cells control the passage of blood through the splenic cord, but in comparison to vascular endothelial cells, they are morphology dissimilar. $P2Y_{12}$ function in these cells is not defined, yet a role in cAMP signalling is postulated (Uehara and Uehara 2011). Several studies have also investigated whether $P2Y_{12}$ receptors are present

on leukocytes and did not find evidence of this (Hollopeter *et al.* 2001; Zhang *et al.* 2001; Haynes *et al.* 2006).

This chapter describes the successful development of a novel ApoE/$P2Y_{12}$ DK mouse strain which, as expected, demonstrated functional platelet $P2Y_{12}$-deficiency. These data also suggest that, given the stimulus of a high-fat diet, $P2Y_{12}$-deficiency results in distinct phenotype differences in ApoE/$P2Y_{12}$ DK mice compared to their $ApoE^{-/-}$ counterparts. Separate to its platelet effects, a potential role for $P2Y_{12}$ in other cell-types, influencing liver function and specifically fat deposition within the liver tissue, was postulated, given the evidence of elevated liver enzymes and fatty livers in $P2Y_{12}$-deficient mice fed a high-fat diet. Many other phenotype parameters, however, including metabolic responses, blood pressure, and lipid profile, were similar to $ApoE^{-/-}$ mice, and so demonstrated that any non-platelet $P2Y_{12}$ differences are relatively limited. In the following chapter, I go on to investigate the role of $P2Y_{12}$ in atherogenesis using this newly developed mouse strain.

5 The role of the $P2Y_{12}$ receptor in atherogenesis

The initiation and development of atherosclerotic plaques is a complex inflammatory response involving a network of cellular processes (Ross 1999; Libby 2002). Platelets have a fundamental role in atherothrombosis, but their role in atherogenesis is less clear. They are known to interact with the endothelium and leukocytes and, upon activation, can elicit an inflammatory response in these cells via both direct adhesion and the release of pro-inflammatory cytokines (Henn *et al.* 1998; Gawaz *et al.* 2000; von Hundelshausen *et al.* 2001). Furthermore, activated platelets can induce mitogenic effects on the vessel wall through secretion of growth factors (Schini-Kerth *et al.* 1997; Massberg *et al.* 2003). Several studies have investigated various aspects of platelet involvement, including adhesion receptors and proteins (Massberg *et al.* 2002; Burger and Wagner 2003; Huo *et al.* 2003; Bultmann *et al.* 2010), alluding to the notion that platelet activation potentiates lesion development.

Given this evidence, and the importance of $P2Y_{12}$ in modulating the vessel wall response to injury, as demonstrated in Chapter 3 (Evans *et al.* 2009), I hypothesised that $P2Y_{12}$ may also be important in atherogenesis. In this chapter I investigated lesion development in ApoE/$P2Y_{12}$ DK mice, to assess the effects of $P2Y_{12}$ deficiency on atherogenesis.

5.1 ApoE/$P2Y_{12}$ double knockout mice demonstrate region-specific differences in lesion development, compared to ApoE$^{-/-}$ mice, when fed a high-fat diet

ApoE$^{-/-}$ and ApoE/$P2Y_{12}$ DK mice were fed a western or a chow diet for 12 weeks, and atherogenesis was assessed in 3 areas of the vasculature prone to atheroma – the thoracic aorta, brachiocephalic artery, and aortic sinus (see Methods, section 2.9).

5.1.1 Aortae

Oil red O staining of whole aortae showed no difference in lesion area, represented as a percentage of the total aortic surface area, between ApoE$^{-/-}$ and ApoE/$P2Y_{12}$ DK mice following 12 weeks on either a western or chow diet (see Figure 5.1a and b): lesion area in western fed mice was 10.26 ± 0.63 vs. 9.1 ± 0.86% (ApoE$^{-/-}$ vs. ApoE/$P2Y_{12}$ DK; *P*=ns) and in chow fed mice was 3.84 ± 0.66 vs. 2.84 ± 0.57% (ApoE$^{-/-}$ vs. ApoE/$P2Y_{12}$ DK; *P*=ns). To assess potential region-specific differences in lesion development, atheroma was quantified in the aortic arch and descending aorta (see Figure 5.1c). ApoE/$P2Y_{12}$ DK mice fed a western diet had significantly attenuated atheroma in the aortic arch, which was reduced by 50% compared to ApoE$^{-/-}$ mice (Figure 5.1d; chow data not shown): aortic arch lesion area

was 16.67 ± 1.25 vs. 8.54 ± 0.85% (ApoE$^{-/-}$ vs. ApoE/P2Y$_{12}$ DK; *P*<0.001). However, there was no significant effect of P2Y$_{12}$ deficiency in the descending aortae: lesion area was 2.99 ± 0.25 vs. 2.24 ± 0.32% (ApoE$^{-/-}$ vs. ApoE/P2Y$_{12}$ DK; *P*=ns).

5.1.2 Brachiocephalic artery

Cross-sections of the brachiocephalic artery stained with alcian blue/elastic van Gieson revealed few lesions in this region of the vasculature, but those present were found close to the bifurcation of the vessel. Western fed mice demonstrated large and complex lesions with notable cholesterol clefts and fibrous caps (see Figure 5.2a), whereas chow fed mice exhibited much smaller and less complex lesions (images not shown). Quantification of the lesion area, represented as a ratio of the total CSA of the vessel, showed ApoE/P2Y$_{12}$ DK mice fed a western diet had significantly reduced lesion area compared to their ApoE$^{-/-}$ counterparts (see Figure 5.2b): 0.089 ± 0.015 vs. 0.046 ± 0.007 (ApoE$^{-/-}$ vs. ApoE/P2Y$_{12}$ DK; *P*<0.05). No difference was seen in chow fed mice: 0.016 ± 0.011 vs. 0.017 ± 0.007 (ApoE$^{-/-}$ vs. ApoE/P2Y$_{12}$ DK; *P*=ns).

5.1.3 Aortic sinus

Despite a clear effect of P2Y$_{12}$ deficiency on lesion development within the aortic arch and brachiocephalic artery of western fed mice, no effect was seen in the aortic sinus. Stained cross-sections revealed large and developed lesions within each of the valve leaflets of the aortic sinus. Both genotypes demonstrated highly complex lesions containing numerous cholesterol clefts, broken elastic laminae, and fibrous caps (see Figure 5.3a). Quantification of lesion area, represented as a ratio of the aortic sinus CSA, showed no difference in atheroma between ApoE$^{-/-}$ or ApoE/P2Y$_{12}$ DK mice for either diet (see Figure 5.3b): lesion area was 0.149 ± 0.015 vs. 0.122 ± 0.016 in western fed mice (ApoE$^{-/-}$ vs. ApoE/P2Y$_{12}$ DK; *P*=ns) and 0.027 ± 0.003 vs. 0.022 ± 0.006 in chow fed animals (ApoE$^{-/-}$ vs. ApoE/P2Y$_{12}$ DK; *P*=ns).

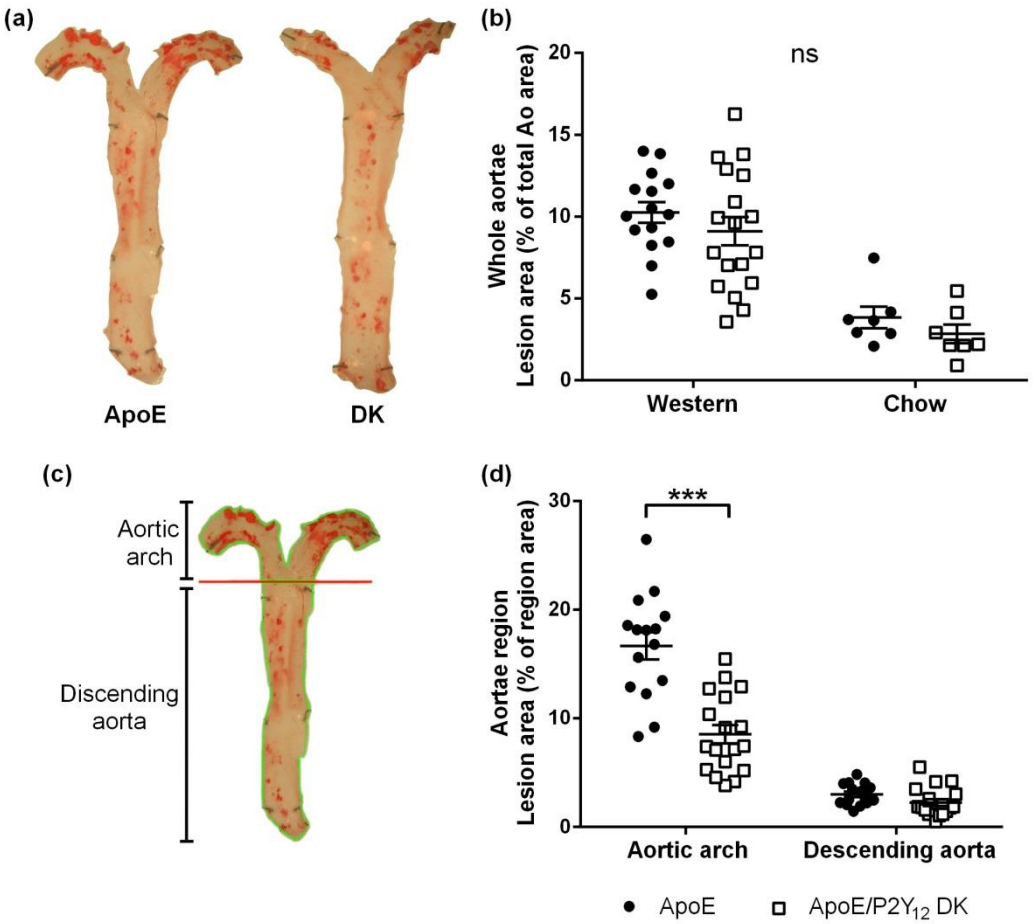

Figure 5.1 – Oil red O staining showed a significant reduction in lesion formation in the aortic arch of ApoE/P2Y$_{12}$ double knockout mice fed a western diet.

ApoE$^{-/-}$ (n=15) and ApoE/P2Y$_{12}$ DK (n=18) male mice were fed a western or chow diet for 12 weeks. Aortae were **(a)** stained with oil red O and **(b)** lesion area was calculated as a percentage of total surface area for the whole aorta. **(c)** Lesion was also assessed in the aortic arch and descending aorta, and **(d)** quantified for mice fed a western diet. Data are mean ± SEM; ****P*<0.001; two-way ANOVA with Bonferroni's multiple comparison.

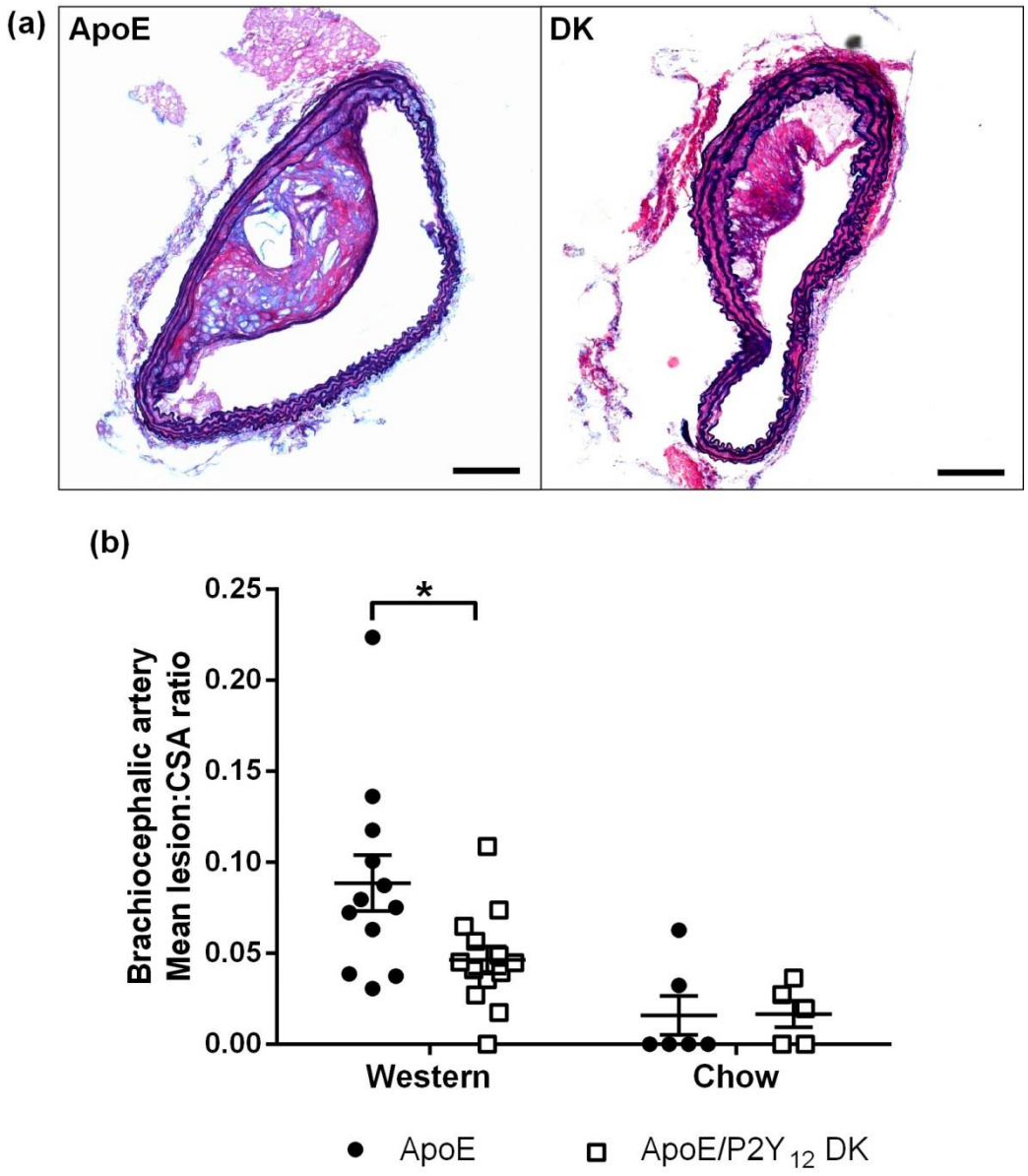

Figure 5.2 – ApoE/P2Y$_{12}$ double knockout mice fed a western diet had reduced lesion formation, compared to ApoE$^{-/-}$, in the brachiocephalic artery.

ApoE$^{-/-}$ (n=12) and ApoE/P2Y$_{12}$ DK (n=13) male mice were fed a western or chow diet for 12 weeks. Brachiocephalic arteries were sectioned and **(a)** stained with alcian blue/elastic van Gieson. Representative cross-sections of western fed mice are shown. Images taken at x100 magnification, scale bar = 100 µm. **(b)** Lesion area was calculated, and is shown as mean lesion:CSA (cross-sectional area) ratio. Data are mean ± SEM; **P*<0.05; two-way ANOVA with Bonferroni's multiple comparison.

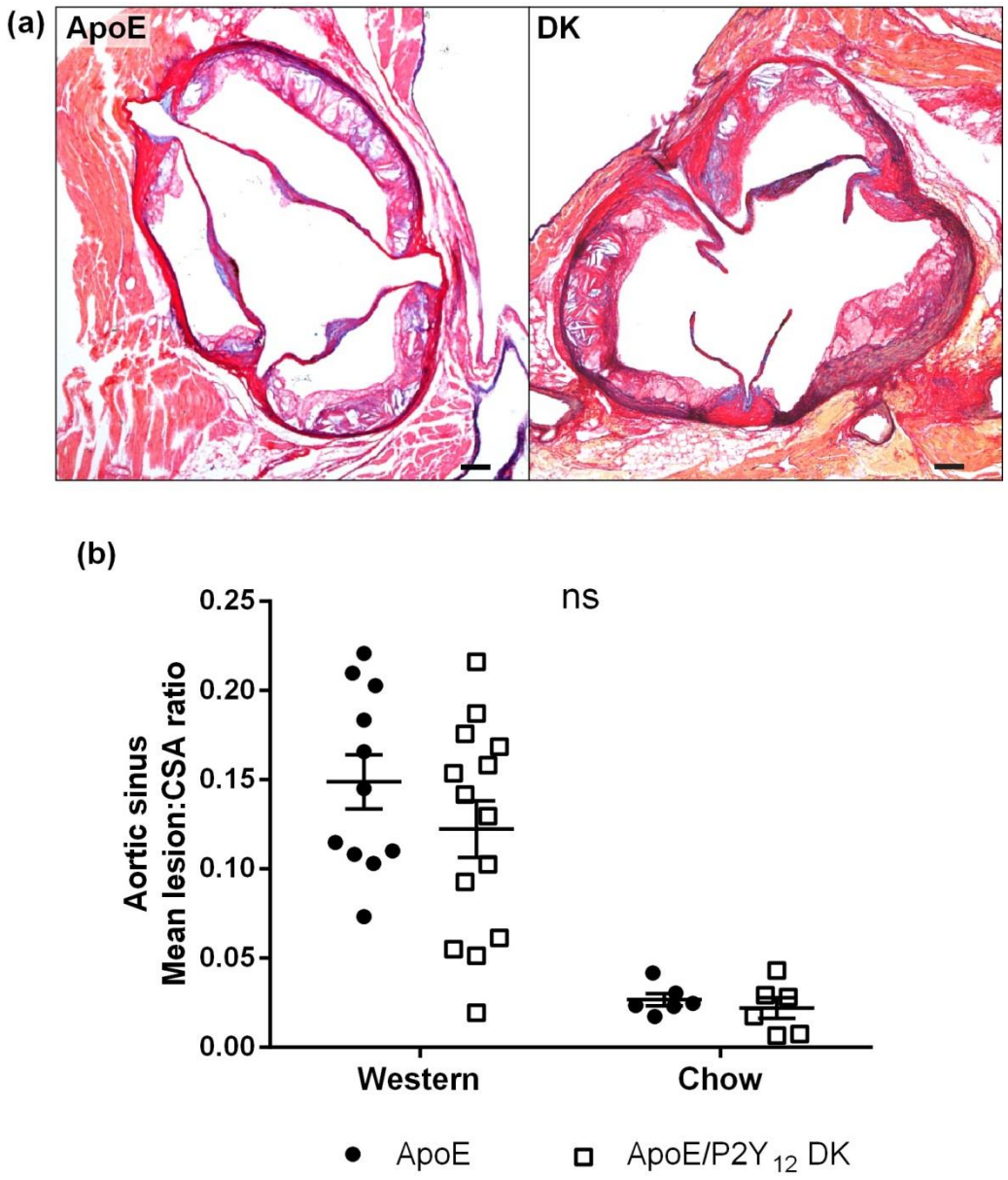

Figure 5.3 – No difference in lesion formation, between ApoE$^{-/-}$ and ApoE/P2Y$_{12}$ double knockout mice, was seen in the aortic sinus for either diet.

ApoE$^{-/-}$ (n=11) and ApoE/P2Y$_{12}$ DK (n=14) male mice were fed a western or chow diet for 12 weeks. Each aortic sinus was sectioned and **(a)** stained with alcian blue/elastic van Gieson. Representative cross-sections of western fed mice are shown. Images taken at x40 magnification, scale bar = 100 µm. **(b)** Lesion area was calculated, and is shown as mean lesion:CSA (cross-sectional area) ratio. Data are mean ± SEM; *P*=ns; two-way ANOVA with Bonferroni's multiple comparison.

5.2 Lesion phenotype was similar in both ApoE$^{-/-}$ and ApoE/P2Y$_{12}$ double knockout mice fed a western diet

As collagen, smooth muscle cell, and macrophage content are key characteristics of developing complex and inflammatory lesions, I went on to further stain the aortic sinus sections of western fed mice with martius scarlet blue (MSB) for collagen, and for α-smooth muscle actin (α-SMA), and macrophage markers, F4-80 and MAC387, using immunohistochemistry.

5.2.1 Collagen

MSB staining provides clear differentiation between fibrin (red) and collagen connective fibres (blue). Staining of the aortic sinus sections showed well-defined bright blue collagen staining of the vessel wall and valve leaflets, including large proportions of positive staining also within the lesions (see Figure 5.4a). Higher magnification images from ApoE$^{-/-}$ and ApoE/P2Y$_{12}$ DK mice highlight that the collagen fibres were predominantly located in the acellular necrotic core, and towards the cap and shoulder regions of the lesions. Quantification of the percentage collagen content within aortic sinus lesions from each genotype showed no difference between ApoE$^{-/-}$ or ApoE/P2Y$_{12}$ DK mice fed a western diet (see Figure 5.4b): collagen content was 29.18 ± 4.6 vs. 28.06 ± 3.49% (ApoE$^{-/-}$ vs. ApoE/P2Y$_{12}$ DK; *P*=ns).

5.2.2 Smooth muscle actin

Smooth muscle actin immunostaining of aortic sinus sections, using DAB as the substrate, revealed brown α-SMA positive cells within the vessel wall. Positive staining was localised to those areas of the vessel wall with visible elastic laminae, but no staining was present in the myocardium (see Figure 5.5a). Negative control sections, where only secondary antibody was applied, showed no non-specific binding of the secondary antibody and therefore displayed no positive staining. Higher magnification images (see Figure 5.5b) demonstrated many α-SMA positive cells within both ApoE$^{-/-}$ and ApoE/P2Y$_{12}$ DK lesions, located predominantly within the fibrous cap and towards the shoulder regions of the lesions. Quantification of α-SMA content within the aortic sinus lesions established no significant difference between ApoE$^{-/-}$ and ApoE/P2Y$_{12}$ DK mice fed a western diet (see Figure 5.5c): % α-smooth muscle actin content was 5.63 ± 1.23 vs. 7.03 ± 2.17% (ApoE$^{-/-}$ vs. ApoE/P2Y$_{12}$ DK; *P*=ns).

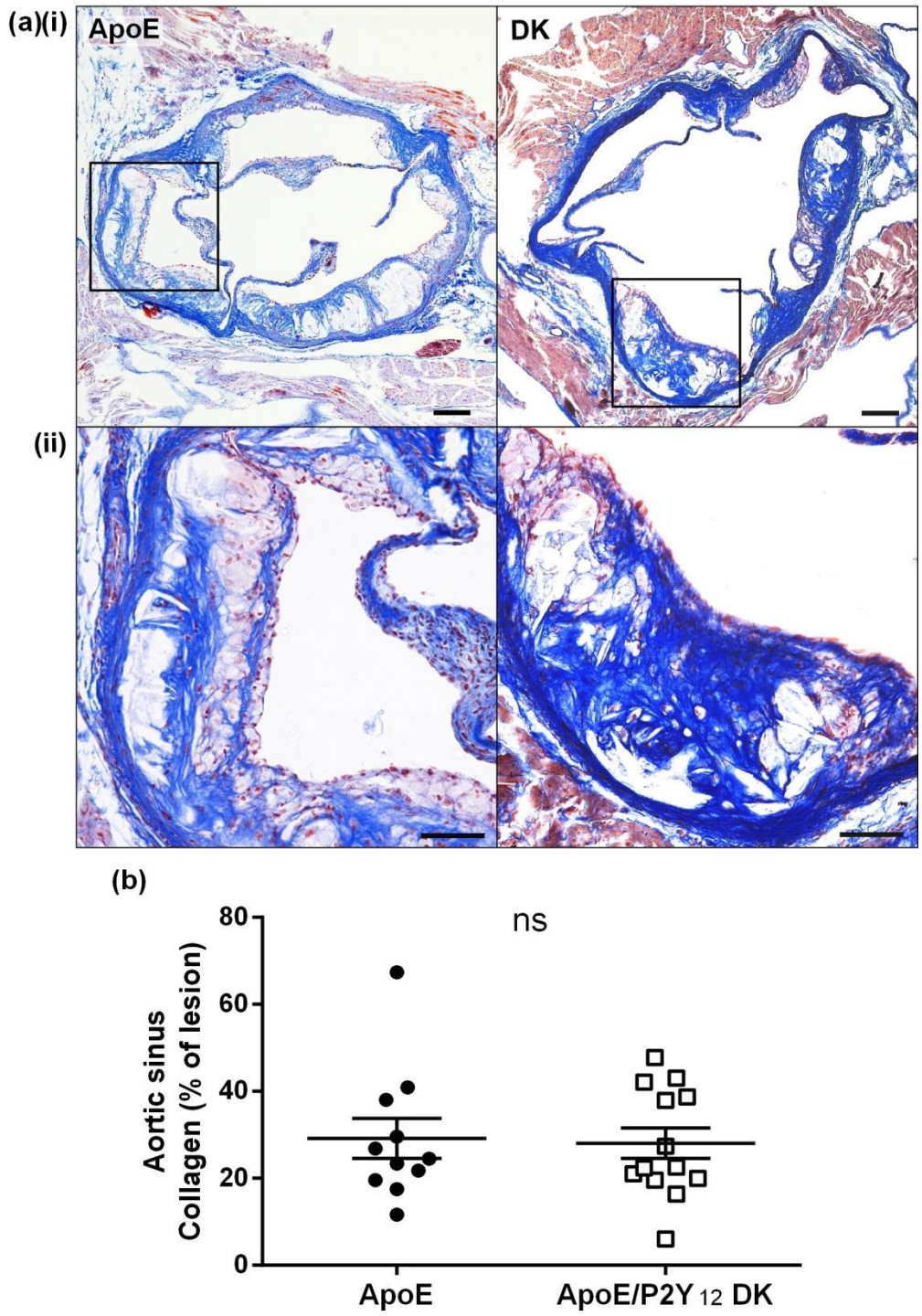

Figure 5.4 – Collagen staining showed no difference in the collagen content of aortic sinus lesions from western fed mice.

ApoE$^{-/-}$ (n=11) and ApoE/P2Y$_{12}$ DK (n=13) male mice were fed a western or chow diet for 12 weeks. **(a)** Aortic sinus sections were stained with martius scarlet blue, from which collagen is stained bright blue. Representative cross-sections of western fed mice are shown. Images taken at **(i)** x40 magnification, scale bar = 100 µm and **(ii)** x200 magnification (highlighted area), scale bar = 50 µm. **(b)** Collagen content within the aortic sinus lesions was quantified, and is shown as a percentage of the total lesion area. Data are mean ± SEM; *P*=ns; Independent samples t test.

Figure 5.5 – No difference was seen in the α-smooth muscle actin content of aortic sinus lesions from western fed mice.

$ApoE^{-/-}$ (n=11) and $ApoE/P2Y_{12}$ DK (n=13) male mice were fed a western or chow diet for 12 weeks. Aortic sinus sections from **(i)** $ApoE^{-/-}$ and **(ii)** $ApoE/P2Y_{12}$ DK mice were stained for α-smooth muscle actin using immunohistochemistry, from which positive cells are stained brown. Representative cross-sections of western fed mice are shown, including **(iii)** a negative control. Images taken at **(a)** x40 magnification, scale bar = 100 µm, and **(b)** x200 magnification (highlighted area), scale bar = 50 µm. **(c)** Smooth muscle actin content within the aortic sinus lesions was quantified, and is shown as a percentage of the total lesion area. Data are mean ± SEM; *P*=ns; Independent samples t test.

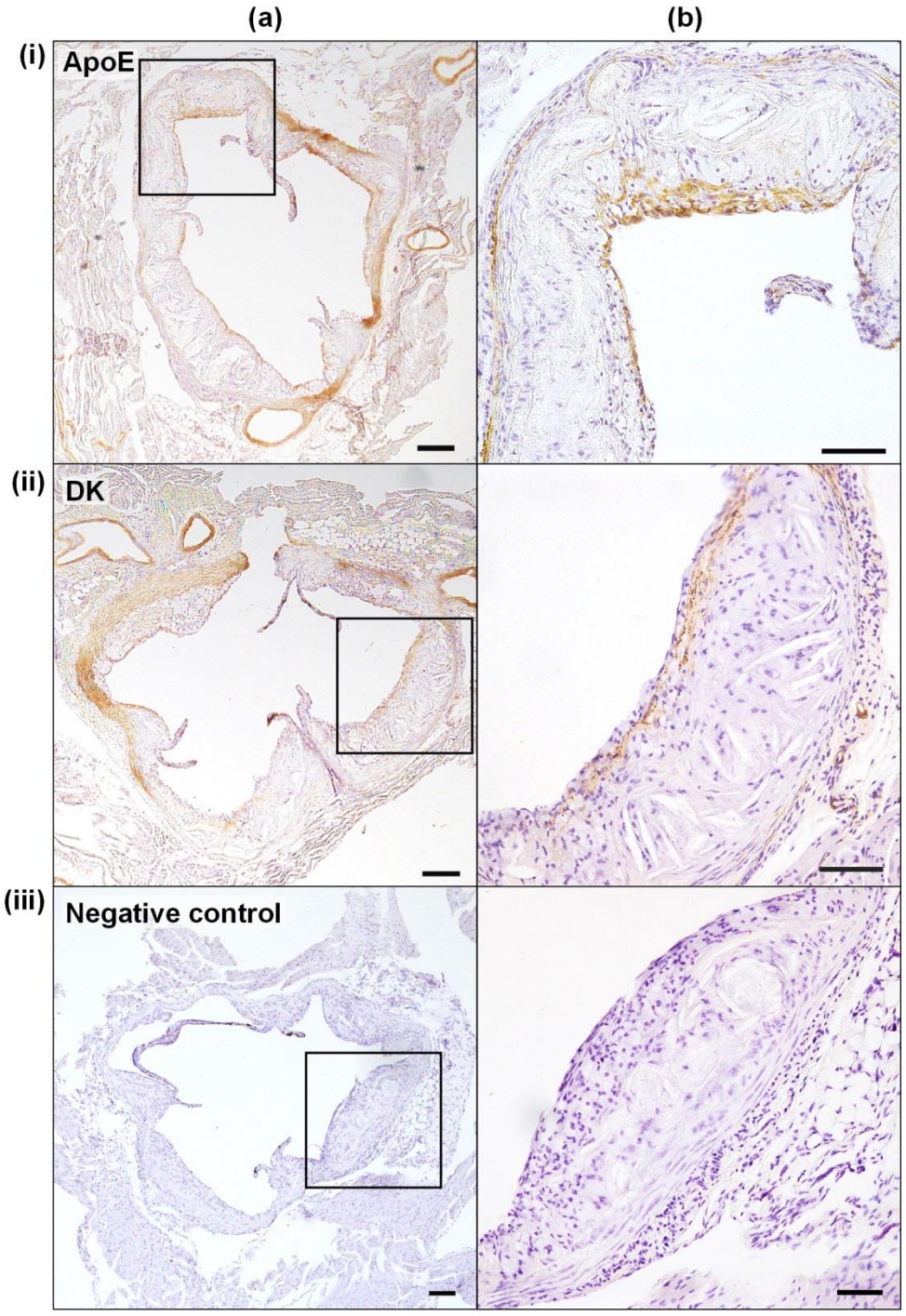
(a)
(b)
(i)
ApoE
(ii)
DK
(iii)
Negative control

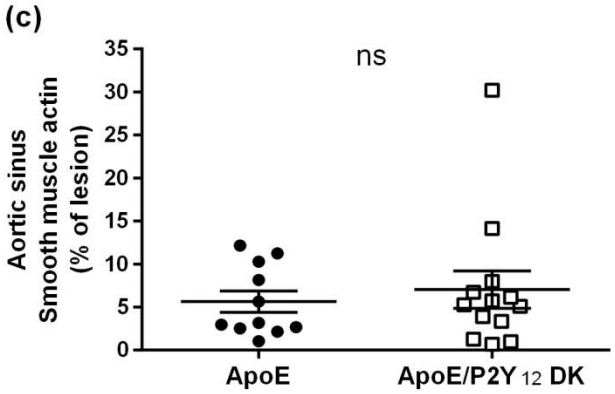
(c)
ns
Aortic sinus
Smooth muscle actin
(% of lesion)
35
30
25
20
15
10
5
0
ApoE
ApoE/P2Y 12 DK

5.2.3 Macrophage markers

Staining for F4/80 and MAC387 macrophage markers by immunohistochemistry, using DAB as the substrate, provided inconclusive results. F4/80 staining of aortic sinus sections showed sparse positive staining, with a few distinct positive cells in the cardiac tissue, but no staining within the lesions (see Figure 5.6a). Negative control sections showed no non-specific binding of the secondary antibody. Spleen cross-sections showed abundant positive staining in the red pulp.

MAC387 staining demonstrated a high level of non-specific staining, as shown in the negative control section (see Figure 5.6b). Despite strong positive staining within spleen cross-sections, no specific staining was observed in the aortic sinus. Pale background staining was particularly evident within the acellular necrotic core of the lesions.

Figure 5.6 – Staining for macrophage markers, F4/80 and MAC387, within aortic sinus lesions provided inconclusive results.

Aortic sinus cross-sections were stained for **(a)** F4/80 and **(b)** MAC387 using immunohistochemistry, from which positive cells are stained brown. Representative cross-sections of ApoE$^{-/-}$ western fed mice are shown. **(i) & (iii)** Images taken at x40 magnification, scale bar = 100 µm, and **(ii)** taken at x200 magnification (highlighted area), scale bar = 50 µm. **(iv)** Spleen positive control sections also taken at x200 magnification.

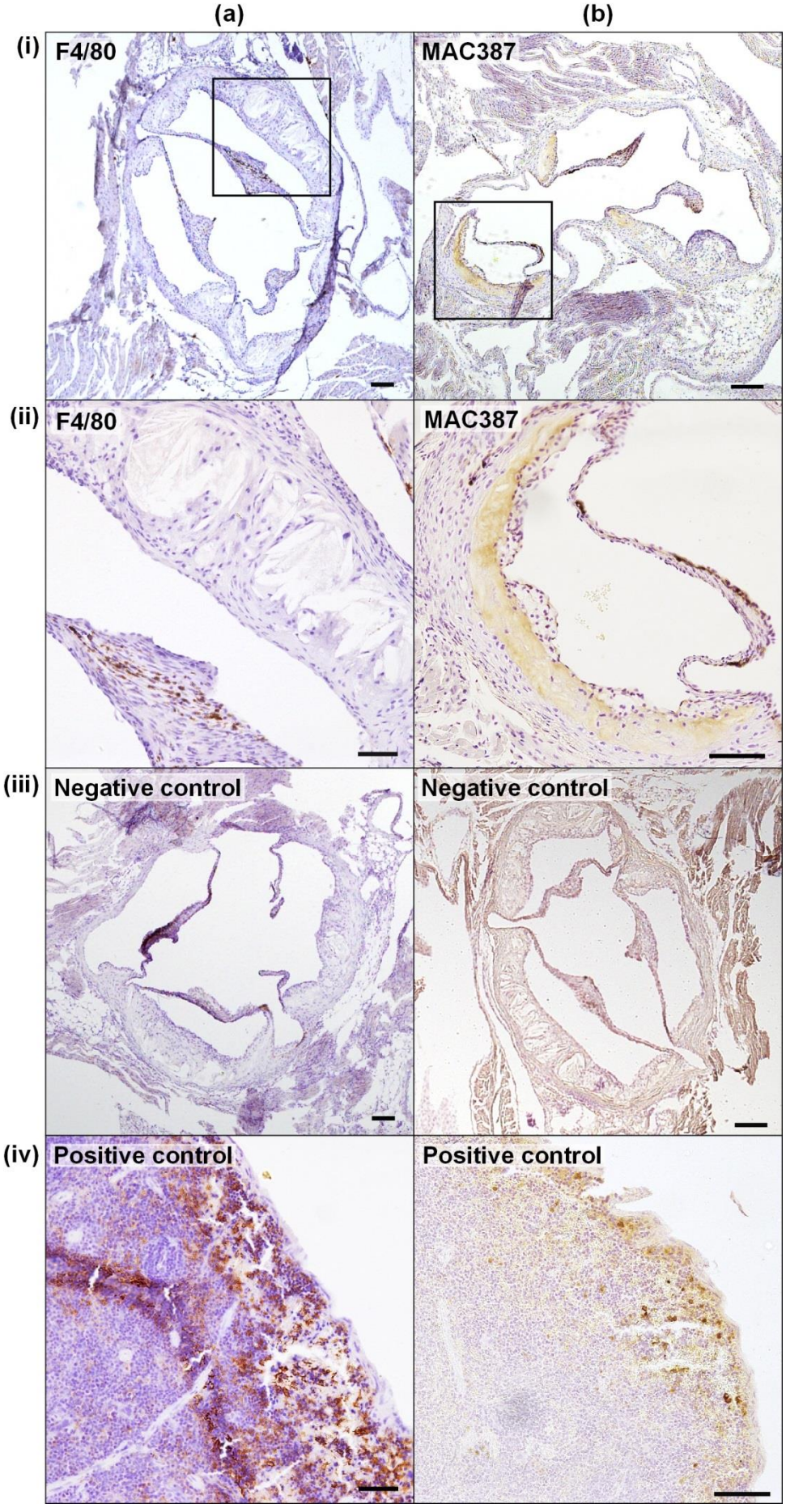
(a)
(b)
(i)
F4/80
MAC387
(ii)
F4/80
MAC387
(iii)
Negative control
Negative control
(iv)
Positive control
Positive control

5.3 Summary

This chapter has described the role of the $P2Y_{12}$ receptor in atherogenesis by examining the extent, structure, and composition of atherosclerotic lesions in ApoE/$P2Y_{12}$ DK mice, and assessing their development across several areas of the vasculature prone to disease. Results were obtained following 12 weeks on a high-fat western diet. In summary:

- $P2Y_{12}$-deficient mice fed a western diet had significantly less atheroma in the aortic arch compared to their $ApoE^{-/-}$ counterparts.
- No difference was observed in the descending aorta, or when assessing lesion area across the entire aorta.
- Western fed ApoE/$P2Y_{12}$ DK mice also had significantly attenuated atheroma in the brachiocephalic artery compared to $ApoE^{-/-}$.
- However, in the aortic sinus, no difference in lesion formation was noted.
- Aortic sinus lesions demonstrated a high degree of collagen staining localised predominantly to the necrotic core, cap, and shoulder regions of the lesion, although there was no overall difference in the percentage collagen content between groups.
- Smooth muscle actin positive cells were found in high numbers within the cap and shoulder regions of aortic sinus lesions from both $ApoE^{-/-}$ and ApoE/$P2Y_{12}$ DK mice; however, no difference in α-SMA content was noted between each group.
- Macrophage staining provided inconclusive results with no evidence of positive staining within the lesions.

5.4 Discussion

Atherogenesis is a process classically described as involving leukocytes and cells of the vessel wall; nevertheless, there is mounting evidence to suggest that platelets should also be considered in this ensemble, as their impact on the inflammatory response becomes more apparent. In Chapter 3, I demonstrated that platelet $P2Y_{12}$ mediated the vessel wall response to injury and so may implicate a role for $P2Y_{12}$ in atherogenesis. In this chapter, I describe a moderate region-specific effect of $P2Y_{12}$–deficiency on atherosclerotic lesion development, which, together with recent findings (Li *et al.* 2012), suggests a role for platelet $P2Y_{12}$ in established disease.

With α granules packed full of cytokines and membrane adhesion proteins, the pro-inflammatory capacity of platelets is evident. Many studies have been conducted to tease out their potential role in propagating lesion development, focussing on the mechanisms by which platelets interact with the inflammatory system, via adhesion and cytokine release. Roles for platelet adhesion proteins and receptors have been implicated, including P-selectin (Burger and Wagner 2003; Huo *et al.* 2003), CD40L (Lievens *et al.* 2010), GPIb (Massberg *et al.* 2002), and VI (Bultmann *et al.* 2010). In addition, the deposition of cytokines, such as

RANTES and PF4, by activated platelets onto endothelial and monocyte membranes has been associated with increased leukocyte recruitment to atherosclerotic and injured vessels (von Hundelshausen *et al.* 2001; Schober *et al.* 2002; Huo *et al.* 2003). The $P2Y_{12}$ receptor, with its central role in platelet reactivity and, importantly, α granule release, was therefore an attractive candidate for investigation, and so formed the basis for this thesis.

Whilst completing my research, Li *et al.* published data using their own ApoE/$P2Y_{12}$ DK mouse strain, presenting evidence to suggest that platelet $P2Y_{12}$ indeed promotes lesion development, and does this via $P2Y_{12}$–mediated granule release of P-selectin and PF4, thus amplifying leukocyte recruitment (Li *et al.* 2012). These findings are consistent with my own data which demonstrated that, at an earlier time point in disease, $P2Y_{12}$ deficiency lead to a moderate reduction in atheroma. However, the magnitude of this attenuation was somewhat lesser in my data compared to the effect seen by Li *et al.* and, furthermore, I observed no significant $P2Y_{12}$ effect in some areas of the vasculature. In the Li study, a high-fat diet similar to our own western diet was used, but mice were fed for 20 weeks as opposed to 12 weeks, as in my experiments. This difference in the length of atherogenic stimulus could therefore explain the variance in $P2Y_{12}$-effect on lesion size between these studies, and interestingly suggests that platelet $P2Y_{12}$ may have a greater influence later in disease.

Although $P2Y_{12}$-deficiency appeared to have only a moderate effect on atherogenesis from my data, perhaps the most fascinating finding was that this effect appeared to be regional, and dependent on the area of the vasculature. Lesion area was attenuated in the brachiocephalic arteries of mice, but not in the aortic sinus. Similarly there was no difference when assessing the whole aorta; however, a substantial reduction in atheroma was identified in the aortic arch. This indicates that the local vascular environment may have been responsible for these regional differences, and so introduces the possibility that flow patterns and shear stress may be exacerbating the effects of $P2Y_{12}$-deficiency on atherogenesis.

Oscillatory flow and low shear stress are known to be key factors in determining the location of atherosclerotic lesions throughout the vasculature (Ku *et al.* 1985; Asakura and Karino 1990). Lesion prone sites have been shown to not only express high levels of leukocyte adhesion molecules, such as VCAM-1 (Nakashima *et al.* 1998), but also increased vWF expression (Theilmeier *et al.* 2002). In this particular study, rabbits fed a high-fat diet demonstrated both increased vWF and, consequently, platelet adhesion at lesion prone sites. Further investigation discovered GP1b-vWF and P-selectin-PSGL-1 platelet-endothelial interactions were responsible for these findings. All of the areas I chose to assess for atherosclerotic burden are renowned lesion prone sites, yet despite this, the aortic sinus and whole aorta showed no difference in atheroma. Interestingly, however, the brachiocephalic artery and aortic arch, which demonstrated the greatest effect of $P2Y_{12}$-

deficiency on atheroma, are perhaps subject to the greatest variations in shear stress (Suo *et al.* 2007). Given that $P2Y_{12}$ activation is required for the firm adhesion of platelets to vWF (Goto *et al.* 2002), these sites may reveal the greatest impact of platelet adhesion, or lack of in $P2Y_{12}$-deficient mice, on lesion development and so may explain why the $P2Y_{12}$ effect was most apparent here.

Although it has been documented that platelets adhere to the endothelium of $ApoE^{-/-}$ mice at as early as 6 weeks of age and that these interactions precede lesion development (Massberg *et al.* 2002), equally there is much evidence to also support a role for platelets in advanced disease. In addition to the Li study, other mouse models have identified that both platelet P-selectin and CD40L not only potentiate atherogenesis, but actively promote a mature lesion phenotype, demonstrating a high smooth muscle cell content and evidence of lesion calcification (Lutgens *et al.* 1999; Burger and Wagner 2003; Lievens *et al.* 2010). Indeed the mitogenic effects of PDGF, released from activated platelets, on VSMCs are well established (Schini-Kerth *et al.* 1997; Massberg *et al.* 2003); yet, α-SMA staining showed no difference in smooth muscle cell content in the aortic sinus after 12 weeks on a western diet. Lesions in this area were assessed for VSMC and collagen content due to the availability of sections and ability to compare similar regions between groups; however, with no difference seen in lesion area, phenotype changes in the lesions were unlikely. Surprisingly, despite assessing collagen and macrophage content of the lesions, the Li study did not perform α-SMA staining.

Collagen content was determined by martius scarlet blue (MSB) trichrome stain, which I selected in preference to traditional trichrome stains, such as Masson's, as it offered clearer differentiation between fibrin, collagen, and RBCs, as well as being a reliable and consistent staining method. Aortic sinus lesions showed no difference in collagen content between groups at 12 weeks, but in the Li study at 20 weeks, $P2Y_{12}$-deficiency resulted in an increase in collagen within the lesions. This is a curious finding since collagen synthesis within atherosclerotic lesions is mainly associated with VSMCs, specifically their migration (Rocnik *et al.* 1998), and platelets are known to induce this effect. In addition, TGF-β and PDGF have both been shown to induce collagen synthesis by VSMC (Amento *et al.* 1991). Although not the only source for these mitogens, other unique platelet releasates have been found within atherosclerotic lesions (Coppinger *et al.* 2004). Given this evidence it could be deduced that, conversely, platelet activation would in fact increase VSMC migration and collagen synthesis, and that $P2Y_{12}$-deficiency would lead to a reduction in both. However, without knowledge of the smooth muscle cell content of the lesions from the Li study, it is difficult to explain their collagen findings.

Macrophages make up a large proportion of the cells within atherosclerotic lesions, and are essential in driving the inflammatory microenvironment, promoting migration, proliferation,

foam cell formation, and ultimately plaque destabilisation. With such an important role in atherogenesis, I sought to quantify macrophage content within the aortic sinus lesions by immunohistochemistry but staining yielded inconclusive results. Initially I stained for F4/80, which is expressed on most tissue macrophages, and obtained positive signals from the surrounding cardiac tissue, though none within the lesion itself. Absence of non-specific antibody binding and abundant positive staining of spleen cross-sections, suggested that the antibody staining had worked, but yielded no F4/80 positive cells within the lesions.

As several macrophage subtypes have been identified, that express different phenotypes and cell markers (Mantovani *et al.* 2009; Ley *et al.* 2011), I decided to try another marker with a broader expression. MAC387 is expressed on granulocytes, monocytes, and tissue macrophages; however, my staining achieved no positive cells within any of the tissue, except in the positive control. Evidence of non-specific antibody binding in the negative control, and background staining in the sinus tissue, suggested the experimental conditions were not optimal. Further workup of this antibody may have yielded positive results, but as macrophages are a heterogeneous population, further work using alternative markers such as CD68, MAC3 and MOMA-2, is also warranted.

These data suggest $P2Y_{12}$-deficiency has a moderate regional effect in advanced atherogenesis, at 12 weeks on a high-fat diet. However, the impact of $P2Y_{12}$ increases as disease progresses and a greater role for platelet $P2Y_{12}$ in late atherogenesis is identified in the Li study. Nevertheless, the influence of VSMC $P2Y_{12}$ must also be considered when interpreting these findings. Little is known of the effect of vessel wall $P2Y_{12}$ on atherogenesis and so, therefore, I went on to investigate the role of platelet versus vessel wall $P2Y_{12}$ in atherogenesis, using bone marrow transplantations; the results of which are discussed in the next chapter.

6 The role of platelet versus vessel wall $P2Y_{12}$ in early atherogenesis

Although predominantly expressed on platelets, $P2Y_{12}$ is also expressed on vascular smooth muscle cells, where it mediates cell contraction (Wihlborg *et al.* 2004), and promotes pro-inflammatory and mitogenic responses via a thrombin-induced pathway (Rauch *et al.* 2010). In the previous chapter, I demonstrated that $P2Y_{12}$ deficiency led to subtle effects on lesion development in some areas of the vasculature. Recent work has suggested that, at a later time point in advanced disease, platelet $P2Y_{12}$ plays a substantial role in the development of mature atherosclerotic plaques in a mouse atherosclerosis model (Li *et al.* 2012). I hypothesised that $P2Y_{12}$ activation may also be important in promoting early atherogenesis, in contrast to later stages of disease when endothelial disruption may promote the role of platelets.

In this chapter, I investigated the role of $P2Y_{12}$ using a model of early atherogenesis, by feeding a western diet for 4 weeks, and employed bone marrow transplantations to examine the contributions of platelet versus vessel wall $P2Y_{12}$ to initial lesion formation.

6.1 Transplanted bone marrow-derived platelets expressed the donor $P2Y_{12}$-phenotype

$ApoE^{-/-}$ and $ApoE/P2Y_{12}$ DK mice underwent BMT to generate 2 control and 2 chimeric groups, deficient in either platelet or vessel wall $P2Y_{12}$. The transplantation method I employed in this study has successfully been used previously by our group (Chamberlain *et al.* 2006; Evans *et al.* 2009). However, to further confirm the bone marrow $P2Y_{12}$ phenotype I assessed the efficacy of transplantation using flow cytometry to measure platelet activation markers, P-selectin and activated GPIIbIIIa receptors, in response to PAR-4 TRAP, a potent platelet agonist.

Platelets from $ApoE^{-/-}$ mice transplanted with $ApoE^{-/-}$ bone marrow displayed high fluorescence of the CD62p and CD41/61 JON-A antibodies, demonstrating these platelets expressed high levels of both P-selectin and activated GPIIbIIIa receptors. In contrast, platelets from $ApoE^{-/-}$ mice transplanted with $ApoE/P2Y_{12}$ DK bone marrow showed attenuated platelet activation, and exhibited much lower fluorescence levels, shown as a shift to the left in the fluorescence peaks for each antibody (see Figure 6.1a and b).

CD62p and CD41/61 JON-A fluorescence was measured in response to a range of PAR-4 TRAP concentrations, in addition to a saline control, which showed the cells were not pre-activated. Expression was measured as an increase in median fluorescence over baseline, determined using an isotype (CD62p) or EDTA unstimulated control (CD41/61 JON-A). At

each concentration, ApoE$^{-/-}$ mice transplanted with ApoE/P2Y$_{12}$ DK bone marrow demonstrated consistently lower P-selectin (Figure 6.1c) and activated GPIIbIIIa receptor expression (Figure 6.1d) compared to ApoE$^{-/-}$ controls. This was particularly evident at 3 mmol/L TRAP, where P-selectin median fluorescence was 1617 ± 828 vs. 115 ± 41 (ApoE$^{-/-}$ vs. ApoE/P2Y$_{12}$ DK bone marrow; *P*=ns) and GPIIbIIIa median fluorescence was 5027 ± 2549 vs. 1753 ± 474 (*P*=ns). Attenuated expression of these activation markers in ApoE$^{-/-}$ mice transplanted with ApoE/P2Y$_{12}$ DK bone marrow confirmed the successful reconstitution of P2Y$_{12}$-deficient donor bone marrow into recipient mice.

6.2 Bone marrow transplanted mice showed no difference in blood coagulation parameters

In order to determine any variation in the potential for thrombin and fibrin generation between the BMT mice, I assessed coagulation parameters. Activated partial thromboplastin time (aPTT) and prothrombin time (PT) were measured to assess the intrinsic (aPTT) and extrinsic (PT) coagulation pathways, and fibrinogen levels were a measure of the final common coagulation pathway. No differences were found between any of the bone marrow chimeric groups for PT, aPTT or fibrinogen levels (see Figure 6.2).

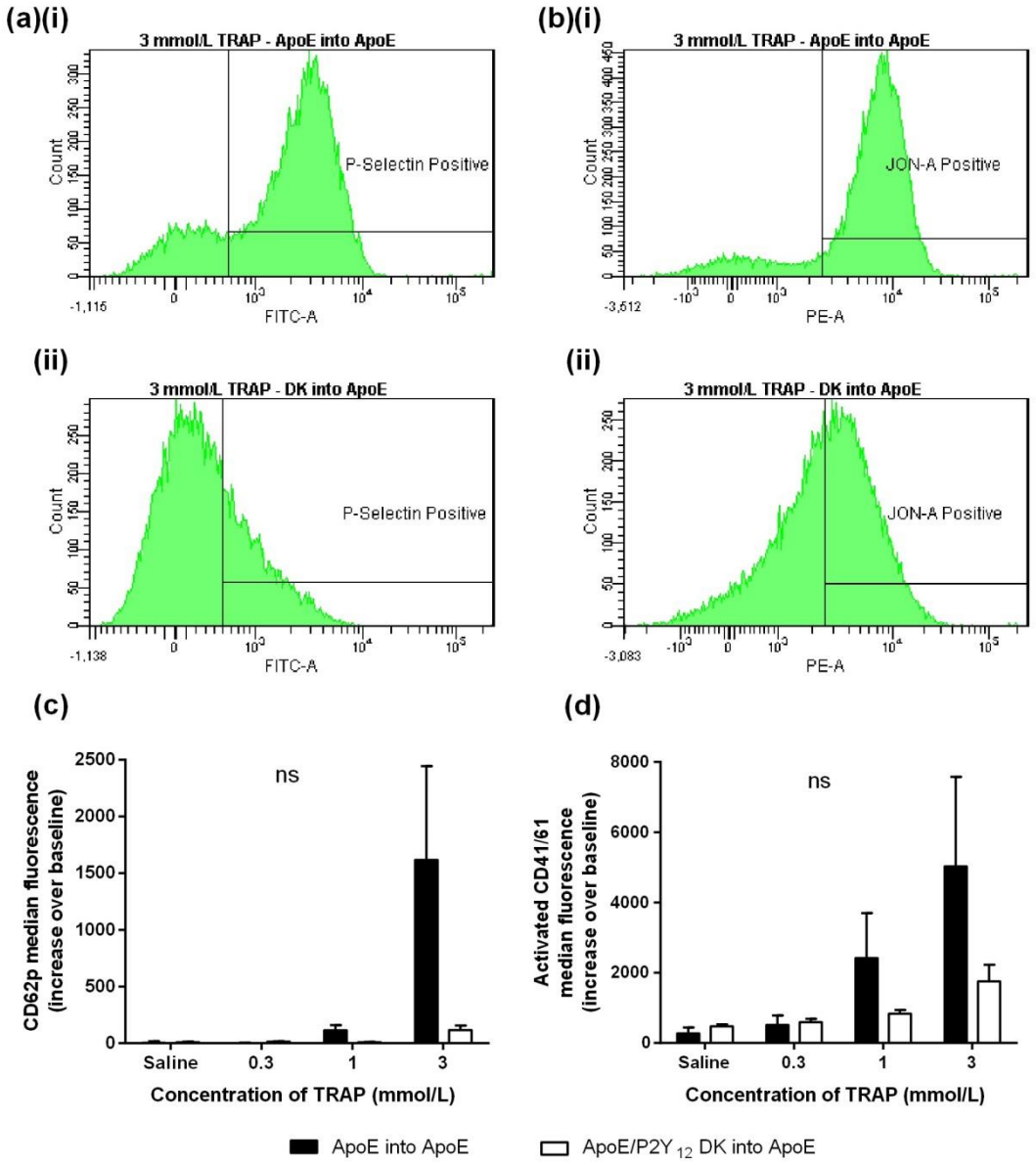

Figure 6.1 – ApoE$^{-/-}$ male mice transplanted with ApoE/P2Y$_{12}$ double knockout bone marrow demonstrated attenuated platelet activation markers compared to control mice.

Blood was taken from ApoE$^{-/-}$ mice transplanted with either ApoE$^{-/-}$ or ApoE/P2Y$_{12}$ DK bone marrow (n=3), and analysed by flow cytometry to assess platelet function, via measurement of **(a)** P-selectin (CD62p) expression and **(b)** activation of the GPIIbIIIa receptor (CD41/61) in response to PAR-4 TRAP. Representative fluorescence histograms are shown for **(i)** ApoE$^{-/-}$ into ApoE$^{-/-}$ and **(ii)** ApoE/P2Y$_{12}$ DK into ApoE$^{-/-}$ mice. Median fluorescence was measured and is shown as increase over baseline for **(c)** CD62p and **(d)** activated CD41/61. Data are mean ± SEM; *P*=ns; Mann-Whitney test (adjusted level of significance *P*<0.01 for multiple group comparisons).

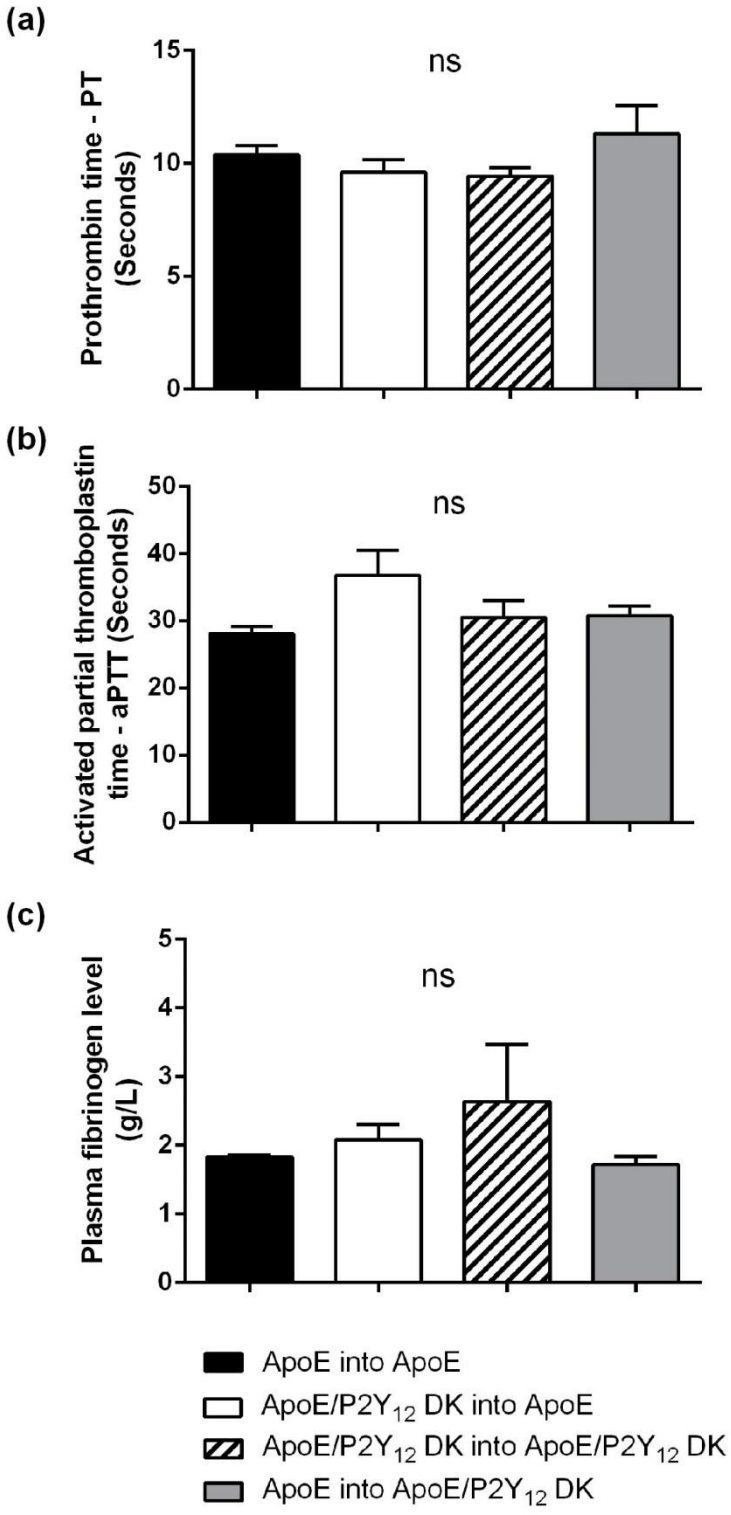

Figure 6.2 – No differences were found in the coagulation response of bone marrow transplanted mice.

Coagulation parameters **(a)** prothrombin time (PT), **(b)** activated partial thromboplastin time (aPTT), and **(c)** fibrinogen levels were measured in each of the bone marrow transplant chimeric groups: ApoE into ApoE, DK into ApoE, DK into DK, and ApoE into DK (n=3, 4, 3 and 5 respectively). Data are mean ± SEM; *P*=ns; one-way ANOVA with Tukey's multiple comparison.

6.3 Vessel wall, not platelet, $P2Y_{12}$ potentiates early atherogenesis

Mice were fed a western diet for 4 weeks, following BMT, before lesion area was assessed.

6.3.1 Aortae

Thoracic aortae stained with oil red O demonstrated a non-significant trend towards reduced percentage atheroma in vessel wall $P2Y_{12}$-deficient mice (see Figure 6.3a and b): lesion area was 3.35 ± 0.36% in control mice, 2.14 ± 0.28% in mice with deficient vessel wall and platelet $P2Y_{12}$ (*P*=0.07 vs. control), and 2.1 ± 0.36% in mice with only deficient vessel wall $P2Y_{12}$ (*P*=0.056 vs. control). When assessing the aortic arch alone, atheroma was also attenuated in vessel wall $P2Y_{12}$-deficient mice (see Figure 6.3c): aortic arch lesion area was 6.7 ± 0.83% in control mice, 4.33 ± 0.4% in mice with deficient vessel wall and platelet $P2Y_{12}$ (*P*=0.033 vs. control), and 4.4 ± 0.54% in mice with only deficient vessel wall $P2Y_{12}$ (*P*=0.039 vs. control). However, there was no significant effect of vessel wall $P2Y_{12}$ in the descending aortae. Mice with absence of only platelet $P2Y_{12}$ exhibited no differences in lesion area compared to controls.

6.3.2 Brachiocephalic artery

Cross-sections of the brachiocephalic artery revealed the presence of few lesions in this region of the vasculature. Those lesions which were visible, were often found close to the bifurcation of the vessel, and were small in size, simple in structure and appeared to be of an early phenotype. In some cases, no lesions were detected along the entire length of the vessel (see Figure 6.4a). Quantification demonstrated that mice deficient in vessel wall $P2Y_{12}$ had significantly attenuated atheroma, an effect which was irrespective of platelet $P2Y_{12}$ expression. Lesion area, represented as a ratio of the total CSA of the vessel, was 0.027 ± 0.002 in control mice, 0.004 ± 0.003 in mice with deficient vessel wall and platelet $P2Y_{12}$ (*P*<0.001 vs. control), and 0.006 ± 0.003 in mice lacking only vessel wall $P2Y_{12}$ (*P*<0.001 vs. control) (see Figure 6.4b). Absence of platelet $P2Y_{12}$ alone appeared to have no effect on lesion size (0.021 ± 0.004; *P*=ns vs. control).

6.3.3 Aortic sinus

Analogous results were observed in the aortic sinus, with notably less atheroma observed in mice deficient in vessel wall $P2Y_{12}$ (see Figure 6.5b): aortic sinus lesion area was 0.071 ± 0.008 in control mice, 0.024 ± 0.003 in mice with deficient vessel wall and platelet $P2Y_{12}$ (*P*<0.001 vs. control), and 0.03 ± 0.006 in mice lacking only vessel wall $P2Y_{12}$ (*P*<0.001 vs. control). Again this effect was independent of platelet $P2Y_{12}$ expression. In contrast to the brachiocephalic artery, the aortic sinus revealed more substantial lesions (see Figure 6.5a); however, these too were simple in structure, and considerably less complex than those seen after 12 weeks of feeding on a western diet (see Figure 5.3a).

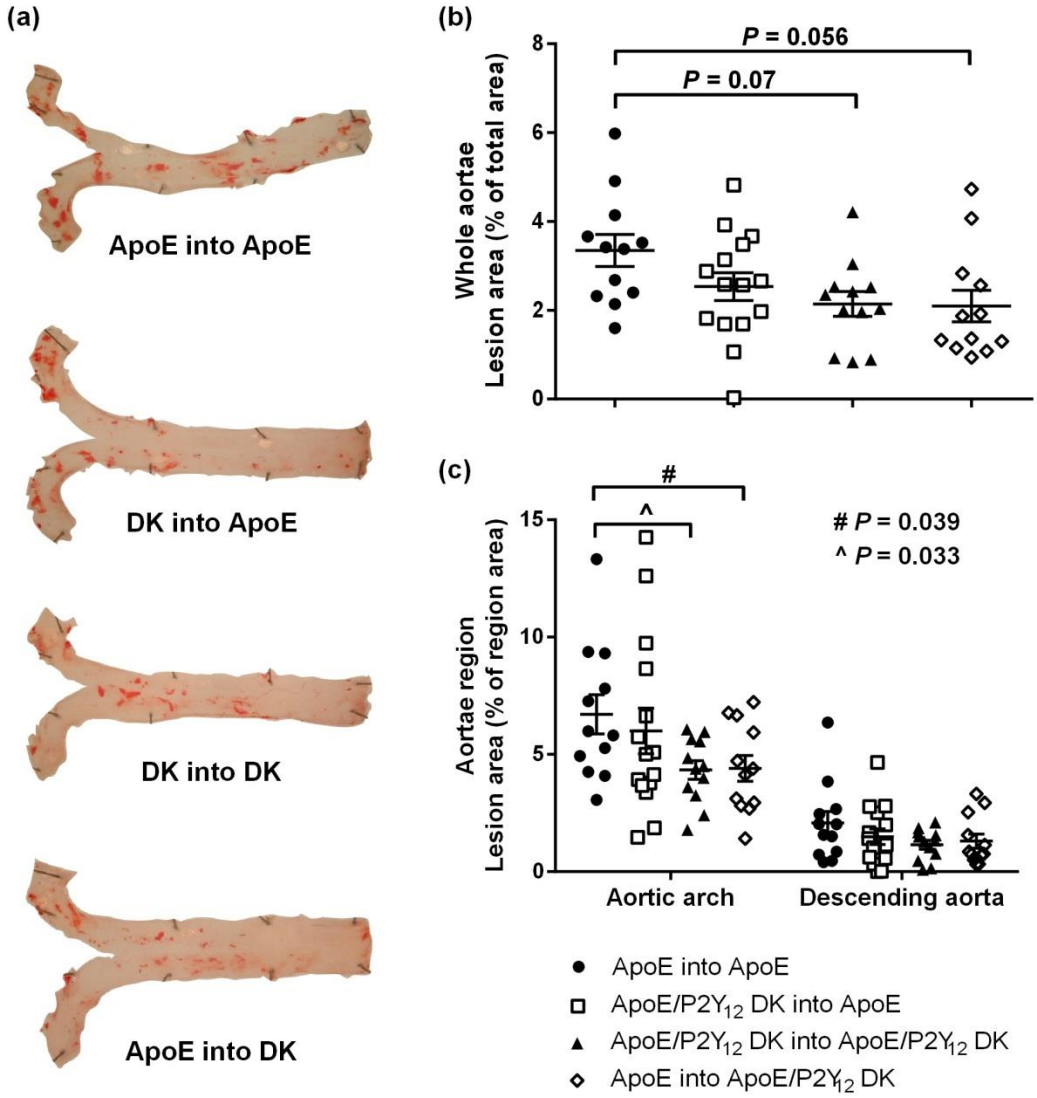

Figure 6.3 – Oil red O staining showed attenuated atheroma in the whole aorta and aortic arch region of vessel wall $P2Y_{12}$-deficient mice.

$ApoE^{-/-}$ and ApoE/$P2Y_{12}$ DK male mice underwent bone marrow transplantation to generate chimeric groups: ApoE into ApoE, DK into ApoE, DK into DK, and ApoE into DK (n=12, 15, 12 and 12 respectively). Following 4 weeks on a western diet, aortae were **(a)** stained with oil red O, and lesion area calculated as a percentage of surface area for the **(b)** whole aorta, and **(c)** aortic arch and descending aorta. Data are mean ± SEM; *P*=ns; **(b)** one-way ANOVA with Tukey's multiple comparison; **(c)** Mann-Whitney test (adjusted level of significance *P*<0.01 for multiple group comparisons).

Figure 6.4 – Attenuated atheroma was seen in the brachiocephalic arteries of vessel wall $P2Y_{12}$-deficient mice, following bone marrow transplantation.

$ApoE^{-/-}$ and $ApoE/P2Y_{12}$ DK male mice underwent bone marrow transplantation to generate chimeric groups: ApoE into ApoE, DK into ApoE, DK into DK, and ApoE into DK (n=10, 13, 8 and 9 respectively). Following 4 weeks on a western diet, the brachiocephalic arteries were sectioned, and **(a)** stained with alcian blue/elastic van Gieson. Representative cross-sections of each chimeric group are shown. Images taken at x100 magnification, scale bar = 100 μm. **(b)** Lesion area was calculated, and is shown as mean lesion:CSA (cross-sectional area) ratio. Data are mean ± SEM; **P*<0.05, ***P*<0.01, ****P*<0.001; one-way ANOVA with Tukey's multiple comparison.

(a)

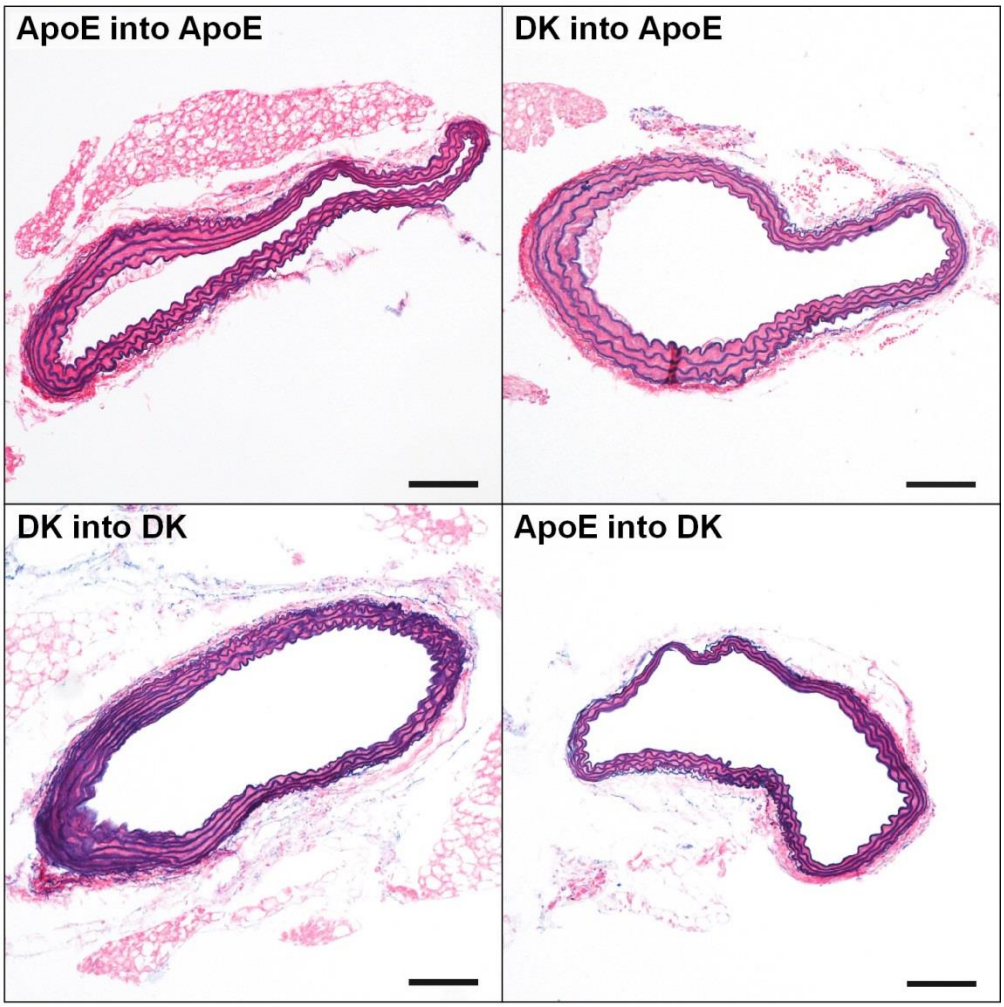
ApoE into ApoE
DK into ApoE
DK into DK
ApoE into DK

(b)

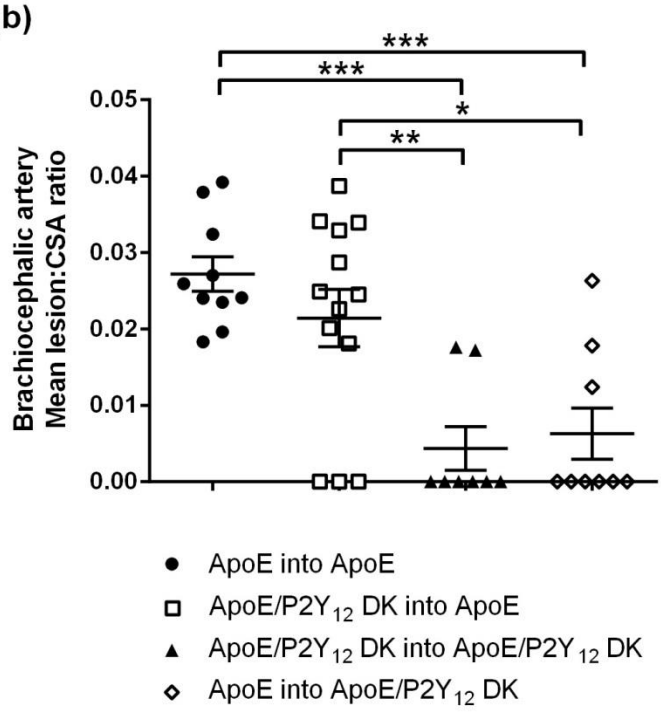
***
***
*
**
Brachiocephalic artery
Mean lesion:CSA ratio
0.05
0.04
0.03
0.02
0.01
0.00
ApoE into ApoE
ApoE/P2Y12 DK into ApoE
ApoE/P2Y12 DK into ApoE/P2Y12 DK
ApoE into ApoE/P2Y12 DK

Figure 6.5 – Lesion formation was significantly attenuated in the aortic sinus of vessel wall $P2Y_{12}$-deficient mice, regardless of platelet $P2Y_{12}$ expression.

$ApoE^{-/-}$ and $ApoE/P2Y_{12}$ DK male mice underwent bone marrow transplantation to generate chimeric groups: ApoE into ApoE, DK into ApoE, DK into DK, and ApoE into DK (n=13, 14, 9 and 10 respectively). Following 4 weeks on a western diet, the aortic sinus was sectioned, and **(a)** stained with alcian blue/elastic van Gieson. Representative cross-sections of each chimeric group are shown. Images taken at x40 magnification, scale bar = 100 μm. **(b)** Lesion area was calculated, and is shown as mean lesion:CSA (cross-sectional area) ratio. Data are mean ± SEM; ****P*<0.001; one-way ANOVA with Tukey's multiple comparison.

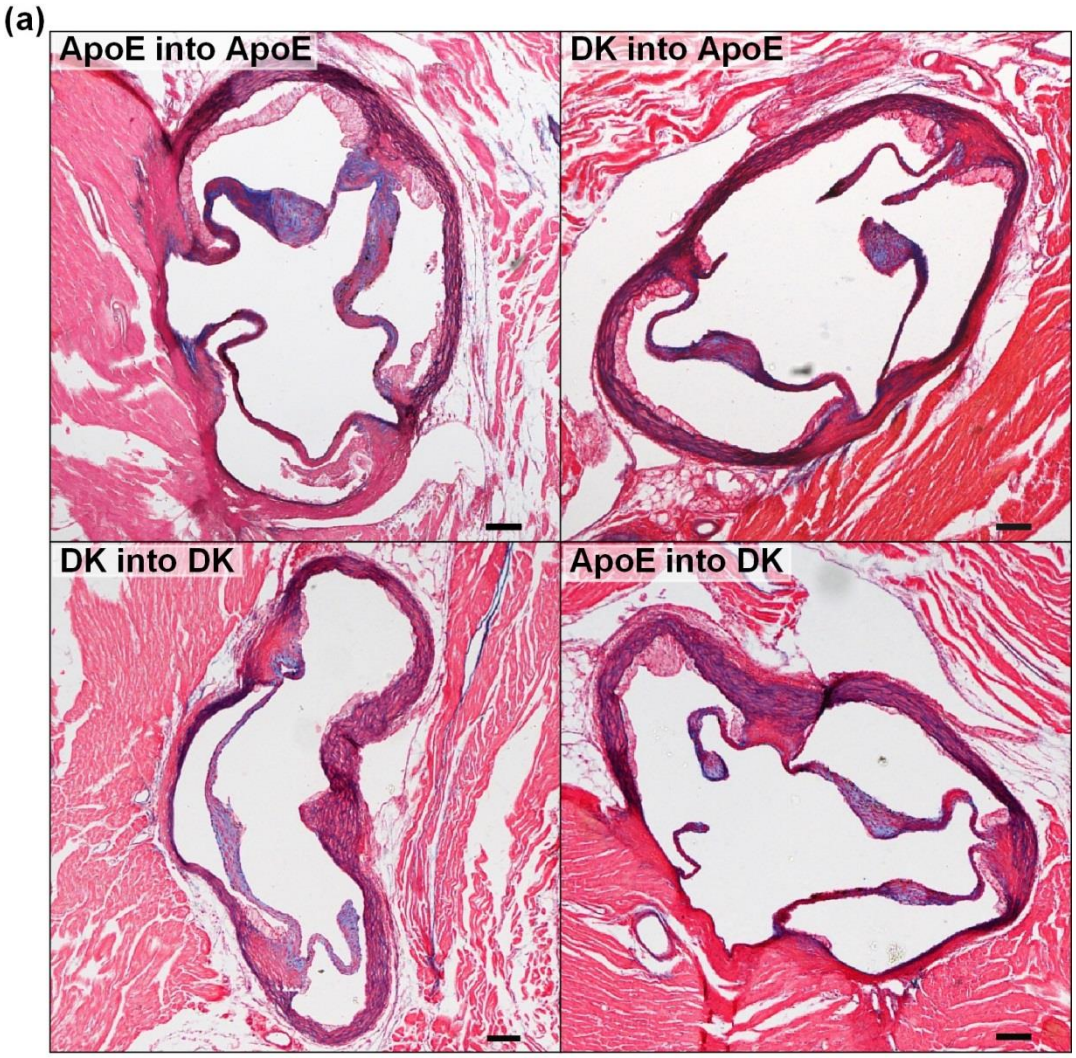
(a)
ApoE into ApoE
DK into ApoE
DK into DK
ApoE into DK

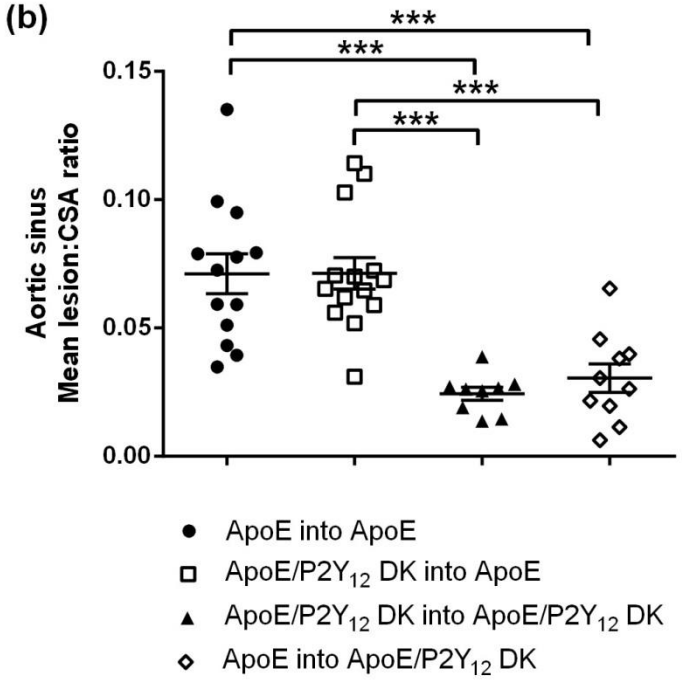
(b)
***
***
***
***
0.15
0.10
0.05
0.00
Aortic sinus
Mean lesion:CSA ratio
ApoE into ApoE
ApoE/P2Y12 DK into ApoE
ApoE/P2Y12 DK into ApoE/P2Y12 DK
ApoE into ApoE/P2Y12 DK

6.4 Vessel wall $P2Y_{12}$-deficiency results in an earlier lesion phenotype

As collagen and smooth muscle cell content are key characteristics of developing complex lesions, I went on to further stain the aortic sinus sections with martius scarlet blue for collagen, and for α-smooth muscle actin by immunohistochemistry.

6.4.1 Collagen

MSB staining of the aortic sinus sections showed well-defined bright blue collagen staining of the vessel wall and valve leaflets. Higher magnification images of $ApoE^{-/-}$ into $ApoE^{-/-}$ and ApoE/$P2Y_{12}$ DK into $ApoE^{-/-}$ lesions, those mice which did express vessel wall $P2Y_{12}$, showed collagen fibres within the lesions, predominantly located towards the cap and shoulder regions (see Figure 6.6b). However, inspection of lesions from mice lacking vessel wall $P2Y_{12}$, ApoE/$P2Y_{12}$ DK into ApoE/$P2Y_{12}$ DK and $ApoE^{-/-}$ into ApoE/$P2Y_{12}$ DK, showed little or no collagen staining within any of the lesions. Quantification of the percentage collagen content within aortic sinus lesions from each group confirmed a non-significant trend towards reduced collagen in vessel wall $P2Y_{12}$-deficient lesions: % collagen was 19.2 ± 4.29 in control mice, 12.08 ± 3.04 in mice lacking only vessel wall $P2Y_{12}$ and 7.94 ± 1.71 in mice with deficient vessel wall and platelet $P2Y_{12}$ (P=0.08 vs. control; Figure 6.7).

6.4.2 Smooth muscle actin

Smooth muscle actin immunostaining of aortic sinus sections, using DAB as the substrate, revealed brown α-SMA positive cells within the vessel wall. As typically seen in the aortic sinus, positive staining was localised to areas of the vessel wall with visible elastic laminae, but no staining was present in the myocardium. Higher magnification images demonstrated again that those mice which expressed vessel wall $P2Y_{12}$, $ApoE^{-/-}$ into $ApoE^{-/-}$ and ApoE/$P2Y_{12}$ DK into $ApoE^{-/-}$, had α-SMA positive cells within their lesions. As with the collagen staining, these cells were predominantly located towards the cap and shoulder regions of the lesions (see Figure 6.8b). Similarly, mice lacking vessel wall $P2Y_{12}$, ApoE/$P2Y_{12}$ DK into ApoE/$P2Y_{12}$ DK and $ApoE^{-/-}$ into ApoE/$P2Y_{12}$ DK, possessed fewer smooth muscle actin positive cells within their lesions. Quantification of α-SMA content within the aortic sinus lesions established again, a non-significant trend towards reduced percentage smooth muscle actin in vessel wall $P2Y_{12}$-deficient lesions: 6.14 ± 1.49% in control mice, 8.06 ± 1.36% in mice lacking platelet $P2Y_{12}$, 2.52 ± 0.6% in mice with deficient vessel wall and platelet $P2Y_{12}$ (P<0.05 vs. platelet $P2Y_{12}$ deficient mice) and 3.85 ± 0.89% in mice lacking only vessel wall $P2Y_{12}$ (P=0.09 vs. platelet $P2Y_{12}$ deficient mice; Figure 6.9).

Figure 6.6 – Aortic sinus lesions from bone marrow transplanted mice demonstrate reduced collagen staining in the lesions of vessel wall $P2Y_{12}$-deficient mice.

$ApoE^{-/-}$ and $ApoE/P2Y_{12}$ DK male mice underwent bone marrow transplantation to generate chimeric groups: **(i)** ApoE into ApoE, **(ii)** DK into ApoE, **(iii)** DK into DK, and **(iv)** ApoE into DK, and were fed western diet for 4 weeks. Representative aortic sinus cross-sections stained with martius scarlet blue are shown, in which collagen is stained bright blue. Images taken at **(a)** x40, scale bar = 100 µm and **(b)** x400 magnification (highlighted area), scale bar = 50 µm.

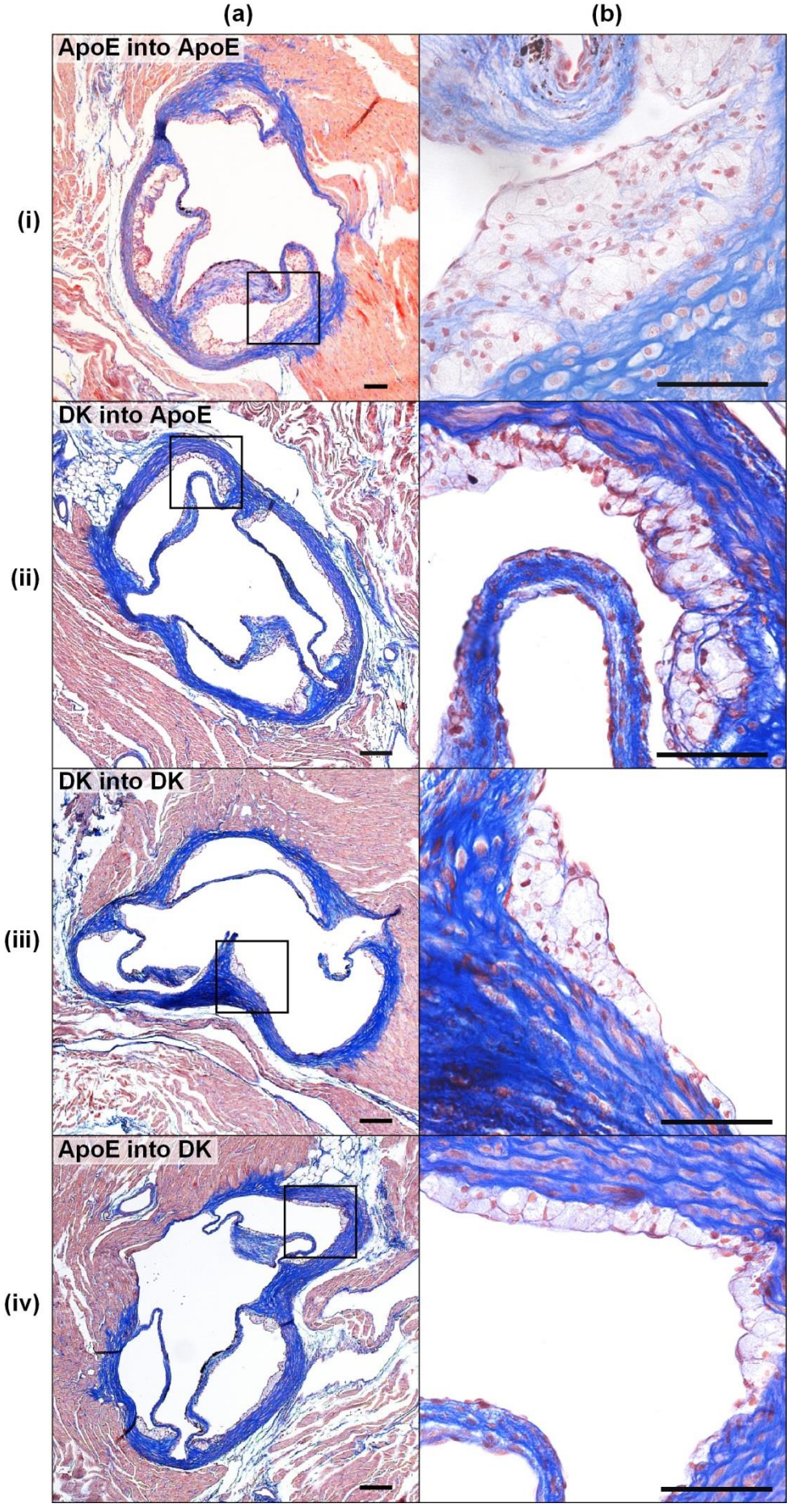
(a)
(b)
(i)
ApoE into ApoE
(ii)
DK into ApoE
(iii)
DK into DK
(iv)
ApoE into DK

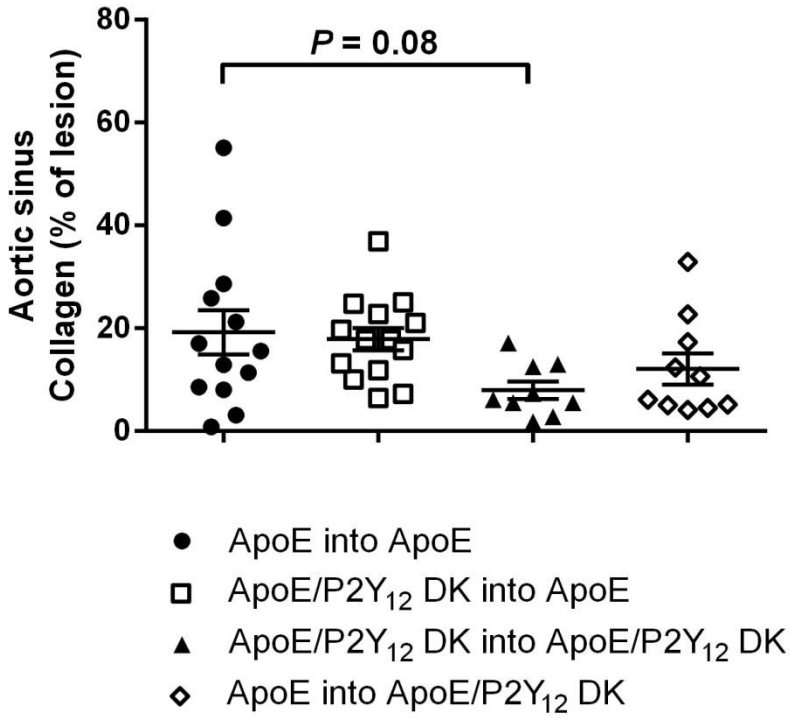

Figure 6.7 – Quantification of collagen content, within aortic sinus lesions, demonstrated that vessel wall $P2Y_{12}$-deficient mice expressed less collagen within their lesions.

$ApoE^{-/-}$ and ApoE/$P2Y_{12}$ DK male mice underwent bone marrow transplantation to generate chimeric groups: ApoE into ApoE, DK into ApoE, DK into DK, and ApoE into DK (n=13, 14, 9 and 10 respectively) and were fed western diet for 4 weeks. Collagen content within the aortic sinus lesions was quantified, and is shown as a percentage of the total lesion area. Data are mean ± SEM; *P*=ns; one-way ANOVA with Tukey's multiple comparison.

Figure 6.8 – Bone marrow transplanted mice demonstrate reduced α-smooth muscle actin staining in the aortic sinus lesions of vessel wall $P2Y_{12}$-deficient mice.

$ApoE^{-/-}$ and $ApoE/P2Y_{12}$ DK male mice underwent bone marrow transplantation to generate chimeric groups: **(i)** ApoE into ApoE, **(ii)** DK into ApoE, **(iii)** DK into DK, and **(iv)** ApoE into DK, and were fed western diet for 4 weeks. Representative aortic sinus cross-sections stained for α-smooth muscle actin using immunohistochemistry are shown, in which positive cells are stained brown. Images taken at **(a)** x40, scale bar = 100 µm and **(b)** x400 magnification (highlighted area), scale bar = 50 µm.

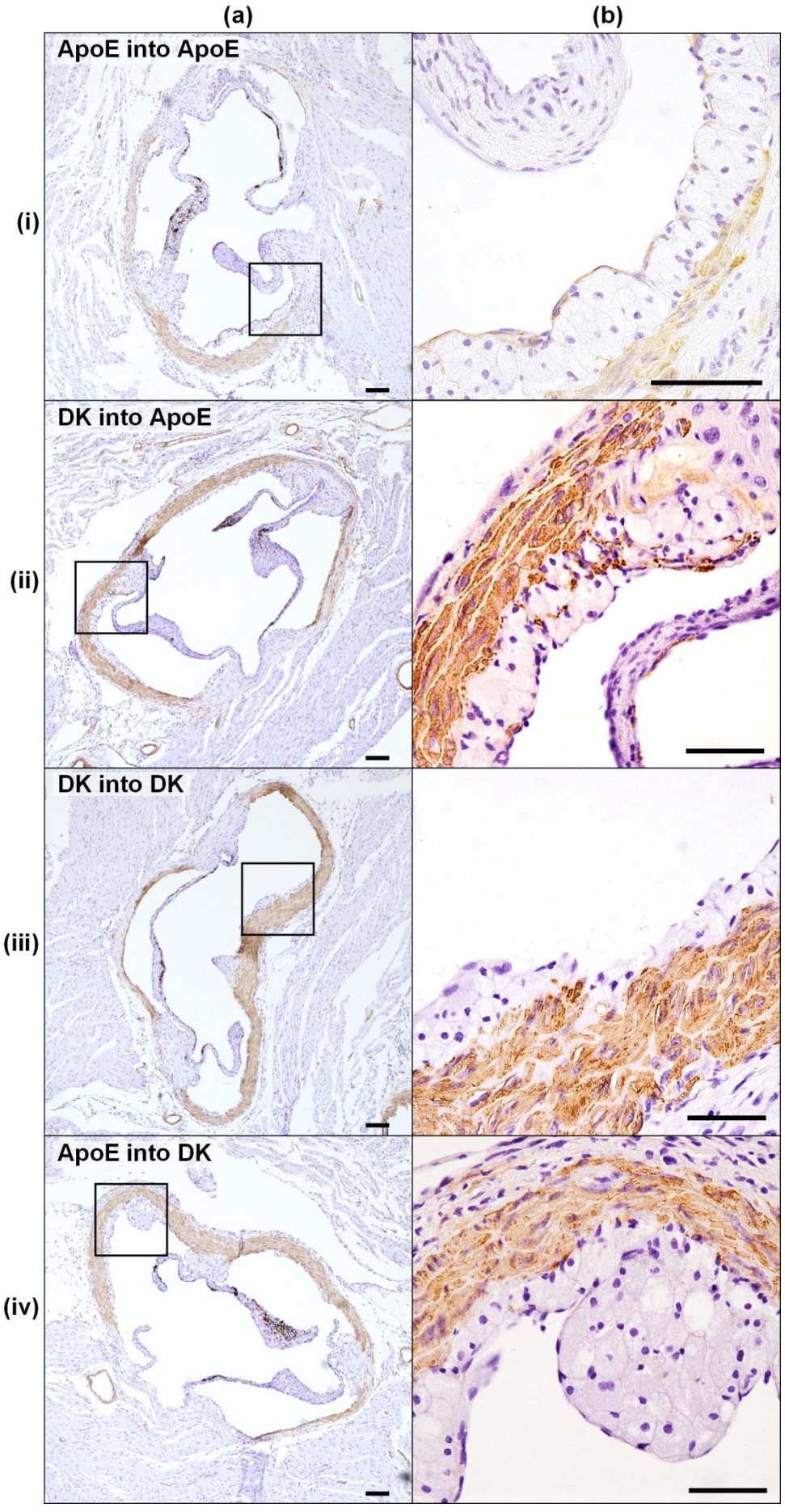
(a)
(b)
(i)
ApoE into ApoE
(ii)
DK into ApoE
(iii)
DK into DK
(iv)
ApoE into DK

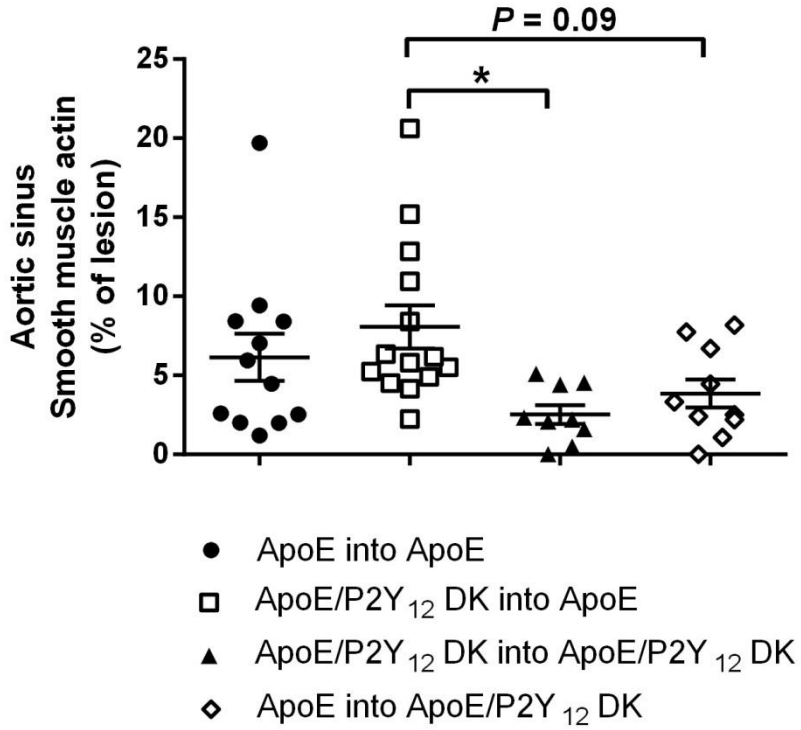

Figure 6.9 – Quantification of α-smooth muscle actin, within aortic sinus lesions, demonstrated that vessel wall $P2Y_{12}$-deficient mice had less smooth muscle actin positive cells within their lesions.

$ApoE^{-/-}$ and $ApoE/P2Y_{12}$ DK male mice underwent bone marrow transplantation to generate chimeric groups: ApoE into ApoE, DK into ApoE, DK into DK, and ApoE into DK (n=12, 14, 9 and 10 respectively) and were fed western diet for 4 weeks. Smooth muscle actin content within the aortic sinus lesions was quantified, and is shown as a percentage of the total lesion area. Data are mean ± SEM; **P*<0.05; one-way ANOVA with Tukey's multiple comparison.

6.5 $P2Y_{12}$ and α-smooth muscle actin dual immunofluorescence staining of aortic sinus lesions

To investigate the localisation of $P2Y_{12}$ expression within the aortic sinus lesions, I developed a dual immunofluorescence staining protocol for $P2Y_{12}$ alongside a smooth muscle cell marker, α-smooth muscle actin. Few commercial $P2Y_{12}$ antibodies were available, and none had been used on murine tissue or for this purpose. I opted to use the APR-012 $P2Y_{12}$ antibody from Alomone Labs (Israel). Various conditions were tested to find the optimum staining conditions, and the results can be seen in Figure 6.10.

The α-SMA antibody (green) produced strong positive staining within the vessel wall of the aortic sinus. Some additional positive cells could also be seen in lesions from $ApoE^{-/-}$ into $ApoE^{-/-}$ and ApoE/$P2Y_{12}$ DK into $ApoE^{-/-}$ mice. As seen with DAB immunostaining, there were no positive cells in the lesions of vessel wall $P2Y_{12}$-deficient mice. The $P2Y_{12}$ antibody (red) in comparison was very weak, and required a much longer exposure time, indicating a lower expression level. However, a positive signal was seen in the vessel wall, and mirrored those areas which were also α-SMA positive. Interestingly, positive staining could be seen in the vessel wall of all groups, despite the ApoE/$P2Y_{12}$ DK into ApoE/$P2Y_{12}$ DK and $ApoE^{-/-}$ into ApoE/$P2Y_{12}$ DK groups being vessel wall $P2Y_{12}$-deficient. Although a weak signal, some positive cells could also be seen in the lesions of $ApoE^{-/-}$ into $ApoE^{-/-}$ and ApoE/$P2Y_{12}$ DK into $ApoE^{-/-}$ mice. Negative and single colour control sections show no evidence of non-specific binding for either antibody.

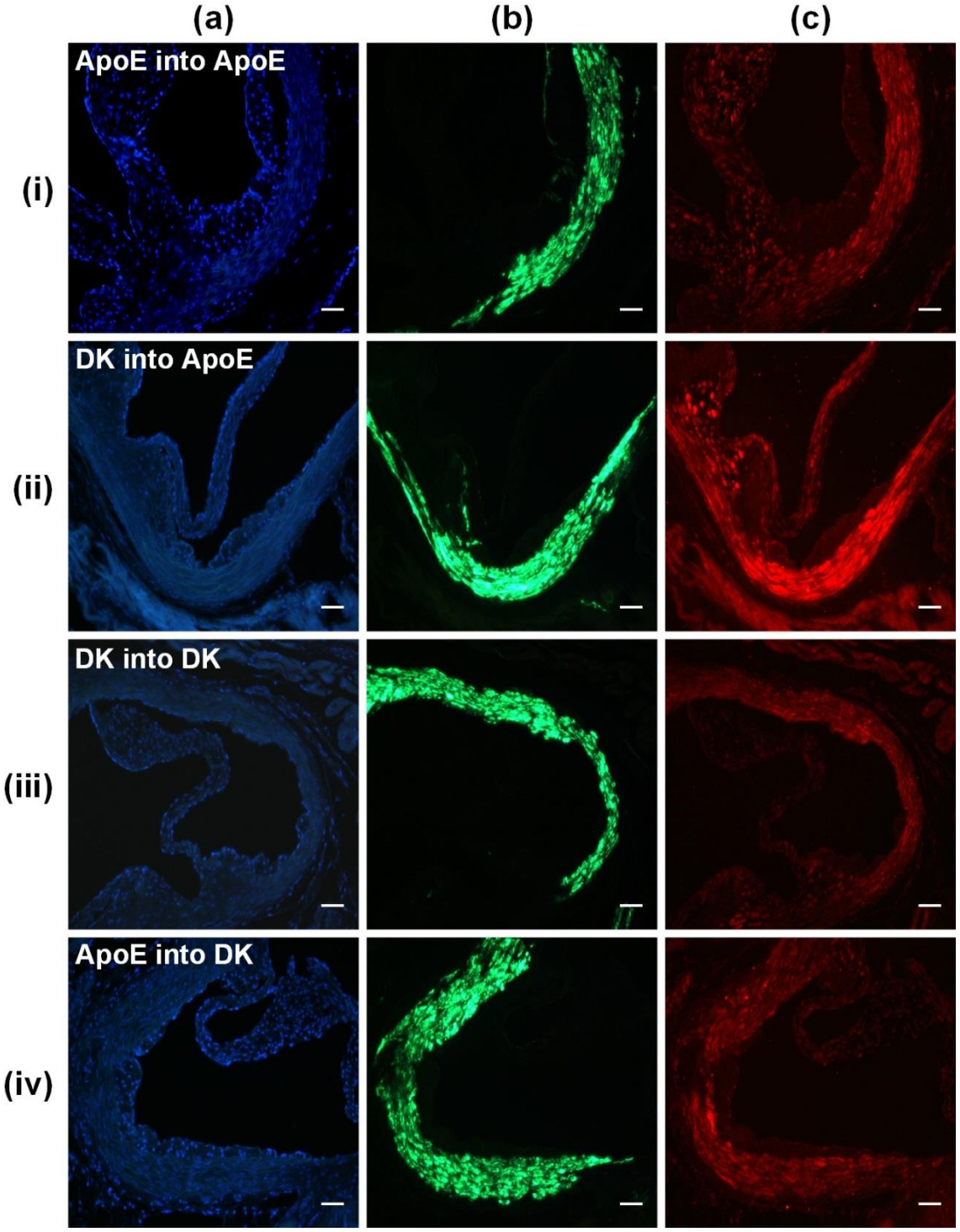
(a)
(b)
(c)
(i)
ApoE into ApoE
(ii)
DK into ApoE
(iii)
DK into DK
(iv)
ApoE into DK

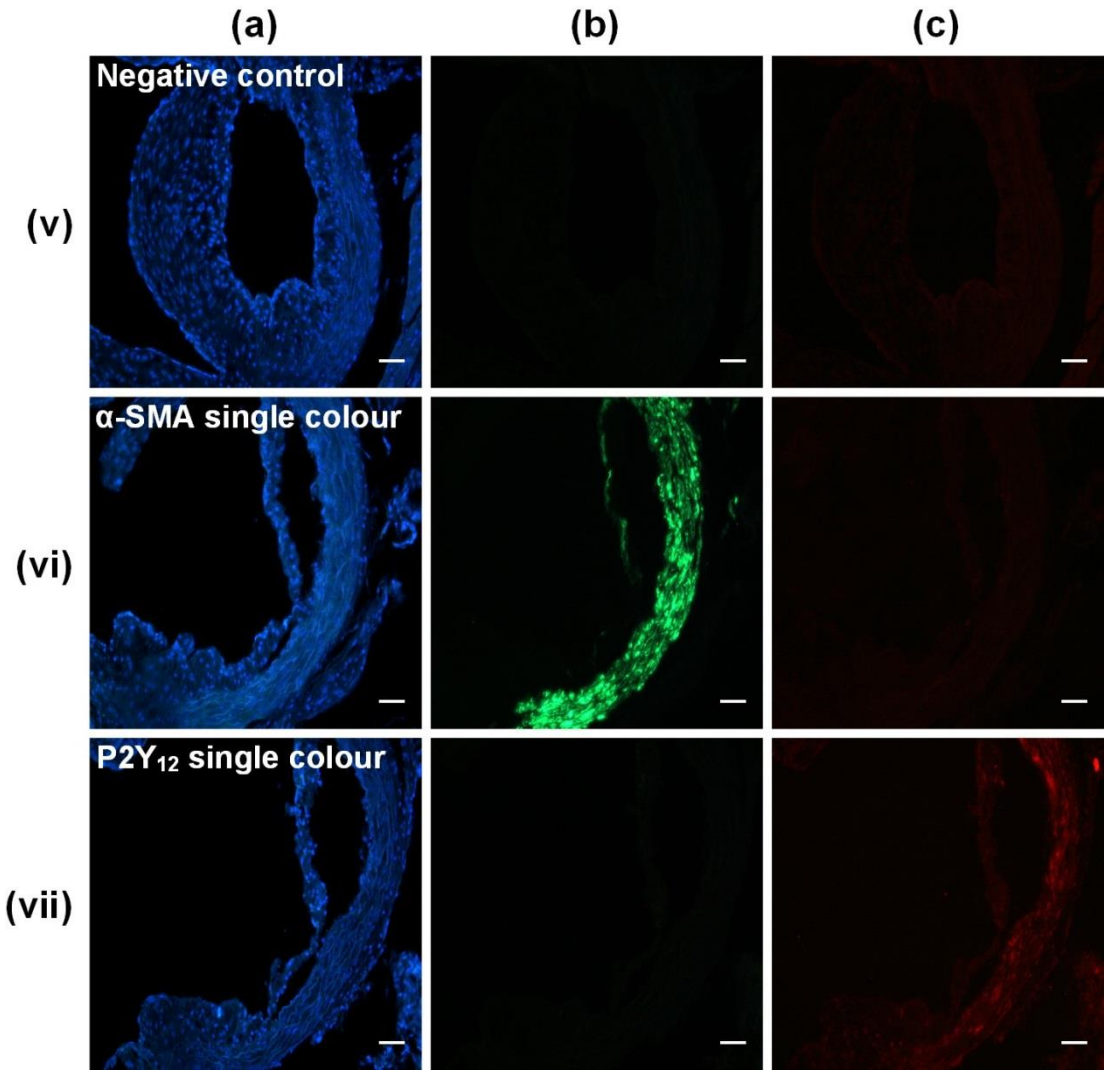

Figure 6.10 – Smooth muscle actin and $P2Y_{12}$ dual immunofluorescent staining of aortic sinus lesions from bone marrow transplanted mice.

$ApoE^{-/-}$ and $ApoE/P2Y_{12}$ DK male mice underwent bone marrow transplantation to generate chimeric groups: **(i)** ApoE into ApoE, **(ii)** DK into ApoE, **(iii)** DK into DK, and **(iv)** ApoE into DK and were fed western diet for 4 weeks. Representative aortic sinus cross-sections are shown, which are stained for **(a)** DAPI (nuclei, blue), **(b)** α-smooth muscle actin (green), and **(c)** $P2Y_{12}$ (red) using immunofluorescence techniques. **(v)** Negative and **(vi-vii) s**ingle colour controls are also shown. Images taken at x200 magnification, scale bar = 50 µm.

6.6 Summary

The work in this chapter further described the role of $P2Y_{12}$ in early atherogenesis, using bone marrow transplantations to delineate the contribution of platelet versus vessel wall $P2Y_{12}$ receptors in this process. Results were obtained following 4 weeks on a high-fat western diet. In summary:

- Reduced expression of platelet activation markers, P-selectin and activated GPIIbIIIa receptor, in $ApoE^{-/-}$ mice transplanted with ApoE/$P2Y_{12}$ DK bone marrow demonstrated the expected bone marrow $P2Y_{12}$ phenotype, and thus confirmed the efficacy of transplantation.
- There were no differences in the coagulation response of bone marrow transplanted mice.
- Vessel wall $P2Y_{12}$-deficient mice had attenuated lesion formation in the whole aorta and aortic arch compared to $ApoE^{-/-}$ control mice.
- In addition, lesion area was significantly reduced in the brachiocephalic arteries and aortic sinus of vessel wall $P2Y_{12}$-deficient mice.
- The effect of vessel wall $P2Y_{12}$-deficiency on lesion development appeared to be independent of platelet $P2Y_{12}$ expression.
- Aortic sinus lesions from mice which expressed vessel wall $P2Y_{12}$ demonstrated collagen fibres within the cap and shoulder regions, and contained an increased percentage collagen content than lesions from those mice lacking vessel wall $P2Y_{12}$, where little or no collagen was observed.
- Similarly, vessel wall $P2Y_{12}$-deficient mice also had fewer α-smooth muscle actin positive cells within their lesions.
- $P2Y_{12}$ and α-smooth muscle actin dual staining provided interesting, but inconclusive results. Some weak $P2Y_{12}$ positive cells were noted in the lesions; however, positive staining was also observed in the aortic sinus wall of vessel wall $P2Y_{12}$-deficient mice.

6.7 Discussion

Fully understanding the role of platelets and $P2Y_{12}$ in atherogenesis could reveal potential mechanisms by which disease progression could be modulated. In the previous chapter, I demonstrated a moderate regional effect of $P2Y_{12}$–deficiency in established disease; yet little is known of its impact in early atherogenesis or likewise, of the role of vessel wall $P2Y_{12}$ in this process. In this chapter, I identify a previously unknown role of vessel wall $P2Y_{12}$ in modulating early atherogenesis, and therefore propose that it is vessel wall, rather than platelet, $P2Y_{12}$ which plays a significant role in the early stages of disease by promoting lesion development.

To my knowledge, all platelet atherogenesis studies to date model established disease, choosing end points from 7 to more than 30 weeks on a chow or high-fat diet (Massberg *et al.* 2002; Burger and Wagner 2003; Hechler *et al.* 2008; Bultmann *et al.* 2010). Cholesterol clefts and fibrous caps are common features in these lesions, and are typically associated with advanced plaques, including those which are susceptible to endothelial erosion and rupture (Stary *et al.* 1995). This is true of my findings from the previous chapter, where mice fed a western diet for 12 weeks had advanced lesions, and also the Li study which assessed atheroma in ApoE/$P2Y_{12}$ DK mice after 20 weeks on a high-fat diet, similar in composition to our own western diet (Li *et al.* 2012). I therefore chose to study a much earlier stage of atherogenesis, after only 4 weeks of feeding, where I could both accurately measure atheroma and also be confident of little risk of endothelial erosion.

To investigate the role of platelet versus vessel wall $P2Y_{12}$ at this earlier time point, I carried out bone marrow transplantations using a method previously employed by our group (Chamberlain *et al.* 2006; Evans *et al.* 2009). To further confirm the successful reconstitution of donor bone marrow into recipient mice I performed a P-selectin assay to assess $P2Y_{12}$ function, and found $ApoE^{-/-}$ mice transplanted with ApoE/$P2Y_{12}$ DK bone marrow had diminished platelet function as expected, compared to control mice. These results were consistent with our previous findings on $P2Y_{12}$ mice (Evans *et al.* 2009).

Recent work by Rauch *et al.* links $P2Y_{12}$ expression with VSMC mitogenesis via a thrombin-induced pathway, and may provide a potential mechanism for the effect I observed (Rauch *et al.* 2010). Interestingly, following exposure to thrombin, they found $P2Y_{12}$ surface expression being significantly upregulated by nuclear factor kappa-light-chain-enhancer of activated B cells (NF-κB), and $P2Y_{12}$-induced mitogenic effects enhanced. In an inflammatory setting such as atherogenesis, where thrombin generation is likely, it is probable that $P2Y_{12}$-potentiated VSMC mitogenesis contributes to lesion progression. Indeed, $P2Y_{12}$-positive VSMCs have been identified within atherosclerotic lesions (Rauch *et al.* 2010). Furthermore, to eliminate the possible impact of differences in thrombin generation on the interpretation of my findings, I conducted PT and aPTT tests and found no difference in response between chimeric groups.

Assessing atheroma in transplanted mice following 4 weeks on a western diet demonstrated that, in contrast to the Li study, it is vessel wall, rather than platelet, $P2Y_{12}$ which is important in the development of early lesions, but perhaps this balance shifts as disease progresses. This hypothesis is supported by my previous work in Chapter 3 showing that platelet, rather than vessel wall, $P2Y_{12}$ plays a profound role in the vessel wall response to injury (Evans *et al.* 2009). Consideration must also be made for the potential influence of vessel wall $P2Y_{12}$ on the results demonstrated by Li *et al* (Li *et al.* 2012). Only ApoE/$P2Y_{12}$ DK mice were chosen as recipients for their bone marrow transplantations and so further investigation

looking at the role of vessel wall $P2Y_{12}$ in later atherogenesis is warranted. Research into the role of the related platelet purine receptor $P2Y_1$ in atherogenesis, which is more widely expressed than $P2Y_{12}$, demonstrated a similar vascular wall effect on atherogenesis, and so also supports the need for further exploration in this area (Hechler *et al.* 2008).

The smaller lesions observed in vessel wall $P2Y_{12}$-deficient mice suggest that VSMC $P2Y_{12}$ expression does influence lesion size, perhaps via VSMC mitogenesis; however, this is yet to be explored. Absence of α-SMA expression within these lesions, compared to positive staining seen in those mice which do express vessel wall $P2Y_{12}$, lends some support to this hypothesis, although whether lesion progression is delayed or altered in the absence of VSMC $P2Y_{12}$ remains to be seen. Indeed, little is known of the true effects of $P2Y_{12}$ deficiency on VSMC development, phenotype, or plasticity and so extensive investigation is required to find the exact mechanism behind these findings.

Given that $P2Y_{12}$-positive VSMCs had been identified in human atherosclerotic lesions (Rauch *et al.* 2010), I was interested to investigate the location of these cells, and in relation to known VSMC marker, α-SMA. I therefore chose to use an immunofluorescence staining approach. Having researched into the few commercially available $P2Y_{12}$ antibodies, I found the literature to be very limited, with few of these antibodies having either been tested on rodent tissue, or for immunohistochemistry or fluorescence techniques. However, of these antibodies, the APR-012 polyclonal antibody from Alomone Labs had successfully been used on both rat spleen and brain tissue for immunofluorescence (Amadio *et al.* 2006; Uehara and Uehara 2011). I therefore endeavoured to use this antibody, in conjunction with the Dako α-SMA antibody, for dual immunofluorescence staining using Alexa Fluor 488 (α-SMA) and Alexa Fluor 594 ($P2Y_{12}$) conjugated secondary antibodies.

Despite a weak signal, $P2Y_{12}$ staining could clearly be seen in the vessel wall which, as expected, corresponded to α-smooth muscle actin positive areas. In addition, some weakly positive cells could to seen in lesions from $ApoE^{-/-}$ into $ApoE^{-/-}$ and $ApoE/P2Y_{12}$ DK into $ApoE^{-/-}$ mice, but further work is necessary to improve the $P2Y_{12}$ staining in order to determine whether these are both $P2Y_{12}$ and α-SMA positive cells. Negative control sections showed no evidence of non-specific binding, yet positive staining could be seen in the vessel wall of all chimeric groups, despite some being vessel wall $P2Y_{12}$-deficient. Given that the biological phenotype of all chimeras were as expected, as is clearly demonstrated in the P-selectin data (see Figure 6.1), there is not a clear explanation for these findings. However, I postulate that as the $P2Y_{12}^{-/-}$ mice were generated using a neomycin insert into the gene, perhaps some protein is still expressed in these mice, but the receptor is not functional. The Alomone $P2Y_{12}$ antibody is specific to the 2^{nd} intracellular loop of the receptor and so, if this amino acid sequence remains, it may explain the positive staining seen in these mice.

These data demonstrate that vessel wall $P2Y_{12}$ is important in early atherogenesis and potentiates lesion formation, perhaps via VSMC mitogenesis. In later disease, it seems that platelet $P2Y_{12}$ plays a greater role in determining lesion size and phenotype. $P2Y_{12}$ inhibitors, ticagrelor and clopidogrel, effectively inhibit platelet reactivity and therefore, in the following chapter, I went on to investigate whether these were able to block the vessel wall $P2Y_{12}$ effect on early atherogenesis.

7 Effect of pharmacological inhibition of $P2Y_{12}$ on early atherogenesis

The $P2Y_{12}$ antagonist clopidogrel and next-generation agents, such as ticagrelor, are routinely used in ACS treatment due to their remarkable effects at preventing thrombosis. Given that vessel wall $P2Y_{12}$ is able to potentiate early atherogenesis; I was interested to investigate if these $P2Y_{12}$ inhibitors were able to modulate the vessel wall $P2Y_{12}$-mediated effect on early atherogenesis in $ApoE^{-/-}$ mice.

In addition, recent data show that ticagrelor also inhibits adenosine re-uptake by RBCs (van Giezen *et al.* 2012), and blocks ADP-induced vasoconstriction in isolated arteries (Hogberg *et al.* 2010; Grzesk *et al.* 2012). Furthermore, ticagrelor offers a reduced mortality risk, compared to clopidogrel, in patients with acute coronary syndromes (Wallentin *et al.* 2009), but the mechanisms for this mortality reduction remain to be established. I therefore aimed to determine any non-$P2Y_{12}$-mediated effects of ticagrelor or clopidogrel on early atherogenesis in ApoE/$P2Y_{12}$ DK mice.

7.1 Voluntary drug delivery of ticagrelor and clopidogrel in jelly results in effective $P2Y_{12}$ inhibition

To investigate the effects of $P2Y_{12}$ inhibitors on early atherogenesis, mice were given either twice-daily doses of ticagrelor (100 mg/kg), daily clopidogrel (20 mg/kg), or mannitol (control) in jelly, in addition to a western diet for 4 weeks. This novel method of voluntary drug delivery was adapted from a published method by Zhang (Zhang 2011) and avoided the need for twice-daily gavage, which would have been highly stressful to the animals.

Mice were first trained for a week with jelly only and then switched to a drug-jelly mixture. All responded well, with 77% of mice eating all or >50% of the jelly cube for each dose, throughout the 4 weeks of drug treatment. The remaining 23% of mice did not eat the jelly on five or more occasions; however, missed doses were sporadic and interleaved with periods where the jelly cubes were consumed. None of the mice missed every dose. Of the mice which missed five or more doses, all but one was in the ticagrelor treatment group. With some mice, particularly those in the ticagrelor group, missing several drug doses, I was keen to investigate the efficacy of drug delivery for this method and so assessed platelet $P2Y_{12}$ inhibition by measuring P-selectin expression in response to PAR-4 TRAP.

Platelets from $ApoE^{-/-}$ mice treated with mannitol (control) demonstrated high fluorescence of the CD62p antibody in response to 1 mmol/L TRAP, indicating these platelets expressed high levels of P-selectin as expected. In contrast, platelets from $ApoE^{-/-}$ mice treated with $P2Y_{12}$ antagonists, ticagrelor and clopidogrel, showed attenuated platelet activation and

exhibited much lower fluorescence levels, shown as a shift to the left in the P-selectin fluorescence peaks (see Figure 7.1a).

Expression was measured as an increase in median fluorescence over baseline, determined using an isotype control antibody. At each concentration, $ApoE^{-/-}$ mice treated with $P2Y_{12}$ inhibitors demonstrated lower P-selectin expression (see Figure 7.1b) compared to control-treated mice. This was particularly evident in response to 1 mmol/L TRAP for which P-selectin median fluorescence was 600 ± 87 for $ApoE^{-/-}$ controls, 166 ± 55 for ticagrelor-treated mice (P<0.001 vs. control), and 141 ± 73 for clopidogrel-treated mice (P<0.001 vs. control; Figure 7.1c). As expected, reduced P-selectin expression was observed in all ApoE/$P2Y_{12}$ DK mouse treatment groups, and there was no additional effect of ticagrelor or clopidogrel (see Figure 7.1b and c). Attenuated expression of these activation markers in $ApoE^{-/-}$ mice treated with ticagrelor and clopidogrel verified effective drug delivery and $P2Y_{12}$ inhibition.

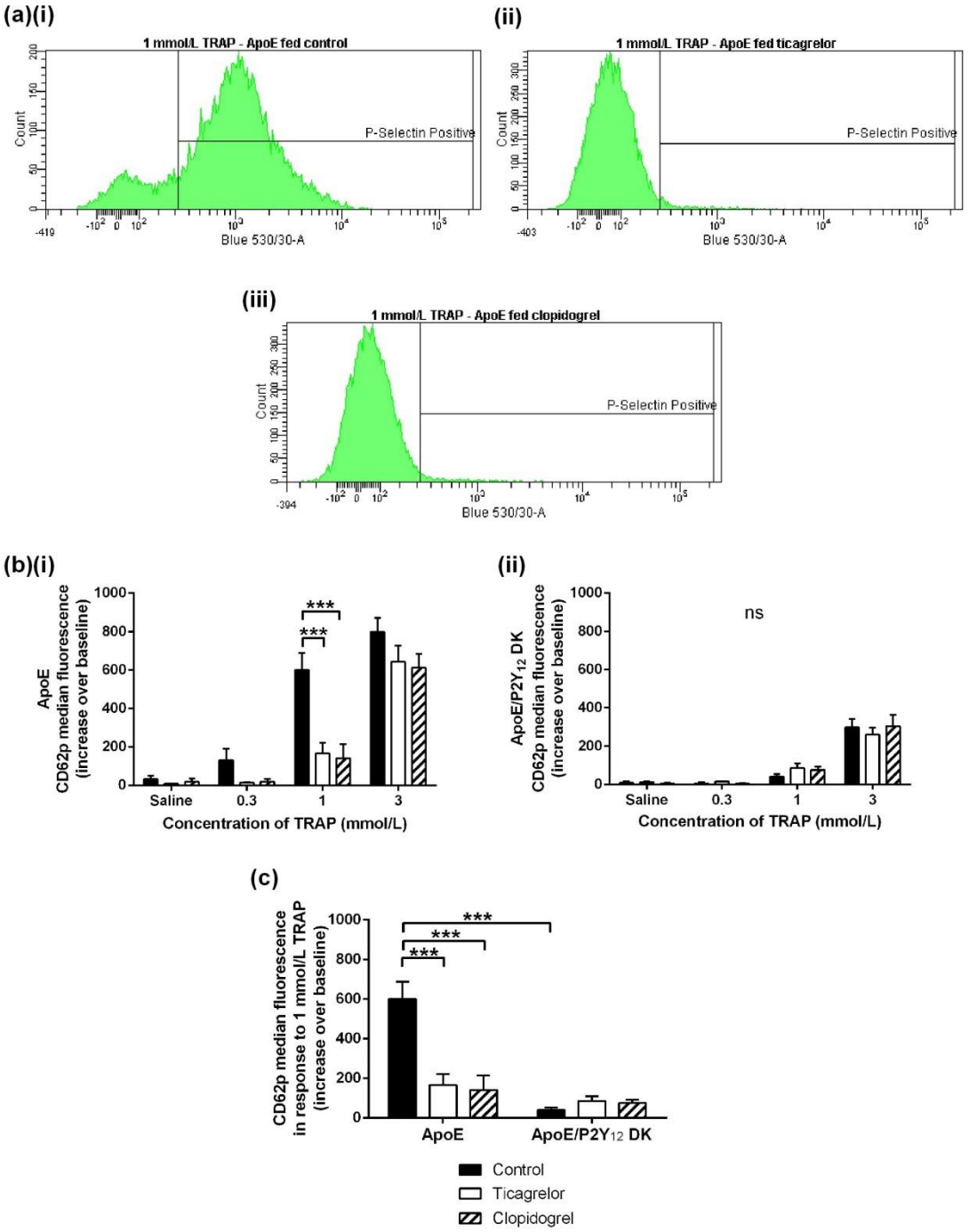

Figure 7.1 – ApoE$^{-/-}$ mice treated with ticagrelor or clopidogrel exhibited reduced P-selectin expression, demonstrating effective platelet P2Y$_{12}$ inhibition.

Blood was taken from ApoE$^{-/-}$ and ApoE/P2Y$_{12}$ DK male mice treated with either ticagrelor (n=7 & 6 respectively), clopidogrel (n=5 & 6), or mannitol (control; n=7 & 6), and analysed by flow cytometry to assess P-selectin (CD62p) expression in response to PAR-4 TRAP. **(a)** Representative fluorescence histograms are shown for ApoE$^{-/-}$ mice from each treatment group. P-selectin expression was measured as median fluorescence, shown as increase over baseline, for **(b)(i)** ApoE$^{-/-}$ and **(ii)** ApoE/P2Y$_{12}$ DK mice and **(c)** in response to 1 mmol/L PAR-4 TRAP. Data are mean ± SEM; ***P<0.001; two-way ANOVA with Tukey's multiple comparison.

7.2 Ticagrelor and clopidogrel have no effect on early atherogenesis

ApoE$^{-/-}$ and ApoE/P2Y$_{12}$ DK male mice were fed either ticagrelor, clopidogrel, or mannitol (control) for 4 weeks, in addition to a western diet, to investigate the effects of pharmacological inhibition of P2Y$_{12}$ on early atherogenesis. Atheroma was assessed in the thoracic aorta and aortic sinus.

7.2.1 Aortae

Whole aortae were stained with oil red O (see Figure 7.2a), and the mean percentage atheroma was calculated for each treatment group and genotype. Ticagrelor or clopidogrel treatment had no effect on lesion development, compared to controls, in either ApoE$^{-/-}$ or ApoE/P2Y$_{12}$ DK mice (see Figure 7.2b). Likewise, further analysis of the aortic arch and descending aorta demonstrated no region-specific differences in lesion formation (descending aorta data not shown). A greater spread of data was noted in the aortic arch lesion area of ApoE$^{-/-}$ compared to ApoE/P2Y$_{12}$ DK mice: lesion area was 1.54 ± 0.35% in control, 1.9 ± 0.51% in ticagrelor and 0.86 ± 0.24% in clopidogrel treated ApoE$^{-/-}$ mice (all *P*=ns vs. control) vs. 1.38 ± 0.3% in control, 1.8 ± 0.29% in ticagrelor and 1.47 ± 0.28% in clopidogrel treated ApoE/P2Y$_{12}$ DK mice (all *P*=ns vs. control).

7.2.2 Aortic sinus

As seen previously with 4 weeks of feeding on a western diet, histological staining revealed the presence of small, simple lesions within the aortic sinus (see Figure 7.3). Quantitative analysis demonstrated similar results to the whole aortae and showed no effect of the P2Y$_{12}$ inhibitors on atherogenesis in either ApoE$^{-/-}$ or ApoE/P2Y$_{12}$ DK mice compared to controls. However, an overall effect of P2Y$_{12}$ deficiency on lesion size continued to be observed in the presence of the P2Y$_{12}$ inhibitors, when comparing all ApoE/P2Y$_{12}$ DK mice with their ApoE$^{-/-}$ counterparts (Mean lesion:CSA ratio 0.023 ± 0.002 [DK] vs. 0.034 ± 0.002 [ApoE]; *P*<0.001; Figure 7.4).

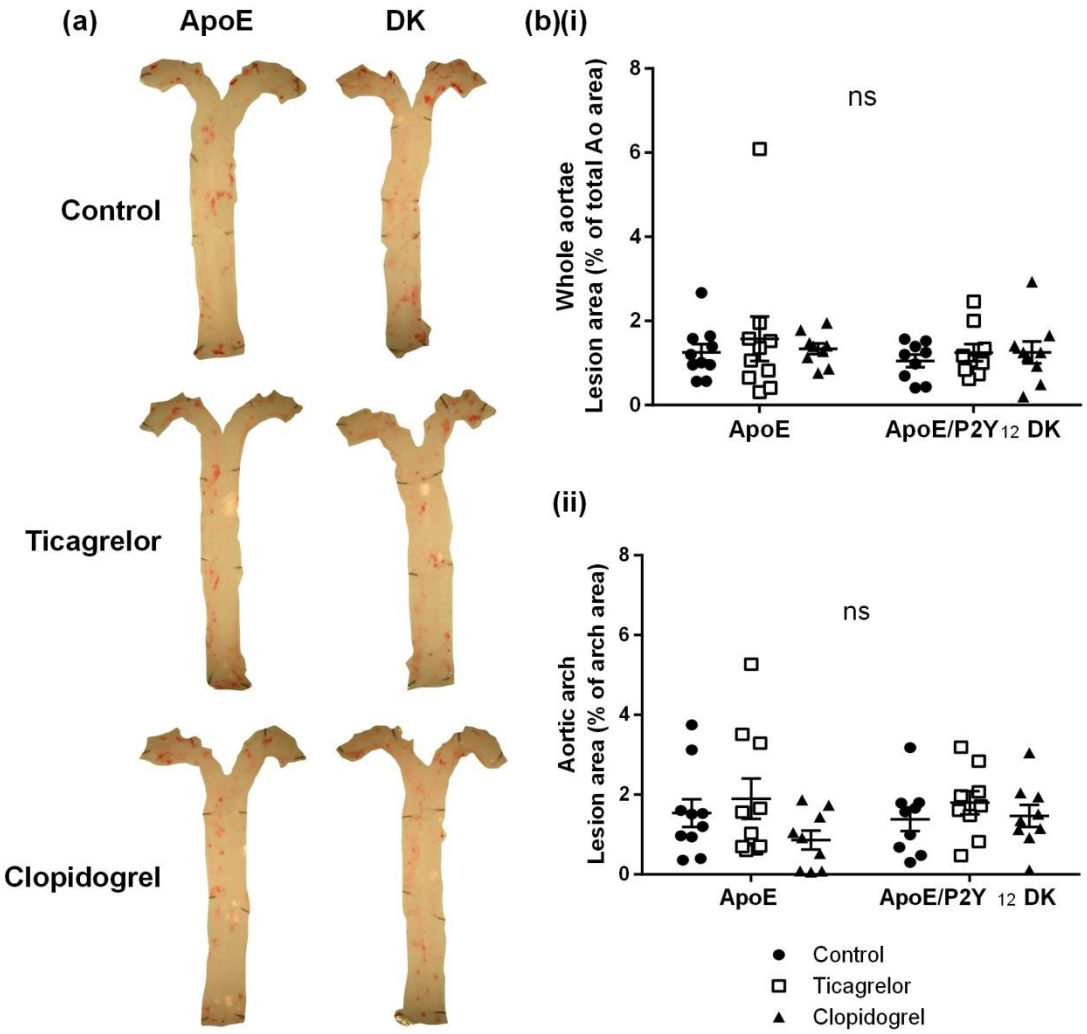

Figure 7.2 – Oil red O staining of whole aortae showed no effect of ticagrelor or clopidogrel treatment on lesion formation compared to control mice.

Whole aortae were excised from ApoE$^{-/-}$ and ApoE/P2Y$_{12}$ DK male mice fed western diet for 4 weeks, in addition to either twice daily doses of ticagrelor (100 mg/kg; n=10 & 9 respectively), daily clopidogrel (20 mg/kg; n=9 & 8), or mannitol (control; n=9). **(a)** Aortae were stained *en face* with oil red O, and lesion area quantified in **(b)(i)** the whole aorta and **(ii)** aortic arch. Data are mean ± SEM; *P*=ns; two-way ANOVA with Tukey's multiple comparison.

Figure 7.3 – ApoE$^{-/-}$ and ApoE/P2Y$_{12}$ double knockout mice treated with ticagrelor, clopidogrel, or control demonstrated small aortic sinus lesions, but no overall difference in the extent of atheroma.

Representative aortic sinus cross-sections stained with alcian blue/elastic van Gieson from **(a)** ApoE$^{-/-}$ and **(b)** ApoE/P2Y$_{12}$ DK male mice fed a western diet for 4 weeks in addition to either **(i)** mannitol (control), **(ii)** ticagrelor, or **(iii)** clopidogrel treatment. Images taken at x40 magnification, scale bar = 100 µm.

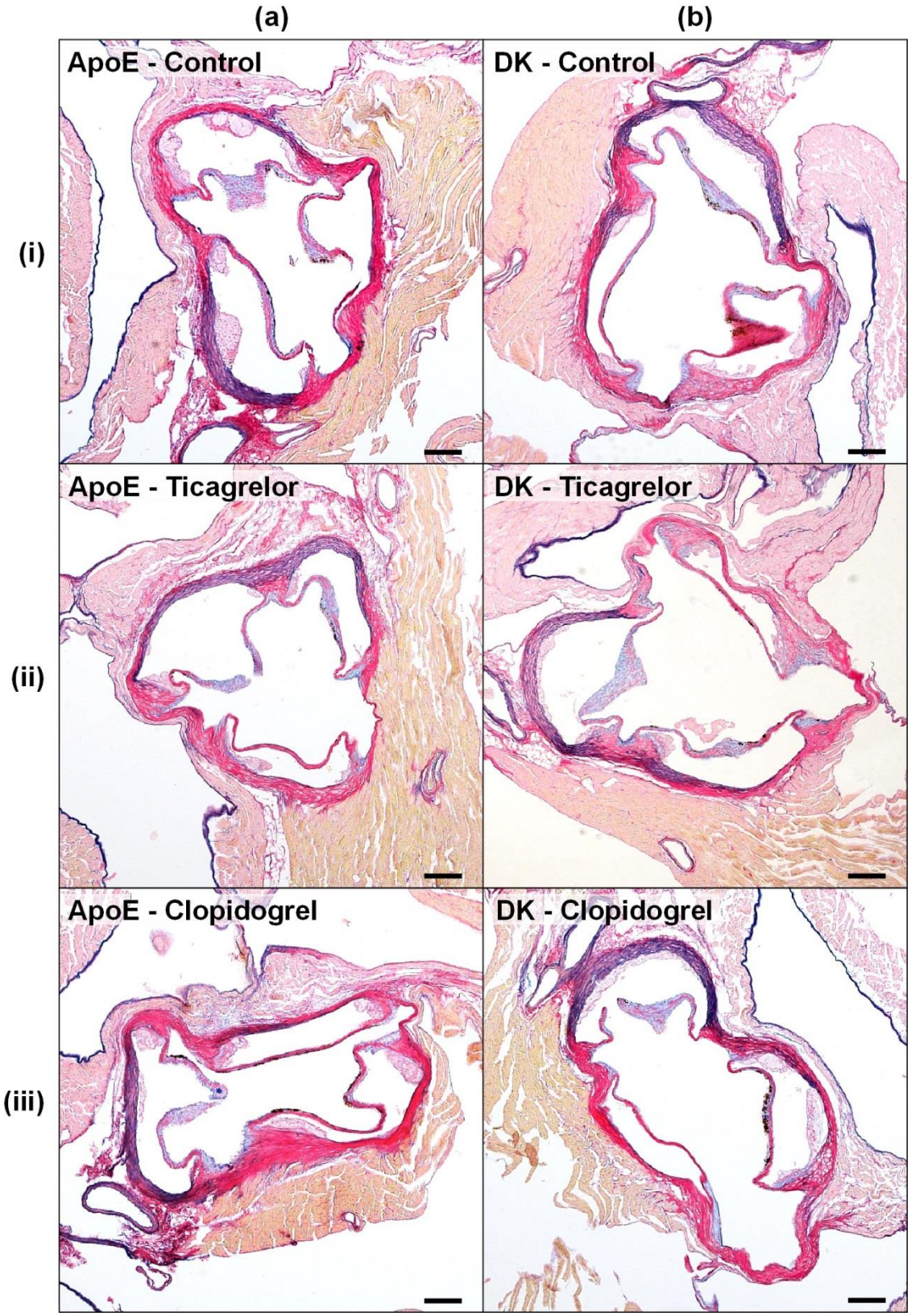
(a)
(b)
(i)
(ii)
(iii)
ApoE - Control
DK - Control
ApoE - Ticagrelor
DK - Ticagrelor
ApoE - Clopidogrel
DK - Clopidogrel

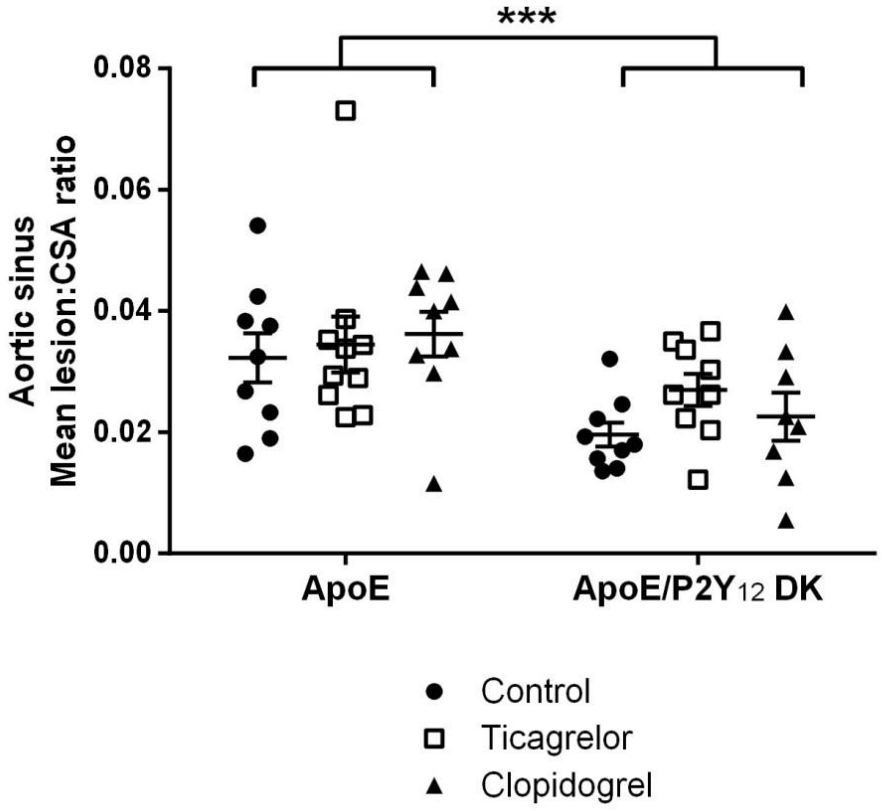

Figure 7.4 – Ticagrelor or clopidogrel treatment had no effect on lesion development in ApoE$^{-/-}$ or ApoE/P2Y$_{12}$ double knockout mice, but an effect of P2Y$_{12}$-deficiency on atheroma was still observed.

Lesion area was quantified in the aortic sinus from ApoE$^{-/-}$ and ApoE/P2Y$_{12}$ DK male mice fed western diet for 4 weeks, in addition to either twice daily doses of ticagrelor (100 mg/kg; n=10 & 9 respectively), daily clopidogrel (20 mg/kg; n=9 & 8), or mannitol (control; n=9). Lesion area is shown as mean lesion:CSA (cross-sectional area) ratio. Data are mean ± SEM; *P*<0.001; Independent samples t test (ApoE vs ApoE/P2Y$_{12}$ DK); *P*=ns; two-way ANOVA with Tukey's multiple comparison.

7.3 Summary

This chapter has examined the use of $P2Y_{12}$ inhibitors, ticagrelor and clopidogrel, in modulating early atherogenesis, and investigated both $P2Y_{12}$- or non-$P2Y_{12}$-mediated effects on this process. In summary:

- Ticagrelor and clopidogrel treatment yielded a significant reduction in the expression of platelet activation marker, P-selectin, in $ApoE^{-/-}$ mice compared to those treated with control, demonstrating effective platelet $P2Y_{12}$ inhibition.
- Oil red O staining revealed ticagrelor and clopidogrel treatment had no effect on lesion formation, compared to control, in the whole aorta of $ApoE^{-/-}$ or ApoE/$P2Y_{12}$ DK mice.
- In addition, there were no region-specific differences in lesion development.
- Likewise, in the aortic sinus, $P2Y_{12}$ inhibitors had no effect on lesion area compared to control treatment in either $ApoE^{-/-}$ or ApoE/$P2Y_{12}$ DK mice.
- An overall effect of $P2Y_{12}$ deficiency on lesion formation was still observed in the aortic sinus, when comparing all ApoE/$P2Y_{12}$ DK mice with their $ApoE^{-/-}$ counterparts.

7.4 Discussion

The potential therapeutic impact of $P2Y_{12}$ antagonist treatment in the prevention or management of atherosclerosis, before the onset of life-threatening acute coronary syndromes, is of great interest. In the previous chapter, I demonstrated that vessel wall, but not platelet, $P2Y_{12}$ potentiated early atherogenesis, which then poses the question, are $P2Y_{12}$ antagonists able to block this vessel wall effect? In this chapter, I show that ticagrelor and clopidogrel effectively inhibited platelet $P2Y_{12}$, but had no effect on lesion development in early atherogenesis. These findings therefore indicate that prophylactic use of $P2Y_{12}$ inhibitors may not be beneficial in preventing early atherosclerotic disease.

In this study, I utilised a novel approach to drug dosing as an alternative to gavage in order to minimise animal stress, whilst maintaining a satisfactory level of drug delivery and $P2Y_{12}$ inhibition. The doses used of ticagrelor and clopidogrel were based on previous studies that established these as optimal for providing a high, sustained level of $P2Y_{12}$ inhibition (Evans *et al.* 2009; Patil *et al.* 2010). Although the voluntary method of drug delivery did not achieve the accuracy and compliance of drug dosage compared to gavage, it did attain a high level of platelet $P2Y_{12}$ inhibition.

Clopidogrel is widely used in ACS treatment, but next-generation agents, such as ticagrelor, are increasingly employed due to their superior inhibitory effects, and greater clinical efficacy. Although particularly effective at preventing secondary thrombosis, evidence of

their effects on atherogenesis itself is limited, and existing studies offer conflicting results. Schulz *et al*. investigated the effects of prophylactic treatment, with aspirin and clopidogrel, on lesion development in ApoE$^{-/-}$ mice and found that whilst these drugs effectively prevented thrombosis following plaque rupture, they had no effect on atherogenesis (Schulz *et al.* 2008). However, a later study published contradictory results showing that mice treated with clopidogrel had reduced atheroma, as well as a stable lesion phenotype compared to untreated animals (Afek *et al.* 2009). With such controversy, I was interested to explore whether P2Y$_{12}$ antagonists were able to inhibit the vessel wall effect on atherogenesis, as demonstrated in Chapter 6. I found that, despite effective platelet P2Y$_{12}$ inhibition, neither ticagrelor nor clopidogrel had any effect on lesion development in ApoE$^{-/-}$ mice after 4 weeks of treatment. Though whether these drugs are able to penetrate the vessel wall, and so would be available to block VSMC P2Y$_{12}$ receptors, is debatable.

Studies have shown that ticagrelor (Hogberg *et al.* 2010; Grzesk *et al.* 2012) and another reversibly-binding P2Y$_{12}$ antagonist, cangrelor (Wihlborg *et al.* 2004), are able to inhibit ADP-induced VSMC contraction, advocating the notion that these drugs are capable of binding to, and blocking the action of, VSMC P2Y$_{12}$ receptors as they similarly do in platelets. However, such experiments were conducted in denuded arteries, therefore suggesting these effects may not have been evident when the endothelium was intact, although this was not specified. Interestingly, clopidogrel was shown to have no effect on vessel contraction, with the short half-life of the active metabolite being postulated as a potential contributory factor to this lack of effect (Wihlborg *et al.* 2004).

Without evidence to demonstrate whether drugs such as ticagrelor and clopidogrel are able to permeate the vessel wall and, if so, at what concentration they effectively inhibit P2Y$_{12}$-mediated effects in VSMCs, it is difficult to draw conclusions from my findings. Nonetheless, it can be deduced that, at doses which yield high levels of platelet P2Y$_{12}$ inhibition, ticagrelor and clopidogrel are unable to inhibit VSMC P2Y$_{12}$-mediated effects on atherogenesis, whether this be via actual lack of effect on the cells or an inability of the drugs to physically reach the receptor. Further investigation is needed to elucidate the action of these agents on VSMC P2Y$_{12}$ receptors *in vivo*, and deduce their ability to penetrate the endothelium.

In addition to its effects on platelets, ticagrelor has also been shown to block adenosine re-uptake by RBCs (van Giezen *et al.* 2012), and so may have other, non-P2Y$_{12}$-mediated effects on the vessel wall, which I was keen to explore further. Uptake of adenosine is a process by which extracellular levels of this important purine are regulated. Adenosine signalling evokes physiological effects in many tissues including the heart, and an accumulation of adenosine also protects against tissue damage following ischaemia or inflammation (Noji *et al.* 2004). Acting on the vessel wall, adenosine is a vasodilator and is known to induce nitric oxide production in both VSMC (Dubey *et al.* 1998) and endothelial

cells (Smits *et al.* 1995), which suppresses expression of leukocyte adhesion molecules, such as VCAM-1 (De Caterina *et al.* 1995). Adenosine has also been shown to inhibit VSMC proliferation (Garg and Hassid 1989), all of which are important processes in the initiation and progression of atherogenesis. Furthermore, the PLATO clinical study showed that ticagrelor offered a reduced mortality risk from non-cardiovascular causes, compared to clopidogrel (Wallentin *et al.* 2009) and, additionally, ticagrelor treated patients were less likely to experience pulmonary adverse events such as infection and sepsis (Storey *et al.* 2012). The mechanisms for these beneficial effects though, remain to be established.

Therefore given the potential athero-protective effects of ticagrelor, I chose to investigate non-$P2Y_{12}$-mediated effects of ticagrelor and clopidogrel on atherogenesis using ApoE/$P2Y_{12}$ DK mice. However, neither ticagrelor nor clopidogrel treatment had any effect on lesion development after 4 weeks of treatment. As these mice were $P2Y_{12}$-deficient, drug activity could not be assessed via P-selectin expression. Nevertheless, given that these mice were treated and monitored alongside $ApoE^{-/-}$ mice, which achieved effective platelet $P2Y_{12}$ inhibition using the same treatment regime, it can be assumed that they also had a similar level of drug activity. These findings therefore indicate that any non-$P2Y_{12}$-mediated effects of ticagrelor and clopidogrel are insufficient to influence lesion development, and so do not effect atherogenesis at this early stage. Consideration must also be made for the possible effects of $P2Y_{12}$ deficiency on VSMC development and behaviour in this model, which may negate the vessel wall response to adenosine.

8 General discussion

Preventing blood loss and maintaining haemostasis via thrombosis is the primary function of the platelet; however, further insight has shown these cells can impact upon processes far beyond the blood clot. The purinergic receptor $P2Y_{12}$, responsible for amplifying and sustaining the platelet activation response, is perhaps arguably the most important of the many platelet receptors due to its profound influence on platelet reactivity. In addition, new roles for $P2Y_{12}$ receptors that are expressed on other cell types are beginning to emerge. With the availability of highly effective inhibitors, $P2Y_{12}$ offers a promising target for disease management, and may hold the key to mediating the role of $P2Y_{12}$ in processes such as atherogenesis.

In this thesis, I have demonstrated that platelet $P2Y_{12}$ is crucial in modulating the vessel wall response to injury. Conversely, through the development of a novel ApoE/$P2Y_{12}$ DK mouse strain, I have discovered that vessel wall, but not platelet, $P2Y_{12}$ is important in early atherogenesis and potentiates initial lesion formation. However, the $P2Y_{12}$ inhibitors, ticagrelor and clopidogrel, were ineffective at blocking this vessel wall $P2Y_{12}$ effect on early atherogenesis.

There is an increasing body of evidence demonstrating how individual platelet proteins and adhesion receptors, such as P-selectin, CD40L, and GPVI, contribute to lesion development in atherogenesis (Burger and Wagner 2003; Bultmann *et al.* 2010; Lievens *et al.* 2010). Platelets are known to interact with the inflammatory system via leukocytes, and cells of the vessel wall via cytokine and mitogen release, as a result of platelet activation. Therefore, as a central regulator of platelet reactivity, the $P2Y_{12}$ receptor was felt to be crucial in modulating these effects and, as such, studies into the role of platelet $P2Y_{12}$ in atherogenesis were greatly anticipated. However, my findings have challenged this paradigm, revealing instead a novel role for vessel wall $P2Y_{12}$ in early lesion development. Together with existing literature, these findings offer new insights into the respective roles of platelet and vessel wall $P2Y_{12}$ receptors in atherogenesis, and how the influence of these cell types may change over time as disease progresses. Therefore, to summarise this current knowledge, I propose a suggested timeline of $P2Y_{12}$ involvement in atherogenesis, as demonstrated in murine studies (see Figure 8.1).

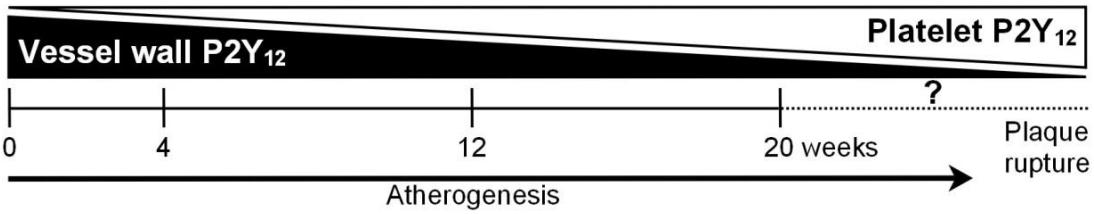

Figure 8.1 – Timeline of $P2Y_{12}$ involvement in atherogenesis.

In the early stages of disease, after 4 weeks on a western diet, vessel wall $P2Y_{12}$ plays a significant role in lesion development, whereas platelet $P2Y_{12}$ has little effect (see Chapter 6). At 12 weeks, when vessels demonstrate characteristics of more advanced disease, the influence of $P2Y_{12}$ is less apparent, except in areas of the vasculature exposed to turbulent flow, where $P2Y_{12}$ is still important in lesion progression. As discussed in Chapter 5, this may reflect an increasing impact of platelet adhesion on atherogenesis, and suggests a lesser role of vessel wall $P2Y_{12}$ at this stage. In later disease, following 20 weeks on a high-fat diet, Li *et al.* document that platelet $P2Y_{12}$ exerts a prominent effect in promoting advanced lesion development (Li *et al.* 2012). This is further supported by my own findings, which demonstrate a profound role for platelet $P2Y_{12}$ in the vessel wall response to injury through mediating thrombus and neointima formation (see Chapter 3).

It is clear that vessel wall and platelet $P2Y_{12}$ appear to have a greater impact at opposing stages of disease, but how they mediate their effects is not yet fully appreciated. A recent study into VSMC $P2Y_{12}$ expression and function, however, may provide a potential mechanism, having revealed that $P2Y_{12}$ promotes VSMC mitogenesis in response to thrombin (Rauch *et al.* 2010). Furthermore, $P2Y_{12}$ expression was found to be regulated by the pro-inflammatory transcription factor, NF-κB. In advanced disease, platelet $P2Y_{12}$ has a more prominent role, where it appears platelet interactions with the inflammatory system become more important to lesion growth, and where endothelial erosion is more likely to occur. Though, exactly when the balance switches from vessel wall to platelet $P2Y_{12}$ is not clear, and further investigation into what influences this process is of great interest.

Given that ticagrelor and clopidogrel were unable to inhibit the vessel wall $P2Y_{12}$ effect on early atherogenesis (see Chapter 7), but are known to be extremely effective inhibitors of platelet $P2Y_{12}$, fully understanding the timeline of $P2Y_{12}$ involvement in atherogenesis could have beneficial consequences to both disease treatment and management. These findings indicate that $P2Y_{12}$ inhibitors may not offer a therapeutic strategy for the prevention of atherosclerosis in people without evidence of atherosclerotic disease. However, where disease is apparent, a greater role of platelets is implicated at this stage, and so indicates that commencing $P2Y_{12}$ inhibitor treatment earlier than when it's conventionally given, following atherothrombosis, may be advantageous in managing lesion progression. Nevertheless, caution must be exercised before considering the prophylactic use of these drugs, and the overall preventative benefit versus bleeding risk fully assessed. Indeed, one such clinical study of clopidogrel plus aspirin, versus aspirin treatment alone, in patients with existing CVD and those which were asymptomatic but high-risk, demonstrated no overall effect of clopidogrel in preventing future CV events, yet indicated a moderate increased bleeding risk (Bhatt *et al.* 2006). Sub-group analysis did, however, show a marginal benefit of clopidogrel treatment for those with existing disease, but not in asymptomatic patients, who demonstrated increased bleeding complications. Clearly further investigation is

necessary to clarify the full effect of antiplatelet drugs, including the new $P2Y_{12}$ antagonist ticagrelor, on primary prophylaxis in patients with existing disease, to determine when this treatment would be indicated and, furthermore, to study their direct effects on lesion progression.

It must also be noted that, although clopidogrel is known to produce a consistently high level of platelet $P2Y_{12}$ inhibition in mice, the response in humans, particularly those with CAD, is much more variable (Gurbel *et al.* 2003). The incidence of clopidogrel 'non-responders' is well-documented, and is a known risk factor for stent thrombosis (Gurbel *et al.* 2005; Mega *et al.* 2010). In light of my findings on the innate relationship between $P2Y_{12}$ inhibition, thrombosis and neointima formation, my data also suggest that inadequate $P2Y_{12}$ inhibition may have an adverse impact on the risk of restenosis in patients who respond poorly to clopidogrel, and therefore effective $P2Y_{12}$ inhibition may be beneficial in the prevention of restenosis.

The recently resolved crystal structure of $P2Y_{12}$ in complex with an agonist and antagonist, will undoubtedly fuel further interest in $P2Y_{12}$ inhibitors and their therapeutic use (Zhang *et al.* 2014; Zhang *et al.* 2014). Along with the emerging evidence of $P2Y_{12}$ involvement in atherogenesis, this newfound knowledge of the receptor binding sites may therefore drive the development of novel agents, and could mark a new era for platelet and potentially VSMC $P2Y_{12}$ inhibitors in disease prevention.

8.1 Limitations

The use of animals in the study of human diseases offers an inherent limitation to the conclusions which may be drawn from such research, including this thesis. There are many arguments both for and against the suitability and relevance of animal models in research. Anatomical and genetic differences between species pose the greatest challenge, in addition to the ability to mimic those diseases which are largely human-specific. This is particularly evident in murine models of atherogenesis, as mice appear to be naturally resistant to atherosclerosis and require genetic manipulation of either the LDL receptor or ApoE gene in order to develop the disease. With the addition of a high-fat diet, disease progression is vastly accelerated in comparison to humans; however, atherosclerotic lesion structure and location are very similar, particularly in $ApoE^{-/-}$ mice (Nakashima *et al.* 1994). When interpreting findings it must therefore be considered that this research was conducted in a non-human species, and so any conclusions drawn may not directly translate into human disease. Yet given the challenges posed by animal models, their advantages far outweigh any potential drawbacks by providing a valuable insight into disease processes not offered by *in vitro* assays alone. In particular, transgenic mouse lines enable the full impact of individual proteins and receptors, such as $P2Y_{12}$ to be revealed, something which cannot be achieved in larger animal models.

Ferric chloride is a useful vessel injury model, which is quick to perform, is not technically difficult as the vessel remains intact and, as a consequence, has a high success rate. However, the extent of injury is not always consistent, and can also result in damage to the surrounding tissue. As injury is inflicted via oxidation rather than by mechanical means, the ensuing tissue factor release is much greater than would occur in a wire injury model, and so perhaps does not provide the ideal conditions in which to accurately model PCI-induced injury. Despite this, it does yield a reliable method for inducing thrombus and neointima formation, and has revealed the dominant effect of platelet $P2Y_{12}$ on these processes, which can then be further investigated in restenosis models.

Performing a dihybrid cross for the generation of a novel transgenic mouse line requires many resources, and is both a time-consuming and costly undertaking. With the time constraints of this project and given the knowledge that both parent strains had already been backcrossed 10 generations with C57/BL6 mice, and so should have an identical genetic background, we chose not to pursue further backcrossing in the ApoE/$P2Y_{12}$ DK colony generated for this thesis. However, in an ideal scenario, where time limitations and resources were not an issue, this strain would too have been backcrossed to fully ensure a common genetic background. Furthermore, given that the significant chi-squared value obtained for the F_2 generation was likely to have been due to small population size, in hindsight a greater number of breeding pairs would have been advantageous to more accurately assess the genotype frequencies in this population.

Phenotype differences in weight gain and liver function between ApoE/$P2Y_{12}$ DK and $ApoE^{-/-}$ mice, when fed a high-fat diet, raise many questions as to the role of $P2Y_{12}$ in other cell-types. Although $P2Y_{12}$ function in these cells was discussed in Chapter 4, along with how these may have resulted in these phenotype disparities, their overall impact on atherogenesis is unknown. It is unlikely that $P2Y_{12}$ function in liver, spleen, pancreatic, or microglial cells could influence lesion development, given that systemic lipid and cholesterol levels were unaltered and metabolic function was similar, nevertheless this should be considered when interpreting these findings.

Similarly, following BMT, mice are described as being platelet or vessel wall $P2Y_{12}$-deficient; however, consideration must be made for the potential influence of other $P2Y_{12}$-expressing cells. Although predominantly expressed on platelets, $P2Y_{12}$ mRNA has also been identified, to a lesser degree, in murine dendritic cells, where it is thought to enhance T cell activation (Ben Addi *et al.* 2010). The contribution of dendritic $P2Y_{12}$ receptors to atherogenesis is unknown; however, although they too are bone marrow-derived, dendritic cells represent only a small population of cells in comparison to platelets (Fearnley *et al.* 1999). Likewise, $P2Y_{12}$ has been found to be expressed on cultured endothelial cells, but its role in these cells is currently unknown. Therefore, although platelets and VSMCs are the

principal source of $P2Y_{12}$ in the bone marrow and vessel wall, it must be acknowledged that they are not the only cell-types to express $P2Y_{12}$. Nevertheless, given the evidence, it is highly likely that the $P2Y_{12}$ effects on vessel injury and atherogenesis demonstrated in this thesis are platelet and VSMC-mediated.

En face oil red O staining of aortae is a standard technique for the quantification of atheroma, but this method is a relatively crude measurement and is not sensitive to the size of lesion, rather the lipid content. As such, the accuracy of this method may be limited by residual fatty tissue on the outside of the vessel. Extensive efforts were made whilst dissecting the aortae to remove all fat from the outer surface of the vessel. Nevertheless, a small amount of fat may have remained on the vessel, and may have been counted towards positive staining; however, the overall impact of this on the results is expected to be minimal. Conversely, quantification of lesion area via histological analysis is considerably more accurate, though when assessing long vessels, cross-sections must be made at intervals to enable full assessment of the vessel. This was the case with both the carotid and brachiocephalic arteries, and so given the intervals between cross-sections, areas of lesion or neointima were inevitably missed, leading to some loss of detail on lesion/neointima size and composition. Despite this, analysis of several sections at regular intervals along the length of the vessel, and taking a mean value, still provides a relatively accurate overview of injury or atheroma within the vessel, and is a sensitive method to detect significant effects of gene deficiency on these processes.

A voluntary method of drug delivery was utilised in Chapter 7 of this thesis as an alternative to twice daily gavage. Ticagrelor, clopidogrel, or mannitol (control) doses were mixed with jelly, which could then be presented to the mice as a small jelly cube containing drug. Mice do not eat large quantities of food and, as this was given in addition to western diet *ad libitum*, jelly cubes needed to be as small as possible. As a result, to achieve the required dosage, drug concentrations were relatively high and so may have affected the taste of the jelly. Some mice, particularly in the ticagrelor group, did not take to the jelly doses and chose to leave the jelly on several occasions. However, despite this non-compliance in some animals, a high level of platelet $P2Y_{12}$ inhibition was still achieved, as measured by P-selectin expression. I believe this method is extremely useful for long-term dosing studies and, following minor modifications, compliance could also be improved. Mice were trained for one week on jelly only, but in future a longer training period may be beneficial. In addition, the method from which this was adapted (Zhang 2011) used added sweeteners. It appears that the addition of the drug alters the taste of the jelly and so using either a more concentrated flavour of jelly or adding additional sweeteners may overcome this issue.

8.2 Future work

The findings of this thesis generate many opportunities in which the research could be taken further. Continuation of this work could not only better inform areas of platelet and $P2Y_{12}$ research, but also facilitate advancements in disease prevention and management through a greater understanding of the cell roles in disease progression. The following sections outline areas in which I feel my research could be elaborated.

Given the clear relationship between thrombus and neointima formation, and the importance of platelet $P2Y_{12}$ in this process, it would be interesting to now test the impact of $P2Y_{12}$ inhibitors in a more clinically relevant injury model. Despite the obvious difficulties involved, due to small vessel size, attempts have been made to directly model PCI in rodents, and recently murine stenting and balloon angioplasty have successfully been developed (Ali *et al.* 2007; Chamberlain *et al.* 2010). Alternatively, the well-established pig angioplasty model of restenosis could be employed (Schwartz *et al.* 1990). Further investigation into the development of restenosis using these models would be of interest, particularly in the application of the superior $P2Y_{12}$ inhibitor ticagrelor in preventing this process.

Likewise, vessel injury models used to study thrombosis and neointima formation have largely been performed on healthy vessels, and were therefore executed in non-inflammatory models. Previous studies have shown that atherosclerotic $ApoE^{-/-}$ mice demonstrate increased neointima formation following injury (Zhu *et al.* 2000). This highlights the huge impact that a pro-inflammatory environment, which is found particularly in atherosclerotic vessels following PCI, may have on neointima formation. Therefore, additional research into the impact of $P2Y_{12}$ inhibition following arterial injury in a pro-inflammatory model is merited. Recently developed mutant pig models of atherosclerosis may be particularly useful for such experiments (Jensen *et al.* 2010; Al-Mashhadi *et al.* 2013). In addition, given the positive impact of $P2Y_{12}$ antagonists on reducing restenosis in animal models, an appropriately powered clinical study into the direct effect of $P2Y_{12}$ antagonists on restenosis rates following PCI is also warranted.

Phenotype differences between $ApoE/P2Y_{12}$ DK and $ApoE^{-/-}$ mice would be of interest to explore in more detail. As mentioned previously, metabolic cages could be employed to accurately measure food intake in $ApoE/P2Y_{12}$ DK mice to study whether increased weight gain was due to greater food consumption. Similarly, the effects of brain $P2Y_{12}$-deficiency on behaviour and activity could be studied, which may shed light on the diet-related weight increase, in addition to providing a better understanding of the long-term impact of $P2Y_{12}$-deficiency on brain development and function.

At the 3 phases of atherogenesis discussed in this thesis, after 4, 12, and 20 weeks on a high-fat diet, it is clear that the influence of platelet and vessel wall $P2Y_{12}$ evolves, and

changes with disease progression. Between the Li study (Li *et al.* 2012) and my own, snapshots into the cellular roles in atherogenesis are emerging; however, further studies are required to build up a detailed picture of $P2Y_{12}$ involvement throughout disease progression.

Regional differences in lesion development observed in ApoE/$P2Y_{12}$ DK mice after 12 weeks of western diet were postulated to be due to the impact of shear stress on platelet adhesion. Flow models have been used previously to investigate the effects of shear on platelet adhesion to the endothelium. This hypothesis could be pursued further using flow models to study the effect of varying shear stress on adhesion of $P2Y_{12}$-deficient platelets to cultured endothelial cells and in explanted atherosclerotic vessels.

Macrophage staining of aortic sinus lesions using markers F4/80 and MAC387 proved inconclusive. Results from the MAC387 staining suggested further workup of the antibody was required and that modification of the experimental conditions may have yielded more definitive results. Given more time, I would like to have pursued this work and if unsuccessful, would have tried alternative markers such as CD68, MAC3 and MOMA-2.

In addition, further smooth muscle actin staining of lesions from ApoE/$P2Y_{12}$ DK mice fed western diet for a longer period of 20 weeks, similar to the Li study, would be of particular interest (Li *et al.* 2012). Li *et al.* demonstrated an increase in collagen at 20 weeks in $P2Y_{12}$-deficient mice, yet carried out no α-smooth muscle actin staining of their own. As discussed in Chapter 5, this finding appears to be contradictory to my own showing a decrease in collagen and α-SMA in the absence of $P2Y_{12}$ due to a possible reduction in $P2Y_{12}$-mediated VSMC mitogenesis. Furthermore, the Li study did not investigate the possible effects of vessel wall $P2Y_{12}$ on atherogenesis, and so further bone marrow transplantations would be of great interest, given my own findings. However, research hypotheses must be carefully considered in accordance with the 3R's principles, in order to justify the further use of animals, prior to embarking on additional time points and bone marrow transplantations.

Following the discovery that vessel wall $P2Y_{12}$-deficiency leads to a reduction in atheroma, further study is needed to better understand exactly how $P2Y_{12}$ signalling in these cells promotes early atherogenesis. I postulated this may be due to $P2Y_{12}$-mediated VSMC mitogenesis in light of recent work by Rauch *et al.*, which demonstrated enhanced $P2Y_{12}$ expression and $P2Y_{12}$-induced mitogenic effects in response to thrombin (Rauch *et al.* 2010). Continuation of this *in vitro* work, including using $P2Y_{12}$-deficient VSMCs, would be of particular interest and may help to address this hypothesis. Studying mitogenic responses in $P2Y_{12}$-deficient cells following exposure to growth factors and chemokines could be performed. Given that little is known of the effect of $P2Y_{12}$-deficiency on VSMC development and phenotype, further investigation into this is also warranted. Clarification on

the expression of definitive VSMC synthetic and contractile phenotype markers will also aid this research.

Identification of $P2Y_{12}$ within atherosclerotic lesions of bone marrow transplanted mice could be confirmed by mRNA expression levels. Additional workup of the α-SMA/$P2Y_{12}$ dual immunofluorescent staining protocol is also required, and would help determine $P2Y_{12}$ expressing VSMCs from platelets that have been incorporated into the lesion. Determination of the APR-012 $P2Y_{12}$ antibody binding site is needed to confirm whether positive signals seen in the aortic sinus of vessel wall $P2Y_{12}$-deficient mice was indeed, as postulated the antibody binding to part of the non-functional receptor or due to non-specific binding. If it was the latter, then the use of other $P2Y_{12}$ antibodies could be pursued.

Despite achieving a high level of platelet-$P2Y_{12}$ inhibition, ticagrelor and clopidogrel treatment did not block vessel wall $P2Y_{12}$-mediated effects on atherogenesis. However, this lack of effect could be due to the drugs not penetrating the endothelium and so never reaching the receptor. $P2Y_{12}$ antagonists have been shown to block $P2Y_{12}$-mediated contraction, but these experiments were carried out on denuded vessels. Further *ex vivo* studies could be carried out using vessels with an intact endothelium, to investigate if these drugs are able to penetrate to the receptor. Additional work utilising labelled inhibitors may also be able to measure drug permeability and detect inhibitors bound to VSMC $P2Y_{12}$.

Finally, given the indication of platelet $P2Y_{12}$ involvement in late atherogenesis, investigation into the effect of $P2Y_{12}$ antagonists on lesion progression would be of interest and could be performed in murine or porcine models of advanced atherosclerosis. In the long-term, clinical studies into the prophylactic use of these drugs in patients with evidence of atherosclerotic disease could be investigated, and should assess both any benefit, by a reduction in CV events, but also any associated bleeding risk.

8.3 Concluding remarks

In conclusion, this thesis presents novel findings to support my original hypothesis that the $P2Y_{12}$ receptor is important in modulating the vessel wall response to both injury and inflammation. Furthermore, I describe a previously unknown role of vessel wall, but not platelet, $P2Y_{12}$ in early atherogenesis, which is in contrast to published data that documents the involvement of platelet $P2Y_{12}$ in later atherogenesis and its thrombotic complications (Li *et al.* 2012). This work emphasises the complexity of cellular roles within atherogenesis, and how the nature and impact of these cell populations may change as disease evolves. Further investigation is necessary to clarify the full extent to which vessel wall and platelet $P2Y_{12}$ influence atherogenesis throughout the course of disease. However, it is clear that this work offers a new perspective on atherogenesis, and so has great relevance to, and

impact on, disease management and prevention, which may alter the therapeutic approach to atherosclerosis in the future.

9 References

Afek, A., E. Kogan, S. Maysel-Auslender, A. Mor, E. Regev, A. Rubinstein*, et al.* (2009). Clopidogrel attenuates atheroma formation and induces a stable plaque phenotype in apolipoprotein E knockout mice. *Microvasc Res* **77**(3): 364-369.

Aird, W. C. (2011). Discovery of the cardiovascular system: from Galen to William Harvey. *J Thromb Haemost* **9 Suppl 1**: 118-129.

Al-Mashhadi, R. H., C. B. Sorensen, P. M. Kragh, C. Christoffersen, M. B. Mortensen, L. P. Tolbod*, et al.* (2013). Familial hypercholesterolemia and atherosclerosis in cloned minipigs created by DNA transposition of a human PCSK9 gain-of-function mutant. *Sci Transl Med* **5**(166): 166ra161.

Ali, Z. A., N. J. Alp, H. Lupton, N. Arnold, T. Bannister, Y. Hu*, et al.* (2007). Increased in-stent stenosis in ApoE knockout mice: insights from a novel mouse model of balloon angioplasty and stenting. *Arterioscler Thromb Vasc Biol* **27**(4): 833-840.

Alon, R., T. Feizi, C. T. Yuen, R. C. Fuhlbrigge and T. A. Springer (1995). Glycolipid ligands for selectins support leukocyte tethering and rolling under physiologic flow conditions. *J Immunol* **154**(10): 5356-5366.

Alpini, G., S. Roberts, S. M. Kuntz, Y. Ueno, S. Gubba, P. V. Podila*, et al.* (1996). Morphological, molecular, and functional heterogeneity of cholangiocytes from normal rat liver. *Gastroenterology* **110**(5): 1636-1643.

Amadio, S., G. Tramini, A. Martorana, M. T. Viscomi, G. Sancesario, G. Bernardi*, et al.* (2006). Oligodendrocytes express P2Y12 metabotropic receptor in adult rat brain. *Neuroscience* **141**(3): 1171-1180.

Amento, E. P., N. Ehsani, H. Palmer and P. Libby (1991). Cytokines and growth factors positively and negatively regulate interstitial collagen gene expression in human vascular smooth muscle cells. *Arterioscler Thromb* **11**(5): 1223-1230.

Anderson, H. V., J. McNatt, F. J. Clubb, M. Herman, J. P. Maffrand, F. DeClerck*, et al.* (2001). Platelet inhibition reduces cyclic flow variations and neointimal proliferation in normal and hypercholesterolemic-atherosclerotic canine coronary arteries. *Circulation* **104**(19): 2331-2337.

Anderson, K. M., P. W. Wilson, P. M. Odell and W. B. Kannel (1991). An updated coronary risk profile. A statement for health professionals. *Circulation* **83**(1): 356-362.

Andre, P., S. M. Delaney, T. LaRocca, D. Vincent, F. DeGuzman, M. Jurek*, et al.* (2003). P2Y12 regulates platelet adhesion/activation, thrombus growth, and thrombus stability in injured arteries. *J Clin Invest* **112**(3): 398-406.

Andre, P., C. V. Denis, J. Ware, S. Saffaripour, R. O. Hynes, Z. M. Ruggeri*, et al.* (2000). Platelets adhere to and translocate on von Willebrand factor presented by endothelium in stimulated veins. *Blood* **96**(10): 3322-3328.

Angiolillo, D. J., M. S. Firstenberg, M. J. Price, P. E. Tummala, M. Hutyra, I. J. Welsby*, et al.* (2012). Bridging antiplatelet therapy with cangrelor in patients undergoing cardiac surgery: a randomized controlled trial. *JAMA* **307**(3): 265-274.

Antiplatelet_Trialists'_Collaboration (1994). Collaborative overview of randomised trials of antiplatelet therapy--I: Prevention of death, myocardial infarction, and stroke by prolonged antiplatelet therapy in various categories of patients. Antiplatelet Trialists' Collaboration. *BMJ* **308**(6921): 81-106.

Asa, D., L. Raycroft, L. Ma, P. A. Aeed, P. S. Kaytes, A. P. Elhammer*, et al.* (1995). The P-selectin glycoprotein ligand functions as a common human leukocyte ligand for P- and E-selectins. *J Biol Chem* **270**(19): 11662-11670.

Asakura, T. and T. Karino (1990). Flow patterns and spatial distribution of atherosclerotic lesions in human coronary arteries. *Circ Res* **66**(4): 1045-1066.

Babaev, V. R., Y. V. Bobryshev, O. V. Stenina, E. M. Tararak and G. Gabbiani (1990). Heterogeneity of smooth muscle cells in atheromatous plaque of human aorta. *Am J Pathol* **136**(5): 1031-1042.

Ball, R. Y., E. C. Stowers, J. H. Burton, N. R. Cary, J. N. Skepper and M. J. Mitchinson (1995). Evidence that the death of macrophage foam cells contributes to the lipid core of atheroma. *Atherosclerosis* **114**(1): 45-54.

Barrett, T. B. and E. P. Benditt (1987). sis (platelet-derived growth factor B chain) gene transcript levels are elevated in human atherosclerotic lesions compared to normal artery. *Proc Natl Acad Sci U S A* **84**(4): 1099-1103.

Battegay, E. J., E. W. Raines, R. A. Seifert, D. F. Bowen-Pope and R. Ross (1990). TGF-beta induces bimodal proliferation of connective tissue cells via complex control of an autocrine PDGF loop. *Cell* **63**(3): 515-524.

Baumhueter, S., N. Dybdal, C. Kyle and L. A. Lasky (1994). Global vascular expression of murine CD34, a sialomucin-like endothelial ligand for L-selectin. *Blood* **84**(8): 2554-2565.

Bauriedel, G., R. Hutter, U. Welsch, R. Bach, H. Sievert and B. Luderitz (1999). Role of smooth muscle cell death in advanced coronary primary lesions: implications for plaque instability. *Cardiovasc Res* **41**(2): 480-488.

Ben Addi, A., D. Cammarata, P. B. Conley, J. M. Boeynaems and B. Robaye (2010). Role of the P2Y12 receptor in the modulation of murine dendritic cell function by ADP. *J Immunol* **185**(10): 5900-5906.

Bentzon, J. F., C. Weile, C. S. Sondergaard, J. Hindkjaer, M. Kassem and E. Falk (2006). Smooth muscle cells in atherosclerosis originate from the local vessel wall and not circulating progenitor cells in ApoE knockout mice. *Arterioscler Thromb Vasc Biol* **26**(12): 2696-2702.

Bertrand, M. E., H. J. Rupprecht, P. Urban, A. H. Gershlick and C. Investigators (2000). Double-blind study of the safety of clopidogrel with and without a loading dose in combination with aspirin compared with ticlopidine in combination with aspirin after coronary stenting : the clopidogrel aspirin stent international cooperative study (CLASSICS). *Circulation* **102**(6): 624-629.

Bhatt, D. L., K. A. Fox, W. Hacke, P. B. Berger, H. R. Black, W. E. Boden*, et al.* (2006). Clopidogrel and aspirin versus aspirin alone for the prevention of atherothrombotic events. *N Engl J Med* **354**(16): 1706-1717.

Bhatt, D. L., A. M. Lincoff, C. M. Gibson, G. W. Stone, S. McNulty, G. Montalescot*, et al.* (2009). Intravenous platelet blockade with cangrelor during PCI. *N Engl J Med* **361**(24): 2330-2341.

Bhatt, D. L., G. W. Stone, K. W. Mahaffey, C. M. Gibson, P. G. Steg, C. W. Hamm*, et al.* (2013). Effect of platelet inhibition with cangrelor during PCI on ischemic events. *N Engl J Med* **368**(14): 1303-1313.

Bizzozero, J. (1882). Ueber einen neuen Forrnbestandteil des Blutes und dessen Rolle bei der Thrombose und Blutgerinnung. *Archiv für pathologische Anatomie und Physiologie und für klinische Medicin* **90**: 261-332.

Blair, P. and R. Flaumenhaft (2009). Platelet alpha-granules: basic biology and clinical correlates. *Blood Rev* **23**(4): 177-189.

Bobik, A. (2006). Transforming growth factor-betas and vascular disorders. *Arterioscler Thromb Vasc Biol* **26**(8): 1712-1720.

Bolliger, D., F. Szlam, N. Suzuki, T. Matsushita and K. A. Tanaka (2010). Heterozygous antithrombin deficiency improves in vivo haemostasis in factor VIII-deficient mice. *Thromb Haemost* **103**(6): 1233-1238.

Boring, L., J. Gosling, M. Cleary and I. F. Charo (1998). Decreased lesion formation in CCR2-/- mice reveals a role for chemokines in the initiation of atherosclerosis. *Nature* **394**(6696): 894-897.

Boyle, J. J., P. L. Weissberg and M. R. Bennett (2003). Tumor necrosis factor-alpha promotes macrophage-induced vascular smooth muscle cell apoptosis by direct and autocrine mechanisms. *Arterioscler Thromb Vasc Biol* **23**(9): 1553-1558.

Braun, M., P. Pietsch, S. B. Felix and G. Baumann (1995). Modulation of intercellular adhesion molecule-1 and vascular cell adhesion molecule-1 on human coronary smooth muscle cells by cytokines. *J Mol Cell Cardiol* **27**(12): 2571-2579.

Brewer, D. B. (2006). Max Schultze (1865), G. Bizzozero (1882) and the discovery of the platelet. *Br J Haematol* **133**(3): 251-258.

Brown, M. S. and J. L. Goldstein (1986). A receptor-mediated pathway for cholesterol homeostasis. *Science* **232**(4746): 34-47.

Bultmann, A., Z. Li, S. Wagner, M. Peluso, T. Schonberger, C. Weis*, et al.* (2010). Impact of glycoprotein VI and platelet adhesion on atherosclerosis--a possible role of fibronectin. *J Mol Cell Cardiol* **49**(3): 532-542.

Burger, P. C. and D. D. Wagner (2003). Platelet P-selectin facilitates atherosclerotic lesion development. *Blood* **101**(7): 2661-2666.

Cannon, C. P. and E. Braunwald (2008). Unstable angina and Non-ST elevation myocardial infarction. Braunwald's Heart Disease: A Textbook of Cardiovascular Medicine. P. Libby, R. O. Bonow, D. L. Mann and D. P. Zipes. Philadelphia, Saunders Elsevier. **2:** 1319-1351.

Cannon, C. P. and T. H. Lee (2008). Approach to the patient with chest pain. Braunwald's Heart Disease: A Textbook of Cardiovascular Medicine. P. Libby, R. O. Bonow, D. L. Mann and D. P. Zipes. Philadelphia, Saunders Elsevier. **2:** 1195-1205.

Capodanno, D., J. L. Ferreiro and D. J. Angiolillo (2013). Antiplatelet therapy: new pharmacological agents and changing paradigms. *J Thromb Haemost* **11 Suppl 1**: 316-329.

CAPRIE (1996). A randomised, blinded, trial of clopidogrel versus aspirin in patients at risk of ischaemic events (CAPRIE). CAPRIE Steering Committee. *Lancet* **348**(9038): 1329-1339.

Carr, M. W., S. J. Roth, E. Luther, S. S. Rose and T. A. Springer (1994). Monocyte chemoattractant protein 1 acts as a T-lymphocyte chemoattractant. *Proc Natl Acad Sci U S A* **91**(9): 3652-3656.

Cattaneo, M. (2012). Response variability to clopidogrel: is tailored treatment, based on laboratory testing, the right solution? *J Thromb Haemost* **10**(3): 327-336.

Chamberlain, J., D. Evans, A. King, R. Dewberry, S. Dower, D. Crossman*, et al.* (2006). Interleukin-1beta and signaling of interleukin-1 in vascular wall and circulating cells modulates the extent of neointima formation in mice. *Am J Pathol* **168**(4): 1396-1403.

Chamberlain, J., S. Francis, Z. Brookes, G. Shaw, D. Graham, N. J. Alp*, et al.* (2009). Interleukin-1 regulates multiple atherogenic mechanisms in response to fat feeding. *PLoS One* **4**(4): e5073.

Chamberlain, J., M. Wheatcroft, N. Arnold, H. Lupton, D. C. Crossman, J. Gunn*, et al.* (2010). A novel mouse model of in situ stenting. *Cardiovasc Res* **85**(1): 38-44.

Chandrasekar, B. and J. F. Tanguay (2000). Platelets and restenosis. *J Am Coll Cardiol* **35**(3): 555-562.

Chen, C. N., Y. S. Li, Y. T. Yeh, P. L. Lee, S. Usami, S. Chien*, et al.* (2006). Synergistic roles of platelet-derived growth factor-BB and interleukin-1beta in phenotypic modulation of human aortic smooth muscle cells. *Proc Natl Acad Sci U S A* **103**(8): 2665-2670.

Christen, T., V. Verin, M. Bochaton-Piallat, Y. Popowski, F. Ramaekers, P. Debruyne*, et al.* (2001). Mechanisms of neointima formation and remodeling in the porcine coronary artery. *Circulation* **103**(6): 882-888.

Ciferri, S., C. Emiliani, G. Guglielmini, A. Orlacchio, G. G. Nenci and P. Gresele (2000). Platelets release their lysosomal content in vivo in humans upon activation. *Thromb Haemost* **83**(1): 157-164.

Cipollone, F., M. Fazia, G. Mincione, A. Iezzi, B. Pini, C. Cuccurullo*, et al.* (2004). Increased expression of transforming growth factor-beta1 as a stabilizing factor in human atherosclerotic plaques. *Stroke* **35**(10): 2253-2257.

Clarkson, T. B., R. W. Prichard, T. M. Morgan, G. S. Petrick and K. P. Klein (1994). Remodeling of coronary arteries in human and nonhuman primates. *JAMA* **271**(4): 289-294.

Clinton, S. K., R. Underwood, L. Hayes, M. L. Sherman, D. W. Kufe and P. Libby (1992). Macrophage colony-stimulating factor gene expression in vascular cells and in experimental and human atherosclerosis. *Am J Pathol* **140**(2): 301-316.

Collins, G. S. and D. G. Altman (2012). Predicting the 10 year risk of cardiovascular disease in the United Kingdom: independent and external validation of an updated version of QRISK2. *BMJ* **344**: e4181.

Coppinger, J. A., G. Cagney, S. Toomey, T. Kislinger, O. Belton, J. P. McRedmond*, et al.* (2004). Characterization of the proteins released from activated platelets leads to localization of novel platelet proteins in human atherosclerotic lesions. *Blood* **103**(6): 2096-2104.

Crossey, P. A., J. S. Jones and J. P. Miell (2000). Dysregulation of the insulin/IGF binding protein-1 axis in transgenic mice is associated with hyperinsulinemia and glucose intolerance. *Diabetes* **49**(3): 457-465.

Cushing, S. D., J. A. Berliner, A. J. Valente, M. C. Territo, M. Navab, F. Parhami*, et al.* (1990). Minimally modified low density lipoprotein induces monocyte chemotactic protein 1 in human endothelial cells and smooth muscle cells. *Proc Natl Acad Sci U S A* **87**(13): 5134-5138.

D'Souza, S. E., V. J. Byers-Ward, E. E. Gardiner, H. Wang and S. S. Sung (1996). Identification of an active sequence within the first immunoglobulin domain of intercellular cell adhesion molecule-1 (ICAM-1) that interacts with fibrinogen. *J Biol Chem* **271**(39): 24270-24277.

Dahlback, B. (2000). Blood coagulation. *Lancet* **355**(9215): 1627-1632.

Danese, S., C. de la Motte, B. M. Reyes, M. Sans, A. D. Levine and C. Fiocchi (2004). Cutting edge: T cells trigger CD40-dependent platelet activation and granular RANTES release: a novel pathway for immune response amplification. *J Immunol* **172**(4): 2011-2015.

Dangelmaier, C., J. Jin, J. B. Smith and S. P. Kunapuli (2001). Potentiation of thromboxane A2-induced platelet secretion by Gi signaling through the phosphoinositide-3 kinase pathway. *Thromb Haemost* **85**(2): 341-348.

Daniel, J. L., C. Dangelmaier, J. Jin, B. Ashby, J. B. Smith and S. P. Kunapuli (1998). Molecular basis for ADP-induced platelet activation. I. Evidence for three distinct ADP receptors on human platelets. *J Biol Chem* **273**(4): 2024-2029.

Daniel, J. L., C. Dangelmaier and J. B. Smith (1994). Evidence for a role for tyrosine phosphorylation of phospholipase C gamma 2 in collagen-induced platelet cytosolic calcium mobilization. *Biochem J* **302 (Pt 2)**: 617-622.

Davalos, D., J. Grutzendler, G. Yang, J. V. Kim, Y. Zuo, S. Jung*, et al.* (2005). ATP mediates rapid microglial response to local brain injury in vivo. *Nat Neurosci* **8**(6): 752-758.

De Caterina, R., P. Libby, H. B. Peng, V. J. Thannickal, T. B. Rajavashisth, M. A. Gimbrone, Jr.*, et al.* (1995). Nitric oxide decreases cytokine-induced endothelial activation. Nitric oxide selectively reduces endothelial expression of adhesion molecules and proinflammatory cytokines. *J Clin Invest* **96**(1): 60-68.

Dent, T. H. (2010). Predicting the risk of coronary heart disease I. The use of conventional risk markers. *Atherosclerosis* **213**(2): 345-351.

Dent, T. H. (2010). Predicting the risk of coronary heart disease. II: the role of novel molecular biomarkers and genetics in estimating risk, and the future of risk prediction. *Atherosclerosis* **213**(2): 352-362.

Diacovo, T. G., S. J. Roth, J. M. Buccola, D. F. Bainton and T. A. Springer (1996). Neutrophil rolling, arrest, and transmigration across activated, surface-adherent platelets via sequential action of P-selectin and the beta 2-integrin CD11b/CD18. *Blood* **88**(1): 146-157.

DiCorleto, P. E. and D. F. Bowen-Pope (1983). Cultured endothelial cells produce a platelet-derived growth factor-like protein. *Proc Natl Acad Sci U S A* **80**(7): 1919-1923.

Dole, V. S., W. Bergmeier, H. A. Mitchell, S. C. Eichenberger and D. D. Wagner (2005). Activated platelets induce Weibel-Palade-body secretion and leukocyte rolling in vivo: role of P-selectin. *Blood* **106**(7): 2334-2339.

Dole, V. S., W. Bergmeier, I. S. Patten, J. Hirahashi, T. N. Mayadas and D. D. Wagner (2007). PSGL-1 regulates platelet P-selectin-mediated endothelial activation and shedding of P-selectin from activated platelets. *Thromb Haemost* **98**(4): 806-812.

Dopheide, S. M., M. J. Maxwell and S. P. Jackson (2002). Shear-dependent tether formation during platelet translocation on von Willebrand factor. *Blood* **99**(1): 159-167.

Dorsam, R. T. and S. P. Kunapuli (2004). Central role of the P2Y12 receptor in platelet activation. *J Clin Invest* **113**(3): 340-345.

Drechsler, M., Y. Doring, R. T. Megens and O. Soehnlein (2011). Neutrophilic granulocytes - promiscuous accelerators of atherosclerosis. *Thromb Haemost* **106**(5): 839-848.

Dubey, R. K., D. G. Gillespie and E. K. Jackson (1998). Cyclic AMP-adenosine pathway induces nitric oxide synthesis in aortic smooth muscle cells. *Hypertension* **31**(1 Pt 2): 296-302.

Dutta, P., G. Courties, Y. Wei, F. Leuschner, R. Gorbatov, C. S. Robbins*, et al.* (2012). Myocardial infarction accelerates atherosclerosis. *Nature* **487**(7407): 325-329.

Eckly, A., B. Hechler, M. Freund, M. Zerr, J. P. Cazenave, F. Lanza*, et al.* (2011). Mechanisms underlying FeCl3-induced arterial thrombosis. *J Thromb Haemost* **9**(4): 779-789.

ERASER (1999). Acute platelet inhibition with abciximab does not reduce in-stent restenosis (ERASER study). The ERASER Investigators. *Circulation* **100**(8): 799-806.

Erlinge, D. and G. Burnstock (2007). P2 receptors in cardiovascular regulation and disease. *Purinergic Signalling* **Online first**.

Evans, D. J., L. E. Jackman, J. Chamberlain, D. J. Crosdale, H. M. Judge, K. Jetha*, et al.* (2009). Platelet P2Y(12) receptor influences the vessel wall response to arterial injury and thrombosis. *Circulation* **119**(1): 116-122.

Evsikova, C. M. and K. L. Svenson (2014). Activity and food and water intake of 14 inbred strains of mice at 6 months of age. MPD:24761, Mouse Phenome Database web site, The Jackson Laboratory, Bar Harbor, Maine USA.

Fabre, J. E., M. Nguyen, A. Latour, J. A. Keifer, L. P. Audoly, T. M. Coffman*, et al.* (1999). Decreased platelet aggregation, increased bleeding time and resistance to thromboembolism in P2Y1-deficient mice. *Nat Med* **5**(10): 1199-1202.

Fajadet, J., W. Wijns, G. J. Laarman, K. H. Kuck, J. Ormiston, T. Munzel*, et al.* (2006). Randomized, double-blind, multicenter study of the Endeavor zotarolimus-eluting phosphorylcholine-encapsulated stent for treatment of native coronary artery lesions: clinical and angiographic results of the ENDEAVOR II trial. *Circulation* **114**(8): 798-806.

Farb, A., D. K. Weber, F. D. Kolodgie, A. P. Burke and R. Virmani (2002). Morphological predictors of restenosis after coronary stenting in humans. *Circulation* **105**(25): 2974-2980.

Farrehi, P. M., C. K. Ozaki, P. Carmeliet and W. P. Fay (1998). Regulation of arterial thrombolysis by plasminogen activator inhibitor-1 in mice. *Circulation* **97**(10): 1002-1008.

Faxon, D. P., T. A. Sanborn, C. C. Haudenschild and T. J. Ryan (1984). Effect of antiplatelet therapy on restenosis after experimental angioplasty. *Am J Cardiol* **53**(12): 72C-76C.

Fearnley, D. B., L. F. Whyte, S. A. Carnoutsos, A. H. Cook and D. N. Hart (1999). Monitoring human blood dendritic cell numbers in normal individuals and in stem cell transplantation. *Blood* **93**(2): 728-736.

Ferns, G. A., E. W. Raines, K. H. Sprugel, A. S. Motani, M. A. Reidy and R. Ross (1991). Inhibition of neointimal smooth muscle accumulation after angioplasty by an antibody to PDGF. *Science* **253**(5024): 1129-1132.

Fischman, D. L., M. B. Leon, D. S. Baim, R. A. Schatz, M. P. Savage, I. Penn*, et al.* (1994). A randomized comparison of coronary-stent placement and balloon angioplasty in the treatment of coronary artery disease. Stent Restenosis Study Investigators. *N Engl J Med* **331**(8): 496-501.

Forrester, J. S., M. Fishbein, R. Helfant and J. Fagin (1991). A paradigm for restenosis based on cell biology: clues for the development of new preventive therapies. *J Am Coll Cardiol* **17**(3): 758-769.

Foster, C. J., D. M. Prosser, J. M. Agans, Y. Zhai, M. D. Smith, J. E. Lachowicz*, et al.* (2001). Molecular identification and characterization of the platelet ADP receptor targeted by thienopyridine antithrombotic drugs. *J Clin Invest* **107**(12): 1591-1598.

Frenette, P. S., C. V. Denis, L. Weiss, K. Jurk, S. Subbarao, B. Kehrel*, et al.* (2000). P-Selectin glycoprotein ligand 1 (PSGL-1) is expressed on platelets and can mediate platelet-endothelial interactions in vivo. *J Exp Med* **191**(8): 1413-1422.

Frenette, P. S., C. Moyna, D. W. Hartwell, J. B. Lowe, R. O. Hynes and D. D. Wagner (1998). Platelet-endothelial interactions in inflamed mesenteric venules. *Blood* **91**(4): 1318-1324.

Fuster, V., P. R. Moreno, Z. A. Fayad, R. Corti and J. J. Badimon (2005). Atherothrombosis and high-risk plaque: part I: evolving concepts. *J Am Coll Cardiol* **46**(6): 937-954.

Galis, Z. S., M. Muszynski, G. K. Sukhova, E. Simon-Morrissey, E. N. Unemori, M. W. Lark*, et al.* (1994). Cytokine-stimulated human vascular smooth muscle cells synthesize a complement of enzymes required for extracellular matrix digestion. *Circ Res* **75**(1): 181-189.

Galis, Z. S., G. K. Sukhova, M. W. Lark and P. Libby (1994). Increased expression of matrix metalloproteinases and matrix degrading activity in vulnerable regions of human atherosclerotic plaques. *J Clin Invest* **94**(6): 2493-2503.

Garcia, A., S. Kim, K. Bhavaraju, S. M. Schoenwaelder and S. P. Kunapuli (2010). Role of phosphoinositide 3-kinase beta in platelet aggregation and thromboxane A2 generation mediated by Gi signalling pathways. *Biochem J* **429**(2): 369-377.

Garg, U. C. and A. Hassid (1989). Nitric oxide-generating vasodilators and 8-bromo-cyclic guanosine monophosphate inhibit mitogenesis and proliferation of cultured rat vascular smooth muscle cells. *J Clin Invest* **83**(5): 1774-1777.

Gawaz, M., K. Brand, T. Dickfeld, G. Pogatsa-Murray, S. Page, C. Bogner*, et al.* (2000). Platelets induce alterations of chemotactic and adhesive properties of endothelial cells mediated through an interleukin-1-dependent mechanism. Implications for atherogenesis. *Atherosclerosis* **148**(1): 75-85.

Gebuhrer, V., J. F. Murphy, J. C. Bordet, M. P. Reck and J. L. McGregor (1995). Oxidized low-density lipoprotein induces the expression of P-selectin (GMP140/PADGEM/CD62) on human endothelial cells. *Biochem J* **306 (Pt 1)**: 293-298.

Gerszten, R. E., E. A. Garcia-Zepeda, Y. C. Lim, M. Yoshida, H. A. Ding, M. A. Gimbrone, Jr.*, et al.* (1999). MCP-1 and IL-8 trigger firm adhesion of monocytes to vascular endothelium under flow conditions. *Nature* **398**(6729): 718-723.

Getz, G. S. and C. A. Reardon (2006). Diet and murine atherosclerosis. *Arterioscler Thromb Vasc Biol* **26**(2): 242-249.

Giesen, P. L., U. Rauch, B. Bohrmann, D. Kling, M. Roque, J. T. Fallon*, et al.* (1999). Blood-borne tissue factor: another view of thrombosis. *Proc Natl Acad Sci U S A* **96**(5): 2311-2315.

Glagov, S., E. Weisenberg, C. K. Zarins, R. Stankunavicius and G. J. Kolettis (1987). Compensatory enlargement of human atherosclerotic coronary arteries. *N Engl J Med* **316**(22): 1371-1375.

Glover, C., X. Ma, Y. X. Chen, H. Miller, J. Veinot, M. Labinaz*, et al.* (2002). Human in-stent restenosis tissue obtained by means of coronary atherectomy consists of an abundant proteoglycan matrix with a paucity of cell proliferation. *Am Heart J* **144**(4): 702-709.

Goto, S., N. Tamura, K. Eto, Y. Ikeda and S. Handa (2002). Functional significance of adenosine 5'-diphosphate receptor (P2Y(12)) in platelet activation initiated by binding of von Willebrand factor to platelet GP Ibalpha induced by conditions of high shear rate. *Circulation* **105**(21): 2531-2536.

Grainger, D. J., J. Reckless and E. McKilligin (2004). Apolipoprotein E modulates clearance of apoptotic bodies in vitro and in vivo, resulting in a systemic proinflammatory state in apolipoprotein E-deficient mice. *J Immunol* **173**(10): 6366-6375.

Gruntzig, A. (1978). Transluminal dilatation of coronary-artery stenosis. *Lancet* **1**(8058): 263.

Grzesk, G., M. Kozinski, E. P. Navarese, M. Krzyzanowski, E. Grzesk, A. Kubica*, et al.* (2012). Ticagrelor, but not clopidogrel and prasugrel, prevents ADP-induced vascular smooth muscle cell contraction: a placebo-controlled study in rats. *Thromb Res* **130**(1): 65-69.

Gurbel, P. A., K. P. Bliden, K. Butler, U. S. Tantry, T. Gesheff, C. Wei*, et al.* (2009). Randomized double-blind assessment of the ONSET and OFFSET of the antiplatelet effects of ticagrelor versus clopidogrel in patients with stable coronary artery disease: the ONSET/OFFSET study. *Circulation* **120**(25): 2577-2585.

Gurbel, P. A., K. P. Bliden, B. L. Hiatt and C. M. O'Connor (2003). Clopidogrel for coronary stenting: response variability, drug resistance, and the effect of pretreatment platelet reactivity. *Circulation* **107**(23): 2908-2913.

Gurbel, P. A., K. P. Bliden, W. Samara, J. A. Yoho, K. Hayes, M. Z. Fissha*, et al.* (2005). Clopidogrel effect on platelet reactivity in patients with stent thrombosis: results of the CREST Study. *J Am Coll Cardiol* **46**(10): 1827-1832.

Hajjar, K. A., D. P. Hajjar, R. L. Silverstein and R. L. Nachman (1987). Tumor necrosis factor-mediated release of platelet-derived growth factor from cultured endothelial cells. *J Exp Med* **166**(1): 235-245.

Hamm, C. W., J. P. Bassand, S. Agewall, J. Bax, E. Boersma, H. Bueno*, et al.* (2011). ESC Guidelines for the management of acute coronary syndromes in patients presenting without persistent ST-segment elevation: The Task Force for the management of acute coronary syndromes (ACS) in patients presenting without persistent ST-segment elevation of the European Society of Cardiology (ESC). *Eur Heart J* **32**(23): 2999-3054.

Hansson, G. K., J. Holm and L. Jonasson (1989). Detection of activated T lymphocytes in the human atherosclerotic plaque. *Am J Pathol* **135**(1): 169-175.

Harats, D., A. Shaish, J. George, M. Mulkins, H. Kurihara, H. Levkovitz*, et al.* (2000). Overexpression of 15-lipoxygenase in vascular endothelium accelerates early atherosclerosis in LDL receptor-deficient mice. *Arterioscler Thromb Vasc Biol* **20**(9): 2100-2105.

Hardy, A. R., M. L. Jones, S. J. Mundell and A. W. Poole (2004). Reciprocal cross-talk between P2Y1 and P2Y12 receptors at the level of calcium signaling in human platelets. *Blood* **104**(6): 1745-1752.

Harker, L. A. (1987). Role of platelets and thrombosis in mechanisms of acute occlusion and restenosis after angioplasty. *Am J Cardiol* **60**(3): 20B-28B.

Harrington, R. A., G. W. Stone, S. McNulty, H. D. White, A. M. Lincoff, C. M. Gibson*, et al.* (2009). Platelet inhibition with cangrelor in patients undergoing PCI. *N Engl J Med* **361**(24): 2318-2329.

Hartwig, J. H. (2006). The platelet cytoskeleton. Platelets. A. D. Michelson. Burlington, MA, Academic Press**:** 75-98.

Hautmann, M. B., C. S. Madsen and G. K. Owens (1997). A transforming growth factor beta (TGFbeta) control element drives TGFbeta-induced stimulation of smooth muscle alpha-actin gene expression in concert with two CArG elements. *J Biol Chem* **272**(16): 10948-10956.

Haynes, S. E., G. Hollopeter, G. Yang, D. Kurpius, M. E. Dailey, W. B. Gan*, et al.* (2006). The P2Y12 receptor regulates microglial activation by extracellular nucleotides. *Nat Neurosci* **9**(12): 1512-1519.

Hechler, B., A. Eckly, P. Ohlmann, J. P. Cazenave and C. Gachet (1998). The P2Y1 receptor, necessary but not sufficient to support full ADP-induced platelet aggregation, is not the target of the drug clopidogrel. *Br J Haematol* **103**(3): 858-866.

Hechler, B., M. Freund, C. Ravanat, S. Magnenat, J. P. Cazenave and C. Gachet (2008). Reduced atherosclerotic lesions in P2Y1/apolipoprotein E double-knockout mice: the contribution of non-hematopoietic-derived P2Y1 receptors. *Circulation* **118**(7): 754-763.

Hechler, B., N. Lenain, P. Marchese, C. Vial, V. Heim, M. Freund*, et al.* (2003). A role of the fast ATP-gated P2X1 cation channel in thrombosis of small arteries in vivo. *J Exp Med* **198**(4): 661-667.

Henn, V., J. R. Slupsky, M. Grafe, I. Anagnostopoulos, R. Forster, G. Muller-Berghaus*, et al.* (1998). CD40 ligand on activated platelets triggers an inflammatory reaction of endothelial cells. *Nature* **391**(6667): 591-594.

Henney, A. M., P. R. Wakeley, M. J. Davies, K. Foster, R. Hembry, G. Murphy*, et al.* (1991). Localization of stromelysin gene expression in atherosclerotic plaques by in situ hybridization. *Proc Natl Acad Sci U S A* **88**(18): 8154-8158.

Herbert, J. M., F. Dol, A. Bernat, R. Falotico, A. Lale and P. Savi (1998). The antiaggregating and antithrombotic activity of clopidogrel is potentiated by aspirin in several experimental models in the rabbit. *Thromb Haemost* **80**(3): 512-518.

Herman, M. P., G. K. Sukhova, P. Libby, N. Gerdes, N. Tang, D. B. Horton*, et al.* (2001). Expression of neutrophil collagenase (matrix metalloproteinase-8) in human atheroma: a novel collagenolytic pathway suggested by transcriptional profiling. *Circulation* **104**(16): 1899-1904.

Hlatky, M. A., D. B. Boothroyd, D. M. Bravata, E. Boersma, J. Booth, M. M. Brooks*, et al.* (2009). Coronary artery bypass surgery compared with percutaneous coronary interventions for multivessel disease: a collaborative analysis of individual patient data from ten randomised trials. *Lancet* **373**(9670): 1190-1197.

Hogberg, C., H. Svensson, R. Gustafsson, A. Eyjolfsson and D. Erlinge (2010). The reversible oral P2Y12 antagonist AZD6140 inhibits ADP-induced contractions in murine and human vasculature. *Int J Cardiol* **142**(2): 187-192.

Hollopeter, G., H. M. Jantzen, D. Vincent, G. Li, L. England, V. Ramakrishnan*, et al.* (2001). Identification of the platelet ADP receptor targeted by antithrombotic drugs. *Nature* **409**(6817): 202-207.

Holmes, D. R., Jr., R. E. Vlietstra, H. C. Smith, G. W. Vetrovec, K. M. Kent, M. J. Cowley*, et al.* (1984). Restenosis after percutaneous transluminal coronary angioplasty

(PTCA): a report from the PTCA Registry of the National Heart, Lung, and Blood Institute. *Am J Cardiol* **53**(12): 77C-81C.

Horton, D. B., P. Libby and U. Schonbeck (2001). Ligation of CD40 onvascular smooth muscle cells mediates loss of interstitial collagen via matrix metalloproteinase activity. *Ann N Y Acad Sci* **947**: 329-336.

Hu, Y., F. Davison, B. Ludewig, M. Erdel, M. Mayr, M. Url*, et al.* (2002). Smooth muscle cells in transplant atherosclerotic lesions are originated from recipients, but not bone marrow progenitor cells. *Circulation* **106**(14): 1834-1839.

Huang, J., E. M. Driscoll, M. L. Gonzales, A. M. Park and B. R. Lucchesi (2000). Prevention of arterial thrombosis by intravenously administered platelet P2T receptor antagonist AR-C69931MX in a canine model. *J Pharmacol Exp Ther* **295**(2): 492-499.

Huo, Y., A. Schober, S. B. Forlow, D. F. Smith, M. C. Hyman, S. Jung*, et al.* (2003). Circulating activated platelets exacerbate atherosclerosis in mice deficient in apolipoprotein E. *Nat Med* **9**(1): 61-67.

Hutter, R., C. Valdiviezo, B. V. Sauter, M. Savontaus, I. Chereshnev, F. E. Carrick*, et al.* (2004). Caspase-3 and tissue factor expression in lipid-rich plaque macrophages: evidence for apoptosis as link between inflammation and atherothrombosis. *Circulation* **109**(16): 2001-2008.

Inwald, D. P., A. McDowall, M. J. Peters, R. E. Callard and N. J. Klein (2003). CD40 is constitutively expressed on platelets and provides a novel mechanism for platelet activation. *Circ Res* **92**(9): 1041-1048.

Ishibashi, S., M. S. Brown, J. L. Goldstein, R. D. Gerard, R. E. Hammer and J. Herz (1993). Hypercholesterolemia in low density lipoprotein receptor knockout mice and its reversal by adenovirus-mediated gene delivery. *J Clin Invest* **92**(2): 883-893.

Italiano, J. E., Jr., P. Lecine, R. A. Shivdasani and J. H. Hartwig (1999). Blood platelets are assembled principally at the ends of proplatelet processes produced by differentiated megakaryocytes. *J Cell Biol* **147**(6): 1299-1312.

Iwata, H., I. Manabe, K. Fujiu, T. Yamamoto, N. Takeda, K. Eguchi*, et al.* (2010). Bone marrow-derived cells contribute to vascular inflammation but do not differentiate into smooth muscle cell lineages. *Circulation* **122**(20): 2048-2057.

Jawien, J., P. Nastalek and R. Korbut (2004). Mouse models of experimental atherosclerosis. *J Physiol Pharmacol* **55**(3): 503-517.

Jensen, T. W., M. J. Mazur, J. E. Pettigew, V. G. Perez-Mendoza, J. Zachary and L. B. Schook (2010). A cloned pig model for examining atherosclerosis induced by high fat, high cholesterol diets. *Anim Biotechnol* **21**(3): 179-187.

Jin, J., J. L. Daniel and S. P. Kunapuli (1998). Molecular basis for ADP-induced platelet activation. II. The P2Y1 receptor mediates ADP-induced intracellular calcium mobilization and shape change in platelets. *J Biol Chem* **273**(4): 2030-2034.

Jin, J. and S. P. Kunapuli (1998). Coactivation of two different G protein-coupled receptors is essential for ADP-induced platelet aggregation. *Proc Natl Acad Sci U S A* **95**(14): 8070-8074.

Joris, I., T. Zand, J. J. Nunnari, F. J. Krolikowski and G. Majno (1983). Studies on the pathogenesis of atherosclerosis. I. Adhesion and emigration of mononuclear cells in the aorta of hypercholesterolemic rats. *Am J Pathol* **113**(3): 341-358.

Kahner, B. N., R. T. Dorsam and S. P. Kunapuli (2008). Role of P2Y receptor subtypes in platelet-derived microparticle generation. *Front Biosci* **13**: 433-439.

Kaikita, K., H. Ogawa, H. Yasue, M. Takeya, K. Takahashi, T. Saito*, et al.* (1997). Tissue factor expression on macrophages in coronary plaques in patients with unstable angina. *Arterioscler Thromb Vasc Biol* **17**(10): 2232-2237.

Kamari, Y., R. Werman-Venkert, A. Shaish, A. Werman, A. Harari, A. Gonen*, et al.* (2007). Differential role and tissue specificity of interleukin-1alpha gene expression in atherogenesis and lipid metabolism. *Atherosclerosis* **195**(1): 31-38.

Kastrati, A., H. Schuhlen, J. Hausleiter, H. Walter, E. Zitzmann-Roth, M. Hadamitzky*, et al.* (1997). Restenosis after coronary stent placement and randomization to a 4-week combined antiplatelet or anticoagulant therapy: six-month angiographic follow-up of the Intracoronary Stenting and Antithrombotic Regimen (ISAR) Trial. *Circulation* **96**(2): 462-467.

Kauffenstein, G., W. Bergmeier, A. Eckly, P. Ohlmann, C. Leon, J. P. Cazenave*, et al.* (2001). The P2Y(12) receptor induces platelet aggregation through weak activation

of the alpha(IIb)beta(3) integrin--a phosphoinositide 3-kinase-dependent mechanism. *FEBS Lett* **505**(2): 281-290.

Keele, K. D. (1951). Leonardo da Vinci, and the movement of the heart. *Proc R Soc Med* **44**(3): 209-213.

Khan, B. V., S. S. Parthasarathy, R. W. Alexander and R. M. Medford (1995). Modified low density lipoprotein and its constituents augment cytokine-activated vascular cell adhesion molecule-1 gene expression in human vascular endothelial cells. *J Clin Invest* **95**(3): 1262-1270.

Kirii, H., T. Niwa, Y. Yamada, H. Wada, K. Saito, Y. Iwakura*, et al.* (2003). Lack of interleukin-1beta decreases the severity of atherosclerosis in ApoE-deficient mice. *Arterioscler Thromb Vasc Biol* **23**(4): 656-660.

Komatsu, R., M. Ueda, T. Naruko, A. Kojima and A. E. Becker (1998). Neointimal tissue response at sites of coronary stenting in humans: macroscopic, histological, and immunohistochemical analyses. *Circulation* **98**(3): 224-233.

Konishi, H., Y. Katoh, N. Takaya, Y. Kashiwakura, S. Itoh, C. Ra*, et al.* (2002). Platelets activated by collagen through immunoreceptor tyrosine-based activation motif play pivotal role in initiation and generation of neointimal hyperplasia after vascular injury. *Circulation* **105**(8): 912-916.

Konstantinides, S., K. Schafer, S. Koschnick and D. J. Loskutoff (2001). Leptin-dependent platelet aggregation and arterial thrombosis suggests a mechanism for atherothrombotic disease in obesity. *J Clin Invest* **108**(10): 1533-1540.

Kotowicz, K., G. L. Dixon, N. J. Klein, M. J. Peters and R. E. Callard (2000). Biological function of CD40 on human endothelial cells: costimulation with CD40 ligand and interleukin-4 selectively induces expression of vascular cell adhesion molecule-1 and P-selectin resulting in preferential adhesion of lymphocytes. *Immunology* **100**(4): 441-448.

Kozaki, K., W. E. Kaminski, J. Tang, S. Hollenbach, P. Lindahl, C. Sullivan*, et al.* (2002). Blockade of platelet-derived growth factor or its receptors transiently delays but does not prevent fibrous cap formation in ApoE null mice. *Am J Pathol* **161**(4): 1395-1407.

Ku, D. N., D. P. Giddens, C. K. Zarins and S. Glagov (1985). Pulsatile flow and atherosclerosis in the human carotid bifurcation. Positive correlation between plaque location and low oscillating shear stress. *Arteriosclerosis* **5**(3): 293-302.

Kurz, K. D., B. W. Main and G. E. Sandusky (1990). Rat model of arterial thrombosis induced by ferric chloride. *Thromb Res* **60**(4): 269-280.

Lamb, D. J., T. Y. Avades and G. A. Ferns (2001). Endogenous neutralizing antibodies against platelet-derived growth factor-aa inhibit atherogenesis in the cholesterol-fed rabbit. *Arterioscler Thromb Vasc Biol* **21**(6): 997-1003.

Larsen, E., A. Celi, G. E. Gilbert, B. C. Furie, J. K. Erban, R. Bonfanti*, et al.* (1989). PADGEM protein: a receptor that mediates the interaction of activated platelets with neutrophils and monocytes. *Cell* **59**(2): 305-312.

Larson, M. K., H. Chen, M. L. Kahn, A. M. Taylor, J. E. Fabre, R. M. Mortensen*, et al.* (2003). Identification of P2Y12-dependent and -independent mechanisms of glycoprotein VI-mediated Rap1 activation in platelets. *Blood* **101**(4): 1409-1415.

Leon, C., B. Hechler, M. Freund, A. Eckly, C. Vial, P. Ohlmann*, et al.* (1999). Defective platelet aggregation and increased resistance to thrombosis in purinergic P2Y(1) receptor-null mice. *J Clin Invest* **104**(12): 1731-1737.

Leon, C., C. Ravanat, M. Freund, J. P. Cazenave and C. Gachet (2003). Differential involvement of the P2Y1 and P2Y12 receptors in platelet procoagulant activity. *Arterioscler Thromb Vasc Biol* **23**(10): 1941-1947.

Ley, K., M. Allietta, D. C. Bullard and S. Morgan (1998). Importance of E-selectin for firm leukocyte adhesion in vivo. *Circ Res* **83**(3): 287-294.

Ley, K., Y. I. Miller and C. C. Hedrick (2011). Monocyte and macrophage dynamics during atherogenesis. *Arterioscler Thromb Vasc Biol* **31**(7): 1506-1516.

Leytin, V., M. Mody, J. W. Semple, B. Garvey and J. Freedman (2000). Flow cytometric parameters for characterizing platelet activation by measuring P-selectin (CD62) expression: theoretical consideration and evaluation in thrombin-treated platelet populations. *Biochem Biophys Res Commun* **269**(1): 85-90.

Li, D., Y. Wang, L. Zhang, X. Luo, J. Li, X. Chen*, et al.* (2012). Roles of purinergic receptor P2Y, G protein-coupled 12 in the development of atherosclerosis in apolipoprotein E-deficient mice. *Arterioscler Thromb Vasc Biol* **32**(8): e81-89.

Li, H., M. I. Cybulsky, M. A. Gimbrone, Jr. and P. Libby (1993). An atherogenic diet rapidly induces VCAM-1, a cytokine-regulatable mononuclear leukocyte adhesion molecule, in rabbit aortic endothelium. *Arterioscler Thromb* **13**(2): 197-204.

Li, Z., M. K. Delaney, K. A. O'Brien and X. Du (2010). Signaling during platelet adhesion and activation. *Arterioscler Thromb Vasc Biol* **30**(12): 2341-2349.

Libby, P. (2002). Inflammation in atherosclerosis. *Nature* **420**(6917): 868-874.

Lievens, D., W. J. Eijgelaar, E. A. Biessen, M. J. Daemen and E. Lutgens (2009). The multi-functionality of CD40L and its receptor CD40 in atherosclerosis. *Thromb Haemost* **102**(2): 206-214.

Lievens, D., A. Zernecke, T. Seijkens, O. Soehnlein, L. Beckers, I. C. Munnix*, et al.* (2010). Platelet CD40L mediates thrombotic and inflammatory processes in atherosclerosis. *Blood* **116**(20): 4317-4327.

Lindemann, S., N. D. Tolley, D. A. Dixon, T. M. McIntyre, S. M. Prescott, G. A. Zimmerman*, et al.* (2001). Activated platelets mediate inflammatory signaling by regulated interleukin 1beta synthesis. *J Cell Biol* **154**(3): 485-490.

Liu, J., D. P. Thewke, Y. R. Su, M. F. Linton, S. Fazio and M. S. Sinensky (2005). Reduced macrophage apoptosis is associated with accelerated atherosclerosis in low-density lipoprotein receptor-null mice. *Arterioscler Thromb Vasc Biol* **25**(1): 174-179.

Loppnow, H., M. Buerke, K. Werdan and S. Rose-John (2011). Contribution of vascular cell-derived cytokines to innate and inflammatory pathways in atherogenesis. *J Cell Mol Med* **15**(3): 484-500.

Lugo-Garcia, L., B. Nadal, R. Gomis, P. Petit, R. Gross and A. D. Lajoix (2008). Human pancreatic islets express the purinergic P2Y11 and P2Y12 receptors. *Horm Metab Res* **40**(11): 827-830.

Lutgens, E., K. B. Cleutjens, S. Heeneman, V. E. Koteliansky, L. C. Burkly and M. J. Daemen (2000). Both early and delayed anti-CD40L antibody treatment induces a stable plaque phenotype. *Proc Natl Acad Sci U S A* **97**(13): 7464-7469.

Lutgens, E., M. Gijbels, M. Smook, P. Heeringa, P. Gotwals, V. E. Koteliansky*, et al.* (2002). Transforming growth factor-beta mediates balance between inflammation and fibrosis during plaque progression. *Arterioscler Thromb Vasc Biol* **22**(6): 975-982.

Lutgens, E., L. Gorelik, M. J. Daemen, E. D. de Muinck, I. S. Grewal, V. E. Koteliansky*, et al.* (1999). Requirement for CD154 in the progression of atherosclerosis. *Nat Med* **5**(11): 1313-1316.

Mach, F., U. Schonbeck, J. Y. Bonnefoy, J. S. Pober and P. Libby (1997). Activation of monocyte/macrophage functions related to acute atheroma complication by ligation of CD40: induction of collagenase, stromelysin, and tissue factor. *Circulation* **96**(2): 396-399.

Mach, F., U. Schonbeck, R. P. Fabunmi, C. Murphy, E. Atkinson, J. Y. Bonnefoy*, et al.* (1999). T lymphocytes induce endothelial cell matrix metalloproteinase expression by a CD40L-dependent mechanism: implications for tubule formation. *Am J Pathol* **154**(1): 229-238.

Mach, F., U. Schonbeck, G. K. Sukhova, E. Atkinson and P. Libby (1998). Reduction of atherosclerosis in mice by inhibition of CD40 signalling. *Nature* **394**(6689): 200-203.

Mach, F., U. Schonbeck, G. K. Sukhova, T. Bourcier, J. Y. Bonnefoy, J. S. Pober*, et al.* (1997). Functional CD40 ligand is expressed on human vascular endothelial cells, smooth muscle cells, and macrophages: implications for CD40-CD40 ligand signaling in atherosclerosis. *Proc Natl Acad Sci U S A* **94**(5): 1931-1936.

MacKenzie, A. B., M. P. Mahaut-Smith and S. O. Sage (1996). Activation of receptor-operated cation channels via P2X1 not P2T purinoceptors in human platelets. *J Biol Chem* **271**(6): 2879-2881.

Maeda, N. (2011). Development of apolipoprotein E-deficient mice. *Arterioscler Thromb Vasc Biol* **31**(9): 1957-1962.

Mahley, R. W. (1988). Apolipoprotein E: cholesterol transport protein with expanding role in cell biology. *Science* **240**(4852): 622-630.

Mallat, Z., B. Hugel, J. Ohan, G. Leseche, J. M. Freyssinet and A. Tedgui (1999). Shed membrane microparticles with procoagulant potential in human atherosclerotic plaques: a role for apoptosis in plaque thrombogenicity. *Circulation* **99**(3): 348-353.

Manka, D., R. G. Collins, K. Ley, A. L. Beaudet and I. J. Sarembock (2001). Absence of p-selectin, but not intercellular adhesion molecule-1, attenuates neointimal growth after arterial injury in apolipoprotein e-deficient mice. *Circulation* **103**(7): 1000-1005.

Manka, D., S. B. Forlow, J. M. Sanders, D. Hurwitz, D. K. Bennett, S. A. Green*, et al.* (2004). Critical role of platelet P-selectin in the response to arterial injury in apolipoprotein-E-deficient mice. *Arterioscler Thromb Vasc Biol* **24**(6): 1124-1129.

Mantovani, A., C. Garlanda and M. Locati (2009). Macrophage diversity and polarization in atherosclerosis: a question of balance. *Arterioscler Thromb Vasc Biol* **29**(10): 1419-1423.

Massberg, S., K. Brand, S. Gruner, S. Page, E. Muller, I. Muller*, et al.* (2002). A critical role of platelet adhesion in the initiation of atherosclerotic lesion formation. *J Exp Med* **196**(7): 887-896.

Massberg, S., F. Vogt, T. Dickfeld, K. Brand, S. Page and M. Gawaz (2003). Activated platelets trigger an inflammatory response and enhance migration of aortic smooth muscle cells. *Thromb Res* **110**(4): 187-194.

Masyuk, A. I., S. A. Gradilone, J. M. Banales, B. Q. Huang, T. V. Masyuk, S. O. Lee*, et al.* (2008). Cholangiocyte primary cilia are chemosensory organelles that detect biliary nucleotides via P2Y12 purinergic receptors. *Am J Physiol Gastrointest Liver Physiol* **295**(4): G725-734.

Matsuno, H., J. M. Stassen, J. Vermylen and H. Deckmyn (1994). Inhibition of integrin function by a cyclic RGD-containing peptide prevents neointima formation. *Circulation* **90**(5): 2203-2206.

Mause, S. F., P. von Hundelshausen, A. Zernecke, R. R. Koenen and C. Weber (2005). Platelet microparticles: a transcellular delivery system for RANTES promoting monocyte recruitment on endothelium. *Arterioscler Thromb Vasc Biol* **25**(7): 1512-1518.

McNicol, A. and S. J. Israels (1999). Platelet dense granules: structure, function and implications for haemostasis. *Thromb Res* **95**(1): 1-18.

Mega, J. L., T. Simon, J. P. Collet, J. L. Anderson, E. M. Antman, K. Bliden*, et al.* (2010). Reduced-function CYP2C19 genotype and risk of adverse clinical outcomes among patients treated with clopidogrel predominantly for PCI: a meta-analysis. *JAMA* **304**(16): 1821-1830.

Mehta, S. R., S. Yusuf, R. J. Peters, M. E. Bertrand, B. S. Lewis, M. K. Natarajan*, et al.* (2001). Effects of pretreatment with clopidogrel and aspirin followed by long-term therapy in patients undergoing percutaneous coronary intervention: the PCI-CURE study. *Lancet* **358**(9281): 527-533.

Momi, S., S. C. Pitchford, P. F. Alberti, P. Minuz, P. Del Soldato and P. Gresele (2005). Nitroaspirin plus clopidogrel versus aspirin plus clopidogrel against platelet thromboembolism and intimal thickening in mice. *Thromb Haemost* **93**(3): 535-543.

Morel, D. W., P. E. DiCorleto and G. M. Chisolm (1984). Endothelial and smooth muscle cells alter low density lipoprotein in vitro by free radical oxidation. *Arteriosclerosis* **4**(4): 357-364.

Moses, J. W., M. B. Leon, J. J. Popma, P. J. Fitzgerald, D. R. Holmes, C. O'Shaughnessy*, et al.* (2003). Sirolimus-eluting stents versus standard stents in patients with stenosis in a native coronary artery. *N Engl J Med* **349**(14): 1315-1323.

Muller, W. A. (1995). The role of PECAM-1 (CD31) in leukocyte emigration: studies in vitro and in vivo. *J Leukoc Biol* **57**(4): 523-528.

Nagaoka, N., T. Matsubara, K. Okazaki, N. Masuda, K. Shikaura and A. Hotta (2001). Comparison of ticlopidine and cilostazol for the prevention of restenosis after percutaneous transluminal coronary angioplasty. *Jpn Heart J* **42**(1): 43-54.

Naghavi, M., P. Libby, E. Falk, S. W. Casscells, S. Litovsky, J. Rumberger*, et al.* (2003). From vulnerable plaque to vulnerable patient: a call for new definitions and risk assessment strategies: Part I. *Circulation* **108**(14): 1664-1672.

Nakashima, Y., A. S. Plump, E. W. Raines, J. L. Breslow and R. Ross (1994). ApoE-deficient mice develop lesions of all phases of atherosclerosis throughout the arterial tree. *Arterioscler Thromb.* **14**(1): 133-140.

Nakashima, Y., E. W. Raines, A. S. Plump, J. L. Breslow and R. Ross (1998). Upregulation of VCAM-1 and ICAM-1 at atherosclerosis-prone sites on the endothelium in the ApoE-deficient mouse. *Arterioscler Thromb Vasc Biol* **18**(5): 842-851.

Napoli, C., F. P. D'Armiento, F. P. Mancini, A. Postiglione, J. L. Witztum, G. Palumbo*, et al.* (1997). Fatty streak formation occurs in human fetal aortas and is greatly enhanced by maternal hypercholesterolemia. Intimal accumulation of low density lipoprotein and its oxidation precede monocyte recruitment into early atherosclerotic lesions. *J Clin Invest* **100**(11): 2680-2690.

Nieswandt, B., C. Brakebusch, W. Bergmeier, V. Schulte, D. Bouvard, R. Mokhtari-Nejad*, et al.* (2001). Glycoprotein VI but not alpha2beta1 integrin is essential for platelet interaction with collagen. *EMBO J* **20**(9): 2120-2130.

Nieswandt, B., I. Pleines and M. Bender (2011). Platelet adhesion and activation mechanisms in arterial thrombosis and ischaemic stroke. *J Thromb Haemost* **9 Suppl 1**: 92-104.

Nieswandt, B., V. Schulte, A. Zywietz, M. P. Gratacap and S. Offermanns (2002). Costimulation of Gi- and G12/G13-mediated signaling pathways induces integrin alpha IIbbeta 3 activation in platelets. *J Biol Chem* **277**(42): 39493-39498.

Nieswandt, B. and S. P. Watson (2003). Platelet-collagen interaction: is GPVI the central receptor? *Blood* **102**(2): 449-461.

Nilsson, J., M. Sjolund, L. Palmberg, J. Thyberg and C. H. Heldin (1985). Arterial smooth muscle cells in primary culture produce a platelet-derived growth factor-like protein. *Proc Natl Acad Sci U S A* **82**(13): 4418-4422.

Noji, T., A. Karasawa and H. Kusaka (2004). Adenosine uptake inhibitors. *Eur J Pharmacol* **495**(1): 1-16.

Norman, K. E., K. L. Moore, R. P. McEver and K. Ley (1995). Leukocyte rolling in vivo is mediated by P-selectin glycoprotein ligand-1. *Blood* **86**(12): 4417-4421.

Nunnari, J. J., T. Zand, I. Joris and G. Majno (1989). Quantitation of oil red O staining of the aorta in hypercholesterolemic rats. *Exp Mol Pathol* **51**(1): 1-8.

Nurden, A. T. (2011). Platelets, inflammation and tissue regeneration. *Thromb Haemost* **105 Suppl 1**: S13-33.

O'Brien, K. A., T. K. Gartner, N. Hay and X. Du (2012). ADP-stimulated activation of Akt during integrin outside-in signaling promotes platelet spreading by inhibiting glycogen synthase kinase-3beta. *Arterioscler Thromb Vasc Biol* **32**(9): 2232-2240.

Offermanns, S., C. F. Toombs, Y. H. Hu and M. I. Simon (1997). Defective platelet activation in G alpha(q)-deficient mice. *Nature* **389**(6647): 183-186.

Ohlmann, P., A. Eckly, M. Freund, J. P. Cazenave, S. Offermanns and C. Gachet (2000). ADP induces partial platelet aggregation without shape change and potentiates collagen-induced aggregation in the absence of Galphaq. *Blood* **96**(6): 2134-2139.

Ohlmann, P., K. L. Laugwitz, B. Nurnberg, K. Spicher, G. Schultz, J. P. Cazenave*, et al.* (1995). The human platelet ADP receptor activates Gi2 proteins. *Biochem J* **312 (Pt 3)**: 775-779.

Ohta, H., H. Wada, T. Niwa, H. Kirii, N. Iwamoto, H. Fujii*, et al.* (2005). Disruption of tumor necrosis factor-alpha gene diminishes the development of atherosclerosis in ApoE-deficient mice. *Atherosclerosis* **180**(1): 11-17.

Oury, C., E. Toth-Zsamboki, J. Vermylen and M. F. Hoylaerts (2002). P2X(1)-mediated activation of extracellular signal-regulated kinase 2 contributes to platelet secretion and aggregation induced by collagen. *Blood* **100**(7): 2499-2505.

Owens, A. P., 3rd and N. Mackman (2011). Microparticles in hemostasis and thrombosis. *Circ Res* **108**(10): 1284-1297.

Owens, G. K., M. S. Kumar and B. R. Wamhoff (2004). Molecular regulation of vascular smooth muscle cell differentiation in development and disease. *Physiol Rev* **84**(3): 767-801.

Paigen, B., A. Morrow, C. Brandon, D. Mitchell and P. Holmes (1985). Variation in susceptibility to atherosclerosis among inbred strains of mice. *Atherosclerosis* **57**(1): 65-73.

Palm, M., L. Frankenberg, M. Johansson and E. Jalkesten (1997). Evaluation of coagulation tests in mouse plasma. *Comparative Haematology International* **7**(4): 243-246.

Palmerini, T., G. Biondi-Zoccai, D. Della Riva, C. Stettler, D. Sangiorgi, F. D'Ascenzo*, et al.* (2012). Stent thrombosis with drug-eluting and bare-metal stents: evidence from a comprehensive network meta-analysis. *Lancet* **379**(9824): 1393-1402.

Panes, O., V. Matus, C. G. Saez, T. Quiroga, J. Pereira and D. Mezzano (2007). Human platelets synthesize and express functional tissue factor. *Blood* **109**(12): 5242-5250.

Papadopoulou, C., V. Corrigall, P. R. Taylor and R. N. Poston (2008). The role of the chemokines MCP-1, GRO-alpha, IL-8 and their receptors in the adhesion of monocytic cells to human atherosclerotic plaques. *Cytokine* **43**(2): 181-186.

Patel, S. R., J. H. Hartwig and J. E. Italiano, Jr. (2005). The biogenesis of platelets from megakaryocyte proplatelets. *J Clin Invest* **115**(12): 3348-3354.

Patel, S. R., J. L. Richardson, H. Schulze, E. Kahle, N. Galjart, K. Drabek*, et al.* (2005). Differential roles of microtubule assembly and sliding in proplatelet formation by megakaryocytes. *Blood* **106**(13): 4076-4085.

Patil, S. B., L. E. Jackman, S. E. Francis, H. M. Judge, S. Nylander and R. F. Storey (2010). Ticagrelor effectively and reversibly blocks murine platelet P2Y12-mediated thrombosis and demonstrates a requirement for sustained P2Y12 inhibition to prevent subsequent neointima. *Arterioscler Thromb Vasc Biol* **30**(12): 2385-2391.

Patrono, C. (1994). Aspirin as an antiplatelet drug. *N Engl J Med* **330**(18): 1287-1294.

Paul, B. Z., J. L. Daniel and S. P. Kunapuli (1999). Platelet shape change is mediated by both calcium-dependent and -independent signaling pathways. Role of p160 Rho-associated coiled-coil-containing protein kinase in platelet shape change. *J Biol Chem* **274**(40): 28293-28300.

Paul, B. Z., J. Jin and S. P. Kunapuli (1999). Molecular mechanism of thromboxane A(2)-induced platelet aggregation. Essential role for p2t(ac) and alpha(2a) receptors. *J Biol Chem* **274**(41): 29108-29114.

Peng, H. B., P. Libby and J. K. Liao (1995). Induction and stabilization of I kappa B alpha by nitric oxide mediates inhibition of NF-kappa B. *J Biol Chem* **270**(23): 14214-14219.

Pfisterer, M., H. P. Brunner-La Rocca, P. T. Buser, P. Rickenbacher, P. Hunziker, C. Mueller*, et al.* (2006). Late clinical events after clopidogrel discontinuation may limit the benefit of drug-eluting stents: an observational study of drug-eluting versus bare-metal stents. *J Am Coll Cardiol* **48**(12): 2584-2591.

Phillips, J. W., K. G. Barringhaus, J. M. Sanders, S. E. Hesselbacher, A. C. Czarnik, D. Manka*, et al.* (2003). Single injection of P-selectin or P-selectin glycoprotein ligand-1 monoclonal antibody blocks neointima formation after arterial injury in apolipoprotein E-deficient mice. *Circulation* **107**(17): 2244-2249.

Pidkovka, N. A., O. A. Cherepanova, T. Yoshida, M. R. Alexander, R. A. Deaton, J. A. Thomas*, et al.* (2007). Oxidized phospholipids induce phenotypic switching of vascular smooth muscle cells in vivo and in vitro. *Circ Res* **101**(8): 792-801.

Piedrahita, J. A., S. H. Zhang, J. R. Hagaman, P. M. Oliver and N. Maeda (1992). Generation of mice carrying a mutant apolipoprotein E gene inactivated by gene targeting in embryonic stem cells. *Proc Natl Acad Sci U S A* **89**(10): 4471-4475.

Quinn, M. T., S. Parthasarathy, L. G. Fong and D. Steinberg (1987). Oxidatively modified low density lipoproteins: a potential role in recruitment and retention of monocyte/macrophages during atherogenesis. *Proc Natl Acad Sci U S A* **84**(9): 2995-2998.

Quinton, T. M., S. Kim, C. Dangelmaier, R. T. Dorsam, J. Jin, J. L. Daniel*, et al.* (2002). Protein kinase C- and calcium-regulated pathways independently synergize with Gi pathways in agonist-induced fibrinogen receptor activation. *Biochem J* **368**(Pt 2): 535-543.

Raines, E. W., S. K. Dower and R. Ross (1989). Interleukin-1 mitogenic activity for fibroblasts and smooth muscle cells is due to PDGF-AA. *Science* **243**(4889): 393-396.

Raines, E. W. and N. Ferri (2005). Thematic review series: The immune system and atherogenesis. Cytokines affecting endothelial and smooth muscle cells in vascular disease. *J Lipid Res* **46**(6): 1081-1092.

Raines, E. W. and R. Ross (1993). Smooth muscle cells and the pathogenesis of the lesions of atherosclerosis. *Br Heart J* **69**(1 Suppl): S30-37.

Rajavashisth, T. B., A. Andalibi, M. C. Territo, J. A. Berliner, M. Navab, A. M. Fogelman*, et al.* (1990). Induction of endothelial cell expression of granulocyte and macrophage colony-stimulating factors by modified low-density lipoproteins. *Nature* **344**(6263): 254-257.

Rauch, B. H., A. C. Rosenkranz, S. Ermler, A. Bohm, J. Driessen, J. W. Fischer*, et al.* (2010). Regulation of functionally active P2Y12 ADP receptors by thrombin in human smooth muscle cells and the presence of P2Y12 in carotid artery lesions. *Arterioscler Thromb Vasc Biol* **30**(12): 2434-2442.

Rauch, U., D. Bonderman, B. Bohrmann, J. J. Badimon, J. Himber, M. A. Riederer*, et al.* (2000). Transfer of tissue factor from leukocytes to platelets is mediated by CD15 and tissue factor. *Blood* **96**(1): 170-175.

Reddick, R. L., S. H. Zhang and N. Maeda (1994). Atherosclerosis in mice lacking apo E. Evaluation of lesional development and progression. *Arterioscler Thromb.* **14**(1): 141-147.

Rendu, F. and B. Brohard-Bohn (2001). The platelet release reaction: granules' constituents, secretion and functions. *Platelets* **12**(5): 261-273.

Reusch, P., H. Wagdy, R. Reusch, E. Wilson and H. E. Ives (1996). Mechanical strain increases smooth muscle and decreases nonmuscle myosin expression in rat vascular smooth muscle cells. *Circ Res* **79**(5): 1046-1053.

Richter, G. M., J. C. Palmaz, G. Noeldge and F. Tio (2000). Blood flow and thrombus formation determine the development of stent neointima. *J Long Term Eff Med Implants* **10**(1-2): 69-77.

Rocnik, E. F., B. M. Chan and J. G. Pickering (1998). Evidence for a role of collagen synthesis in arterial smooth muscle cell migration. *J Clin Invest* **101**(9): 1889-1898.

Roderick, P. J., H. C. Wilkes and T. W. Meade (1993). The gastrointestinal toxicity of aspirin: an overview of randomised controlled trials. *Br J Clin Pharmacol* **35**(3): 219-226.

Romo, G. M., J. F. Dong, A. J. Schade, E. E. Gardiner, G. S. Kansas, C. Q. Li*, et al.* (1999). The glycoprotein Ib-IX-V complex is a platelet counterreceptor for P-selectin. *J Exp Med* **190**(6): 803-814.

Rosenberg, R. D. and J. S. Rosenberg (1984). Natural anticoagulant mechanisms. *J Clin Invest* **74**(1): 1-6.

Rosenberg, S., A. Stracher and R. C. Lucas (1981). Isolation and characterization of actin and actin-binding protein from human platelets. *J Cell Biol* **91**(1): 201-211.

Ross, R. (1993). The pathogenesis of atherosclerosis: a perspective for the 1990s. *Nature* **362**(6423): 801-809.

Ross, R. (1999). Atherosclerosis--an inflammatory disease. *N Engl J Med* **340**(2): 115-126.

Ross, R., J. Glomset and L. Harker (1977). Response to injury and atherogenesis. *Am J Pathol* **86**(3): 675-684.

Ross, R., J. Glomset, B. Kariya and L. Harker (1974). A platelet-dependent serum factor that stimulates the proliferation of arterial smooth muscle cells in vitro. *Proc Natl Acad Sci U S A* **71**(4): 1207-1210.

Ross, R. and J. A. Glomset (1976). The pathogenesis of atherosclerosis (second of two parts). *N Engl J Med* **295**(8): 420-425.

Ross, R. and S. J. Klebanoff (1971). The smooth muscle cell. I. In vivo synthesis of connective tissue proteins. *J Cell Biol* **50**(1): 159-171.

Roth, S. J., M. W. Carr and T. A. Springer (1995). C-C chemokines, but not the C-X-C chemokines interleukin-8 and interferon-gamma inducible protein-10, stimulate transendothelial chemotaxis of T lymphocytes. *Eur J Immunol* **25**(12): 3482-3488.

Rotzius, P., S. Thams, O. Soehnlein, E. Kenne, C. N. Tseng, N. K. Bjorkstrom*, et al.* (2010). Distinct infiltration of neutrophils in lesion shoulders in ApoE-/- mice. *Am J Pathol* **177**(1): 493-500.

Rubin, K., A. Tingstrom, G. K. Hansson, E. Larsson, L. Ronnstrand, L. Klareskog*, et al.* (1988). Induction of B-type receptors for platelet-derived growth factor in vascular inflammation: possible implications for development of vascular proliferative lesions. *Lancet* **1**(8599): 1353-1356.

Russell, P. J. (2002). Population genetics. iGenetics. San Francisco, CA, Benjamin Cummings**:** 623-672.

Sachais, B. S., T. Turrentine, J. M. Dawicki McKenna, A. H. Rux, D. Rader and M. A. Kowalska (2007). Elimination of platelet factor 4 (PF4) from platelets reduces atherosclerosis in C57Bl/6 and apoE-/- mice. *Thromb Haemost* **98**(5): 1108-1113.

Samama, C. M., P. Bonnin, M. Bonneau, G. Pignaud, E. Mazoyer, O. Bailliart*, et al.* (1992). Comparative arterial antithrombotic activity of clopidogrel and acetyl salicylic acid in the pig. *Thromb Haemost* **68**(5): 500-505.

Sano, H., T. Sudo, M. Yokode, T. Murayama, H. Kataoka, N. Takakura*, et al.* (2001). Functional blockade of platelet-derived growth factor receptor-beta but not of receptor-alpha prevents vascular smooth muscle cell accumulation in fibrous cap lesions in apolipoprotein E-deficient mice. *Circulation* **103**(24): 2955-2960.

Saren, P., H. G. Welgus and P. T. Kovanen (1996). TNF-alpha and IL-1beta selectively induce expression of 92-kDa gelatinase by human macrophages. *J Immunol* **157**(9): 4159-4165.

Sasaki, Y., M. Hoshi, C. Akazawa, Y. Nakamura, H. Tsuzuki, K. Inoue*, et al.* (2003). Selective expression of Gi/o-coupled ATP receptor P2Y12 in microglia in rat brain. *Glia* **44**(3): 242-250.

Sata, M., A. Saiura, A. Kunisato, A. Tojo, S. Okada, T. Tokuhisa*, et al.* (2002). Hematopoietic stem cells differentiate into vascular cells that participate in the pathogenesis of atherosclerosis. *Nat Med* **8**(4): 403-409.

Sata, M., A. Takahashi, K. Tanaka, M. Washida, N. Ishizaka, J. Ako*, et al.* (2002). Mouse genetic evidence that tranilast reduces smooth muscle cell hyperplasia via a p21(WAF1)-dependent pathway. *Arterioscler Thromb Vasc Biol* **22**(8): 1305-1309.

Scarborough, P., P. Bhatnagar, K. Wickramasinghe, K. Smolina, C. Mitchell and M. Rayner (2010). Coronary heart disease statistics. University of Oxford, British Heart Foundation Health Promotion Research Group.

Schaar, J. A., J. E. Muller, E. Falk, R. Virmani, V. Fuster, P. W. Serruys*, et al.* (2004). Terminology for high-risk and vulnerable coronary artery plaques. Report of a meeting on the vulnerable plaque, June 17 and 18, 2003, Santorini, Greece. *Eur Heart J* **25**(12): 1077-1082.

Schafer, K., S. Konstantinides, C. Riedel, T. Thinnes, K. Muller, C. Dellas*, et al.* (2002). Different mechanisms of increased luminal stenosis after arterial injury in mice deficient for urokinase- or tissue-type plasminogen activator. *Circulation* **106**(14): 1847-1852.

Schall, T. J., K. Bacon, K. J. Toy and D. V. Goeddel (1990). Selective attraction of monocytes and T lymphocytes of the memory phenotype by cytokine RANTES. *Nature* **347**(6294): 669-671.

Schatz, R. A., D. S. Baim, M. Leon, S. G. Ellis, S. Goldberg, J. W. Hirshfeld*, et al.* (1991). Clinical experience with the Palmaz-Schatz coronary stent. Initial results of a multicenter study. *Circulation* **83**(1): 148-161.

Schini-Kerth, V. B., S. Bassus, B. Fisslthaler, C. M. Kirchmaier and R. Busse (1997). Aggregating human platelets stimulate the expression of thrombin receptors in cultured vascular smooth muscle cells via the release of transforming growth factor-beta1 and platelet-derived growth factorAB. *Circulation* **96**(11): 3888-3896.

Schlegelmilch, T., K. Henke and F. Peri (2011). Microglia in the developing brain: from immunity to behaviour. *Curr Opin Neurobiol* **21**(1): 5-10.

Schober, A., D. Manka, P. von Hundelshausen, Y. Huo, P. Hanrath, I. J. Sarembock*, et al.* (2002). Deposition of platelet RANTES triggering monocyte recruitment requires P-selectin and is involved in neointima formation after arterial injury. *Circulation* **106**(12): 1523-1529.

Schober, A., A. Zernecke, E. A. Liehn, P. von Hundelshausen, S. Knarren, W. A. Kuziel*, et al.* (2004). Crucial role of the CCL2/CCR2 axis in neointimal hyperplasia after arterial injury in hyperlipidemic mice involves early monocyte recruitment and CCL2 presentation on platelets. *Circ Res* **95**(11): 1125-1133.

Schonbeck, U., F. Mach, J. Y. Bonnefoy, H. Loppnow, H. D. Flad and P. Libby (1997). Ligation of CD40 activates interleukin 1beta-converting enzyme (caspase-1) activity in vascular smooth muscle and endothelial cells and promotes elaboration of active interleukin 1beta. *J Biol Chem* **272**(31): 19569-19574.

Schonbeck, U., F. Mach, G. K. Sukhova, E. Atkinson, E. Levesque, M. Herman*, et al.* (1999). Expression of stromelysin-3 in atherosclerotic lesions: regulation via CD40-CD40 ligand signaling in vitro and in vivo. *J Exp Med* **189**(5): 843-853.

Schonbeck, U., F. Mach, G. K. Sukhova, M. Herman, P. Graber, M. R. Kehry*, et al.* (2000). CD40 ligation induces tissue factor expression in human vascular smooth muscle cells. *Am J Pathol* **156**(1): 7-14.

Schonbeck, U., G. K. Sukhova, K. Shimizu, F. Mach and P. Libby (2000). Inhibition of CD40 signaling limits evolution of established atherosclerosis in mice. *Proc Natl Acad Sci U S A* **97**(13): 7458-7463.

Schonherr, E., H. T. Jarvelainen, M. G. Kinsella, L. J. Sandell and T. N. Wight (1993). Platelet-derived growth factor and transforming growth factor-beta 1 differentially affect the synthesis of biglycan and decorin by monkey arterial smooth muscle cells. *Arterioscler Thromb* **13**(7): 1026-1036.

Schrijvers, D. M., G. R. De Meyer, M. M. Kockx, A. G. Herman and W. Martinet (2005). Phagocytosis of apoptotic cells by macrophages is impaired in atherosclerosis. *Arterioscler Thromb Vasc Biol* **25**(6): 1256-1261.

Schultze, M. (1865). Ein heizbarer Objecttisch und seine Verwendung bei Untersuchungen des Blutes. *Archiv für mikroscopische Anatomie* **1**(1): 1-42.

Schulz, C., I. Konrad, S. Sauer, L. Orschiedt, M. Koellnberger, R. Lorenz*, et al.* (2008). Effect of chronic treatment with acetylsalicylic acid and clopidogrel on atheroprogression and atherothrombosis in ApoE-deficient mice in vivo. *Thromb Haemost* **99**(1): 190-195.

Schulz, S., D. Sibbing, S. Braun, T. Morath, J. Mehilli, S. Massberg*, et al.* (2010). Platelet response to clopidogrel and restenosis in patients treated predominantly with drug-eluting stents. *Am Heart J* **160**(2): 355-361.

Schwartz, R. S., K. C. Huber, J. G. Murphy, W. D. Edwards, A. R. Camrud, R. E. Vlietstra*, et al.* (1992). Restenosis and the proportional neointimal response to coronary artery injury: results in a porcine model. *J Am Coll Cardiol* **19**(2): 267-274.

Schwartz, R. S., J. G. Murphy, W. D. Edwards, A. R. Camrud, R. E. Vliestra and D. R. Holmes (1990). Restenosis after balloon angioplasty. A practical proliferative model in porcine coronary arteries. *Circulation* **82**(6): 2190-2200.

Schwenke, D. C. and T. E. Carew (1989). Initiation of atherosclerotic lesions in cholesterol-fed rabbits. II. Selective retention of LDL vs. selective increases in LDL permeability in susceptible sites of arteries. *Arteriosclerosis* **9**(6): 908-918.

Schwertz, H., N. D. Tolley, J. M. Foulks, M. M. Denis, B. W. Risenmay, M. Buerke*, et al.* (2006). Signal-dependent splicing of tissue factor pre-mRNA modulates the thrombogenicity of human platelets. *J Exp Med* **203**(11): 2433-2440.

Semple, J. W., J. E. Italiano, Jr. and J. Freedman (2011). Platelets and the immune continuum. *Nat Rev Immunol* **11**(4): 264-274.

Shanker, G., J. L. Kontos, D. M. Eckman, D. Wesley-Farrington and D. C. Sane (2006). Nicotine upregulates the expression of P2Y12 on vascular cells and megakaryoblasts. *J Thromb Thrombolysis* **22**(3): 213-220.

Shattil, S. J. and P. J. Newman (2004). Integrins: dynamic scaffolds for adhesion and signaling in platelets. *Blood* **104**(6): 1606-1615.

Shaw, S. K., S. Ma, M. B. Kim, R. M. Rao, C. U. Hartman, R. M. Froio*, et al.* (2004). Coordinated redistribution of leukocyte LFA-1 and endothelial cell ICAM-1 accompany neutrophil transmigration. *J Exp Med* **200**(12): 1571-1580.

Shimokado, K., E. W. Raines, D. K. Madtes, T. B. Barrett, E. P. Benditt and R. Ross (1985). A significant part of macrophage-derived growth factor consists of at least two forms of PDGF. *Cell* **43**(1): 277-286.

Shuldiner, A. R., J. R. O'Connell, K. P. Bliden, A. Gandhi, K. Ryan, R. B. Horenstein*, et al.* (2009). Association of cytochrome P450 2C19 genotype with the antiplatelet effect and clinical efficacy of clopidogrel therapy. *JAMA* **302**(8): 849-857.

Smith, J. D., E. Trogan, M. Ginsberg, C. Grigaux, J. Tian and M. Miyata (1995). Decreased atherosclerosis in mice deficient in both macrophage colony-stimulating factor (op) and apolipoprotein E. *Proc Natl Acad Sci U S A* **92**(18): 8264-8268.

Smits, P., S. B. Williams, D. E. Lipson, P. Banitt, G. A. Rongen and M. A. Creager (1995). Endothelial release of nitric oxide contributes to the vasodilator effect of adenosine in humans. *Circulation* **92**(8): 2135-2141.

Smolenski, A. (2012). Novel roles of cAMP/cGMP-dependent signaling in platelets. *J Thromb Haemost* **10**(2): 167-176.

Springer, T. A. (1995). Traffic signals on endothelium for lymphocyte recirculation and leukocyte emigration. *Annu Rev Physiol* **57**: 827-872.

Stary, H. C., A. B. Chandler, R. E. Dinsmore, V. Fuster, S. Glagov, W. Insull, Jr.*, et al.* (1995). A definition of advanced types of atherosclerotic lesions and a histological classification of atherosclerosis. A report from the Committee on Vascular Lesions of the Council on Arteriosclerosis, American Heart Association. *Arterioscler Thromb Vasc Biol* **15**(9): 1512-1531.

Stary, H. C., A. B. Chandler, S. Glagov, J. R. Guyton, W. Insull, Jr., M. E. Rosenfeld*, et al.* (1994). A definition of initial, fatty streak, and intermediate lesions of atherosclerosis. A report from the Committee on Vascular Lesions of the Council on Arteriosclerosis, American Heart Association. *Arterioscler Thromb Vasc Biol* **14**(5): 840-856.

Steele, P. M., J. H. Chesebro, A. W. Stanson, D. R. Holmes, Jr., M. K. Dewanjee, L. Badimon*, et al.* (1985). Balloon angioplasty. Natural history of the pathophysiological response to injury in a pig model. *Circ Res* **57**(1): 105-112.

Steinhubl, S. R., P. B. Berger, J. T. Mann III, E. T. A. Fry, A. DeLago, C. Wilmer*, et al.* (2002). Early and Sustained Dual Oral Antiplatelet Therapy Following Percutaneous Coronary Intervention: A Randomized Controlled Trial. *JAMA* **288**(19): 2411-2420.

Stone, G. W., S. G. Ellis, D. A. Cox, J. Hermiller, C. O'Shaughnessy, J. T. Mann*, et al.* (2004). A polymer-based, paclitaxel-eluting stent in patients with coronary artery disease. *N Engl J Med* **350**(3): 221-231.

Storey, R. F. (2006). Biology and pharmacology of the platelet P2Y12 receptor. *Curr Pharm Des.* **12**(10): 1255-1259.

Storey, R. F., D. J. Angiolillo, S. B. Patil, B. Desai, R. Ecob, S. Husted*, et al.* (2010). Inhibitory effects of ticagrelor compared with clopidogrel on platelet function in patients with acute coronary syndromes: the PLATO (PLATelet inhibition and patient Outcomes) PLATELET substudy. *J Am Coll Cardiol* **56**(18): 1456-1462.

Storey, R. F., H. M. Judge, R. G. Wilcox and S. Heptinstall (2002). Inhibition of ADP-induced P-selectin expression and platelet-leukocyte conjugate formation by clopidogrel and the P2Y12 receptor antagonist AR-C69931MX but not aspirin. *Thromb Haemost* **88**(3): 488-494.

Storey, R. F., H. M. Sanderson, A. E. White, J. A. May, K. E. Cameron and S. Heptinstall (2000). The central role of the P_{2T} receptor in amplification of human platelet activation, aggregation, secretion and procoagulant activity. *Br J Haematol* **110**(4): 925-934.

Storey, R. F., P. Steg, S. James, S. Husted, C. Cannon, R. Becker*, et al.* (2012). Reduction in pulmonary adverse events and associated sepsis and mortality in acute coronary syndrome patients teated with ticagrelor compared to clopidogrel: A post hoc analysis of the PLATO study. *Journal of the American College of Cardiology* **59**(13s1): E482-E482.

Storey, R. F., R. G. Wilcox and S. Heptinstall (2002). Comparison of the pharmacodynamic effects of the platelet ADP receptor antagonists clopidogrel and AR-C69931MX in patients with ischaemic heart disease. *Platelets* **13**(7): 407-413.

Sugidachi, A., T. Ogawa, A. Kurihara, K. Hagihara, J. A. Jakubowski, M. Hashimoto*, et al.* (2007). The greater in vivo antiplatelet effects of prasugrel as compared to clopidogrel reflect more efficient generation of its active metabolite with similar antiplatelet activity to that of clopidogrel's active metabolite. *J Thromb Haemost* **5**(7): 1545-1551.

Sukhova, G. K., U. Schonbeck, E. Rabkin, F. J. Schoen, A. R. Poole, R. C. Billinghurst*, et al.* (1999). Evidence for increased collagenolysis by interstitial collagenases-1 and -3 in vulnerable human atheromatous plaques. *Circulation* **99**(19): 2503-2509.

Suo, J., D. E. Ferrara, D. Sorescu, R. E. Guldberg, W. R. Taylor and D. P. Giddens (2007). Hemodynamic shear stresses in mouse aortas: implications for atherogenesis. *Arterioscler Thromb Vasc Biol* **27**(2): 346-351.

Tabas, I. (2005). Consequences and therapeutic implications of macrophage apoptosis in atherosclerosis: the importance of lesion stage and phagocytic efficiency. *Arterioscler Thromb Vasc Biol* **25**(11): 2255-2264.

Tanaka, K., M. Sata, Y. Hirata and R. Nagai (2003). Diverse contribution of bone marrow cells to neointimal hyperplasia after mechanical vascular injuries. *Circ Res* **93**(8): 783-790.

Theilmeier, G., C. Michiels, E. Spaepen, I. Vreys, D. Collen, J. Vermylen*, et al.* (2002). Endothelial von Willebrand factor recruits platelets to atherosclerosis-prone sites in response to hypercholesterolemia. *Blood* **99**(12): 4486-4493.

Theroux, P., H. Ouimet, J. McCans, J. G. Latour, P. Joly, G. Levy*, et al.* (1988). Aspirin, heparin, or both to treat acute unstable angina. *N Engl J Med* **319**(17): 1105-1111.

Thyberg, J. and A. Hultgardh-Nilsson (1994). Fibronectin and the basement membrane components laminin and collagen type IV influence the phenotypic properties of subcultured rat aortic smooth muscle cells differently. *Cell Tissue Res* **276**(2): 263-271.

Thyberg, J., L. Palmberg, J. Nilsson, T. Ksiazek and M. Sjolund (1983). Phenotype modulation in primary cultures of arterial smooth muscle cells. On the role of platelet-derived growth factor. *Differentiation* **25**(2): 156-167.

Topper, J. N., J. Cai, D. Falb and M. A. Gimbrone, Jr. (1996). Identification of vascular endothelial genes differentially responsive to fluid mechanical stimuli: cyclooxygenase-2, manganese superoxide dismutase, and endothelial cell nitric oxide synthase are selectively up-regulated by steady laminar shear stress. *Proc Natl Acad Sci U S A* **93**(19): 10417-10422.

Toschi, V., R. Gallo, M. Lettino, J. T. Fallon, S. D. Gertz, A. Fernandez-Ortiz*, et al.* (1997). Tissue factor modulates the thrombogenicity of human atherosclerotic plaques. *Circulation* **95**(3): 594-599.

Trumel, C., B. Payrastre, M. Plantavid, B. Hechler, C. Viala, P. Presek*, et al.* (1999). A key role of adenosine diphosphate in the irreversible platelet aggregation induced by the PAR1-activating peptide through the late activation of phosphoinositide 3-kinase. *Blood* **94**(12): 4156-4165.

Tsai, T. N., J. P. Kirton, P. Campagnolo, L. Zhang, Q. Xiao, Z. Zhang*, et al.* (2012). Contribution of stem cells to neointimal formation of decellularized vessel grafts in a novel mouse model. *Am J Pathol* **181**(1): 362-373.

Tsao, P. S., R. Buitrago, J. R. Chan and J. P. Cooke (1996). Fluid flow inhibits endothelial adhesiveness. Nitric oxide and transcriptional regulation of VCAM-1. *Circulation* **94**(7): 1682-1689.

Tseng, M. T., A. Dozier, B. Haribabu and U. M. Graham (2005). Transendothelial migration of ferric ion in FeCl(3) injured murine common carotid artery. *Thromb Res*.

Turner, N. A., J. L. Moake and L. V. McIntire (2001). Blockade of adenosine diphosphate receptors P2Y(12) and P2Y(1) is required to inhibit platelet aggregation in whole blood under flow. *Blood* **98**(12): 3340-3345.

Tzima, E., M. Irani-Tehrani, W. B. Kiosses, E. Dejana, D. A. Schultz, B. Engelhardt*, et al.* (2005). A mechanosensory complex that mediates the endothelial cell response to fluid shear stress. *Nature* **437**(7057): 426-431.

Uehara, K. and A. Uehara (2011). P2Y1, P2Y6, and P2Y12 receptors in rat splenic sinus endothelial cells: an immunohistochemical and ultrastructural study. *Histochem Cell Biol* **136**(5): 557-567.

Unterberg, C., D. Sandrock, K. Nebendahl and A. B. Buchwald (1995). Reduced acute thrombus formation results in decreased neointimal proliferation after coronary angioplasty. *J Am Coll Cardiol* **26**(7): 1747-1754.

van der Loop, F. T., G. Gabbiani, G. Kohnen, F. C. Ramaekers and G. J. van Eys (1997). Differentiation of smooth muscle cells in human blood vessels as defined by smoothelin, a novel marker for the contractile phenotype. *Arterioscler Thromb Vasc Biol* **17**(4): 665-671.

van der Meijden, P. E., S. M. Schoenwaelder, M. A. Feijge, J. M. Cosemans, I. C. Munnix, R. Wetzker*, et al.* (2008). Dual P2Y 12 receptor signaling in thrombin-stimulated platelets--involvement of phosphoinositide 3-kinase beta but not gamma isoform in Ca2+ mobilization and procoagulant activity. *FEBS J* **275**(2): 371-385.

van der Wal, A. C., A. E. Becker, C. M. van der Loos and P. K. Das (1994). Site of intimal rupture or erosion of thrombosed coronary atherosclerotic plaques is characterized by an inflammatory process irrespective of the dominant plaque morphology. *Circulation* **89**(1): 36-44.

van Giezen, J. J., J. Sidaway, P. Glaves, I. Kirk and J. A. Bjorkman (2012). Ticagrelor inhibits adenosine uptake in vitro and enhances adenosine-mediated hyperemia responses in a canine model. *J Cardiovasc Pharmacol Ther* **17**(2): 164-172.

Vial, C., M. G. Rolf, M. P. Mahaut-Smith and R. J. Evans (2002). A study of P2X1 receptor function in murine megakaryocytes and human platelets reveals synergy with P2Y receptors. *Br J Pharmacol* **135**(2): 363-372.

Virchow, R. (1971). Cellular pathology: as based upon physiological and pathological histology. New York, Dover Publications.

von Hundelshausen, P., K. S. Weber, Y. Huo, A. E. Proudfoot, P. J. Nelson, K. Ley*, et al.* (2001). RANTES deposition by platelets triggers monocyte arrest on inflamed and atherosclerotic endothelium. *Circulation* **103**(13): 1772-1777.

Wallentin, L., R. C. Becker, A. Budaj, C. P. Cannon, H. Emanuelsson, C. Held*, et al.* (2009). Ticagrelor versus clopidogrel in patients with acute coronary syndromes. *N Engl J Med* **361**(11): 1045-1057.

Wallentin, L. C. (1991). Aspirin (75 mg/day) after an episode of unstable coronary artery disease: long-term effects on the risk for myocardial infarction, occurrence of severe

angina and the need for revascularization. Research Group on Instability in Coronary Artery Disease in Southeast Sweden. *J Am Coll Cardiol* **18**(7): 1587-1593.
Wang, L., C. Miller, R. F. Swarthout, M. Rao, N. Mackman and M. B. Taubman (2009). Vascular smooth muscle-derived tissue factor is critical for arterial thrombosis after ferric chloride-induced injury. *Blood* **113**(3): 705-713.
Wang, X. and L. Xu (2005). An optimized murine model of ferric chloride-induced arterial thrombosis for thrombosis research. *Thromb Res* **115**(1-2): 95-100.
Wang, Y., M. Sakuma, Z. Chen, V. Ustinov, C. Shi, K. Croce*, et al.* (2005). Leukocyte engagement of platelet glycoprotein Ibalpha via the integrin Mac-1 is critical for the biological response to vascular injury. *Circulation* **112**(19): 2993-3000.
West, L. E., T. Steiner, H. M. Judge, S. E. Francis and R. F. Storey (2014). Vessel wall, not platelet, P2Y12 potentiates early atherogenesis. *Cardiovasc Res* **102**(3): 429-435.
Westrick, R. J., M. E. Winn and D. T. Eitzman (2007). Murine models of vascular thrombosis (Eitzman series). *Arterioscler Thromb Vasc Biol* **27**(10): 2079-2093.
Wheatcroft, S. B., A. M. Shah, J. M. Li, E. Duncan, B. T. Noronha, P. A. Crossey*, et al.* (2004). Preserved glucoregulation but attenuation of the vascular actions of insulin in mice heterozygous for knockout of the insulin receptor. *Diabetes* **53**(10): 2645-2652.
White, J. G. (2006). Platelet structure. Platelets. A. D. Michelson. Burlington, MA, Academic Press**:** 45-74.
WHO (2008). The global burden of disease: 2004 update. Geneva, World Health Organization.
Wihlborg, A. K., L. Wang, O. O. Braun, A. Eyjolfsson, R. Gustafsson, T. Gudbjartsson*, et al.* (2004). ADP receptor P2Y12 is expressed in vascular smooth muscle cells and stimulates contraction in human blood vessels. *Arterioscler Thromb Vasc Biol* **24**(10): 1810-1815.
Wilcox, J. N., K. M. Smith, S. M. Schwartz and D. Gordon (1989). Localization of tissue factor in the normal vessel wall and in the atherosclerotic plaque. *Proc Natl Acad Sci U S A* **86**(8): 2839-2843.
Willerson, J. T., S. K. Yao, J. McNatt, C. R. Benedict, H. V. Anderson, P. Golino*, et al.* (1991). Frequency and severity of cyclic flow alternations and platelet aggregation predict the severity of neointimal proliferation following experimental coronary stenosis and endothelial injury. *Proc Natl Acad Sci U S A* **88**(23): 10624-10628.
Wiviott, S. D., E. Braunwald, C. H. McCabe, G. Montalescot, W. Ruzyllo, S. Gottlieb*, et al.* (2007). Prasugrel versus clopidogrel in patients with acute coronary syndromes. *N Engl J Med* **357**(20): 2001-2015.
Woollard, K. J., S. Sturgeon, J. P. Chin-Dusting, H. H. Salem and S. P. Jackson (2009). Erythrocyte hemolysis and hemoglobin oxidation promote ferric chloride-induced vascular injury. *J Biol Chem* **284**(19): 13110-13118.
Yu, H., V. Stoneman, M. Clarke, N. Figg, H. B. Xin, M. Kotlikoff*, et al.* (2011). Bone marrow-derived smooth muscle-like cells are infrequent in advanced primary atherosclerotic plaques but promote atherosclerosis. *Arterioscler Thromb Vasc Biol* **31**(6): 1291-1299.
Yusuf, S., S. Reddy, S. Ounpuu and S. Anand (2001). Global burden of cardiovascular diseases: part I: general considerations, the epidemiologic transition, risk factors, and impact of urbanization. *Circulation* **104**(22): 2746-2753.
Yusuf, S., F. Zhao, S. R. Mehta, S. Chrolavicius, G. Tognoni and K. K. Fox (2001). Effects of clopidogrel in addition to aspirin in patients with acute coronary syndromes without ST-segment elevation. *N Engl J Med* **345**(7): 494-502.
Zhan, Y., R. C. Paolicelli, F. Sforazzini, L. Weinhard, G. Bolasco, F. Pagani*, et al.* (2014). Deficient neuron-microglia signaling results in impaired functional brain connectivity and social behavior. *Nat Neurosci* **17**(3): 400-406.
Zhang, F. L., L. Luo, E. Gustafson, J. Lachowicz, M. Smith, X. Qiao*, et al.* (2001). ADP is the cognate ligand for the orphan G protein-coupled receptor SP1999. *J Biol Chem* **276**(11): 8608-8615.
Zhang, J., K. Zhang, Z. G. Gao, S. Paoletta, D. Zhang, G. W. Han*, et al.* (2014). Agonist-bound structure of the human P2Y12 receptor. *Nature* **509**(7498): 119-122.
Zhang, K., J. Zhang, Z. G. Gao, D. Zhang, L. Zhu, G. W. Han*, et al.* (2014). Structure of the human P2Y12 receptor in complex with an antithrombotic drug. *Nature* **509**(7498): 115-118.

Zhang, L. (2011) Voluntary oral administration of drugs in mice. Protocol Exchange.
Zhang, P. (2011) Glucose tolerance test in mice. Bio-protocol **1**.
Zhang, S. H., R. L. Reddick, J. A. Piedrahita and N. Maeda (1992). Spontaneous hypercholesterolemia and arterial lesions in mice lacking apolipoprotein E. *Science.* **258**(5081): 468-471.
Zhu, B., D. G. Kuhel, D. P. Witte and D. Y. Hui (2000). Apolipoprotein E inhibits neointimal hyperplasia after arterial injury in mice. *Am J Pathol* **157**(6): 1839-1848.
Zhu, Y., P. M. Farrehi and W. P. Fay (2001). Plasminogen activator inhibitor type 1 enhances neointima formation after oxidative vascular injury in atherosclerosis-prone mice. *Circulation* **103**(25): 3105-3110.

10 Appendices

10.1 Appendix I – Diets and antibiotic water

10.1.1 Chow diet

2018S - Teklad Global 18% protein rodent diet purchased from Harlan (Indiana, IN). Autoclaved and stored at room temperature.

Ingredients

Ground wheat, ground corn, wheat middlings, dehulled soybean meal, corn gluten meal, soybean oil, calcium carbonate, brewers dried yeast, dicalcium phosphate, iodized salt, L-lysine, DL-methionine, choline chloride, thiamine mononitrate, biotin, niacin, vitamin A acetate, pyridoxine hydrochloride, vitamin D3 supplement, folic acid, menadione sodium bisulphite complex (source of vitamin K activity), calcium pantothenate, vitamin E supplement, vitamin B12 supplement, riboflavin, ferrous sulphate, magnesium oxide, manganous oxide, zinc oxide, copper sulphate, calcium iodate, cobalt carbonate, chromium potassium sulphate, kaolin.

Specification	*% (w/w)*	*% KCal*	*Kcal/g*
Crude fat	6	17	
Crude protein	18.8	23	
Crude fibre	3.8	/	
Ash	5.9	/	
Carbohydrate	50	60	
****Starch***	*45		
****Sugar***	*5		
Digestible energy			3.4
Metabolised energy			3.3

10.1.2 Western diet

829100 - Western rodent diet purchased from Special Diet Services (Witham, UK). Purified diet, stored at 4°C to prolong shelf-life.

Ingredients

Sucrose, milk fat anhydrous, casein, maltodextrin, corn starch, cellulose, corn oil, calcium carbonate, L-cystine, choline bitartrate, cholesterol (0.15%), antioxidant, AIN-76A-MX, AIN-76A-VX.

Specification	*% (w/w)*	*% KCal*	*Kcal/g*
Crude fat	21.4	42	1.93
Crude protein	17.5	15	0.7
Crude fibre	3.5	/	/
Ash	4.1	/	/
Carbohydrate	50	43	2
Energy			4.63

10.1.3 Antibiotic drinking water

Antibiotic stocks

Neomycin trisulphate salt hydrate (N1876; Sigma, Poole, UK): 0.1 mol/L in 10 mL aliquots
Polymyxin B sulphate salt (P1004; Sigma): 1 million USP units in 2 mL aliquots

Antibiotic water

An aliquot of each antibiotic is added to 1 litre of sterile water making the final concentrations: 1 mmol/L neomycin, 1000 USP units/mL polymyxin B.

10.2 Appendix II - PCR parameters and buffers

All reagents listed in Materials (see section 2.3.1), unless otherwise stated.

10.2.1 ApoE PCR parameters

Reaction mix

BioMix™ red	12.5 µL	
Primer 180	0.5 µL	0.4 µmol/L final concentration
Primer 181	0.5 µL	
Primer 182	0.5 µL	
Sample DNA	2 µL	
Sterile water	9 µL	

Cycle program

	94°C for 3 minutes (denaturation step)
X 35	94°C for 20 seconds (denaturation step)
	68°C for 40 seconds (annealing step)
	72°C for 2 minutes (elongation step)
	72°C for 7 minutes (final elongation step)
	4°C holding temperature

10.2.2 $P2Y_{12}$ PCR parameters

Reaction mix

25 mmol/L nucleotides	0.2 µL	0.2 mmol/L final concentration
25 mmol/L $MgCl_2$	1.5 µL	1.5 mmol/L final concentration
GoTaq® DNA polymerase (5 U/µL)	0.2 µL	1 unit
5 x GoTaq® green buffer	5 µL	1 x final concentration
Primer NEO	0.3 µL	0.25 µmol/L final concentration
Primer DP308	0.93 µL	0.75 µmol/L final concentration
Primer DP310	0.93 µL	0.75 µmol/L final concentration
Sample DNA	2 µL	
Sterile water	13.94 µL	

Cycle program

	94°C for 3 minutes (denaturation step)
X 35	94°C for 30 seconds (denaturation step)
	62°C for 30 seconds (annealing step)
	72°C for 1 minute (elongation step)
	72°C for 7 minutes (final elongation step)
	4°C holding temperature

10.2.3 Agarose gels

ApoE - 1.5% w/v gel: 2.25 g agarose to 150 mL TAE buffer
$P2Y_{12}$ - 2% w/v gel: 3 g agarose to 150 mL TAE buffer

In each case, the agarose/TAE mixture was heated in a microwave on full power for 2 minutes until the agarose had dissolved and the liquid was clear. The solution was cooled before adding 10 µL ethidium bromide. The gel poured and allowed to set for 1 hour before placing in an electrophoresis tank. The gel was submerged in TAE buffer before loading samples.

10.2.4 TAE buffer

To make x 50 stock: 2 mol/L Tris (hydroxymethyl) methylamine (VWR, Lutterworth, UK)
28.55 mL glacial acetic acid (100% v/v) (VWR)
50 mmol/L EDTA (pH 8.0) (Sigma)
Make up to 500 mL with distilled water
Dilute with distilled water to x 1 working solution.

10.2.5 DNA marker

1 µL Phix174/HAEIII marker + 3 µL orange/green 6x loading dye + 14 µL sterile water

10.3 Appendix III – Histology and immunohistochemistry

All reagents listed in Materials (see section 2.8.1 and 2.9.1).

10.3.1 Fixatives

Neutral buffered formalin (10% v/v)

To make 1 litre: 4 g sodium phosphate [NaH_2PO_4]
7.1 g di-sodium hydrogen orthophosphate [Na_2HPO_4]
100 mL formaldehyde (37% w/v)
900 mL distilled water

Paraformaldehyde in PBS (PFA) (4% w/v)

To make 100 mL: 4 g paraformaldehyde
100 mL PBS

Run the bottle under a hot tap to heat the solution to approximately 60°C. Then add several drops of sodium hydroxide [NaOH] to raise the solution to pH 7.0. The solution should now become clear.

10.3.2 Dehydration protocol

Tissue is placed in plastic histological cassettes and submerged in increasing concentrations of alcohol for 1 hour per grade alcohol (50%, 70%, 90%, 100% and 100% v/v ethanol), including a change of ethanol after the first 100% step. Tissue is then placed in a 1:1 mixture of ethanol (100%) and xylene for 1 hour. Followed by 2 x 1 hour steps in xylene, with a change of liquid after the first xylene step. Tissue is then placed in molten paraffin wax and left in an oven (60°C) overnight.

To ensure successful infiltration of the wax into the tissue, molten wax should only be held at 1-2°C above its melting point. In this case the melting point was 58°C and so the wax oven was set to a maximum temperature of 60°C. Storing wax at much higher temperatures

above its melting point, for prolonged periods of time, can alter the properties of the wax and in my experience reduce the ability of the wax to infiltrate the tissues. Further preventative measures include replacing molten wax every 6 months and avoid allowing the wax to set and re-melt.

10.3.3 Histological staining protocols

10.3.3.1 Oil red O

Making oil red O stain

1. Add 1 mL distilled water to 99 mL isopropanol (Propan-2-ol).
2. Add oil red O powder to the solution until it is saturated.
3. Filter the saturated solution using Whatman® grade 1 filter paper.
4. Dilute the final stain to 60% v/v using distilled water.

Staining protocol

1. Carry out the staining process in individual 1.5 mL eppendorf tubes.
2. Rinse aortae in distilled water followed by 60% v/v isopropanol for 2 minutes.
3. Immerse in oil red O for 10-15 minutes.
4. Rinse in 60% v/v isopropanol for 2 minutes, followed by distilled water.

10.3.3.2 Alcian blue/elastic van Gieson (EVG)

Staining protocol

1. Dewax slides for 10 minutes in xylene and rehydrate through graded alcohols (100%, 90%, 70% and 50% v/v ethanol) for 2 minutes each, finishing in water.
2. Oxidise with aqueous potassium permanganate (0.25% w/v) for 3 minutes, then rinse in water.
3. Bleach with oxalic acid (1% w/v) for 3 minutes, then rinse in water.
4. Stain nuclei with Carazzi's haematoxylin for 2 minutes.
5. Differentiate with acid alcohol (1% v/v HCl in 70% v/v ethanol) for 5 seconds.
6. "Blue" with hot running tap water for 5 minutes.
7. Stain with alcian blue (1% w/v in 3% aqueous acetic acid) for 5 minutes.
8. Rinse in water, followed by 95% v/v ethanol.
9. Stain with Miller's elastin stain for 30 minutes.
10. Differentiate in 95% ethanol and rinse in water.
11. Stain with Curtis' modified van Gieson reagent (10 mL 1% w/v ponceau S in 90 mL saturated aqueous picric acid, 1ml glacial acetic acid) for 6 minutes, then rinse in water.
12. Dehydrate through graded alcohols (reverse step 1) ending in xylene.
13. Mount with coverslips using DPX resin.

Interpretation

Elastin coarse and fine fibres	Blue/black
Acid mucopolysaccharides	Black
Collagen	Red
Muscle	Yellow

10.3.3.3 Haematoxylin and eosin (H&E)

Staining protocol

1. Dewax slides for 10 minutes in xylene and rehydrate through graded alcohols (100%, 90%, 70% and 50% v/v ethanol) for 2 minutes each, finishing in water.
2. Stain with Carazzi's haematoxylin for 2 minutes, then rinse in water.

3. Stain with eosin (1% w/v) for 30 seconds.
4. Rinse briefly in water and quickly dehydrate through graded alcohols for 30 seconds each step, beginning at 90% ethanol and ending in xylene.
5. Mount with coverslips using DPX resin.

10.3.3.4 Martius scarlet blue (MSB)

Staining protocol

1. Dewax slides for 10 minutes in xylene and rehydrate through graded alcohols (100%, 90%, 70% and 50% v/v ethanol) for 2 minutes each, finishing in water.
2. Stain with celestine blue (1% w/v) for 5 minutes.
3. Stain with Harris' haematoxylin for 5 minutes, then rinse in water.
4. Differentiate in acid alcohol (1% v/v HCl in 70% v/v ethanol) for a few seconds and then 'blue' in tap water for 5 minutes.
5. Rinse in 95% v/v ethanol.
6. Stain with martius yellow (0.5% w/v martius yellow, 2% w/v phosphotungstic acid in 95% ethanol) for 2 minutes and rinse in water.
7. Stain with ponceau de xylidine (1% w/v ponceau de xylidine in 2% v/v glacial acetic acid) for 10 minutes.
8. Differentiate in 1% w/v phosphotungstic acid for 5 minutes and drain (do not wash in water).
9. Stain with methyl blue (5% w/v methyl blue in 10% v/v glacial acetic acid) for 10 minutes.
10. Rinse in 1% v/v glacial acetic acid for 10 minutes.
11. Dehydrate in 100% v/v ethanol, then xylene for 2 minutes each.
12. Mount with coverslips using DPX resin.

Interpretation

Nuclei	Black/purple
RBCs	Yellow
Fibrin	Red
Collagen/adventitia/connective tissue	Bright blue
Smooth muscle	Pink/red

10.3.4 Immunohistochemistry protocols

Reagents

Vectastain® ABC-HRP reagent - Add 1 drop each of reagent A and B into 2.5 mL PBS (make 30 minutes prior to use).
Sigma*FAST*™ DAB - Add one DAB and one urea hydrogen peroxide tablet to 15 mL water.

General staining protocol

1. Dewax slides for 10 minutes in xylene and rehydrate through graded alcohols (100%, 90%, 70% and 50% v/v ethanol) for 2 minutes each, finishing in water.
2. Block endogenous peroxidases by incubation in 3% v/v hydrogen peroxide in PBS for 10 minutes, then rinse in water.
3. Antigen retrieval step if necessary.
4. Block non-specific secondary antibody binding with 1% w/v skimmed milk powder in PBS for 30 minutes at room temperature.
5. Tip off milk buffer (don't wash) and blot away excess.
6. Incubate with primary antibody.
7. Wash in 3 changes of PBS, for 5 minutes each.

8. Incubate with biotinylated secondary antibody (1:200 dilution in PBS) for 30 minutes at room temperature.
9. Wash in 3 changes of PBS, for 5 minutes each.
10. Incubate with Vectastain® ABC-HRP reagent for 30 minutes at room temperature.
11. Wash in 3 changes of PBS, for 5 minutes each.
12. Add DAB substrate for 5 minutes and rinse in water.
13. Counterstain using Carazzi's haematoxylin for 1 minute and rinse in water.
14. Dehydrate through graded alcohols (reverse step 1) ending in xylene.
15. Mount with coverslips using DPX resin.

10.3.4.1 α-Smooth muscle actin (α-SMA)

Primary antibody

Mouse monoclonal anti-human α-smooth muscle actin (M0851); 1:150 dilution in PBS for 1 hour at room temperature.

Secondary antibody

Biotinylated goat anti-mouse IgG secondary antibody.

10.3.4.2 F4/80

Primary antibody

Rat anti-mouse F4/80 (ab6640); 1:100 dilution in PBS, overnight at 4°C.

Secondary antibody

Biotinylated goat anti-rat IgG secondary antibody.

Antigen retrieval

Incubate in citrate buffer for 20 minutes at 95°C. Cool for 20 minutes at room temperature, then permeabilise by incubation in 0.5% v/v triton X-100 in PBS for 10 minutes at room temperature.

Citrate buffer (10 mmol/L, pH 6.0)

2.1 g citric acid monohydrate
900 mL distilled water

Adjust pH to 6.0 using 2 mol/L sodium hydroxide [NaOH], then dilute to 1 litre for use.

10.3.4.3 MAC387

Primary antibody

Mouse monoclonal anti-human MAC387 (M074701); 1:100 dilution in PBS for 1 hour at room temperature.

Secondary antibody

Biotinylated goat anti-mouse IgG secondary antibody.

Antigen retrieval

Incubate in 0.1% w/v trypsin in TBS (pH 8.0) for 10 minutes at 37°C. Tip off trypsin and add PBS to stop digestion.

10.3.5 $P2Y_{12}$ / α-smooth muscle actin immunofluorescence protocol

Primary antibodies

Mouse monoclonal anti-human α-smooth muscle actin (M0851).
Rabbit polyclonal anti-$P2Y_{12}$ (APR-012).

Secondary antibodies

Alexa Fluor® 488 goat anti-mouse IgG, H+L, highly cross adsorbed (A-11034).
Alexa Fluor® 594 goat anti-rabbit IgG, H+L, highly cross adsorbed (A-11037).

Staining protocol

1. Dewax slides for 10 minutes in xylene and rehydrate through graded alcohols (100%, 90%, 70% and 50% v/v ethanol) for 2 minutes each, finishing in water for 5 minutes.
2. Block non-specific secondary antibody binding in blocking buffer (5% v/v goat serum, 1% w/v BSA, 0.5% v/v triton in PBS) for 30 minutes at room temperature.
3. Tip off blocking buffer (don't wash) and blot away excess.
4. Incubate with α-smooth muscle actin (1:150) and $P2Y_{12}$ primary antibodies (1:100) in dilution buffer (1% w/v BSA, 0.5% triton v/v in PBS) overnight at 4°C.
5. Wash in 3 changes of PBS, for 5 minutes each.
6. Incubate with fluorescent secondary antibodies (1:200 dilution with 1% w/v BSA in PBS) in the dark for 1 hour at room temperature.
7. Wash in 3 changes of PBS, for 5 minutes each.
8. Mount with coverslips using Vectashield® mounting medium with DAPI, seal with nail varnish and keep in the dark.

10.4 Appendix IV – *In vitro* assays

All reagents listed in Materials (see section 2.10.1).

10.4.1 HEPES-Tyrode's (HT) buffer

To make 2 litres:
- 15.15 g Sodium chloride [NaCl]
- 1.48 g Sodium bicarbonate [$NaHCO_3$]
- 0.4176 g Potassium chloride [KCl]
- 0.218 g Potassium phosphate [KH_2PO_4]
- 2.04 g Dextrose (D-glucose)
- 4.78 g N-2-hydroxyethylpiperazine-N′-2-ethanesulfonic acid (HEPES)
- 2 L ultra pure water